



This document was produced
by scanning the original publication.

Ce document est le produit d'une
numérisation par balayage
de la publication originale.

GEOLOGICAL SURVEY OF CANADA
BULLETIN 390

**UPPERMOST DEVONIAN AND LOWER CARBONIFEROUS
STRATIGRAPHY, SEDIMENTATION, AND DIAGENESIS,
SOUTHWESTERN DISTRICT OF MACKENZIE AND
SOUTHEASTERN YUKON TERRITORY**

B.C. RICHARDS

1989



Energy, Mines and
Resources Canada

Énergie, Mines et
Ressources Canada

Canada

THE ENERGY OF OUR RESOURCES

THE POWER OF OUR IDEAS

GEOLOGICAL SURVEY OF CANADA
BULLETIN 390

**UPPERMOST DEVONIAN AND LOWER CARBONIFEROUS
STRATIGRAPHY, SEDIMENTATION, AND DIAGENESIS,
SOUTHWESTERN DISTRICT OF MACKENZIE AND
SOUTHEASTERN YUKON TERRITORY
(NTS 95 B, C, F, and G)**

B.C. RICHARDS

with appendices on paleontology by
B.L. Mamet, E.W. Bamber, A.C. Higgins
D.C. McGregor, and J. Utting

1989

© Minister of Supply and Services Canada 1989

Available in Canada through

authorized bookstore agents and other bookstores

or by mail from

Canadian Government Publishing Centre
Supply and Services Canada
Ottawa, Canada K1A 0S9

and from

Geological Survey of Canada offices:

601 Booth Street
Ottawa, Canada K1A 0E8

3303-33rd Street N.W.,
Calgary, Alberta T2L 2A7

A deposit copy of this publication is also available for reference
in public libraries across Canada

Cat. No. M42-390E
ISBN 0-660-13430-6

Price subject to change without notice

Critical readers

E.W. Bamber
D. Morrow

Scientific editor

N.C. Ollerenshaw

Authors' address

Institute of Sedimentary and Petroleum Geology
3303 - 33rd Street, N.W.
Calgary, Alberta T2L 2A7

Original manuscript submitted: 87.05.05
Approved for publication: 87.08.11

PREFACE

The thick succession of Lower Carboniferous strata in southwestern District of Mackenzie and southeastern Yukon Territory represents a significant episode in the geological history of northwestern Canada. This bulletin is the first well documented, truly comprehensive treatment of the Lower Carboniferous in the area. It contains a wealth of information on several different aspects of stratigraphy, sedimentology and diagenesis, and will become a standard, widely read reference for future studies of correlative rocks in Western Canada. The detailed information presented in this report will contribute to the accurate assessment of petroleum resources in this frontier region. Anomalies in the stratigraphic nomenclature have been corrected, thereby placing the lithostratigraphy of the succession on a firm basis. The interpretation of the origins of the abundant large-scale truncation surfaces, so characteristic of the Lower Carboniferous carbonate lithofacies, are particularly illuminating. This bulletin also presents the detailed paleontological control essential to local and interregional correlation.

Elkanah A. Babcock
Assistant Deputy Minister
Geological Survey of Canada

PRÉFACE

L'épaisse succession de strates du Carbonifère inférieur que l'on retrouve dans le sud-ouest du district de Mackenzie et dans le sud-est du Yukon représente un épisode important de l'histoire géologique du Nord-ouest canadien. Le présent bulletin constitue la première étude bien documentée et vraiment complète du Carbonifère inférieur dans cette région. Véritable mine d'information sur plusieurs questions différentes se rapportant à la stratigraphie, à la sédimentologie et à la diagenèse, ce bulletin deviendra un document de référence très lu auquel on fera appel pour l'étude des roches de corrélation dans l'ouest du Canada. Les renseignements détaillés qui sont présentés ici nous aideront à mieux évaluer les ressources pétrolières de cette région pionnière. Les anomalies dans la nomenclature stratigraphique ont été corrigées; de ce fait, la lithostratigraphie de la succession se retrouve placée sur de solides assises. Par ailleurs, la façon dont on a interprété l'origine des abondantes et vastes surfaces de troncature, lesquelles caractérisent si bien le lithofaciès des roches carbonatées du Carbonifère inférieur, s'est avérée particulièrement éclairante. Le présent bulletin fait également état des contrôles paléontologiques détaillés qui sont essentiels à l'établissement de corrélations à l'échelle locale et entre les régions.

Elkanah A. Babcock
Sous-ministre adjoint
Commission géologique du Canada

CONTENTS

1	Abstract/Résumé
2	Introduction
2	Previous work
2	Present work
3	Acknowledgments
3	Lithostratigraphic framework
3	Formational nomenclature
5	Underlying and overlying strata
6	Besa River Formation
6	Type section
6	Previous work in the study area
9	Distribution
9	Thickness
9	Lithostratigraphic relationships
9	Lithofacies
9	Shale and sandstone lithofacies
9	Dark-shale lithofacies
10	Spiculite and spicule-lime-packstone lithofacies
12	Environmental interpretations
12	Shale and sandstone lithofacies
13	Dark-shale lithofacies
13	Spiculite and spicule-lime-packstone lithofacies
13	Age
13	Banff Formation
13	Type section
13	Previous work in the study area
14	Distribution
14	Thickness
14	Lithostratigraphic relationships
14	Lithofacies
14	Dark-shale lithofacies
15	Limestone and siltstone lithofacies
17	Environmental interpretations
17	Dark-shale lithofacies
18	Limestone and siltstone lithofacies
19	Age
19	Yohin Formation
19	Type section
19	Previous work
19	Distribution
20	Thickness
20	Lithostratigraphic relationships
20	Lithology
22	Diagenesis
22	Calcite
22	Calcite cement fabrics
23	Replacement calcite
23	Cements in sandstone and siltstone
23	Lithofacies
23	Graded-bed lithofacies
25	Crossbedded sandstone lithofacies
26	Environmental interpretations
26	Graded-bed lithofacies
27	Crossbedded sandstone lithofacies
28	Shoaling-upward depositional episode
28	Age
28	Pekisko Formation
28	Type section and previous work
28	Distribution and thickness
28	Lithostratigraphic relationships
29	Lithology
29	Environmental interpretations
29	Age
29	Clausen Formation
29	Type section
30	Previous work
30	Distribution
30	Thickness
30	Lithostratigraphic relationships
30	Lithology

31	Lithofacies
31	Dark-shale lithofacies
32	Spiculite lithofacies
32	Lime-grainstone and packstone lithofacies
32	Siltstone lithofacies
33	Environmental interpretations
33	Dark-shale lithofacies
33	Spiculite lithofacies
33	Lime grainstone and packstone lithofacies
33	Siltstone lithofacies
33	Age
34	Prophet Formation
34	Type section
34	Previous work
34	Distribution
34	Thickness
34	Lithostratigraphic relationships
36	Lithology
38	Diagenesis
38	Sponge spicules
38	Chert
39	Calcite
39	Replacement calcite
39	Passively precipitated calcite
40	Neomorphic calcite
40	Displacive calcite
41	Dolomite
42	Pyrite
42	Lithofacies
42	Spiculite and spicule-lime-packstone lithofacies
48	Dark-shale lithofacies
48	Mixed-skeletal lime-packstone lithofacies
49	Multibed sequences
50	Environmental interpretations
50	Spiculite and spicule-lime-packstone lithofacies
50	Dark-shale lithofacies
51	Mixed-skeletal lime-packstone lithofacies
51	Terrigenous influx and carbonate buildup development
52	Age
52	Flett Formation
52	Type section
53	Previous work
53	Distribution
54	Thickness
54	Lithostratigraphic relationships
54	Members
54	Tlogotsho Member
54	Jackfish Gap Member
55	Meilleur Member
55	Lithology
57	Diagenesis
57	Chert
58	Calcite
59	Dolomite
61	Other authigenic minerals
61	Lithofacies
61	Mixed-skeletal lime-packstone lithofacies
65	Lime-grainstone lithofacies
66	Siltstone and sandstone lithofacies
67	Shale and mudstone lithofacies
69	Spicule-lime-packstone lithofacies
70	Multibed sequences
70	Environmental interpretations
70	Mixed-skeletal lime-packstone lithofacies
71	Lime-grainstone lithofacies
72	Siltstone and sandstone lithofacies
72	Shale and mudstone lithofacies
73	Spicule-lime-packstone lithofacies
73	Carbonate buildup development and terrigenous influx

74	Age
74	Golata Formation
74	Type section
74	Previous work
74	Distribution
75	Thickness
75	Lithostratigraphic relationships
75	Lithology
76	Diagenesis
76	Chert
76	Dolomite
76	Other authigenic minerals
77	Lithofacies
77	Dark-shale lithofacies
77	Dolostone lithofacies
78	Sandstone lithofacies
78	Environmental interpretations
79	Age
79	Concave-upward truncation surfaces
79	Distribution and general characteristics
81	Submarine channels and fills
83	Slump scars
83	Truncation surfaces of undetermined origin
84	Origin of multibed carbonate-bearing sequences
84	Asymmetric progradational sequences
85	Asymmetric abandonment sequences
86	Symmetric sequences
86	Carbonate buildups
86	Style of buildup
87	Shelf-margin characteristics
87	Effects of terrigenous input
87	Provenance of siliciclastics
87	Golata, upper Besa River, and Mattson formations
89	Formations between the Exshaw and Golata formations
91	Paleogeography
92	Depositional summary
92	Early Tournaisian to late middle Tournaisian (Tn1a to Tn2)
93	Latest middle and late Tournaisian (Tn2 and Tn3)
95	Latest Tournaisian through latest middle Viséan (Tn3 to V2)
97	Latest middle Viséan (V2) to early Serpukhovian
99	References
110	Appendix A. Foraminifers and calcareous algae, identified by B.L. Mamet
125	Appendix B. Corals, identified by E.W. Bamber
129	Appendix C. Conodonts, identified by A.C. Higgins
130	Appendix D. Palynomorphs, identified by D.C. McGregor
131	Appendix E. Palynomorphs, identified by J. Utting
134	Appendix F. Point count analyses
135	Appendix G. X-ray analyses

Illustrations

Figures

4	1. Map of project area showing locations of sections and outcrops studied.
6	2. Lithostratigraphic units in project area.
7	3. Correlation of Carboniferous lithostratigraphic units.
in pocket	4. Cross-section between localities 1 and 7 (Fig. 1, cross-section A-A').
in pocket	5. Cross-section between localities 8 and 26 (Fig. 1, cross-section B-B').
in pocket	6. Cross-section between localities 19 and 20 (Fig. 1, cross-section C-C').
10	7. Partly schematic, restored cross-section between localities 2 and 9, illustrating relationship of Mattson deltaic deposits to deposits in underlying formations.
11	8. Type section of the Mattson Formation at Jackfish Gap.
11	9. Outcrop of Besa River and Mattson formations at Tika Creek.
11	10. Outcrop of Besa River and Prophet formations at Locality 11.
12	11. Outcrop of Besa River spiculite and spicule-lime-packstone lithofacies.
12	12. Polished slab of turbidites from Besa River Formation at Ram Creek.
12	13. Outcrop of Banff(?) and Yohin formations at Bluefish Mountain.
15	14. Photomicrograph of lime grainstone from Banff(?) Formation.

Figures

- 15 15, 16. Outcrops and sedimentary structures of limestone and siltstone lithofacies in the Banff(?) Formation.
- 16 17, 18. Photomicrographs of Banff lithologies.
- 16 19. Diagram showing carbonate diagenetic environments.
- 17, 18 20-22. Sedimentary structures in limestone and siltstone lithofacies of the Banff(?) Formation.
- 19 23. Type section of the Yohin Formation at Jackfish Gap.
- in pocket 24. Stratigraphic column and descriptions for type Yohin, Clausen, and Flett formations, the type Tlogotsho, Jackfish Gap, and Meilleur members of the Flett, and the Prophet and Golata formations.
- 21 25. Photomicrographs of Yohin lithologies and cements.
- 24 26. The Yohin graded-bed lithofacies at Locality 29.
- 24 27. Polished slab of a Yohin siltstone turbidite.
- 24 28. Polished slab of a Yohin graded limestone and sandstone bed.
- 26 29, 30. Sedimentary structures in the Yohin crossbedded sandstone lithofacies.
- 29 31. Photomicrograph of lime-grainstone from the Pekisko(?) Formation.
- 31 32. Outcrops of Clausen, Prophet, and Flett formations at Jackfish Gap; large-scale truncation surface in the Flett.
- 32 33. Outcrop of Clausen dark-shale lithofacies.
- 32 34. Photomicrograph of Clausen lime-grainstone.
- 35 35. Outcrops of Prophet, Golata, and Mattson formations at Ram Creek; large-scale truncation surfaces and multibed sequences in the Prophet.
- 37-41 36-40. Photomicrographs of Prophet rock types, cement, chert, and dolomite.
- 42 41. Outcrop of Prophet spiculite and spicule-lime-packstone lithofacies.
- 43-46 42-45. Polished slabs of Prophet Formation turbidites.
- 47 46. Nodular spicule lime packstone in the Prophet Formation.
- 48 47, 48. Prophet Formation, mixed-skeletal lime-packstone lithofacies.
- 49 49. Multibed sequences in Prophet and Flett formations.
- 51 50. Cross-sections illustrating phases of carbonate-buildup development.
- 53 51. Type sections of Flett Formation and the Tlogotsho, Jackfish Gap, and Meilleur members.
- 56-60 52-57. Photomicrographs of Flett lithologies, cements, and chert.
- 60-63 58-60. Outcrops and sedimentary structures of the Flett mixed-skeletal lime-packstone lithofacies.
- 63 61. *Zoophycos* sp. from the Flett Formation.
- 63-65 62-65. Outcrops and sedimentary structures of the Flett lime-grainstone lithofacies.
- 67 66. Outcrops and sedimentary structures of Flett siltstone and sandstone lithofacies.
- 68 67. Type section of Jackfish Gap Member of Flett; shows lithofacies.
- 68 68. Outcrop of the Flett shale and mudstone lithofacies.
- 68 69. Outcrop of Flett spicule-lime-packstone lithofacies.
- 69 70. Multibed sequences and a large-scale truncation surface in the Meilleur Member.
- 73 71. Outcrop of Golata Formation.
- 76 72. Photomicrograph of Golata sandstone.
- 76, 77 73-75. Outcrops and sedimentary structures of the Golata Formation.
- 80-81 76. Large-scale truncation surfaces in the Flett Formation.
- 84-85 77. Large-scale truncation surfaces and multibed sequences in the Prophet and Flett formation.
- 86, 88-89 78, 79. Large-scale truncation surfaces and levee-like deposits in the Flett Formation.
- 90 80. Large-scale truncation surfaces and related fills in the Yohin graded-bed lithofacies.
- 91 81. Truncation surfaces and foreset-like beds in the Flett Formation.
- 92 82. Large-scale truncation surfaces and multibed sequence in the Yohin Formation.
- 93 83, 84. Slump deposits and related truncation surfaces in the Prophet Formation.
- 93, 94 85, 86. Large-scale truncation surface and related mound-like structure in the Prophet Formation.
- 96-97 87. Models of a carbonate platform and ramp.
- 97 88. Rose diagram of paleocurrent directions.
- 98 89. Map showing western depositional limits of Flett and Prophet formations.

Table

- 8 1. Thickness of lithostratigraphic units.

UPPERMOST DEVONIAN AND LOWER CARBONIFEROUS STRATIGRAPHY, SEDIMENTATION,
AND DIAGENESIS, SOUTHWESTERN DISTRICT OF MACKENZIE AND SOUTHEASTERN
YUKON TERRITORY (NTS 95 B, C, F, AND G)

Abstract

The uppermost Devonian and Lower Carboniferous in this region consist of a succession of continental terrace wedge deposits. These comprise a shale lithosome that intertongues eastward with the following: a lower interval of dominantly terrigenous slope and shelf facies (upper Banff Formation and coeval Yohin Formation); a middle succession with carbonate platform and ramp facies (in ascending order: Pekisko and Prophet formations, Formation F, and Flett Formation); and an upper interval of delta facies (Mattson Formation). Basinal and prodelta shale in the Besa River Formation constitute the western part of the shale lithosome, and, proceeding upward, the lower Banff, Clausen, and Golata formations are its eastern tongues. The lower Banff is mainly basinal shale, whereas shelf limestone and sandstone predominate in the upper Banff. Graded beds dominate the slope to shelf facies of the western and lower Yohin, which overlies mainly the Besa River; the upper Yohin in the east is chiefly shallow shelf sandstone. Four carbonate buildups are present, and each successive buildup prograded farther westward than its predecessor. Platform shelf limestone constitutes most of the Pekisko, which abruptly overlies the upper Banff. The Prophet ramp and platform facies, which overlie Besa River and Clausen basinal shale, comprise slope spiculite and limestone that both underlie, and pass eastward into, more proximal, ramp and platform deposits of Formation F and the Flett. The Flett, which overlies the Prophet and Formation F, is mainly shelf margin and slope limestone. Yohin, Prophet, and Flett slope facies have submarine channel scars. The Golata, mostly prodelta shale, conformably overlies the Prophet and Flett and is conformably overlain by Mattson deltaic sandstone. Siliciclastics in this succession had a northern provenance. The calcite cement was precipitated in the meteoric-phreatic and subsurface zones; spicules provided silica for chert.

The name Rundle Group is extended into the area; Etanda Formation is abandoned. Also, the Flett is redefined and subdivided into the Tlogotsho, Jackfish Gap, and Meilleur members.

Keywords: *Lower Carboniferous, stratigraphy, carbonates, sedimentation, diagenesis, basin deposits, slope deposits, shelf-margin deposits, submarine paleochannels, deltaic deposits, biostratigraphy, carbonate cements, Rundle Group, Etanda Formation, Flett Formation.*

Résumé

Dans cette région, les sédiments du Dévonien supérieur et du Carbonifère inférieur forment une séquence de dépôts en forme de biseau de terrasse continentale. Ces dépôts forment un lithosome de schiste argileux avec intercalations vers l'est des sédiments suivants: un intervalle inférieur de faciès terrigènes de talus et de plate-forme (partie supérieure de la formation de Banff et formation contemporaine de Yohin); une séquence intermédiaire comportant des faciès carbonatés de plate-forme et de rampe (en ordre ascendant: formations de Pekisko et de Prophet, formation F et formation de Flett); et un intervalle supérieur de faciès deltaïques (formation de Mattson). La partie ouest du lithosome contient des schistes argileux de bassin et de prodelta de la formation de Besa River, tandis que les biseaux à l'est se composent des formations suivantes, données en ordre ascendant: partie inférieure de la formation de Banff, formation de Clausen et formation de Golata. La partie inférieure de la formation de Banff se compose surtout de schiste argileux de bassin, et la partie supérieure, de grès et de calcaire de plate-forme. Des couches granoclassées prédominent dans les faciès de talus et de plate-forme des parties ouest et inférieure de la formation de Yohin, qui repose en grande partie sur la formation de Besa River. La partie supérieure de la formation de Yohin à l'est se compose principalement de grès de plate-forme peu profonde. On y trouve quatre accumulations de carbonates, chacune d'entre elles s'étant avancée plus loin vers l'ouest que la précédente. La formation de Pekisko se compose surtout de calcaire de plate-forme et repose en discordance sur la partie supérieure de la formation de Banff. Les faciès de rampe et de plate-forme de la formation de Prophet, qui recouvrent les schistes argileux de bassin des formations de Besa River et de Clausen, se composent de spiculite et de calcaire de talus sous-jacents aux dépôts de rampe et de plate-forme d'origine plus proximale des formations F et de Flett en lesquels ils se transforment vers l'est. La formation de Flett, sus-jacente à la formation de Prophet et à la formation F, se compose surtout de calcaire de talus et de marge de plate-forme. Les faciès de talus des formations de Yohin, de Prophet et de Flett contiennent des cicatrices de chenaux sous-marins. La formation de Golata, qui se compose principalement de schiste argileux de prodelta, repose en concordance sur les formations de Prophet et de Flett, et en concordance sous le grès deltaïque de Mattson. La source des roches silicoclastiques de cette séquence se trouvait au nord. Le ciment calcitique s'est précipité dans la zone météorique-phréatique et dans la zone de la subsurface; la silice du chert provient de spicules.

On utilise maintenant le nom du groupe de Rundle dans la région; celui de la formations d'Etanda est abandonné. La formation de Flett est définie à nouveau et subdivisée en trois membres, soit ceux de Tlogotsho, de Jackfish Creek et de Meilleur.

Mots clés: *Carbonifère inférieur, stratigraphie, carbonates, sédimentation, diagenèse, dépôts de bassin, dépôts de talus, dépôts de marge de plate-forme, paléochenaux sous-marins, dépôts deltaïques, biostratigraphie, ciments de carbonate, groupe de Rundle, formation d'Etanda, formation de Flett.*

INTRODUCTION

The uppermost Devonian and Lower Carboniferous in the southwestern District of Mackenzie and southeastern Yukon Territory (Figs. 1-3) form a thick shallowing-upward succession of continental terrace wedge deposits (Figs. 4-6). This succession, which comprises terrigenous clastics, carbonates, chert, and minor coal, was deposited on the downwarped western margin of the ancestral North American plate and possibly the western cratonic platform. It is widely exposed in the southern Mackenzie fold belt south of 61°30'N, and underlies a moderately extensive area on the adjacent interior platform (Fig. 1). Various aspects of the uppermost Devonian and Lower Carboniferous in this region have been examined in previous reconnaissance studies, but little detailed work has been done, and several important stratigraphic and sedimentological problems require attention.

This report deals mainly with the uppermost Devonian and Lower Carboniferous strata that lie between the Mattson and Exshaw formations in a region bounded by latitudes 60°00'N and 61°20'N and by longitudes 122°30'W and 125°00'W (Figs. 1-3). Specific subjects addressed are: regional lithostratigraphy; characteristics, distribution, and depositional environments of the lithofacies; and the latest Devonian and Early Carboniferous depositional history of the project area. Some aspects of the diagenesis of the deposits are also discussed.

Previous work

Geological work on the uppermost Devonian (lowest Tournaisian) and Lower Carboniferous (Tournaisian to lower Serpukhovian) in the project area began in 1887 when McConnell collected fossils from limestone outcrops along the banks of the Liard River north of Fort Liard. These fossils were examined by Whiteaves, who suggested that they were of Carboniferous age (McConnell, 1891, p. 55D, 56D). Hume (1923) examined the same exposures, made a brief traverse onto Carboniferous outcrops in the Liard Range west of the river, and suggested a Kinderhookian age for these exposures on the basis of brachiopods and bryozoans.

During an extensive reconnaissance expedition, Hage (1945, p. 8-15) measured sections and collected invertebrate fossils from a number of localities between the La Biche Range and Bluefish Mountain (Fig. 1). Hage did not name any rock units of Carboniferous age, but he determined that the Carboniferous in the region comprises shale and limestone units of Mississippian age, overlain by a unit of interbedded sandstone and shale of Late Mississippian or possible Early Pennsylvanian age.

Patton (1958) initiated detailed stratigraphic work on the Carboniferous in the project area. He measured and described the Carboniferous section at Jackfish Gap (Fig. 1, Loc. 4) and proposed the name Mattson Formation (Fig. 2) for the thick sequence of sandstone, with subordinate shale, limestone, dolostone, and minor coal, that occurs at the top of the section.

Douglas and Norris (1959, 1960) published preliminary geological maps (NTS map areas 95 B, C, F, and G) and accounts of regional geology. They did not introduce formal names for rock units but proposed several informal Devonian and Carboniferous units and gave them numerical designations (Fig. 2). Revised editions of the maps for areas 95 B, C, F, and G were published by Douglas (1976) and Douglas and Norris (1976a, b, c).

In a preliminary report, Harker (1961) named the Yohin, Clausen, Flett, and Etanda formations of Early Carboniferous age and divided the Mattson Formation into three informal members (Fig. 2). In addition, he provided descriptions of these formations and members, correlated them with the informal map units of Douglas and Norris (1959, 1960), and briefly discussed their ages. Subsequently, Harker (1963) described and discussed these formations in greater detail, and Douglas et al. (1963) published a geological map of the region that showed their distribution.

Pelzer (1966, p. 275, 315-317), Bamber et al. (1968, p. 8, 9, 16), and Bamber and Mamet (1978, p. 4-9) discussed the lateral relationships between Carboniferous formations in northeastern British Columbia and those north of latitude 60°00'N. Also, Bamber and Mamet described the type section of the Flett Formation, and Pelzer gave a detailed account of the stratigraphy, mineralogy, and geochemistry of the Devonian to Carboniferous Besa River Formation in British Columbia and southeastern Yukon Territory. Bamber et al. (1980) and Richards (1983b, p. A57) briefly described the Carboniferous System in the project area and discussed the depositional environments of major lithofacies.

Using palynological data, Braman (1976, p. 40, 42), and Braman and Hills (1977, p. 596) determined that Patton (1958, p. 323) and Harker (1961, p. 7; 1963, p. 33) had included an interval of Lower Cretaceous strata in the Mattson type section. Moreover, they briefly discussed the lithology and depositional environments of the Mattson Formation at its type locality.

The sub-Mattson, Tournaisian and Viséan strata, in the subsurface on the interior platform, have received little coverage in the literature, and the unpublished nomenclature used is generally similar to that which Macauley (1958) used in the Peace River region of northwestern Alberta. Early, unpublished nomenclature for formations of Tournaisian to Viséan age, in the subsurface of northern Alberta and northeastern British Columbia, was an extension of that employed in southwestern Alberta. It included the Exshaw, Banff, Pekisko, Shunda, Turner Valley, and Mount Head formations. Macauley (1958), in a report on the Carboniferous of the Peace River area, retained the first four names but introduced the name Debolt Formation for equivalents of the Turner Valley and Mount Head. Alternatively, Harker (1963, p. 15) assigned to the Flett Formation much of the sub-Mattson, Tournaisian and Viséan strata that underlie the interior platform in the report area. Finally, Douglas and Norris (1976a) subdivided that succession into the Exshaw, Banff and Flett formations.

Numerous geologists, including Hacquebard and Barss (1957, p. 3), Patton (1958), Harker (1961, 1963), Sullivan (1965), Bamber et al. (1968, p. 8, 11, 16), Braman and Hills (1977), Bamber and Mamet (1978), and Bamber et al. (1980), have discussed the biostratigraphy, correlations, and ages of Tournaisian and Viséan formations in the project area.

Present work

This study is based chiefly on data from the outcrop belt of the Tournaisian and Viséan in the southern Mackenzie fold belt, but incorporates some data from well sections in the project area and the region to the east (Figs. 5, 6). Parts of the field seasons of 1975, 1976 and 1978 were spent in the study area. At type localities and other selected sites that have good exposures, 13 detailed surface sections were measured (Fig. 1, Locs. 1-13; Table 1). Observations were made at four other localities where exposures are good (Fig. 1, Locs. 29-32), but stratigraphic sections were not

measured. During the course of this fieldwork, the overlying Mattson Formation was measured at five localities in the outcrop belt, for the separate studies of Bamber et al. (1980, 1984) and Richards (in progress). The samples, electric logs, and lithological logs from 15 well sections were examined to determine the distribution, thickness, and gross lithology of the sub-Mattson Tournaisian and Viséan formations in the subsurface of the project area (Fig. 1, Locs. 14-28; Table 1). Of these 15 well sections, core was available only from the Pan Am. Beaver YT G-01 well (Fig. 1, Loc. 19). Also, the core and cuttings from the Banff and Exshaw formations in the Imperial Island River No. 1 well, 75.5 km east of the project area (Table 1, Loc. 33), were logged.

Laboratory work included X-ray diffraction analyses, examination of thin sections and polished rock surfaces, and identification of fossils. Dunham's (1962) carbonate rock classification, Folk's (1974b) sandstone classification, and Folk's (1965, p. 25) size scale for crystals were used. Colour terms are from the colour chart of the Geological Society of America. Foraminifers, calcareous algae, conodonts, corals, and palynomorphs were used for biostratigraphic control.

B.L. Mamet identified the foraminifers and calcareous algae, and assigned them to the informal Oppel zones of Mamet and Skipp (1970a, b). Eleven foraminiferal zones, ranging in age from middle Tournaisian through late Viséan (Tn2 to V3), are recognized within the Lower Carboniferous of northeastern British Columbia and southwestern District of Mackenzie (Bamber and Mamet, 1978, p. 9-15 and Fig. 4). Bamber and Mamet listed the characteristic microbiota of these zones. The observed occurrences of these zones in the project area are indicated on Figure 3, and pertinent sections of Mamet (pers. comms., 1977, 1981), including taxon lists for individual samples from the study area, are in Appendix A.

E.W. Bamber identified corals that were collected during this study (Bamber, pers. comm., 1977; Appendix B). A.C. Higgins identified conodonts from the Banff(?), Yohin, and Clausen formations (Higgins, pers. comm., 1981; Appendix C). M.S. Barss identified many of the palynomorphs and assigned them to informal assemblage zones. Richards (1983a, Appendix D) provided the pertinent parts of the report of Barss (pers. comm., 1977). Finally, D.C. McGregor identified palynomorphs obtained from the Kotcho and Banff formations, and J. Utting identified miospores from several formations. Relevant sections of their reports (McGregor, pers. comm., 1980; Utting, pers. comm., 1981) are in Appendices D and E, respectively.

In this report, the Devonian/Carboniferous boundary is placed in the Tournaisian Series at the position advocated by Sandberg et al. (1972, 1978) and Sandberg and Poole (1977). They recommended that this boundary be placed at the base of the *Siphonodella sulcata* conodont Zone. The base of that zone is either close to or at the base of the *Gattendorfia subinvoluta* cephalopod Zone, which is the position for the basal Carboniferous boundary recommended by the second International Congress of Carboniferous Stratigraphy and Geology at Heerlen, 1935 (Sandberg et al., 1978, p. 117). Most biostratigraphers now accept the position recommended by that congress, although it requires that the lower part of the Tournaisian Series (Tn1a and basal Tn1b) be placed below the base of the Carboniferous System (Clayton et al., 1977, p. 4). The European Tournaisian is subdivided, mainly on biostratigraphic criteria, into three parts, which are referred to in ascending order as Tn1, Tn2, and Tn3 (Fig. 3). Also, the Tn1 has been subdivided in ascending order into the Tn1a and Tn1b.

Acknowledgments

This report is based on an unpublished University of Kansas doctoral dissertation (Richards, 1983a). I thank all persons who contributed to that study: R.A. Robison, who supervised the project; P. Enos, L.F. Dellwig, W. Dort Jr., and C.J. Sorenson, who served on the thesis advisory committee, critically read the manuscript, and suggested helpful modifications; E.W. Bamber, D.W. Morrow, G. Morin, and D.K. Strickland for useful discussions; and Terry Weiss and Chris Steudtler for able field assistance. E.W. Bamber and D.W. Morrow critically read a revised draft of this report.

Project 750085, initiated by D.W. Morrow of the Geological Survey of Canada, funded field and logistics support in the summers of 1975 and 1976. A research grant from the Geological Society of America provided part of the support for fieldwork in the summer of 1978, and the University of Kansas Department of Geology gave generous financial support throughout my graduate program.

B.L. Mamet at the University of Montreal identified foraminifers and calcareous algae, and A.C. Higgins at the University of Sheffield identified conodonts. At the Geological Survey of Canada, E.W. Bamber identified corals; M.S. Barss, D.C. McGregor, and J. Utting identified the palynomorphs; and A.G. Heinrich made semiquantitative X-ray diffraction analyses.

LITHOSTRATIGRAPHIC FRAMEWORK

Formational nomenclature

The published formational nomenclature currently used in the project area is based largely on the work of the Geological Survey of Canada. In the southern Mackenzie fold belt, the Tournaisian and Viséan have generally been subdivided, in ascending order, into the Besa River, Yohin, Clausen, Flett, and Mattson formations (Harker, 1963; Douglas, 1976; Douglas and Norris, 1976a, b, c; Bamber et al., 1980) (Fig. 2). Immediately eastward, on the interior platform, they have been subdivided in ascending order into the Exshaw, Banff, Flett, and Mattson formations (Douglas and Norris, 1976a).

For this report, the Tournaisian and Viséan in the project area are subdivided into 11 formations, five of which are in the Rundle Group of Douglas (1958, p. 36, 37) (Figs. 2, 3). The Besa River, Yohin, Clausen, Exshaw, Banff, and Mattson formations are used as previously defined. The names Rundle Group, and Pekisko, Prophet, and Golata formations, as currently used in northeastern British Columbia and western Alberta (see Macauley et al., 1964; Bamber and Mamet, 1978), are extended into this region and applied to the Lower Carboniferous strata. In addition, the informal name, Formation F, is introduced for an unnamed unit that in northeastern British Columbia has been called the "Shunda" by Bamber and Mamet (1978). On the interior platform north of latitude 60°00'N, the Pekisko, Clausen, Formation F, Prophet, and Flett constitute the Rundle Group. In the Mackenzie fold belt, the Rundle comprises the Flett and Prophet formations. The Flett is redefined to exclude strata that I reassign to the Prophet and Golata, and the name Etanda (Harker, 1961), formerly used in the area, is abandoned. Lithostratigraphic relationships of the 11 formations are summarized in three cross-sections (Figs. 4-6).

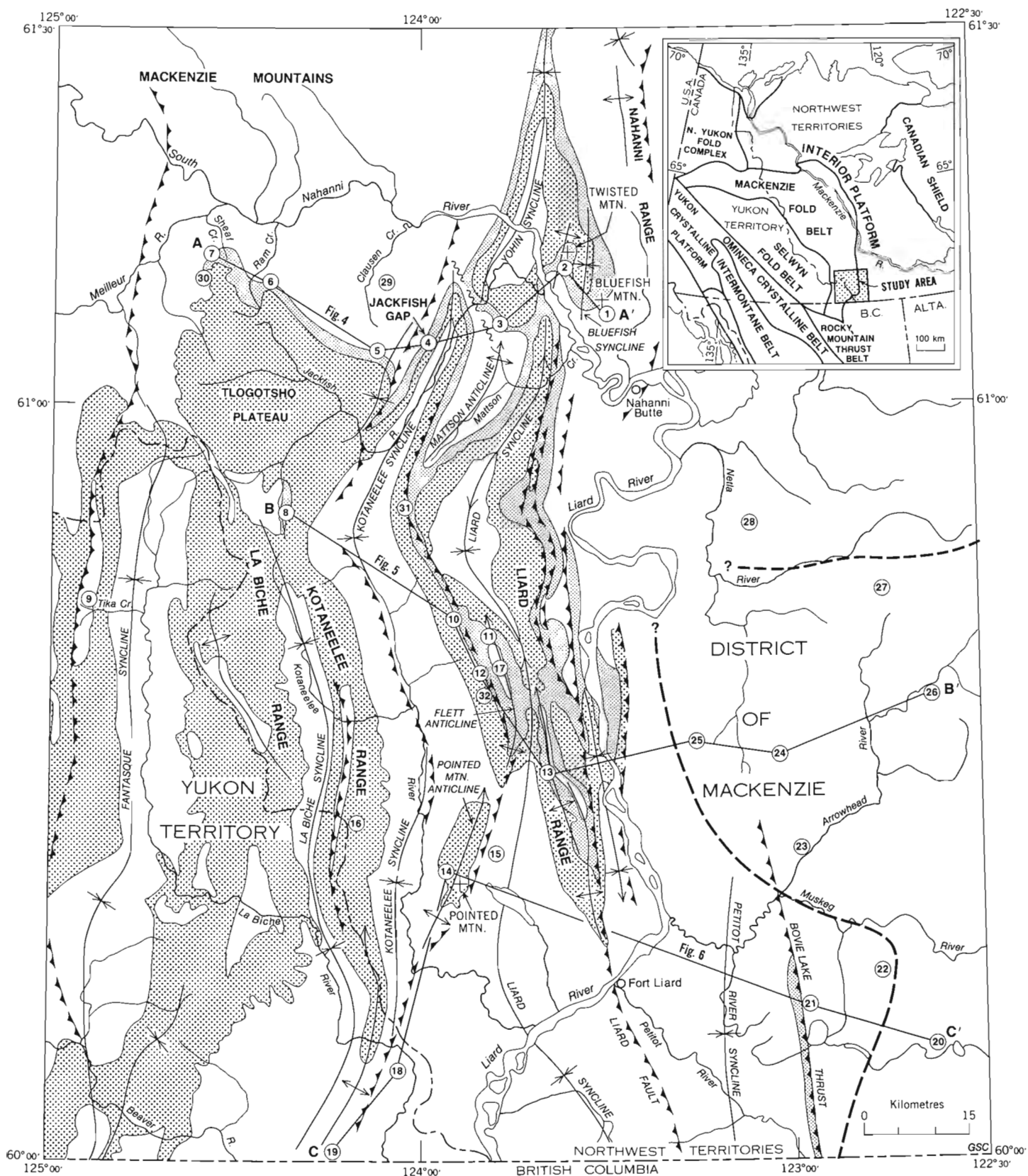



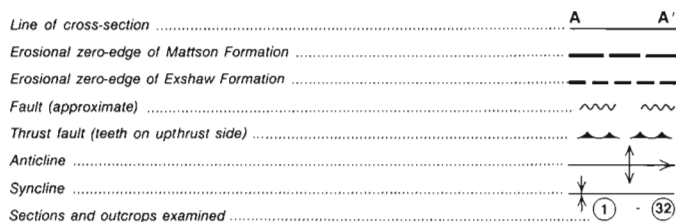
Figure 1. Map of project area showing locations of sections and outcrops studied (geology after Douglas et. al., 1963). Index map illustrates relationship of project area to principal geological elements in northwestern Canada (after Douglas et al., 1970, p. 368).

LEGEND

CARBONIFEROUS

 **PROPHET, FLETT AND GOLATA formations: Carbonates, spiculite and shale**

 **MATTSO FORMATION: Sandstone, siltstone, shale and carbonates**



SURFACE SECTIONS

1. BLUEFISH MOUNTAIN: 61°07'23"N/123°29'13"W, NTS 95 G/3
2. TWISTED MOUNTAIN: 61°11'00"N/123°37'38"W, NTS 95 G/4
3. NORTH END MATTSO ANTICLINE: 61°06'38"N/123°45'54"W, NTS 95 G/4
4. JACKFISH GAP: 61°05'54"N/123°59'26"W, NTS 95 G/4
5. NORTHEAST CORNER TLOGOTSHO PLATEAU: 61°03'55"N/124°07'08"W, NTS 95 F/1
6. RAM CREEK: 61°09'50"N/124°24'47"W, NTS 95 F/1
7. SHEAF CREEK: 61°12'23"N/124°33'32"W, NTS 95 F/2
8. ETANDA LAKES: 60°50'30"N/124°22'01"W, NTS 95 C/16
9. TIKA CREEK: 60°43'47"N/124°53'29"W, NTS 95 C/10
10. CENTRAL LIARD RANGE: 60°45'15"N/123°55'27"W, NTS 95 B/13
11. NORTH END FLETT ANTICLINE: 60°41'20"N/123°48'20"W, NTS 95 B/12
12. WEST FLANK FLETT ANTICLINE: 60°33'50"N/123°48'20"W, NTS 95 B/12
13. SOUTHERN LIARD RANGE: 60°29'46"N/123°38'53"W, NTS 95 B/5

SUBSURFACE SECTIONS

14. PAN AM. A-1 POINTED MTN. P-53: 60°22'46"N/123°54'34"W, NTS 95 B/5
15. AMOCO POINTED MTN. P-24: 60°23'54"N/123°48'57"W, NTS 95 B/5
16. PAN AM. KOTANEELEE Q-67: 60°26'51"N/124°11'56"W, NTS 95 C/8
17. AMOCO FLETT N-19: 60°38'48"N/123°48'07"W, NTS 95 B/12
18. CANADA SOUTHERN ET AL. N. BEAVER R. YT-127: 60°07'N/124°04'W, NTS 95 C/1
19. PAN AM. BEAVER YT Q-01: 60°00'25"N/124°15'48"W, NTS 95 C/1
20. PAN AM. HOME SIGNAL C.S.P. CELIBETA NO. 7: 60°09'25"N/122°37'44"W, NTS 95 B/2
21. TEXACO N.F.A. BOVIE LAKE J-72: 60°11'39"N/122°58'44"W, NTS 95 B/2
22. I.O.E. AMOCO BOVIE M-05: 60°14'46"N/122°46'39"W, NTS 95 B/2
23. B.A. TEXACO ARROWHEAD B-76: 60°25'02"N/122°59'02"W, NTS 95 B/7
24. B.A. TEXACO ARROWHEAD N-2: 60°31'46"N/123°01'18"W, NTS 95 B/11
25. AMOCO B-1 EAST FLETT H-13: 60°32'28"N/123°17'15"W, NTS 95 B/11
26. IMP. SUN ARROWHEAD AURORA M-47: 60°36'54"N/122°38'55"W, NTS 95 B/10
27. IMP. SUN NETLA C-07: 60°46'15"N/122°46'15"W, NTS 95 B/15
28. MURPHY ET AL. NETLA M-31: 60°50'52"N/123°07'15"W, NTS 95 B/14

OTHER OUTCROPS EXAMINED

29. CLAUSEN CREEK: 61°08'01"N/124°02'01"W, NTS 95 F/1
30. NORTHWEST TIP TLOGOTSHO PLATEAU: 61°10'55"N/124°36'14"W, NTS 95 F/2
31. SOUTH END MATTSO ANTICLINE: 60°52'04"N/124°01'58"W, NTS 95 C/16
32. SOUTH END FLETT ANTICLINE: 60°38'04"N/123°49'22"W, NTS 95 B/12

GSC

Underlying and overlying strata

On the interior platform, east of about longitude 123°15'W, the radioactive, brownish black, bituminous to siliceous shale of the widespread Exshaw Formation (Figs. 5, 6) gradationally underlies the Banff Formation. Also, the Exshaw possibly underlies the Banff(?) in the Bluefish Mountain region of the Mackenzie fold belt. According to Pelzer (1966), geochemical methods can be used to identify lithological equivalents of the Exshaw Formation in the Besa River Formation to the west. The Exshaw in much of northeastern British Columbia was deposited at a moderate water depth under anaerobic conditions in an extensive, density stratified basin (Pelzer, 1966, p. 306, 313-315). Moreover, it was probably deposited during a marine transgression (Macqueen and Sandberg, 1970, p. 43; Douglas et al., 1970, p. 399; Griffin, 1967, p. 819; Sandberg and Mapel, 1967; Porter et al., 1982, p. 182). The underlying Kotcho Formation and correlative formations of Famennian age in northeastern British Columbia and southwestern District of Mackenzie were also deposited in transgressive seas (Bassett and Stout, 1967, p. 749; Griffin, 1967, p. 819). The Exshaw in the project area is probably of late Famennian (Devonian) age. During this study, it was determined that palynomorphs of middle Famennian age occur 2 m below the Exshaw, and spores of earliest Tournaisian (Tn1a or early Tn1b) age are 55.5 m above it (Appendix D) in the Imperial Island River No. 1 well (Table 1, Loc. 33), 75.5 km east of the project area.

On the extreme western side of the interior platform and in most of the southern Mackenzie fold belt, shale of Middle to latest Devonian age, in the Besa River Formation, underlies the Carboniferous. The major marine transgression that terminated Devonian, shelf carbonate sedimentation in the region and resulted in deposition of this shale began during the Eifelian (Morrow, 1978).

The formations analysed in this report are overlain by the Mattson Formation (Figs. 7-9) in the southern Mackenzie fold belt and on the southwestern side of the interior platform. In these areas, this formation conformably overlies the Golata and Besa River formations and is of late Viséan (V3) to early Serpukhovian age (Bamber et al., 1980; Appendix E, this report; Richards, 1983a). The Mattson consists mainly of lithofacies that were deposited in deltaic and related environments during several delta cycles (Fig. 7). Using the classification criteria of Galloway (1975), Elliot (1978a), and Fisher et al. (1969, p. 31, 32), the deltas can be classified mainly as fluvial-dominated, wave- and tide-influenced deltas of lobate form. Braided streams of Platte type (Miall, 1977a) dominated the delta plains. Sandstone, and subordinate shale, dolostone, limestone, chert, and coal constitute the Mattson. The sandstone is quartzarenite with subordinate subchertarenite and chertarenite. Most siliciclastic rocks in the Mattson had a northern sedimentary provenance (Bamber et al., 1984, p. 473; Richards, in progress).

Regional unconformities beneath Permian and Lower Cretaceous strata define the upper boundary of the Carboniferous System in the region (Harker, 1963, p. 18; Braman and Hills, 1977; Douglas and Norris, 1976a, b, c) (Fig. 2). Permian strata are present mainly where the Mattson is preserved, but the sub-Permian unconformity cuts down toward the east and overlies older Carboniferous units in small areas on the western side of the interior platform. Similarly, the sub-Cretaceous unconformity cuts down section toward the northeast, where the Cretaceous overlies strata of Late Devonian age (Harker, 1963, p. 18; Douglas and Norris, 1976a, c). On most of the interior platform east of the erosional zero-edge of the Mattson (Fig. 1), strata of

The stratigraphy, sedimentology, and diagenesis of the Besa River, Banff, Yohin, Clausen, Pekisko, Prophet, Flett, and Golata formations and Formation F are discussed herein. Emphasis is on the Yohin, Prophet, and Flett. In view of the existence of Pelzer's (1966) comprehensive report, only the upper Besa River Formation is discussed here. The Pekisko is a relatively thin unit, which occurs mainly in the subsurface, and the only subsurface samples available from it are cuttings. Consequently, it is discussed only briefly. Because it is a subsurface unit that is of only marginal importance to this project and was not cored, Formation F is not discussed separately. The stratigraphic relationships and ages of all these formations are shown on Figure 50, in terms of the carbonate buildups.

SYSTEM	JACKFISH GAP, MACKENZIE FOLD BELT				TWISTED MOUNTAIN, MACKENZIE FOLD BELT		BLUEFISH MOUNTAIN AREA, MACKENZIE FOLD BELT		INTERIOR PLATFORM	ETANDA LAKES, MACKENZIE FOLD BELT	
	This report	Harker, 1961, 1963	Douglas and Norris, 1959	Douglas and Norris, 1960	This report	Harker, 1961, 1963	This report	Douglas and Norris, 1960	This report	This report	Harker, 1961, 1963
CRETACEOUS	FORT ST. JOHN GROUP	FORT ST. JOHN GROUP	FORT ST. JOHN GROUP	FORT ST. JOHN GROUP	FORT ST. JOHN GROUP	FORT ST. JOHN GROUP			FORT ST. JOHN GROUP	FORT ST. JOHN GROUP	FORT ST. JOHN GROUP
PERMIAN									FANTASQUE FM.		
CARBONIFEROUS	MATTSON FORMATION (Type section)	MATTSON FORMATION	MATTSON FORMATION	MATTSON FORMATION	MATTSON FORMATION	MATTSON FORMATION	MATTSON FORMATION	MATTSON FORMATION	MATTSON FORMATION	MATTSON FORMATION	MATTSON FORMATION
	GOLATA FORMATION				GOLATA FORMATION		GOLATA FORMATION		GOLATA FORMATION	GOLATA FORMATION	ETANDA FORMATION
	Meilleur Member (Type section)	FLETT FORMATION (Type section)	Map Unit 7	Map Unit 32	Meilleur Member	FLETT FORMATION	Meilleur Member	Map Unit 32	Meilleur Member	Meilleur Member	PROPHET FORMATION
	Jackfish Gap Mbr. (Type section)				Jackfish Gap Mbr.		Jackfish Gap Mbr.		Jackfish Gap Mbr.	Tlogotsho Member	Base of section
	Tlogotsho Member (Type section)				Tlogotsho Member		Tlogotsho Member		Tlogotsho Member		
	PROPHET FORMATION				PROPHET FORMATION		PROPHET (?) FORMATION		PROPHET FM.		
	CLAUSEN FORMATION (Type section)	CLAUSEN FORMATION	Map Unit 6	Map Unit 31	CLAUSEN FORMATION	FLETT FORMATION	CLAUSEN FORMATION	Map Unit 31	CLAUSEN FM.	PEKISKO FM.	BESA RIVER FORMATION
	YOHIN FORMATION (Type section)	YOHIN FORMATION	Map Unit 5	Map Unit 30	YOHIN FORMATION		YOHIN FORMATION		?		
		Base of section			Base of section				BANFF FORMATION		
	BESA RIVER FORMATION		Map Unit 4	Map Unit 29					EXSHAW FM.		
DEVONIAN							UNNAMED SILTSTONE FORMATION	Map Unit 27	KOTCHO FORMATION		

GSC

Figure 2. Lithostratigraphic units in study area.

Early Cretaceous age disconformably overlies the latest Devonian and the Carboniferous formations discussed here (Figs. 5, 6).

BESA RIVER FORMATION

Type section

Kidd (1963, p. 369-372) proposed the name Besa River Formation and designated its type section, which is at the western edge of the Rocky Mountain Foothills in the core of the Muskwa River anticline. The locality is 1.2 km north of the Muskwa River, in the Kluachesi Lake area (NTS 94 G/13), at latitude 57°57'N, longitude 123°43'W, in northeastern British Columbia.

Previous work in the study area

In the study area, strata that are here assigned to the Besa River Formation have been included previously in

several map units. The Besa River is equivalent to Douglas and Norris's (1959, p. 8-10) Map unit 4 on the Fort Liard and La Biche maps (NTS 95 B and 95 C) and to Map unit 29 of Douglas and Norris (1960, p. 17) in the Virginia Falls map area (NTS 95 F). The Besa River corresponds to the upper part of Map unit Psh of Douglas (1970), which is of possible Ordovician to Early Carboniferous age. Furthermore, most of Map units 3 and 8 of Douglas et al. (1963), and part of the succession that Harker (1961, p. 6, 7; 1963) assigned to the former Etanda Formation in the region west of the axis of the La Biche syncline, belong to the Besa River Formation.

All of the strata that Harker (1961, 1963) and Douglas et al. (1963) assigned to the Etanda were included in the Besa River Formation by Douglas (1976) and Bamber et al. (1980). However, strata that I reassign to the Prophet and Golata formations were included in the Etanda by Harker and Douglas et al. They included the Prophet and Golata equivalents in the Etanda at its type locality (Fig. 1, Loc. 8) and in much of the La Biche syncline to the south.

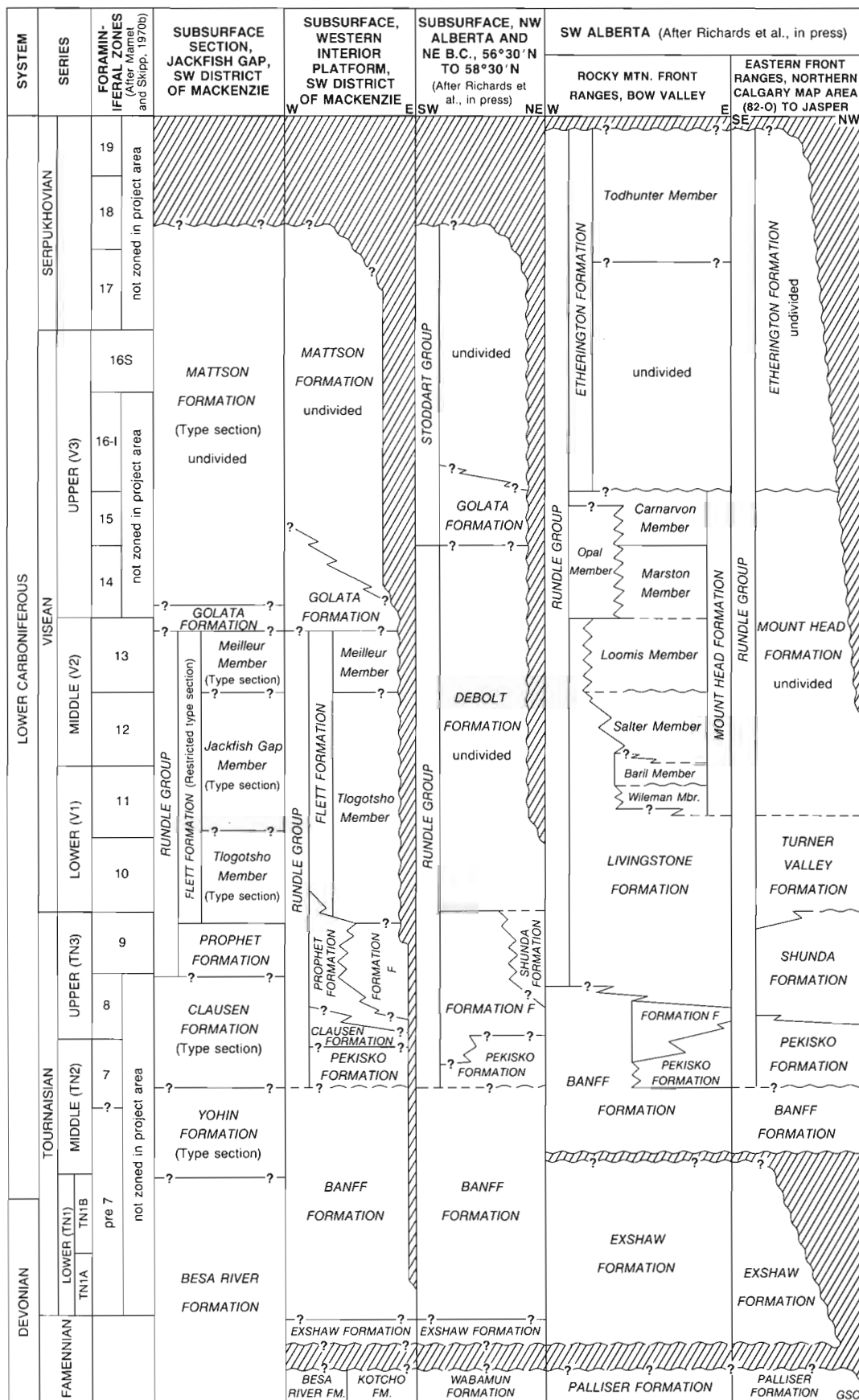


Figure 3. Correlation of Carboniferous lithostratigraphic units with foraminiferal zones of Mamet and Skipp (1970b). Dashed lines indicate nature of contacts uncertain; question marks indicate position of lines uncertain.

TABLE 1

Thicknesses (in metres) of lithostratigraphic units in sections studied. Localities 1 to 28 correspond to localities on Figure 1. Locality 33 is the Imperial Island River No. 1 well (lat. 60°19'29"W, long. 121°08'16"W), NTS 95 A/3, 75.5 km east of the project area, southwestern District of Mackenzie.

Localities	Besa River Formation	Exshaw Formation	Banff Formation	Yohin Formation	Pekisko Formation	Clausen Formation	Prophet Formation	Formation F	Flett Formation	Tlogotsho Mbr. of Flett	Jackfish Gap Mbr. of Flett	Meilleur Mbr. of Flett	Golara Formation	Mattson Formation
1	--	?	413.7 x	81.0	--	P	?	--	P*	P	?	?	--	--
2	?	?	?	129.4 x	--	134.4	44.4	--	280.4	103.3 (?)	79.5	97.6	15.4	274.0
3	P	--	--	46.3 x	--	195.0 (?)	151.5	--	358.1 +	125.2	118.1	114.8 +	P	P
4	P	--	--	157.2 x	--	193.2 (?)	127.0	--	347.3	130.9	80.0	136.4	8.0	1008.7
5	316.0 x	--	--	--	--	--	375.0	--	234.0	--	20.0	214.0	8.5	603.5 *
6	P	--	--	--	--	--	203.6 x	--	--	--	--	--	78.0	P*
7	P	--	--	--	--	--	239.5	--	118.5	--	--	Ur	38.5	P*
8	P	--	--	--	--	--	74.2 x	--	--	--	--	--	518.8	275.0 *
9	25.0 x	--	--	--	--	--	--	--	--	--	--	--	--	1411.8
10	P	--	--	--	--	--	203.7	--	74.5 (?)	--	--	74.5 (?)	23.4	P
11	230.5 x	--	--	--	--	--	204.0 +	--	P	P	--	P	P	P
12	31.0 x	--	--	--	18.0	220.0	280.0	--	246.3	116.5	--	129.8	11.5	P
13	P	--	--	--	?	?	147.2 x	--	291.3 +	149.8	--	141.5	P	P
14	1654.8	--	--	--	--	--	664.8	--	87.5	--	--	87.5	35.9	P
15	P	--	--	--	--	--	P	--	P	--	--	Ur	93.3 x	887.0
16	1271.0	--	--	--	--	--	216.7	--	--	--	--	--	671.8	--
17	P	--	--	--	--	--	--	--	--	--	--	--	--	--
18	931.6	--	--	--	--	--	766.0	--	--	--	--	--	276.5	692.8
19	980.2	--	--	--	--	--	90.5	--	--	--	--	--	1802.3 (?)	393.5 (?)
20	--	11.0	403.6	--	32.6	28.4	99.7	177.7	--	--	--	--	--	--
21	--	15.8	566.0	--	26.8	111.3	224.6	--	312.1	141.7	--	170.4	21.3	--
22	--	P	P	--	P	P	P	?	58.5 x	58.5 x	--	P	31.4	6.1
23	--	13.7	547.1	--	22.0	89.6	72.9	94.2	152.4	103.6	--	48.8	--	--
24	--	15.5	515.1	--	13.4	101.5	44.8	40.2	--	--	--	--	--	--
25	?	?	?	--	P	60.4	165.2	--	285.0	122.5	--	162.5	--	--
26	--	8.5	395.3	--	--	--	--	--	--	--	--	--	--	--
27	--	3.4	--	--	--	--	--	--	--	--	--	--	--	--
28	--	--	--	--	--	--	--	--	--	--	--	--	--	--
33	--	6.7	400.8	--	5.5 (?)	--	--	--	--	--	--	--	--	--

* top removed x base not seen -- absent Ur Flett undivided

+ top not seen P present (?) possibly present or thickness uncertain

Strata that occur along the north side of the Tlogotsho Plateau and are called Besa River here, were assigned to the Yohin and Clausen formations by Harker (1963, p. 7, 9) and Douglas et al. (1963). Because the Clausen in this area resembles formations that underlie the Yohin Formation, the Clausen cannot be distinguished from them unless the Yohin is present. West of the northeastern corner of the Tlogotsho Plateau, the Yohin is absent (Fig. 4). In that area, the unit that Harker and Douglas et al. provisionally assigned to the Yohin (Fig. 11) differs markedly from the type Yohin.

Distribution

The Besa River Formation is widely distributed in northeastern British Columbia, southeastern Yukon Territory, and southwestern District of Mackenzie (Pelzer, 1966; Bamber et al., 1968; Douglas, 1976; Douglas and Norris, 1976a, b, c). In the project area, it occurs throughout most of the Mackenzie fold belt south of the South Nahanni River, and it underlies part of the interior platform west of the Bovie thrust fault. Its present distribution in the western part of the project area was largely determined by post-Early Carboniferous erosion. To the east, however, lithofacies changes and arbitrary boundaries control the distribution of the Besa River (Figs. 5, 6).

Thickness

The Besa River Formation is thickest near its eastern boundary on the extreme western side of the interior platform (Table 1). For example, near the eastern edge of the Liard Range, at Locality 14, the Besa River is 1654.8 m thick, whereas it is 794.0 m thick in the SOBC Shell Beavercrow YT No. 1 well, which is 71 km to the southwest of the project area. The thickest section encountered is at Locality 14, and 30.5 km to the north the Amoco Flett N-19 well (Fig. 1, Loc. 25) intersects a section of similar thickness. Thickness trends in the Besa River are similar in northeastern British Columbia (Pelzer, 1966, p. 276, 301; Bamber et al., 1968, p. 5, 6). According to Pelzer (1966, p. 302, 303), the westward decrease in its thickness is probably depositional instead of erosional.

Lithostratigraphic relationships

In the eastern half of the project area, the Yohin, Pekisko, and Prophet formations conformably overlie and grade westward into the upper Besa River Formation. Also, the Banff, Clausen, and Golata formations are correlative with the upper Besa River, and much of those units form part of the shale lithosome that constitutes most of the Besa River. Arbitrary cutoffs form the boundaries between the Besa River Formation and the Banff, Clausen, and Golata formations (Figs. 4-6). Additional information on the characteristics and approximate geographic locations of the contacts between the Besa River and its eastern correlatives is given in discussions on the lithostratigraphic relationships of the latter.

The Besa River Formation is overlain by the Mattson Formation in the region that is west of the La Biche syncline and southwest of the northern Tlogotsho Plateau (Fig. 7). At most locations, the Mattson/Besa River contact is arbitrarily placed at the base of a resistant sandstone unit and at a level above which the succession is greater than 25 per cent sandstone (Fig. 9). This contact is gradational through several metres or more, and proportions of sand, silt, and sandstone in the Besa River increase toward it. Also, the sandstone of the Mattson intertongues westward with the shale and mudstone of the Besa River. Toward the west, the Mattson/Besa River contact becomes younger.

Lithofacies

In the project area, the upper Besa River Formation comprises a shale and sandstone lithofacies, a spiculite and spicule-lime-packstone lithofacies, and a dark-shale lithofacies.

Shale and sandstone lithofacies

The shale and sandstone lithofacies of the Besa River Formation (Fig. 9), which constitutes the uppermost Besa River west of the La Biche syncline, is a western extension of the dark-shale and the sandstone lithofacies in the Golata. In this region, the younger part of this Besa River lithofacies also underlies and intertongues eastward with delta-slope deposits in the Mattson Formation that consist of sandstone and subordinate shale deposited by sediment gravity flows. The shale and sandstone lithofacies gradationally overlies the dark-shale lithofacies of the Besa River. Widely separated beds of siltstone and sandstone in the shale and sandstone facies distinguish it from the dark-shale lithofacies.

The shale and sandstone lithofacies is mainly shale and mudstone, but beds and laminae of sandstone and siltstone are moderately common, and minor conglomerate is present. The shale and mudstone are greyish black to olive-black, noncalcareous, commonly silty and sandy, and generally devoid of calcareous macrofossils. Much of the shale is highly fissile, whereas the mudstone is friable. The sandstone is siliceous, submature quartzarenite, and muddy, immature quartzarenite, and it is like sandstone in the lower Mattson Formation. In the siltstone, most silt-sized clasts are quartz, and the siltstone varies from siliceous to argillaceous.

Outcrops of the shale and sandstone lithofacies were studied only at Tika Creek (Fig. 1, Loc. 9). There, planar laminae were the only primary sedimentary structures observed in the shale and mudstone. Most beds and laminae of sandstone and siltstone at Tika Creek have sharp bases and vary from massive to internally stratified. Because these sandstone and siltstone deposits are commonly normally graded and comprise two or more components that correspond well to divisions in the standard Bouma sequence (see Bouma, 1962; Middleton and Hampton, 1973), they are interpreted as being mainly turbidites. Units that are less than one metre thick and consist of contorted sandstone turbidites and shale laminae are locally common in the shale and sandstone lithofacies at Tika Creek. Because the deformation was essentially of syndepositional origin, these contorted deposits are considered to be slumps. A massive, ungraded lens of conglomerate, which is 1.5 m thick and has sharp boundaries, was also observed in this facies at this locality. This lens has most characteristics that Middleton and Hampton (1973) considered diagnostic of debris flow deposits and is, therefore, probably of debris flow origin. Evidence of bioturbation is locally present in the shale and sandstone lithofacies.

Dark-shale lithofacies

The dark-shale lithofacies (Fig. 10), which is the best developed facies in the Besa River Formation, constitutes most of the formation in the project area. West of the western depositional limit of the Prophet Formation, the Besa River shale and sandstone lithofacies gradationally overlies the dark-shale facies. To the east, either the Prophet spiculite and spicule-lime-packstone lithofacies (Figs. 10, 35), or the graded-bed lithofacies of the Yohin Formation overlies and grades westward into the dark shales. In much of the region, the dark-shale lithofacies contains widely separated, westward thinning tongues of spiculite and spicule-lime-packstone facies.

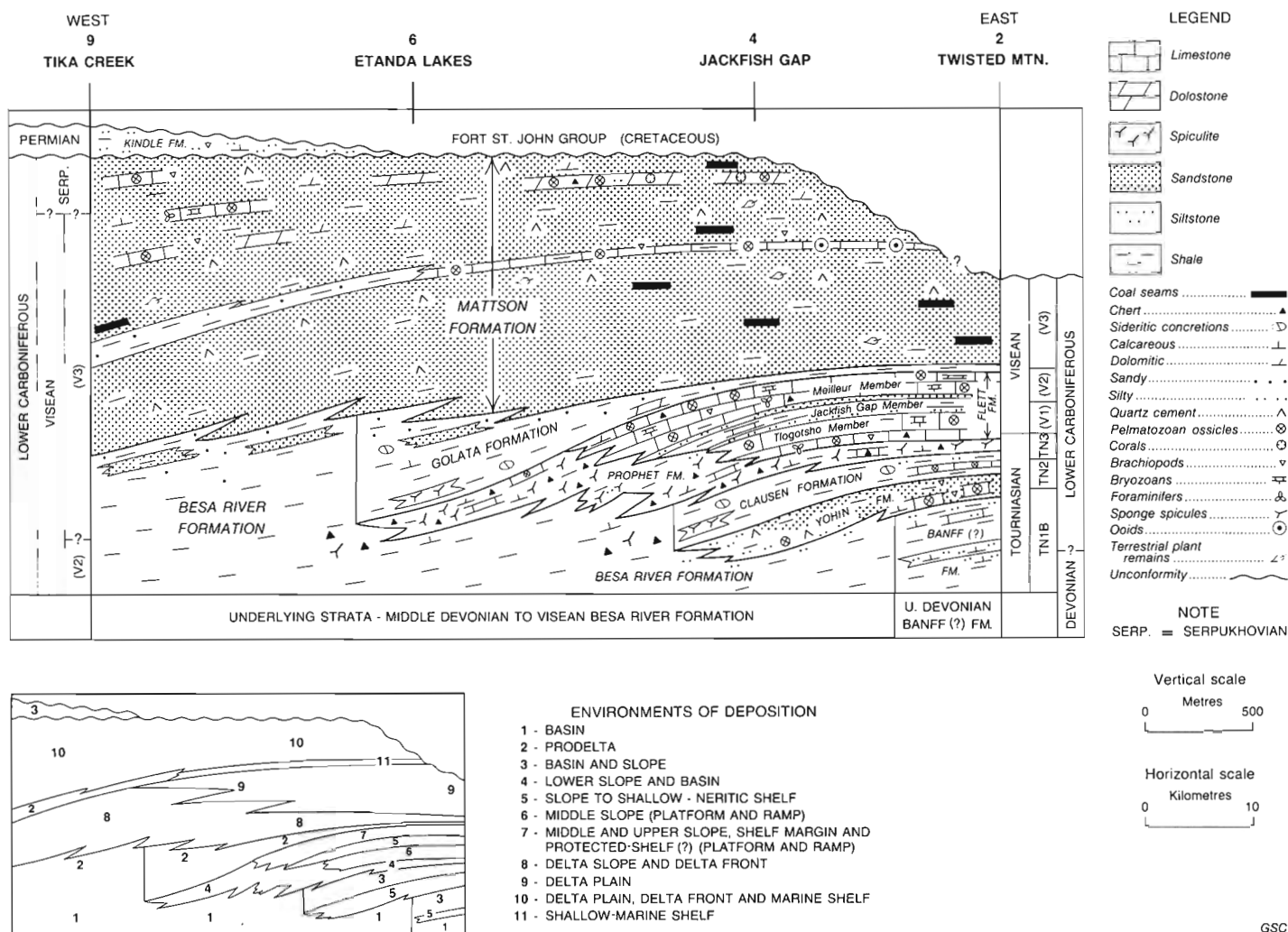


Figure 7. Partly schematic, restored cross-section between Twisted Mountain in southwestern District of Mackenzie, and Tika Creek in southeastern Yukon Territory (Locs. 2 to 9). Figure illustrates relationship of deltaic deposits in the Mattson Formation to deposits in underlying formations.

Most of the dark-shale lithofacies is clay shale, but minor spiculite, spicule lime packstone, and finely crystalline sucrosic dolostone like that in the Prophet Formation (Fig. 36d) occur. The shale is chiefly greyish black to olive-black, highly fissile, siliceous to slightly calcareous and dolomitic, pyritic, and slightly silty. Quartz is the main mineral in the shale (Pelzer, 1966). Sponge spicules are the most common invertebrate remains, and in the uppermost Besa River, they become more abundant toward the basal Prophet. Rare ammonites and bone fragments were also observed.

Units of dark-shale lithofacies are relatively homogeneous, and the diversity of sedimentary structures in them is low. Planar, millimetre-thick laminae, which locally have subtle normal grading, are the main primary sedimentary structures. In the shale, elliptical ironstone concretions, which locally contain macrofossils, are moderately common. Also, lenses of calcite cone-in-cone are locally present. Evidence of bioturbation was not observed in the shale but can be seen in some associated beds and laminae of spiculite and spicule lime packstone.

Spiculite and spicule-lime-packstone lithofacies

Widely separated, westward-thinning tongues of spiculite and spicule-lime-packstone lithofacies (Fig. 11) are intercalated with the dark-shale facies in much of the upper Besa River Formation. These tongues are particularly abundant near the base of the Prophet Formation. Also, many are westward extensions of the spiculite and spicule-lime-packstone lithofacies in the lower Prophet to the east (Fig. 35). This lithofacies in the Besa River is best developed along the north side of the Tlogotsho Plateau, where it occurs as a unit that is 43 m thick, and 200 m or more below the Prophet (Fig. 4).

The spiculite and spicule-lime-packstone lithofacies consists mainly of resistant intervals of dark coloured spiculite and spicule-lime-packstone. Finely crystalline dolostone, bedded chert (Fig. 12), and bryozoan-pelmatozoan lime packstone occur locally.



Figure 8. Type section of the Mattson Formation at Jackfish Gap. Arrow indicates top of Golata Formation (8 m thick) and base of Mattson. The Flett Formation underlies the dark, recessive Golata. ISPG 1281-3.



Figure 9. Upper Besa River Formation and basal Mattson (arrow) at Tika Creek. The Besa River consists of prodelta shale and siltstone. The Mattson is delta-slope sandstone, and contains an erosion surface of a submarine channel. Upper cliff is 6 m high. ISPG 798-26.



Figure 10. Dark-shale lithofacies of upper Besa River Formation, overlain by upper Tournaisian (Tn3) carbonate-platform deposits in the Prophet Formation (204 m thick, arrow points to contact) at Locality 11. The Prophet is mainly spiculite and spicule-lime-packstone lithofacies. ISPG 1764-4.



Figure 11. Units (43 m thick) of spiculite and spicule-lime-packstone lithofacies in the upper Besa River Formation at Locality 5. Flett Formation in background. ISPG 1756-109.

The spiculite and spicule-lime-packstone lithofacies occurs mainly as moderately resistant, thinly laminated to thin bedded units, that are generally less than 40 m thick, have gradational bases, and become more resistant upward. Most of these units consist mainly of planar, millimetre-thick laminae that have sharp to gradational bases and subtle normal grading. The origin of these laminae is discussed in the section on environmental interpretations. Some units contain abundant sharp-based beds and thick laminae that are normally graded and internally stratified (Fig. 12). Platy, bioturbated deposits, of uncertain origin, and rare, sharp-based, massive beds are also present.

The sharp-based graded beds and thick laminae are interpreted as being mainly turbidites, because they generally have two or more components that correspond well to divisions in the standard sequence of Bouma (1962). Planar, millimetre-thick laminae are the most abundant sedimentary structure in the turbidites, but small-scale crossbedding occurs locally. These turbidites generally lack equivalents of the Bouma A and B divisions.

At Locality 5, a one metre thick, massive limestone bed with a sharp base, sharp undulous top, chaotic internal fabric, and numerous pebble-sized intraclasts is present at the top of a unit within this lithofacies. This bed has most of the characteristics that Middleton and Hampton (1973) and Lowe (1979) considered diagnostic of debris flow deposits. It is, therefore, considered to be of debris flow origin.

Environmental interpretations

Shale and sandstone lithofacies

Deposition in the poorly oxygenated water of the dysaerobic zone (Byers, 1977, p. 9) of a prodelta setting is suggested for the shale and sandstone lithofacies. Prodelta deposits are the first terrigenous sediment that a prograding



Figure 12. Polished slab of distal, spiculitic, chert turbidites (GSC loc. C-59103) from upper Besa River Formation at Ram Creek. ISPG 1766-12.



Figure 13. The Banff(?) and Yohin formations at Bluefish Mountain. About 41 m of Yohin are visible (arrow indicates its base). The Banff(?) is mainly dark-shale lithofacies. ISPG 798-78.

delta introduces into a basin (Fisher et al., 1969, p. 18). The shale and sandstone facies in the Besa River Formation conforms with this criterion, because this facies is transitional between delta-slope deposits (Fig. 9) in the overlying Mattson Formation and underlying lithofacies deposited basinward of carbonate buildups (mainly platform deposits). Dark coloured, carbonaceous shale and mudstone, which lack calcareous epifaunal remains, constitute most of this lithofacies and, according to Fisher et al. (1969, p. 18, 19), this is typical of prodelta deposits. Toward the west and the axis of the paleobasin, the age range of the Besa River increases, whereas the formation thins markedly (Pelzer, 1966). Consequently, the shale and sandstone facies was probably deposited on a clinoform, which had a low gradient. Deposition on a clinoform is also indicated by the local presence of syndepositionally deformed turbidites. Finally, because the sediments were locally bioturbated and generally lack evidence of a calcareous epifauna, this lithofacies was deposited, at least partly, in the dysaerobic zone.

Dark-shale lithofacies

The dark-shale lithofacies of the Besa River Formation was deposited in the dysaerobic zone and at moderate water depths in the axial region of an extensive trough-shaped basin. Deposition in the dysaerobic zone is indicated by the local occurrence of bioturbated deposits and general lack of an indigenous calcareous epifauna. Sedimentation in a moderately deep-water basin environment is recorded by the lithology and sedimentary structures of the dark-shale lithofacies and by its spatial relationship to carbonate-platform and deltaic deposits (Figs. 7, 50, 87a). The marked westward (basinward) decrease in the thickness of the Besa River Formation, with a corresponding increase in its age range, indicates that much of the formation and this lithofacies were deposited under starved-basin conditions. Moreover, the westward depositional thinning suggests that the shale of the Besa River was locally deposited at water depths of 760 m or more (Pelzer, 1966).

The depositional origin of most deposits in the dark-shale lithofacies is uncertain, but they possibly resulted from a combination of hemipelagic sedimentation and deposition from dilute, gravity assisted suspension currents. Hemipelagic sedimentation appears to be important in many basins (Jenkyne, 1978; Rupke, 1975; Rupke and Stanley, 1974). Chough and Hesse (1980), Stow and Shanmugam (1980), and others have demonstrated that dilute turbidity currents are important in depositing siliciclastic mud in basins. Deposition by nepheloid-layer flow (Ewing and Thorndike, 1965; Stanley and Unrug, 1972, p. 295) may also be significant in basins.

Spiculite and spicule-lime-packstone lithofacies

Regional lithofacies trends and characteristics of the spiculite and spicule-lime-packstone lithofacies indicate that it was deposited as slope-related tongues in a shale basin. Intervals of this facies are interpreted as mainly basinward-thinning tongues of slope-derived material, because of their similarity and spatial relationship to the Prophet spiculite and spicule-lime-packstone lithofacies, which was deposited largely on the lower slopes of carbonate platforms (Fig. 87a). Also, these intervals in the Besa River Formation are intercalated with westward thickening tongues of the dark-shale lithofacies.

I tentatively interpret the millimetre-thick laminae, which constitute most of the spiculite and spicule-lime-packstone lithofacies, as deposits produced by either dilute

turbidity currents, hemipelagic sedimentation, or a combination of these processes. Dilute, distal turbidity currents probably formed some of these laminae, because these deposits occur with turbidites and either underlie or lie basinward of turbidite-bearing facies. Intervals of this lithofacies were deposited in a deeper water setting basinward of carbonate buildups (Fig. 87). Hemipelagic deposits commonly form broad aprons of fine grained sediment basinward of such buildups. Also, hemipelagic processes produce laminae, like those in this lithofacies, in bottom environments that lack abundant burrowing organisms.

Age

The Besa River Formation ranges in age from Middle Devonian to late Viséan (V3), and it has diachronous upper and lower boundaries (Bamber and Marnet, 1978, p. 7, 8). Fossils from the upper Besa River and directly overlying beds were commonly not suitable for precise dating, but they were sufficient to indicate that the upper boundary of the Besa River ranges in age from early Tournaisian (Tn1) in the east to late Viséan (V3) in the west. The coral *Vesiculophyllum* sp. of probable middle to late Tournaisian age (Tn2 to Tn3) and microfossils of Tournaisian age (Appendices A, B) were collected from the overlying Pekisko Formation in the Liard Range (Fig. 1, Loc. 12). Assemblages of conodonts and palynomorphs (Appendices C, E) indicate that most of the overlying Yohin Formation is of early and middle Tournaisian age (Tn1 and Tn2). Finally, at Tika Creek (Fig. 1, Loc. 9), palynomorphs that probably represent the Densospore Zone (Braman and Hills, 1977) of late Viséan (V3) age were collected from the uppermost Besa River and basal Mattson Formation (Richards, 1983a, Appendix D; Barss, pers. comm., 1977).

BANFF FORMATION

Type section

Kindle (1924) proposed the name Banff Formation. Its type section, established and described by Warren (1927), is at the north end of Mount Rundle, in the Canmore map area (NTS 82 O/3W), of southwestern Alberta (Macqueen and Bamber, 1967, p. 1).

Previous work in the study area

Walton and Mason (1967, p. 155) and de Wit et al. (1973, p. 196) indicated that the Banff was present on the interior platform north of 60°00'N. Douglas and Norris (1976c) assigned a unit on the interior platform to the Banff Formation, and I have accepted this unit as the Banff (Figs. 5, 6).

An interval in the Bluefish and Yohin synclines that I tentatively reassign to the Banff Formation (Fig. 4, Bluefish Mountain section, 0.0–413.7 m) comprises three units that have been variously assigned to the Yohin and Clausen formations and to informal map units (Fig. 2). Douglas and Norris (1976c, Map unit UDsh) included the interval between 0.0 and 150.9 m in an unnamed shale and mudstone unit at Bluefish Mountain. Earlier, Douglas and Norris (1960, p. 17) assigned the same 150.9 m thick unit to Map unit 28, and Harker (1963, p. 60, Units 1 to 3) tentatively assigned it to the Yohin. Also, Harker (1963, p. 7; p. 60 Unit 4) provisionally assigned to the Yohin at Bluefish Mountain the

siltstone and sandstone unit that occurs between 150.9 and 206.4 m in the Banff(?) Formation (Figs. 15, 20) of this report. Douglas and Norris (1960, p. 17) assigned the same siltstone and sandstone unit to Map unit 30, and Douglas and Norris (1976c) mapped it as Yohin in the Bluefish and Yohin synclines. Finally, Harker (1963, p. 9, 60, 61) assigned to the Clausen Formation the shale and limestone unit that occurs between 206.4 and 413.7 m in the Banff(?) at Bluefish Mountain (Fig. 13). Douglas and Norris (1960, p. 18) assigned this third unit to Map unit 31 in the Bluefish Mountain region, and Douglas and Norris (1976c) mapped it as Clausen.

The unit in the Bluefish and Yohin synclines (Fig. 4, Loc. 1, 0.0-413.7 m) is provisionally assigned to the Banff because it is the lithological and stratigraphic equivalent of only the lower two thirds of the Banff on the interior platform. Deposits that are stratigraphically equivalent to the upper Banff on the platform are assigned to the Yohin Formation in this area.

Distribution

The Banff Formation of the project area occurs mainly on the interior platform south of latitude 60°50'N (Figs. 5, 6). In the Mackenzie fold belt, strata that I tentatively assign to this formation occur in the Bluefish and Yohin synclines (Fig. 4), and possibly at the north end of the Mattson anticline. In addition, the Banff is preserved east of the project area, and this formation is widespread in northeastern British Columbia and Alberta (see Macauley et al., 1964, p. 93, 94). North of 60°00'N, the western boundary of the Banff generally coincides with that of the underlying Exshaw Formation. South of 60°50'N this boundary is on the platform between the longitude of the Bovie Lake thrust fault and the Liard Range (Douglas and Norris, 1976a). In the Bluefish Mountain area, the western limit of the Banff(?) coincides with that of the underlying unnamed Devonian siltstone unit (Fig. 2).

Thickness

North of 60°00'N, the thickness of the Banff Formation is moderately variable (Figs. 5, 6; Table 1). Where strata of Carboniferous age overlie it on the interior platform, the Banff thickens quite rapidly westward. For example, it thickens from 403.6 m at Locality 20 to 566.0 m at Locality 21, which is 20.5 km farther west. North of the sub-Cretaceous, erosional zero-edge of overlying Carboniferous formations, the thickness of the Banff decreases fairly rapidly to zero. Over the Celibeta high (de Wit et al., 1973, p. 200), which is an elevated, triangular fault block immediately east of Locality 20, the Banff thins abruptly and is overlain by deposits that are of Cretaceous and possibly Quaternary age.

Lithostratigraphic relationships

Throughout the project area, the Banff Formation conformably overlies the Exshaw Formation. The contact is gradational, and at most localities the Exshaw grades into the Banff through an interval of one metre or more. An upward transition from brownish black, bituminous or siliceous shale to medium-dark grey, nonbituminous shale is characteristic. In addition, the shale becomes markedly less radioactive upward (Figs. 5, 6).

Toward the west, the shale of the Banff Formation merges laterally with that of the Besa River Formation (Figs. 5, 6). The boundary between these units is an arbitrary

cutoff that coincides with the western limit of the Exshaw (Douglas and Norris, 1976a). The Exshaw serves to separate Banff shale from an underlying shale succession of Late Devonian age on the extreme western side of the interior platform. The western limit of the Exshaw is at a location beyond which its equivalents cannot be readily differentiated from underlying and overlying shales without using geochemical methods or gamma ray logs.

On the interior platform of the project area, the Banff is overlain either by the Lower Cretaceous Fort Saint John Group (Douglas and Norris, 1976a), or by limestone and subordinate shale of the Pekisko Formation. Cretaceous strata disconformably overlie the Banff in most of the region north of latitude 60°35'N. Over wide areas of southwestern Alberta and east-central British Columbia, the Banff-Pekisko contact is a minor erosional disconformity (Richards, et al., in press). In the project area, the contact between the Banff and Pekisko is also generally abrupt and, therefore, possibly erosional and disconformable (Figs. 5, 6). It coincides with the base of a moderately resistant transgressive unit comprising locally oolitic, bryozoan-pelmatozoan lime grainstone and packstone with subordinate shale. Beds of siliciclastic siltstone and sandstone are common in the uppermost Banff, but they do not occur in the overlying Pekisko. Moreover, the upper boundary of the Banff coincides with prominent inflections on gamma ray and sonic logs.

In the Bluefish and Yohin synclines, a unit that I tentatively assign to the Banff Formation is conformably overlain by the Yohin Formation. However, the contact between the Banff(?) and Yohin in that region is well exposed only at Bluefish Mountain (Figs. 4, 13), where it is gradational and placed at the base of the first resistant bed above 62.5 m of shale. The shale in the upper 13 m of the Banff at Bluefish Mountain becomes increasingly silty upward and contains numerous thin lenses of siltstone and silty limestone. Above the Banff(?) / Yohin contact at that locality, sandstone, siltstone, and limestone predominate.

The Banff Formation in the project area is probably divisible into formal members but no formal subdivision is attempted in this paper because of insufficient data. On the interior platform, it could be divisible into a lower member, which is mainly shale, and an upper member comprising interbedded shale, sandstone, siltstone, and limestone (Figs. 5, 6). The upper member is lithologically similar to the Yohin Formation, occurs at the same lithostratigraphic position, and is of similar age (middle Tournaisian, Tn2). In the Bluefish Mountain area, the Banff(?) comprises a lower shale unit, a middle unit consisting mainly of sandstone and siltstone (Fig. 15), and an upper shale-dominated unit (Figs. 4, 13).

Lithofacies

A dark-shale lithofacies (Fig. 13) together with a limestone and siltstone lithofacies (Fig. 15) constitute the Banff Formation in the project area.

Dark-shale lithofacies

The dark-shale lithofacies (Fig. 13) constitutes most of the Banff Formation in the project area. Units of this lithofacies are eastward-thinning tongues of the lithosome that constitutes most of the Besa River Formation. On the interior platform of the study area, the dark-shale lithofacies makes up approximately the lower two thirds of the formation, but in the Imperial Island River No. 1 well,

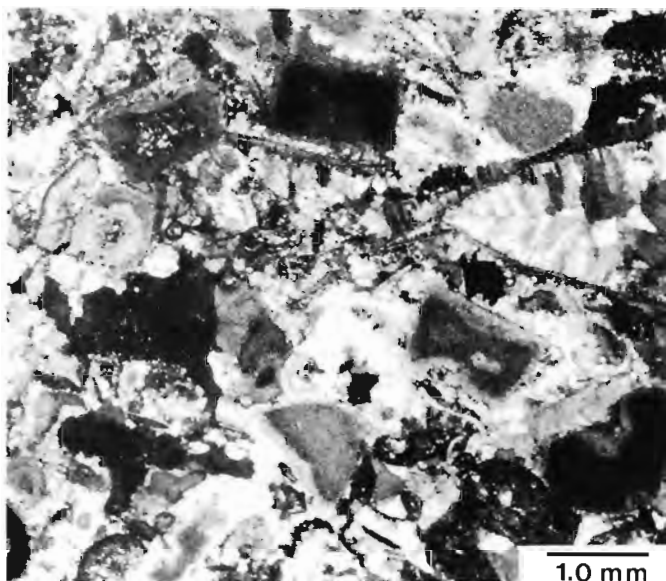


Figure 14. Photomicrograph of pelmatozoan lime grainstone (GSC loc. C-52283) from the dark-shale lithofacies in the Banff(?) Formation at Bluefish Mountain. Bladed fringe cement is present in a brachiopod (upper right); pelmatozoan fragments have monocrystalline syntaxial overgrowths. ISPG 1768-15.



Figure 16. Silty, spiculitic limestone and mudstone in the limestone and siltstone lithofacies of the upper Banff(?) Formation at Bluefish Mountain. Resistant beds resemble turbidites. Jacob's staff in lower left-hand corner is 1.5 m long. ISPG 1756-81.



Figure 15. Limestone and siltstone lithofacies in the middle Banff(?) Formation at Bluefish Mountain. Outcrop shown is the upper three quarters of a 55 m thick, coarsening-upward sequence. ISPG 1764-5.

75.5 km east of the project area, it constitutes only the lower half of the Banff. With the exception of widely separated, resistant units of siltstone (Fig. 15) and silty limestone (Fig. 16), this lithofacies forms most of the Banff(?) in the Bluefish and Yohin synclines (Figs. 1, 4; Loc. 1).

Thick units of shale constitute most of the dark-shale lithofacies (Fig. 13), but locally they contain mudstone and minor siltstone, and skeletal limestone (Fig. 14). The shale and mudstone are medium dark grey, slightly calcareous to noncalcareous, locally silty, slightly pyritic, and sparsely fossiliferous. Planar to wavy, thin laminae are the main sedimentary structures in the shale, but ellipsoidal ironstone concretions are locally common. Lenses, laminae, and thin beds of silty limestone and fossiliferous siltstone are locally present in the shale units. Some of these limestone and siltstone deposits resemble turbidites, because they have sharp bases, subtle normal grading, and two or more components that correspond reasonably well to divisions in the standard Bouma sequence. At Bluefish Mountain, abundant brachiopods, which lack evidence of substantial transport, occur in some thin, nodular limestone beds.

The proportion of silt and the number of lenses to thin beds of siltstone and silty limestone increase upward in units of Banff dark-shale lithofacies that occur near the base of the Yohin Formation. Also, a similar increase in silt content occurs in the dark-shale lithofacies below the thick unit of limestone and siltstone lithofacies in the Banff(?) Formation at Bluefish Mountain. It is apparent, therefore, that units of the dark-shale lithofacies, together with either the lithofacies in the Yohin or units of limestone and siltstone lithofacies in the Banff, form well developed sequences that become coarser grained and more proximal in aspect upward (Fig. 13).

Limestone and siltstone lithofacies

The limestone and siltstone lithofacies forms approximately the upper third of the Banff Formation on the interior platform of the project area, and it occurs as widely separated, resistant units in the Bluefish and Yohin synclines (Figs. 15, 16). It forms westward- and southwestward-thinning sheets that overlie and grade downward into the dark-shale lithofacies of the Banff. For example, in the

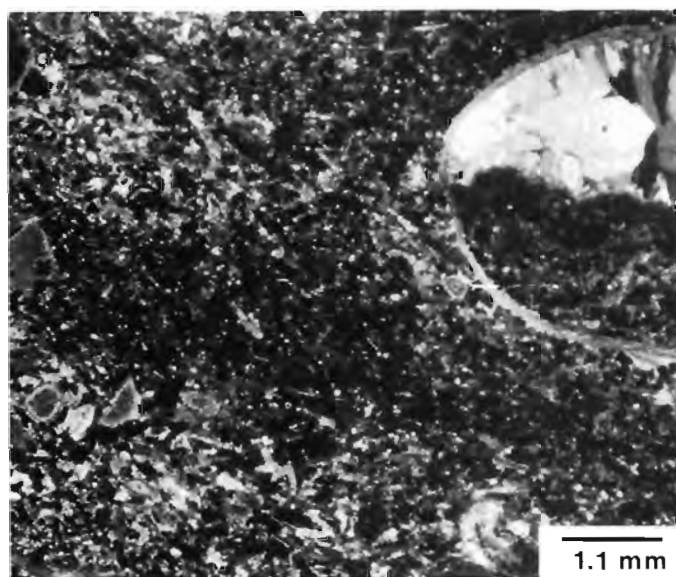


Figure 17. Photomicrograph of silty, pellet-skeletal lime packstone (GSC loc. C-82856D, 749.2 m/2458 ft) from upper Banff Formation, 100 m (328 ft) below top, in the Imperial Island River No. 1 well. Bladed, polycrystalline calcite cement is present in brachiopod. ISPG 1768-18.

Imperial Island River No. 1 well (on the interior platform 75.5 km east of the project area), this lithofacies constitutes the upper 207 m of the formation, but on the interior platform in the project area, this lithofacies generally forms less than the upper 75 m of the Banff. Thick intervals of dark-shale lithofacies overlie units of the limestone and siltstone lithofacies at Bluefish Mountain. On much of the interior platform, skeletal limestone of shallow water aspect, which constitutes the Pekisko Formation, overlies the limestone and siltstone lithofacies in the upper Banff.

Limestone (Figs. 16, 17) with subordinate mudstone, sandstone (Fig. 18), siltstone, and shale constitute the limestone and siltstone lithofacies. At Bluefish Mountain siltstone is predominant. Although limestone predominates at most locations on the interior platform, both within and east of the project area, many beds are sandstone and siltstone. Also, proportions of sandstone and siltstone increase to the north in this area. Most of the sandstone and siltstone is texturally submature to mature subchertarenite, which is light olive-grey, greyish orange weathering, very calcareous, and fossiliferous. The sandstone is mostly very fine to fine grained and commonly grades into limestone and siltstone. Most of the limestone is silty to sandy lime packstone (Fig. 17) and wackestone with subordinate grainstone. Sponge spicules, calcareous algae, pelmatozoan ossicles, brachiopods, intraclasts, ostracods, and peloids are the principal allochems and commonly occur in subequal proportions. Minor coarse crystalline, ferroan dolomite is present in some limestone. Diagenetic chert is also a minor component. The shale and mudstone are mainly medium dark grey to dark greenish grey, silty and calcareous.

Polycrystalline, equant to bladed, fringe cement, and pore-filling mosaics of subequant crystals (Fig. 17) are the principal sparry calcite cement fabrics in the limestone. Much of this cement is strongly ferroan. For reasons similar to those given below, in the section on diagenetic calcite in the Yohin Formation, solutions in Folk's (1973; 1974a, p. 45, 51) meteoric-phreatic and subsurface precipitational environments (Fig. 19) are interpreted as having formed most of this cement.

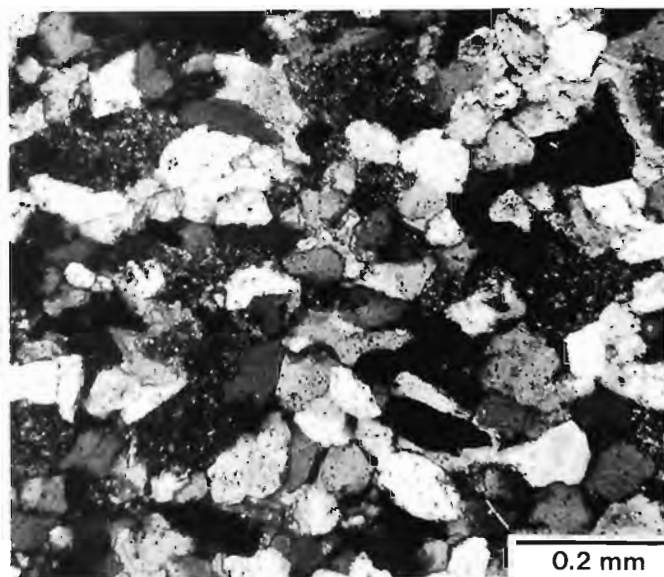


Figure 18. Photomicrograph of very fine sandstone: calcareous, mature subchertarenite (GSC loc. C-82856A, 652.3 m/2140 ft). Sample is from the upper Banff Formation, 3.4 m (11 ft) below top, in the Imperial Island River No. 1 well. ISPG 2026-7.

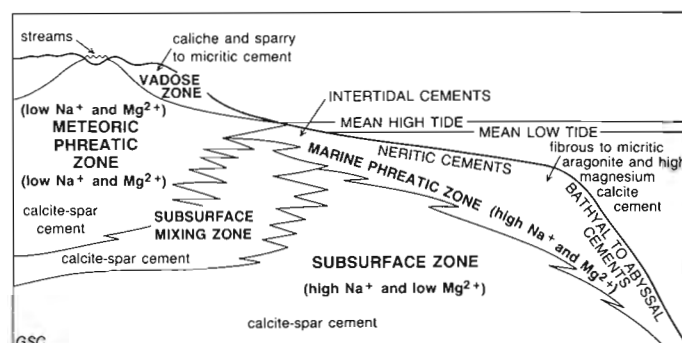


Figure 19. Carbonate diagenetic environments (after Folk, 1974a, Fig. 5).

On the interior platform, in the project area and the region to the east, the limestone and siltstone lithofacies in the upper Banff occurs as a well bedded, cyclic succession similar to that of the Yohin Formation at Bluefish and Twisted mountains. Well samples, and the highly serrated patterns on corresponding gamma ray logs (Figs. 5, 6), indicate that these deposits are well bedded and consist of shale closely interbedded with medium to thin bedded (3-30 cm) limestone, sandstone and siltstone. In addition, the gamma ray profiles indicate that sections of this lithofacies comprise four main styles of multibed sequence: sharp-based sequences, which become less resistant and finer grained upward; sequences that have gradational bases and become coarser and more resistant upward; symmetrical sequences, which are most resistant near their middle; and sequences with sharp tops and bases.

Evidence from a limited amount of core suggests that nodular beds, internally disorganized to graded massive beds, and planar-laminated to crossbedded beds and laminae

constitute much of the limestone and siltstone lithofacies in the upper Banff on the interior platform. The distribution of these deposits in this area is uncertain because north of latitude 60°00'N this lithofacies was cored only in the Imperial Island River No. 1 well.

Thin nodular beds, poorly graded massive beds, and massive beds that have a random internal fabric are common in a 6 m thick interval that was cored about 97 m below the top of the Banff in the above well. The thin beds generally have sharp bases with load casts. They comprise silty, intraclast-rich, fossiliferous limestone, and are either separated by or grade upward into calcareous mudstone. Because they have sharp bases, a basal component that is like the Bouma A division, and an upper component that resembles the Bouma D and E divisions, the graded beds are possibly turbidites. The massive beds that have a disorganized internal fabric commonly have sharp tops and are similar to thin debris flow deposits. Both the graded beds and the massive beds, however, also resemble some tempestites.

Some small-scale crossbedding produced by normal traction currents is present in the limestone and siltstone lithofacies of the upper Banff on the interior platform. Part of a core that was taken from the upper 50 m of this lithofacies in the Imperial Island River No. 1 well, includes intraclast-bearing, glauconitic sandstone containing localized small-scale crossbedding. The crossbedding is not climbing-ripple crossbedding, which is common in turbidites (see Jopling and Walker, 1968). Instead, it is like crossbedding formed by traction currents without significant fallout from suspension. Similar crossbedding is common in shallow marine deposits.

At Bluefish Mountain, the limestone and siltstone lithofacies is preserved mainly in the middle Banff(?) Formation (Fig. 4), where it forms a thick, multibed coarsening-upward sequence (Figs. 15, 20). This sequence, which is about 56 m thick, is laminated to thick bedded and comprises calcareous siltstone and very fine grained sandstone with subordinate shale and limestone. Much of its lower part contains graded beds and laminae that resemble turbidites and some tempestites. These beds and laminae have sharp bases and two or more components that are similar to divisions in the standard Bouma sequence (Fig. 21). The remainder of the sequence consists of mainly medium bedded, bioturbated, and locally crossbedded deposits. However, approximately the upper 3 to 5 m of the sequence are planar-stratified beds of very fine grained, well sorted sandstone that are locally separated by beds containing small-scale crossbedding (Fig. 22). A prominent, undulous scour surface locally separates the interval containing horizontal stratification from the underlying bioturbated and crossbedded deposits.

Elsewhere in the Bluefish Mountain section, the limestone and siltstone lithofacies comprises resistant thin to medium bedded units of rhythmically interbedded shale and silty limestone. The limestone beds, which are internally massive to stratified, have sharp bases and resemble sediment-gravity-flow deposits (Fig. 16).

Environmental interpretations

Dark-shale lithofacies

The dark-shale lithofacies of the Banff Formation is interpreted as having been deposited chiefly below wave base in the relatively poorly oxygenated water of an extensive northwest-trending basin that extended into northeastern

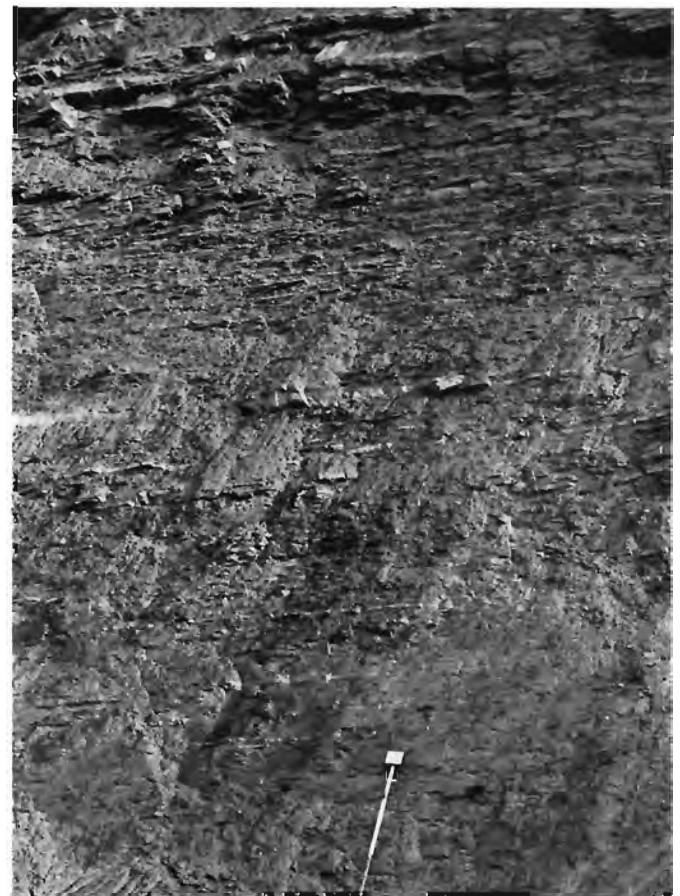


Figure 20. Basal siltstone and mudstone of the 55 m thick, coarsening-upward sequence, which constitutes the middle Banff(?) Formation at Bluefish Mountain (1.5 m scale). ISPG 1756-76.

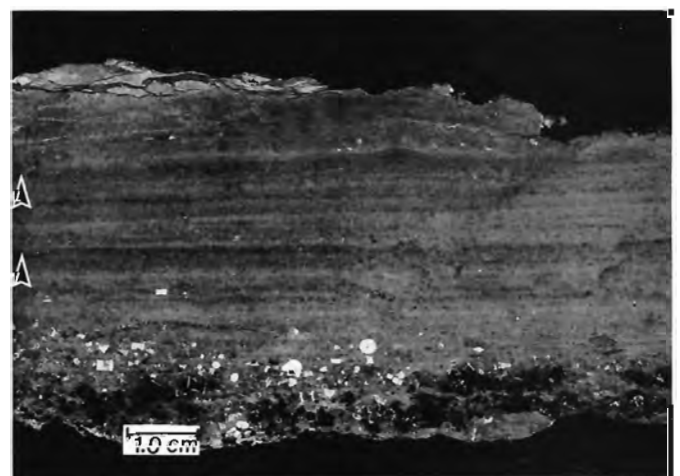


Figure 21. Polished slab of graded, turbidite-like beds of fossiliferous siltstone (GSC loc. C-58525) from the limestone and siltstone lithofacies in the middle Banff(?) Formation at Bluefish Mountain. Arrows indicate tops of thin graded beds. ISPG 1766-9.



Figure 22. Planar stratified, very fine grained, shallow-neritic sandstone in the limestone and siltstone lithofacies of the middle Banff(?) Formation at Bluefish Mountain (vertical bar is 10 cm long). Small-scale crossbedding also is present (arrow). ISPG 1764-6.

British Columbia. Deposition in a basin is indicated by the spatial relationship of the facies to regional lithofacies belts. In the basal Banff, this lithofacies gradationally overlies the black shale of the Exshaw Formation, which was deposited under anaerobic basin conditions (Pelzer, 1966) during a regional transgression. Furthermore, the dark-shale facies occurs as eastward- or landward-thinning tongues of the shale lithosome that constitutes most of the Besa River Formation. The Besa River is mainly basal shale that was deposited in moderately deep water (Pelzer, 1966, p. 306). Overlying lithofacies are of more proximal aspect, but they contain deposits that resemble turbidites and tempestites and form eastward- or landward-thickening units. The dark-shale lithofacies is mainly dark coloured, pyritic, thinly laminated shale, which generally contains impoverished assemblages of calcareous benthos and little evidence of intense bioturbation. Byers (1977) suggested that lithofacies of this type are commonly formed in relatively poorly oxygenated, dysaerobic basin environments. Most of this lithofacies was probably deposited below wave base because the shale is characteristic of that deposited in poorly oxygenated water. Moreover, turbidite-like beds that possibly would have been reworked had they been deposited above wave base are locally associated with it.

The transgression that occurred during deposition of the Exshaw possibly continued during deposition of the dark-shale lithofacies in the basal Banff; however, no conclusive evidence for this is available. Because most of the thick units of this lithofacies grade up into either the regressive Yohin deposits (Fig. 13) or the limestone and siltstone lithofacies in the upper Banff, water depths probably decreased during at least the late depositional stages of these thick units.

Limestone and siltstone lithofacies

Deposition under shoaling-upward conditions on a broad marine shelf that was inclined gently westward or southwestward is suggested for most of the limestone and

siltstone lithofacies on the interior platform. Limited evidence from well core (from the Imperial Island River No. 1 well) demonstrates that this lithofacies in the upper Banff constitutes the upper part of a coarsening- and shoaling-upward succession. Characteristics of the core indicate that this facies is more proximal in aspect than underlying shale deposits in the Banff. They also indicate that the limestone and siltstone lithofacies at least locally comprises intervals that have tempestite- and turbidite-like beds and are overlain by crossbedded strata of shallower marine aspect. The presence of ooid-bearing lime grainstone of shallow water aspect in the overlying Pekisko Formation provides additional evidence of deposition under shoaling-upward conditions. Moreover, most of the Banff in Alberta and much of northeastern British Columbia was deposited under shoaling-upward conditions and commonly contains peritidal and supratidal deposits in its upper part (Richards et al., in press; Morin, 1981; Chatellier, 1983). A combination of increased siliciclastic influx and a possible reduced tectonic subsidence rate in the basin is tentatively interpreted as being the main cause of this shallowing in the study area. On the platform, the extent of the limestone and siltstone lithofacies, which is preserved between Locality 21 and the Imperial Island River No. 1 well (102 km eastward), indicates that the shelf was broad. Moreover, the apparent lack of rapid, major basinward changes in lithology and style of sedimentation across this region suggests that the limestone and siltstone lithofacies was deposited on a surface that had a low gradient.

The thick unit of limestone and siltstone lithofacies that is preserved in the middle Banff(?) at Bluefish Mountain (Figs. 4, 15, 20) is another coarsening-upward sequence that records deposition under shoaling-upward conditions. Because turbidite-like deposits are present, turbidity currents possibly deposited at least part of the interbedded shale, siltstone, and silty limestone in the recessive basal part of the unit (Fig. 20). In comparison, the upper part of the unit (Fig. 22) resembles deposits in shoreline sequences that Howard (1972), Campbell (1971), Harms (1975b) and others have described. However, these upper deposits at Bluefish Mountain are interpreted as shallow-neritic, possibly shoreface, deposits because overlying supratidal deposits are absent, and 207.3 m of marine shale overlie this unit. The planar-stratified beds of very fine grained sandstone in the upper part of this unit are interpreted as shallow-sublittoral deposits that were produced by deposition from lower-flow-regime currents on plane beds. Planar stratification instead of large-scale crossbedding developed because the fine grain size prohibited development of large-scale bed forms (see Southard, 1975, p. 17).

In the intervals of limestone and siltstone lithofacies examined, evidence of slope gradients sufficient to generate turbidity currents by slumping is lacking. A low-gradient basin slope probably existed off the shelf on which the shallow-sublittoral part of this facies was deposited. However, the break in slope would have been subtle and the slope a site of turbidity current deposition rather than generation. The close spatial relationship between turbidite-like deposits and strata deposited above wave base suggests that a slope suitable for slump-generated turbidity currents did not exist.

Like graded beds in the Yohin of the Bluefish-Twisted mountains region, turbidite-like deposits in the limestone and siltstone lithofacies were probably deposited chiefly by storm-generated currents in relatively shallow water. They could be, therefore, mainly tempestites. The proximity to shallow marine strata, and the ichnofossils present, suggest deposition in relatively shallow water. *Planolites* sp. (GSC loc. C-58526) was the only ichnogenus identified, but the

lebensspuren present do not appear to be characteristic of either Seilacher's (1967, 1978) *Nereites* or *Zoophycos* facies, which show typical development in abyssal and bathyal deposits, respectively. Moreover, the work of Aigner (1982), Hamblin and Walker (1979), Anderton (1976), and Mount (1982) suggests that the deposition of graded beds in relatively shallow water by storm generated currents is a common process.

Age

On the interior platform north of latitude 60°00'N, the Banff Formation is mainly of earliest Tournaisian (Tn1a to early Tn1b) to late middle Tournaisian (late Tn2) age; however, slightly older and younger strata are possibly present (Fig. 3). Fossils were not obtained from the basal Banff in that region, and strata of Famennian age are possibly present. Palynomorphs (Appendix D) of earliest Tournaisian (Tn1a to early Tn1b) age (latest Devonian) were collected between 188.3 and 348.3 m below the top of the Banff Formation (52.4 to 212.5 m above its base) in the Imperial Island River No. 1 well. From the same well, palynomorphs of early to middle Tournaisian (late Tn1b to Tn2) (Early Carboniferous) and possibly late Tournaisian (Tn3) ages were collected between 6.7 and 58.5 m below the top of the Banff (Appendices E, F). Consequently, the Devonian/Carboniferous boundary, which is in the upper Tn1b, is in the upper half of the Banff on the platform north of 60°00'N.

At Bluefish Mountain, the Banff(?) Formation is of early Tournaisian (Tn1) age and possibly slightly older. Fossils were not collected from the lower Banff(?) at that location. Palynomorphs of probable late early Tournaisian (late Tn1b) age (earliest Carboniferous) were collected from the middle Banff(?) between 154.9 and 205.9 m above the base of the Bluefish Mountain section (Appendix F). Also, conodonts that are questionably assigned to the *Siphonodella sulcata* Zone (Collinson et al., 1962; Sandberg et al., 1978) of late early Tournaisian (late Tn1b) age (Carboniferous) were obtained from the Banff(?) at 284.1 m above the base of the Bluefish Mountain section (Appendix C). The upper Banff(?) and basal Yohin Formation at Bluefish Mountain contain conodonts that are probably assignable to the *Siphonodella duplicata* Zone of Collinson et al. (1962), which is of latest early Tournaisian (latest Tn1b) age (Appendix C).

YOHIN FORMATION

Type Section

Harker (1961, p. 3) proposed the name Yohin Formation and established its type section (Figs. 6, 23, 24), which outcrops on the west side of Yohin Ridge immediately north of Jackfish Gap (Fig. 1, Loc. 4). The locality is about 32 km west of Nahanni Butte in the Twisted Mountain map area (NTS 95 G/4), at latitude 61°05'54"N, and longitude 123°59'26"W, in the southwestern District of Mackenzie.

Previous work

The Yohin Formation corresponds to Patton's (1958, p. 312) Unit 1 and Douglas and Norris's (1959, p. 10) Map unit 5 at Jackfish Gap. Furthermore, it is synonymous with most of Douglas and Norris's (1960, p. 30) Map unit 30 in the Virginia Falls and Sibbeston Lake map areas (95 F and 95 G), southwestern District of Mackenzie.



Figure 23. Type section of the Yohin Formation at Jackfish Gap. About 157 m of Yohin, mostly graded-bed lithofacies comprising siltstone and sandstone are exposed. Arrows indicate tops of coarsening-upward sequences. ISPG 1303-20.

The distribution of the Yohin Formation, as defined in this report, differs slightly from that reported by Harker (1963) and Douglas and Norris (1976b, c). Harker (1963, p. 48, units 1-7; p. 62, units 1-22) and Douglas and Norris (1976c) assigned to the Flett Formation at Bluefish and Twisted mountains strata that I reassign to the Yohin (Figs. 2, 4). These strata (corresponding to intervals between 413.7 and 494.8 m at Locality 1, and 0.0 and 129.5 m at Locality 2; on Figure 4) are at the same stratigraphic level as the type Yohin and are lithologically similar to it. In comparison, strata that Harker (1963, p. 60, units 1-4) and Douglas and Norris (1976c) assigned to the Yohin at Bluefish Mountain (Fig. 4, Loc. 1, 0-206.4 m) do not closely resemble the Yohin and are stratigraphically lower. Also, Harker (1963, p. 59) and Douglas and Norris (1976b) assigned to the Yohin a unit of spiculite and carbonates that outcrops along the north side of the Tlogotsho Plateau (Fig. 4, 87-130 m in Tlogotsho Plateau section) although it is not representative of that formation. This unit (Fig. 11) and the Yohin are at similar stratigraphic levels but are markedly different lithologically.

Distribution

The Yohin Formation is not widely distributed. It appears to be confined to the Mackenzie fold belt between latitude 60°55'N and 61°45'N in the southwestern District of Mackenzie (Harker, 1963, p. 6, 7; Douglas and Norris, 1976a, b, c), where it is preserved mainly in the Mattson anticline and in the Kotaneelee, Yohin, Liard and Bluefish synclines (Fig. 1). Exposures are in narrow belts on the limbs and noses of these structures, and at most locations the Yohin is moderately resistant but poorly exposed. Its distribution pattern is mainly the result of depositional thinning to the southwest and post-Early Carboniferous erosion to the north and east.

Thickness

Limited stratigraphic data (Table 1) indicate that the Yohin Formation is thickest in the vicinity of its type locality at Jackfish Gap, where it exceeds 157 m in thickness. Southward and westward the formation thins rapidly, diminishing to zero between the type locality and an outcrop 8.5 km westward (Fig. 1, Loc. 5). Similarly, it thins to about 74 m at Bluefish Mountain, 27.5 km east of Jackfish Gap (Fig. 4).

Lithostratigraphic relationships

The Yohin Formation conformably overlies either the Besa River Formation or a unit that I tentatively assign to the Banff Formation. It conformably overlies the shale of this upper Banff(?) at Bluefish Mountain (Fig. 13), in the Bluefish and possibly the Yohin synclines to the north, and possibly at the north end of the Mattson anticline. Elsewhere, including the type locality, the Yohin probably overlies the Besa River, but this contact is seldom exposed in the region. The Yohin/Banff boundary is described in the section dealing with the upper contact of the Banff Formation.

The Yohin Formation grades southwestward into the Besa River Formation. This transition is confined mainly to the subsurface, but it is partly exposed at the extreme northeastern corner of the Tlogotsho Plateau. Unfortunately, because of poor exposure, the relationship between the Yohin and Besa River at that location is unclear, but the Yohin appears to grade laterally into greyish black shale that underlies a unit of silty spiculite and carbonates in the Besa River (Fig. 4). At Locality 30 (Fig. 1), 7.5 km northwest of the Yohin type locality, a thick interval of spiculite, which is possibly equivalent to the unit of spiculite and carbonates noted above, occurs in the Clausen Formation just above, the Yohin.

Shale and mudstone in the Clausen Formation conformably overlie the Yohin. A siltstone or sandstone bed forms the uppermost Yohin, and at most places this is the highest significant occurrence of either lithology below the middle Flett Formation. At Bluefish and Twisted mountains, siltstone beds are a minor rock type in the Clausen. The Yohin/Clausen contact is moderately abrupt, and the Yohin grades into the overlying shale through an interval of 50 cm or less. Because the Clausen is much less resistant, the top of the Yohin coincides with a pronounced break in slope.

Lithology

The Yohin Formation comprises siltstone and sandstone, with subordinate shale, mudstone, and skeletal lime grainstone to packstone (Figs. 4, 24). Siltstone and sandstone (Fig. 25a) occur throughout most of the formation, but the ratio of siltstone to sandstone increases toward the west. Limestone (Fig. 25b) was observed only at Localities 1 and 2, where it occurs in the lower one third of the Yohin. Although shale and mudstone are present throughout, they appear to be most abundant at localities that are northeast of Jackfish Gap.

Sandstone in the Yohin Formation is mainly texturally submature to mature subchertarenite that is sparsely fossiliferous to very fossiliferous, siliceous to calcareous and sideritic, and chiefly fine to very fine grained (Fig. 25a). It is medium to light grey and weathers greyish orange to moderate yellowish brown. Terrigenous clasts in most of these sandstones are poorly to moderately well sorted, but

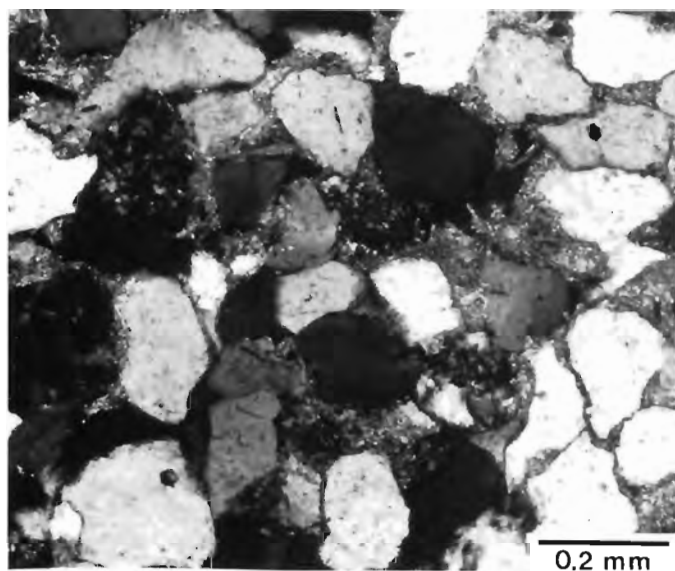
they are well sorted in some of the crossbedded sandstone lithofacies. In some graded sandstone beds and most highly bioturbated sandstone deposits, this rock type is texturally immature. Fine to coarse sand-sized quartz and chert clasts are mainly subangular to subrounded. In the same size range, rounded to well rounded clasts are not abundant, and very angular to angular clasts are moderately common. Siliciclastic silt is common in the very fine grained sandstone. Most sandstone is sparsely fossiliferous, but sandstone in the lower Yohin at Bluefish and Twisted mountains is generally very fossiliferous and grades into sandy limestone. Pelmatozoan ossicles, brachiopods, ostracods, and sponge spicules are the most abundant invertebrate fossils. Foraminifers and corals are generally rare, but calcareous algae are moderately common.

The mean percentages of terrigenous clast types in seven sandstone samples are: quartz 83.3 ± 4.8 , chert rock fragments 12.2 ± 2.9 , other rock fragments (mudstone and subordinate metamorphic rocks) 2.3 ± 1.9 , feldspar 1.1 ± 0.2 , nonopaque heavy minerals (mainly tourmaline, zircon, and sphene) 0.6 ± 0.4 , micas 0.6 ± 0.3 , and opaques 0.3 ± 0.2 (Appendix F). Mean percentages of the types of quartz clasts in six samples are: grains with straight extinction 38.2 ± 3.7 , grains with undulose extinction ($>5^\circ$) 51.0 ± 2.0 , polycrystalline clasts comprising two to three units 4.0 ± 0.8 , and polycrystalline grains with more than three units 6.4 ± 1.3 . These analyses are based on 500 and 400 counts per thin section, respectively. In addition to the constituents listed above, tabular to irregular siliciclastic mudstone and siltstone intraclasts, ranging up to pebble size, occur in many beds and are locally abundant enough to form conglomerate. The provenance of the terrigenous clasts is discussed later in this report.

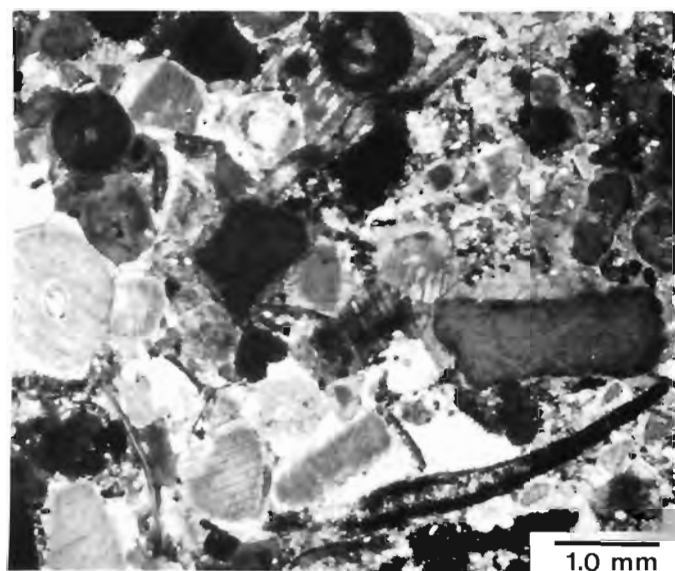
The siltstone is similar in colour and clast composition to the sandstone but commonly contains more mica and mudstone rock fragments. It is mainly texturally immature to submature subchertarenite and subsedarenite that are sandy, unfossiliferous to very fossiliferous, and siliceous to calcareous and sideritic. The clasts are mainly poorly to moderately sorted, and some mud matrix is present in most noncalcareous siltstone. Most of the siltstone is sandy and commonly grades into very fine sandstone. In the lower Yohin Formation at Twisted and Bluefish mountains, most of the siltstone is very calcareous and fossiliferous.

Shale and mudstone in the Yohin Formation are mainly dark grey to greyish black, silty, unfossiliferous, and noncalcareous to slightly calcareous. Mudstone predominates and is friable, whereas the shale is moderately to highly fissile. Invertebrate fossils were observed in these lithologies only in the lower Yohin at Bluefish and Twisted mountains. Elliptical ironstone concretions are common in some beds.

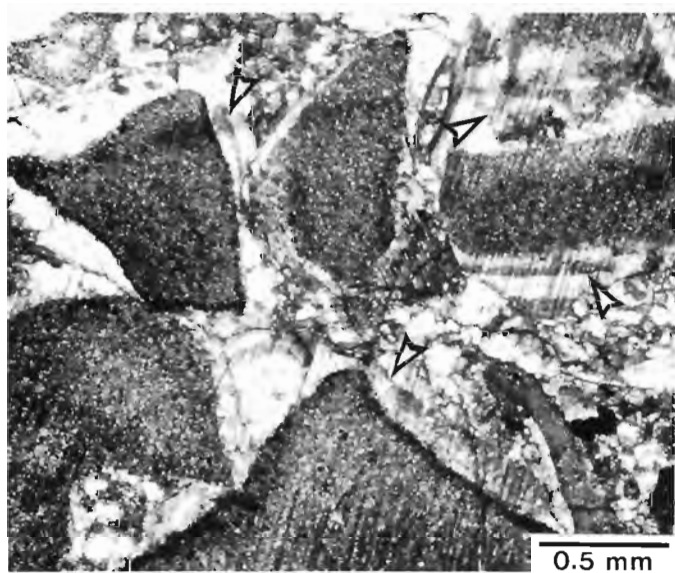
Limestone in the Yohin Formation is mixed-skeletal lime grainstone with subordinate packstone (Fig. 25b). It generally contains abundant quartz and chert silt and sand, and commonly grades into sandstone and siltstone. Pelmatozoan ossicles, brachiopods, sponge spicules, and ostracods are the most abundant bioclasts; in addition, calcareous algae and sand- to pebble-sized intraclasts of siltstone, limestone, and mudstone are common in many beds (Fig. 28). Foraminifers and corals are minor components, but bryozoans, molluscs, and trilobites are locally moderately abundant. Authigenic dolomite and chert occur but are relatively minor constituents. Common limestones in the Yohin are spicule-pelmatozoan, brachiopod-pelmatozoan, and ostracod-spicule lime grainstone and packstone. These limestones are chiefly medium grey to light olive-grey and weather greyish orange.



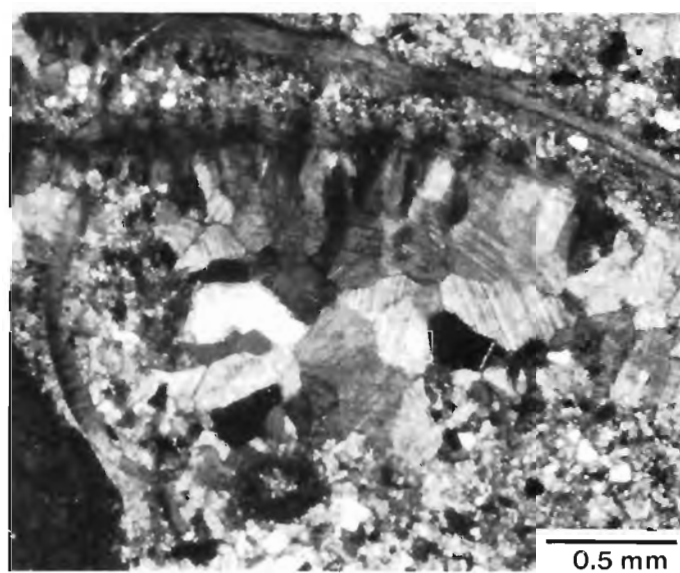
a. Fine sandstone: calcareous submature subchertarenite (GSC loc. C-59012); from the upper Yohin Formation at Twisted Mountain. ISPG 1768-151.



b. Silty, pelmatozoan lime grainstone (GSC loc. C-58530) from the lower Yohin Formation at Bluefish Mountain. Pelmatozoan ossicles have monocrystalline syntaxial overgrowths. ISPG 1768-33.



c. Monocrystalline syntaxial overgrowths on pelmatozoan ossicles in silty lime grainstone (GSC loc. C-58530) from the lower Yohin Formation at Bluefish Mountain. Overgrowths have zones of ferroan and nonferroan calcite; dark bands (arrows) are ferroan. ISPG 1768-27.



d. Ferroan, bladed, polycrystalline fringe cement on a brachiopod shell fragment, and an associated mosaic of blocky calcite cement, in sandy lime grainstone (GSC loc. C-58996) from the lower Yohin Formation at Twisted Mountain. ISPG 1768-139.

Figure 25. Photomicrographs of Yohin Formation lithologies and cements.

Diagenesis

Calcite

Diagenetic calcite forms in four basic ways within sediment: passive precipitation into cavities, replacement of non- CaCO_3 minerals, neomorphism, and displacive precipitation (Folk, 1965, p. 24). In the limestone of the Yohin Formation, authigenic calcite produced in the first three ways is important, whereas calcite formed by replacement and passive precipitation is common in the calcareous sandstone and siltstone. Microspar and pseudospar (Folk, 1965) produced by the recrystallization of micrite are the main neomorphic calcites, but pseudospar produced by inversion of aragonitic skeletons also occurs. Displacive calcite is a minor constituent. Both nonferroan and ferroan diagenetic calcite occur, and the latter predominates.

The ferroan calcite that occurs in the Yohin and other formations discussed in this paper was probably precipitated from solutions in the meteoric-phreatic and subsurface-mixing zone precipitational environments, rather than the vadose and marine-phreatic zones (see Folk, 1973, 1974a, p. 45, 51) (Fig. 19). According to Evamy (1967, p. 791), calcite precipitated in the vadose zone generally lacks Fe^{2+} , because ferroan calcite requires a reducing environment for precipitation. Furthermore, Richter and Füchtbauer (1978, p. 855) stated that ferroan calcite is not formed during the first stages of diagenesis in marine sediment because its precipitation requires a reducing environment and a lack of organic matter, combined with anaerobic, sulphate-reducing bacteria (because the absence of S^{2-} is necessary). Because sulphate-reducing bacteria can be active in older rocks as well as in the uppermost metre of sediment, conditions necessary for Fe^{2+} uptake by calcite may be attained late, if at all, in the marine-connate water realm (Richter and Füchtbauer, 1978, p. 855). However, Richter and Füchtbauer's work demonstrated that caution should be used when the Fe^{2+} content of calcite cement is used to interpret its precipitational environment, because ferroan calcite can replace all nonferroan calcite, particularly high Mg^{2+} calcite.

Calcite cement fabrics

The main fabrics of sparry calcite cement or passively precipitated calcite that occur in the Yohin Formation are: monocrystalline syntaxial overgrowths (Fig. 25b, c); pore-filling mosaics of subequant crystals (Fig. 25d); and polycrystalline fringes of equant to bladed crystals (Fig. 25d). These fabrics exist in subequal proportions and occur both intergranularly and intragranularly.

Monocrystalline syntaxial overgrowths are common on pelmatozoan ossicles (Fig. 25b, c), and syntaxial cement fills their canal systems. These overgrowths are generally relatively clear and lack evidence of acicular calcite and aragonite precursors. The application of Dickson's (1965) staining technique revealed that most of these overgrowths either have two or more cement generations with varying Fe^{2+} content (Fig. 25c) or are strongly ferroan throughout. In the zoned overgrowths, the first generation cement varies from nonferroan to strongly ferroan.

Solutions in the meteoric-phreatic and subsurface zones rather than the marine-phreatic and vadose zones (Fig. 19) probably precipitated most of the monocrystalline syntaxial overgrowths in the Yohin Formation (see Folk, 1973, 1974a, p. 45, 51). Relatively inclusion-free overgrowths like those described above have been reported from numerous limestones. They are believed to precipitate most commonly

from meteoric-phreatic water (Longman, 1980, p. 477; Meyers, 1974; 1978, p. 379; Meyers and Lohmann, 1978, p. 477). In addition, connate solutions in the subsurface zone probably could precipitate this fabric because coarse, sparry calcite cement can form in such environments (see Folk and Land, 1975, p. 66). Although deep-subsurface solutions probably precipitated a portion of these overgrowths, much of this cement probably formed at a relatively early stage, because: effects of compaction are not marked; some of the first-generation cement is not ferroan; and pore-filling mosaics of subequant crystals that are characteristic of later diagenesis commonly overlie the overgrowths. The absence of meniscus cement morphologies, such as those described by Dunham (1971) and Meyers (1974), indicate that these overgrowths were probably not precipitated by vadose solutions. Moreover, Carboniferous vadose processes probably did not affect the Yohin intervals examined, because both this formation and the overlying Clausen appear to lack intraformational unconformities and supratidal lithofacies. The overgrowths did not form pseudomorphs of syndepositional aragonite cement, because evidence of acicular aragonite precursors (see Kendall and Tucker, 1971, 1973; Davies, 1977; Lohmann and Meyers, 1977; Mazzullo, 1980) are absent. According to Longman (1980, p. 477), syntaxial overgrowths on echinoderm fragments form rarely, if ever, in marine-phreatic environments and form most rapidly in the freshwater-phreatic environment. Also, the coarse crystal size and high substrate selectivity of the overgrowths contrasts with modern marine, high magnesium, calcite cements, which are characteristically either fibrous or micritic and have low substrate selectivity (see James et al., 1976; Meyers and Lohmann, 1978, p. 483; Meyers, 1974, p. 855; Folk, 1974a, p. 42). Finally, it is improbable that either marine or vadose solutions precipitated most of this cement because it is mainly ferroan.

Mosaics of subequant, clear, calcite crystals, which are mainly finely to coarsely crystalline, either filled cavities completely or filled the centers of pores lined by other cement fabrics (Fig. 25d). Although some elongation is commonly evident, the length to width ratios of most crystals do not exceed 2:1, which is near Folk's (1965, p. 25) limiting ratio of 1½:1 for equant crystals. Some of these mosaics consist of crystals that increase in size away from pore walls. In lime grainstone and in some very fossiliferous sandstone and siltstone, this mosaic occurs intergranularly and intragranularly, but in other lithologies it exists chiefly in bioclasts and areas of geopetal fabric. This cement is mainly strongly ferroan, with the remainder slightly to moderately ferroan.

Cavity-filling mosaics of equant- to subequant-grained sparry calcite, particularly those which coarsen away from pore walls, are believed to precipitate chiefly from meteoric water (Meyers, 1978, p. 379; Cotter, 1966, p. 771; Friedman and Kolesar, 1971; Buchbinder and Friedman, 1980). However, the mosaics also can precipitate from: vadose water that is low in Mg^{2+} ; meteoric-phreatic solutions; and subsurface solutions, either connate or mixed with meteoric water, that have $\text{Mg}^{2+}/\text{Ca}^{2+}$ ratios below about 2:1 (Folk and Land, 1975, p. 66). A marine origin is unlikely because seawater generally precipitates either micritic or fibrous aragonite and high- Mg^{2+} calcite. The high Mg^{2+} concentration of normal seawater prevents sideward growth of high- Mg^{2+} calcite crystals (Folk, 1974a, p. 44-46). Because the cement fabric in the Yohin is mainly ferroan, and the intervals of Yohin examined were not subaerially exposed during the Early Carboniferous, the cement probably precipitated in either the meteoric-phreatic or subsurface zones of Folk (1974a, Fig. 5) rather than in the vadose zone.

Polycrystalline fringe cement, which exists both intergranularly and intragranularly, is a common cement fabric in most lime grainstone in the Yohin Formation. It also occurs locally in other lithologies. Equant to bladed crystals (Fig. 25d), which are mainly finely to coarsely crystalline and locally relatively inclusion-rich, constitute the fringe cement. Folk's (1965, p. 25) limiting length to width ratios for bladed calcite, which are between 1½:1 and 6:1, are used here. In most samples, bladed fringes of variable thickness are most common, and these fringes commonly interlock with opposing fringes. Away from their foundations, the component crystals decrease in number but increase in size. Also, in bladed fringes the crystals commonly occur in bundles. Subcrystals in the bundles diverge away from their foundations, have irregular subcrystal boundaries, differ in extinction by two or more degrees, and commonly widen outward. This fabric of bundled crystals superficially resembles Bathurst's (1959, p. 11; 1971, p. 426, 427) radial-fibrous mosaic, but the crystals appear to lack the convergent optic axes and curved twins typical of the latter. Although polycrystalline fringes were observed on all bioclasts except echinoderm ossicles and spicules, they are best developed on brachiopods. The fringe cement varies from nonferroan to strongly ferroan, but most is strongly ferroan, and some fringes comprise crystals that have zones containing different amounts of Fe²⁺.

Most polycrystalline fringe cement in the Yohin Formation is interpreted as having been precipitated relatively early in the meteoric-phreatic and shallow-subsurface zones rather than in the marine-phreatic, vadose, or deep-subsurface precipitational environments (see Folk, 1973, 1974a, Fig. 5) (Fig. 19). This cement probably formed at a relatively early stage because: effects of compaction are minimal; the mosaics of elongate crystals contrast with typical late-diagenetic equant mosaics; and pore-filling mosaics of subequant crystals, characteristic of late diagenesis, commonly overlie it. Marine-phreatic solutions probably did not precipitate most of this cement because: it is mainly strongly ferroan; evidence of acicular-aragonite precursors (Kendall and Tucker, 1971, 1973; Lohmann and Meyers, 1977; Mazzullo, 1980) is absent; and its substrate selectivity contrasts with that of marine, fringe cement (see Longman, 1980). Also, the fringe crystals are finely to coarsely crystalline and commonly broad. Marine high-Mg²⁺ calcite cement is either micritic, or bladed to fibrous (acicular), scalenohedral crystals a few microns wide (see James et al., 1976; Folk, 1974a, p. 42, 43). Vadose solutions did not precipitate this cement because: it is mainly ferroan, the Yohin intervals examined were not subaerially exposed, and associated gravity and meniscus cements are lacking. Polycrystalline fringes that consist of either bladed or equant calcite can precipitate in the meteoric-phreatic zone (Longman, 1980; Badiozamani et al., 1977) and in the subsurface-mixing zone (Buchbinder and Friedman, 1980). Moreover, experimental work (Badiozamani et al., 1977, p. 533) suggests that saline connate solutions in the subsurface zone could precipitate these fringes. Finally, crystals in the fringes coarsen toward the centers of pores. This pattern does not appear to occur in cement precipitated by sea water, but it is evident in early cement precipitated by meteoric-phreatic solutions (Loucks, 1977; Longman, 1980) and in calcite precipitated in experimental NaCl solutions (Badiozamani et al., 1977, p. 533).

Replacement calcite

In addition to diagenetic calcite produced by the replacement of quartz cement and silicate clasts, calcite formed by the replacement of opaline sponge spicules is locally important. Most spicules in the Yohin Formation are interpreted to have been opaline for reasons given under the

section on diagenesis of spicules in the Prophet Formation. Where spicules are the main allochems, pseudospar that replaced the biogenic opal commonly constitutes a major part of the calcite. Most of this replacement calcite is strongly ferroan, multicrystalline, and finely to medium crystalline.

Cements in sandstone and siltstone

Most sandstones and siltstones in the Yohin Formation are well cemented and have poor porosity (Fig. 25a). Quartz and strongly ferroan calcite are the principal cement minerals, but clay minerals and very finely to finely crystalline siderite are important in some samples. In most beds, the carbonate cements, particularly calcite, partly replaced quartz cement and to a lesser extent clasts, and in much of the the lower Yohin at Twisted and Bluefish mountains, relict terrigenous clasts float in calcite. Passive precipitation probably formed much of the calcite cement in the very fossiliferous sandstone and siltstone, but in much of the remainder of these rocks, replacement calcite appears to predominate. Replacement textures indicate that quartz was an early cement in many beds and was later partly replaced. Both the passively precipitated and replacement calcite are finely to very coarsely crystalline and locally poikilitic.

Lithofacies

A graded-bed lithofacies (Figs. 24, 26-28), a crossbedded sandstone lithofacies (Figs. 29, 30), and a shale lithofacies constitute the Yohin Formation. The graded-bed lithofacies is complex and, at least locally, divisible into several important subfacies; however, its subdivision is not attempted because of insufficient field data. Dark, grey shale and mudstone with minor siltstone and sandstone constitute the shale lithofacies. This facies, which occurs mainly as thick interbeds between units of crossbedded sandstone lithofacies, is not discussed separately.

Graded-bed lithofacies

The graded-bed lithofacies (Figs. 26-28) is the best exposed and most common of the Yohin lithofacies. In the Jackfish Gap region, it constitutes most of the formation, and only the uppermost Yohin represents the crossbedded sandstone lithofacies and the shale lithofacies. At the north end of the Mattson anticline (Fig. 1, Loc. 3) and northeastward, the graded-bed lithofacies forms at least the lower third of the formation. Northeastward from the Jackfish Gap area, the graded-bed lithofacies grades upward and eastward into the crossbedded sandstone lithofacies. At all locations, the graded-bed facies overlies basinal shale and mudstone of either the Besa River or Banff(?) formations (Fig. 13). In the Jackfish Gap region, west of the type locality, the graded-bed facies is probably overlain by the dark shale of the Clausen Formation. Toward the southwest, the graded-bed lithofacies grades into the basinal shale of the Besa River.

The graded-bed lithofacies includes sandstone and siltstone (Figs. 26, 27) with subordinate shale, mudstone, and limestone (Fig. 28). Siltstone occurs throughout and is the principal lithology in much of the stratotype, but northeastward its abundance decreases. Sandstone is also present throughout this facies and is a major rock type in all sections examined. Limestone occurs at Bluefish and Twisted mountains, but it was not observed southwest of that region. Shale and mudstone occur throughout this lithofacies as laminae and thin to moderately thick, recessive beds, which are most abundant in the northeastern corner of the Yohin outcrop belt.



Figure 26. The Yohin graded-bed lithofacies at Locality 29. Thick, resistant sandstone units of uncertain origin form the upper cliff. Underlying unit is a fining-upward sequence of normally graded, siltstone and sandstone turbidites. ISPG 798-146.

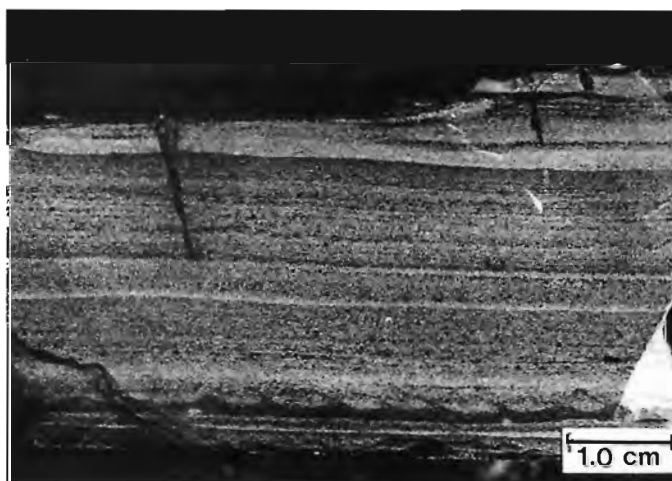


Figure 27. Polished slab of distal (D-E), siltstone turbidite (GSC loc. C-52176) from the Yohin graded-bed lithofacies at Jackfish Gap. Flame structures present at base. ISPG 1766-7.

Beds and laminae of siltstone and sandstone that have sharp bases and vary from massive to stratified and ungraded to graded constitute most of the Yohin graded-bed lithofacies (Figs. 26-28). Some thick, resistant sandstone units of uncertain origin (Fig. 26), and interbeds of shale and mudstone, are associated with them. Deposits in most of the Yohin graded-bed lithofacies are thin to medium bedded, but locally they are either laminated or thick to very thick bedded. These deposits, which consist of siliciclastics and minor limestone, form well defined multibed sequences

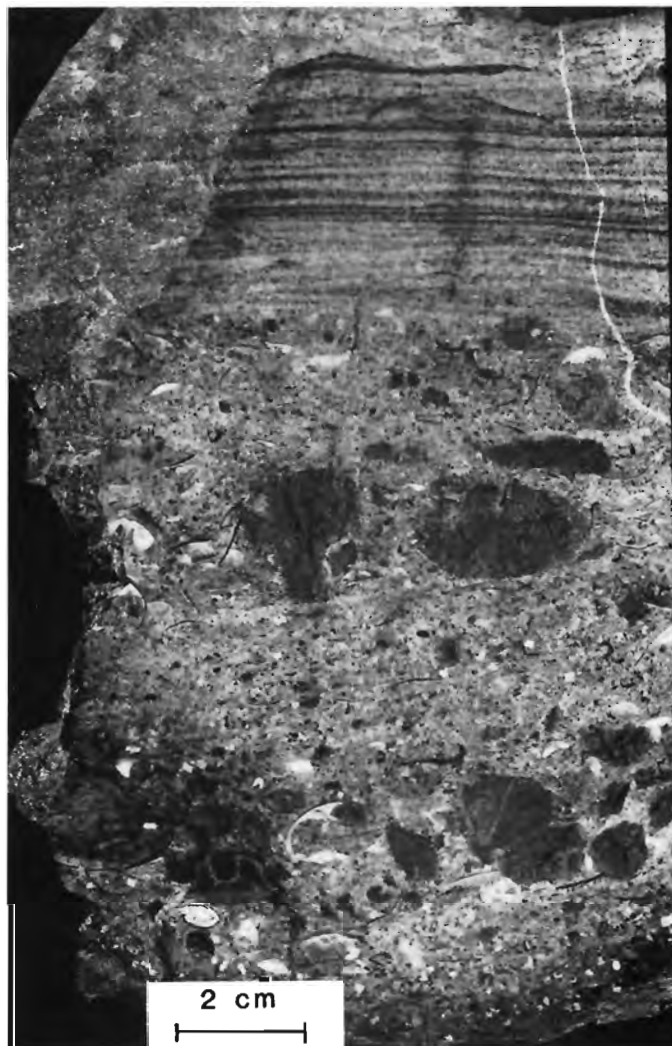


Figure 28. Polished slab of a graded limestone and sandstone bed (GSC loc. C-59000) from the graded-bed lithofacies of the basal Yohin Formation at Twisted Mountain. The bed, interpreted as a storm deposit, has components resembling the Bouma A, C, and possibly the B divisions. ISPG 1766-3.

(Figs. 23, 80). Much of this lithofacies is rhythmically bedded (Fig. 26), and beds commonly have considerable lateral continuity. Large-scale, concave-upward truncation surfaces (Figs. 80, 82), interpreted as being mainly erosion surfaces of submarine channels, locally interrupt bedding continuity. These discontinuities and overlying fill sequences are discussed later, together with similar structures in the Flett and Prophet formations.

Most of the sharp-based beds and laminae in the graded-bed lithofacies comprise two or more components that correspond reasonably well to divisions A to E in the standard Bouma sequence (see Bouma, 1962; Middleton and Hampton, 1973). Many of these deposits, however, also resemble some tempestites. The sharp soles of these deposits commonly have load casts, shallow scours, and trace fossils, but well developed flute- and groove-casts were not observed. The component that resembles the Bouma A division is massive to crudely stratified (Fig. 28) and best

developed in limestone and fossiliferous sandstone. Well developed, millimetre-thick, planar laminae constitute the component that resembles the B division. Small-scale current and climbing-ripple crossbedding, commonly accentuated by dark argillaceous sediment, predominates in the C-like division, but convolute laminae occur in some beds. The D-like division (Fig. 27) is thinly laminated and generally grades up into a darker, more argillaceous, component, which corresponds to the Bouma E division. Evidence of bioturbation is present in many of these laminae and beds, particularly near their tops, and the degree of bioturbation increases toward the northeast.

Few beds and laminae that resemble a complete Bouma sequence of five divisions were observed in the Yohin. At Jackfish Gap, most beds and laminae lack components that correspond to the Bouma A and B divisions. There, they generally have a basal component that is like either the Bouma C or D divisions. Beds with a basal component that resembles the Bouma A or B divisions are common at Twisted and Bluefish mountains, and the A-like component in some of these beds is overlain by a B-like interval. Also the B-like and possibly the A-like divisions appear to be common in beds at Locality 29.

Grading in these sharp-based beds and laminae resembles the distribution grading of Middleton (1967, p. 487), and it is mainly normal. An obvious decrease in mean grain size generally occurs between the base and top of beds, and the A-like division of many beds is distinctly graded. In contrast, in components that correspond to the B, C, D and E divisions, grading, when evident, is generally subtle.

Most sharp-based beds and laminae in the Jackfish Gap area (Fig. 1; Locs. 4, 29) are tentatively interpreted as turbidites, because they have abrupt bases with sole marks, are commonly normally graded, and generally comprise two or more components that correspond well to divisions in the standard Bouma sequence. These beds and laminae are like sandstone turbidites described by Mutti (1977), Sanders (1965), Ricci-Lucchi (1975), and others. Moreover, they are in a succession that is of relatively deep water aspect and is not closely associated with shallow water lithofacies.

The sharp-based beds in the graded bed lithofacies at Bluefish and Twisted mountains resemble turbidites, but it is possible that some were not deposited by turbidity currents. They resemble turbidites because they have the turbidite characteristics listed in the previous paragraph. However, they are closely associated with the Yohin crossbedded sandstone lithofacies, which contains large-scale crossbedding and other structures of shallow water origin. These beds also resemble some storm deposits, particularly those with a massive or planar-stratified basal component, that have been described by Johnson (1978, p. 251, 252), Nelson (1982), Aigner (1982), and others. The origin of these deposits is discussed further in the section on environmental interpretations.

Turbidites that contain Bouma A or B divisions are proximal, and those that lack these divisions are distal (Bouma and Hollister, 1973, p. 89). Therefore, because most turbidites at Jackfish Gap appear to lack the Bouma A and B divisions, they are mainly distal. Proximal turbidites appear to be present at Location 29.

Intervals of distal turbidites in the Yohin are somewhat unusual because the ratio of turbiditic sandstone and siltstone to shale and mudstone is high (commonly greater than 4:1). In this regard they do not resemble Walker and Mutti's (1973, p. 132) classical distal turbidite lithofacies D, but the Yohin deposits do resemble their facies E and the thin-bedded

turbidite facies described by Mutti (1977). The latter facies was deposited in channel margin, channel mouth, inter-channel, and outer-fan environments.

Two principal types of multibed sequence occur in the graded-bed lithofacies of the Yohin: one becomes more resistant upward (Fig. 23) and another that becomes less resistant upward (Figs. 80, 82).

Multibed sequences that occur in the Jackfish Gap region and become more resistant upward generally either overlie the resistant upper part of similar sequences, or grade into underlying units of shale and mudstone. Toward the top of these sequences, the turbidites tend to become thicker, coarser grained, closer together, and more proximal in aspect. The thicker, more extensive sequences commonly consist of two or more subordinate sequences, which are generally less widespread and either become more resistant or less resistant upward. Concave-upward truncation surfaces occur in some compound sequences, but they are generally minor features that exist in the upper half of the sequence. Multibed sequences that become more resistant upward and resemble those in the Jackfish Gap area are present in the graded-bed lithofacies at Twisted and Bluefish mountains.

Yohin sequences that become less resistant upward have erosional bases. Toward the tops of these sequences, resistant beds become thinner, finer grained, more distal in aspect, and to some extent farther apart. Areally extensive sequences of this type are commonly composites comprising several similar but subordinate sequences (Fig. 80). The subordinate sequences are less extensive, and they occur mostly as fill sequences above well developed concave-upward discontinuities, which are chiefly in the lower, resistant half of the main sequences. Although bases of the main, composite sequences are erosional, these sequences generally do not occur above a conspicuous concave-up discontinuity.

Crossbedded sandstone lithofacies

The crossbedded sandstone lithofacies (Figs. 29, 30) forms the upper Yohin Formation in the region northeast of Jackfish Gap and is best developed at Bluefish and Twisted mountains. Also, 3.8 m of sandstone with subordinate siltstone that occur at the top of the Yohin type section are tentatively included in this lithofacies. This lithofacies overlies and grades southwestward into the Yohin graded-bed lithofacies; in addition, it is commonly interbedded with the Yohin shale lithofacies. Dark shale and mudstone in the Clausen Formation overlie the crossbedded sandstone lithofacies and generally grade into it through less than 50 cm. Sandstone and siltstone with minor shale and mudstone constitute the crossbedded sandstone lithofacies.

The crossbedded sandstone lithofacies comprises resistant intervals of sandstone and siltstone, which are commonly intercalated with recessive units of the shale lithofacies. Sandstone and siltstone deposits occur mainly in well developed, progradational, multibed coarsening-upward sequences that are up to 29.5 m thick. In addition, the crossbedded sandstone lithofacies occurs as units that are mainly between 0.5 and 1.5 m thick, have abrupt bases and gradational to sharp tops, and are intercalated with the shale lithofacies. Individual sandstone bodies appear to be sheet-like lenses. Although some thicker sandstone units are exposed along strike for one kilometre or more, they could not be correlated between the sections measured. The ichnofossils observed in the sandstone and siltstone of this lithofacies include: *Asterosoma* sp. (GSC loc. C-59010),

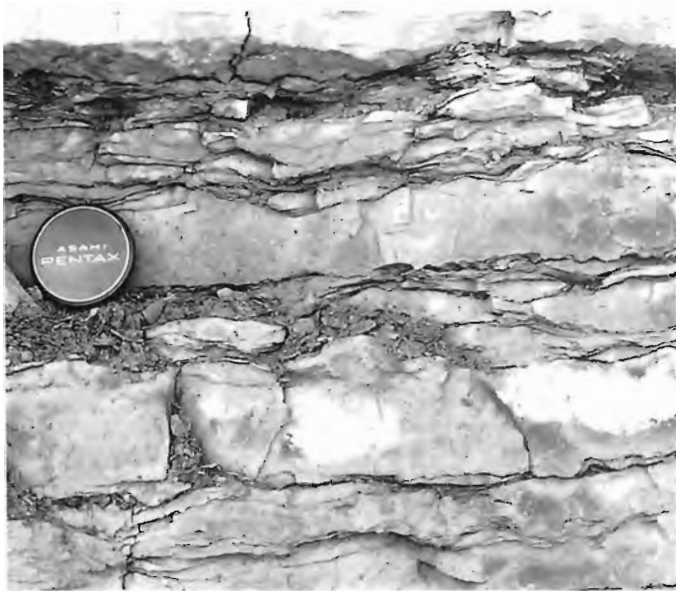


Figure 29. Small-scale crossbedding in bioturbated sandstone of the Yohin crossbedded sandstone lithofacies at Twisted Mountain. ISPG 798-68.



Figure 30. Medium-scale crossbedding in sandstone of the Yohin crossbedded sandstone lithofacies at Twisted Mountain. ISPG 798-70.

Conostichus sp. (GSC loc. C-52185), *Planolites* sp. (GSC loc. C-59010), ?*Phycodes* sp. (GSC loc. C-59010), and ?*Arenicolites* sp. (GSC loc. C-58531). This assemblage is assignable to Seilacher's (1967, 1978) *Cruziana* association.

Individual coarsening-upward sequences become more resistant and proximal in aspect upward. Those that are best developed have a recessive basal division of shale lithofacies and an upper resistant interval consisting of sandstone and siltstone. Most other sequences resemble the upper division

only. Where stacked, the recessive bases of these sequences generally grade downward into the upper resistant strata of an underlying sequence through 20 cm or less. Lenses and very thin beds of sandstone and siltstone become more abundant upward through the shale of the lower division as it grades into the more resistant upper part of the sequence. The upper parts of these sequences are mainly thin to medium bedded (3-30 cm), but thick beds (>30 cm) occur in some and bedding planes are commonly undulatory and erosional. Within the upper division, proportions of shale and mudstone decrease upward, and the beds become thicker and coarser grained. Also, the scale of crossbedding increases, and trace fossils become less abundant. Small-scale crossbedding (Fig. 29) generally predominates in the upper division of most sequences, but wavy lamination is common in lower beds. Both wave- and current-generated, small-scale crossbedding are present. Criteria that de Raaf et al. (1977) provided were used to identify the former. Medium- to large-scale crossbedding (Fig. 30) predominates in the upper parts of the upper division in some thicker sequences; this is mainly trough crossbedding, although tabular sets do occur. Some large-scale sets contain reactivation surfaces and drapes. Because of their similarity to the tidal deposits that Johnson (1978) discussed, it is suggested that tidal currents influenced their formation. A few beds in the upper division of some sequences are probably storm deposits, and they resemble storm beds described by Johnson (1978, p. 251, 252). These beds have erosional bases, and they are either massive to crudely stratified, or have a lower, massive interval and upper, crossbedded deposits. Finally, mudstone flasers and drapes may occur throughout the upper part of the sequences, and intraclasts produced by their erosion are locally common.

Environmental interpretations

Graded-bed lithofacies

Because of their similarity to sequences in siliciclastic submarine fan deposits, deposition on fan-like lobes situated on a gentle slope basinward of submarine channel systems is interpreted as being the origin of most sequences in the Jackfish Gap region that become more resistant upward (Fig. 23). The gradual progradation and aggradation of such lobes has generally been interpreted as the origin of coarsening- and thickening-upward sequences like those in the Yohin. On submarine fans consisting of siliciclastic material, fan-like lobes develop immediately basinward from fan channels (Mutti and Ricci-Lucchi, 1972; Mutti, 1974, 1977; Ricci-Lucchi, 1975; Walker and Mutti, 1973). Subsequent basinward progradation of the channels is interpreted as having produced channelled deposits that commonly overlie this type of sequence (Walker and Mutti, 1973, p. 143; Walker, 1976, p. 32, 33; 1978).

Multibed sequences, which become more resistant upward and resemble those discussed above, occur in the graded-bed lithofacies at Twisted and Bluefish mountains (Fig. 13). Their origin, however, appears to be related to the progradation of shelf deposits instead of lobes on submarine fans and slopes. They are probably not fan deposits because the crossbedded sandstone lithofacies, which was deposited in neritic and possible tidal flat environments, directly overlies them. Overlying slope lithofacies are absent. Furthermore, these sequences neither contain evidence of submarine channels nor appear to be related to them.

Because of their similarity to sequences in submarine-fan deposits, Yohin sequences that become less resistant upward (Figs. 26, 80) are interpreted as the result of channel abandonment and subsequent reduced deposition rates on

related interchannel areas and fan-like lobes. Sequences of this type are the opposite of those that become more resistant upward; consequently they are interpreted as the result of progressive abandonment instead of progradation. Fining- and thinning-upward trends are common in channel fills of siliciclastic submarine fan deposits, and they are generally interpreted as resulting from deposition under conditions of gradual channel abandonment (Mutti and Ghibaudo, 1972; Ricci-Lucci, 1975; Mutti, 1977; Walker and Mutti, 1973). Based on these considerations, it appears probable that upward trends in the resistant, basal, channelled portions of the Yohin sequences resulted from abandonment of channels on a fan. Because of their distal aspect and similarity to interchannel deposits and strata deposited on fan-like lobes basinward of channels, recessive intervals above the channelled component of fining-upward Yohin sequences probably record deposition on either lobes or in interchannel settings.

Turbidity currents, generated on slopes by slumping, probably deposited most of the turbidites documented in the geological record (Hamblin and Walker, 1979, p. 1684). However, sediment gravity flows generated by this process probably did not form many of the sharp-based, graded beds at Bluefish and Twisted mountains. Evidence of a slope suitable for the generation of turbidity currents by slumping is lacking in the Yohin of that area. In fact, shallow-neritic deposits of the Yohin crossbedded sandstone lithofacies gradationally overlie the graded bed lithofacies, and intervening slope deposits are lacking. A basin slope with a low gradient possibly existed basinward of the shelf environment on which the crossbedded sandstone lithofacies was deposited. If present, the slope was chiefly a site of graded bed deposition rather than one of turbidity current generation. This is indicated by the close spatial relationship between the graded bed and the crossbedded sandstone lithofacies, and the apparent lack of slumps, slump scars, and channel systems in these facies. In the absence of an obvious slope, the shelf would have been the depositional setting of the graded beds. Finally, unlike turbidites deposited in relatively deep toe-of-slope environments, the graded bed lithofacies at Bluefish and Twisted mountains was deposited in moderately shallow water.

It is preferable to classify the graded beds at Bluefish and Twisted mountains as shallow marine, graded beds or tempestites instead of turbidites. Field evidence, given in previous paragraphs, indicates that the Yohin graded-bed lithofacies in this region was deposited in a relatively shallow marine setting. The upper Fernie Formation of western Canada contains similar deposits and was deposited in a comparable environment (Hamblin and Walker, 1979). Hamblin and Walker stated that density currents generated by storms probably deposited the turbidites of the upper Fernie, and they developed a model to explain the genesis of the currents. Moreover, the work of Anderton (1976), Hayes (1967), Nelson (1982), and others indicates that the storm generation of shallow marine, graded beds is a major geological process. However, Hunter and Clifton (1982, p. 137, 138) and Nelson (1982) provided evidence that suggests storm related processes other than density currents can produce shallow marine, turbidite-like beds. In order for a deposit to be a turbidite, it must have been deposited by a density current. It is, therefore, probably inappropriate to use the genetic term turbidite for the shallow marine, graded beds at Bluefish and Twisted mountains.

In conclusion, the graded-bed lithofacies of the Yohin Formation was probably deposited in two different and possibly unrelated environments. For reasons given above, this facies, in the vicinity of Bluefish and Twisted mountains, is interpreted as having been deposited largely by storm

generated currents in relatively shallow water on either a gentle basin slope or the basinward margin of a shallow marine shelf. With the possible exception of the uppermost beds, most of the Yohin graded-bed lithofacies in the Jackfish Gap area (Figs. 23, 26, 80) was probably deposited on a submarine-fan complex in moderately deep water on the basin slope and at its base. Evidence for a submarine-fan system is the abundance of probable submarine-channel fills and related progradational thickening- and coarsening-upward sequences that are characteristic of fan-like lobes deposited basinward of channel systems on submarine fans. Submarine fans composed of siliciclastic deposits typically develop in a base-of-slope setting, where a decreased gradient promotes deposition (see Walker and Mutti, 1973; Walker, 1979; Mutti, 1977). Deposition in moderately deep water (below storm wave base) is indicated by the geometry of the deposits (a fan complex), the absence of wave- and tide-generated structures, and the presence of numerous thin, undisturbed planar laminae. The lack of a calcareous epifauna and the presence of a trace fossil assemblage that has a low diversity and is dominated by grazing trails, also suggest deposition at moderate depth.

Crossbedded sandstone lithofacies

Coarsening-upward sequences in the Yohin crossbedded sandstone lithofacies resemble deposits of shallow-marine sand that Spearing (1975, p. 104-114) and Johnson (1978) have described. They are also similar to offshore and shoreface siliciclastic deposits of beaches and to some tidal flat deposits. Although the vertical sequence of rock types and stratification types in the Yohin coarsening-upward sequences is similar to those of prograding sandy shorelines (see Howard, 1972; Davidson-Arnott and Greenwood, 1976; Harms, 1975b; Elliott, 1978b), major differences occur. For example, desiccation structures, fluvial and floodplain deposits, aeolian deposits, and other evidence of emergence do not appear to be present either in or above any of the Yohin sequences. Instead, offshore marine shale and mudstone underlie and overlie the sandstone intervals in these sequences. In addition, the sequences resemble only the offshore and shoreface deposits of beaches because the low-angle to horizontal stratification characteristic of the foreshore environment of beaches (Clifton, 1969; Clifton et al., 1971) is absent. Suspension mud layers are rare in the foreshore or upper shoreface deposits of most beach sequences (Spearing, 1975, p. 114), but they are common in many tidal flat deposits and in most Yohin sequences, including their upper parts. In conclusion, the coarsening-upward sequences in the crossbedded sandstone lithofacies of the Yohin are interpreted as having been deposited mainly in neritic, offshore environments. Some deposits of tidal flat origin are possibly present, but definite evidence of emergence was not observed.

The thin, sheet-like units of sandstone and siltstone that have sharp bases and are intercalated with the shale lithofacies are of uncertain depositional origin. These units occur locally in much of the upper two thirds of the Yohin Formation, but they are best developed near the middle of the formation at Twisted Mountain, and in its upper part at Locality 3. Hummocky bedding is locally evident in some, but small-scale crossbedding appears to be the principal primary sedimentary structure in most beds that were not strongly bioturbated. These resistant units were produced by the episodic deposition of sand and silt in an environment where mud was normally deposited. Deposition in a neritic setting is indicated by the primary sedimentary structures and close association with progradational coarsening-upward sequences, which are characteristic of shallow-neritic environments. The sharp bases, locally with load casts, suggest deposition at least in part by storm generated currents.

The Yohin crossbedded sandstone lithofacies is interpreted as having been deposited in a shallow, sublittoral environment on a broad, progradational marine shelf that had a gentle paleoslope inclined to the west or southwest. This is probably the most regressive lithofacies in the Lower Carboniferous succession below the delta deposits of the Mattson Formation, and it prograded basinward over the progradational deposits of the Yohin graded-bed lithofacies. Deposition in the shallow-neritic zone is indicated by the common occurrence of stratification sequences, particularly coarsening-upward sequences, which are characteristic of the shallow-neritic zone on marine shelves. It is also indicated by the presence of a trace fossil assemblage assignable to Seilacher's (1967, 1978) *Cruziana* association, which is considered diagnostic of shallow-sublittoral shelf deposits. This facies is preserved between Bluefish Mountain and Jackfish Gap, which are separated by a distance of 27.5 km in a direction that is probably subperpendicular to the depositional strike. The distribution of this lithofacies demonstrates that the shelf was broad. Also, the apparent width of the shelf and the lack of rapid facies changes across it toward the basin suggest that the gradient of the paleoslope was low. During deposition of the Yohin, the paleobasin was either west or southwest of the Jackfish Gap area. Evidence for this is the decrease in thickness of the crossbedded sandstone lithofacies toward the southwest, and the spatial relationship between the Yohin and the dark-shale lithofacies of the Besa River Formation to the west.

Water depths began to increase in the area during deposition of the uppermost Yohin Formation. In the region northeast of Jackfish Gap, deposits in the crossbedded sandstone lithofacies that are of most shallow water aspect occur between 15 and 70 m below the top of the Yohin. Also, the overlying Clausen Formation consists mainly of greyish black marine shale. Similar black shale is often formed in marine environments during transgression maxima (Wetzel, 1982). According to Vail et al. (1977b, Fig. 1), sea level was rising eustatically. Therefore, rising global sea level and a corresponding reduction in sedimentation rates probably contributed to this deepening. However, increased tectonic subsidence was possibly a more important factor than a eustatic rise because global sea level was apparently rising at a constant rate throughout the deposition of the Yohin, without causing any apparent increase in the depth of water prior to deposition of the uppermost Yohin.

Shoaling-upward depositional episode

Below the uppermost Yohin Formation, the lithofacies of the Yohin and the underlying dark-shale lithofacies of the upper Besa River and upper Banff(?) formations form a megasequence that becomes more proximal and resistant upward (Fig. 13). This sequence records a transition from shale deposition in the moderately deep water of an extensive basin to the formation of crossbedded sandstone in the shallow-neritic zone and, possibly, tidal flat environments on a marine shelf. The sequence correlates with a similar, coeval succession in the Banff Formation on the interior platform (Figs. 5, 6), and together they record a major episode of shoaling. Because global sea level was rising (Vail et al., 1977b, Fig. 1), uplift in the source areas of the siliciclastic material and possible low tectonic subsidence rates in the basin are tentatively interpreted as the main causes of this decrease in water depth, until the reversal (referred to above) to increasing tectonic subsidence and water depth during deposition of the uppermost Yohin.

Age

Most of the Yohin Formation is probably of early Tournaisian to late middle Tournaisian (late Tn1b to Tn2) age (Fig. 3), but slightly younger strata are possibly present in the uppermost Yohin. Conodonts that are probably assignable to the *Siphonodella duplicata* Zone (Collinson et al., 1962) of early Tournaisian (late Tn1b) age (earliest Carboniferous) were collected from 12.2 m above the base of the Yohin at Bluefish Mountain (Appendix C). Strata at a slightly higher stratigraphic position in the lower Yohin at Twisted Mountain contain conodonts that are of early middle Tournaisian (Tn2) age and assignable to the Lower *Siphonodella crenulata* Zone of Voges (1959, 1960). Palynomorphs of middle Tournaisian to possibly early late Tournaisian (Tn2 to Tn3) age were collected from the upper Yohin at Twisted Mountain and Jackfish Gap (Appendix F).

PEKISKO FORMATION

Type section and previous work

Douglas (1958, p. 39) proposed the name Pekisko Formation and established its type section. The type section is between 2398.8 and 2551.2 m (7870-8370 ft) in the Anglo Canadian Devonian test well (LSD 2, Sec. 25, Tp. 19, Rge. 3, W5) Turner Valley oil field, southwestern Alberta.

The Pekisko of the project area (Figs. 2, 3, 5, 6) has received little study. The unit that is assigned to the Pekisko was included in the Flett Formation by Douglas and Norris (1976c).

Distribution and thickness

In the project area, the Pekisko Formation is a thin unit (Table 1) that is present on most of the interior platform south of latitude 60°35'N and east of longitude 123°30'W (Figs. 5, 6). Also, a unit that I tentatively assign to the Pekisko is present in the Mackenzie fold belt southeast of Locality 12. The thickest section encountered is at the Pan American Home Signal C.S.P. Celibeta No. 7 well (Fig. 1, Loc. 20), which intersects 32.6 m of Pekisko. Toward the north and west, the Pekisko thins gradually beneath the Clausen Formation, but north of the sub-Cretaceous zero-edge of the Clausen it thins rapidly to zero.

Lithostratigraphic relationships

In the District of Mackenzie, the Pekisko Formation overlies the Banff Formation and probably the Besa River Formation (Figs. 5, 6). Characteristics of the Pekisko/Banff boundary are given in the discussion on lithostratigraphic relationships of the Banff. Limited data suggest that the Pekisko locally overlies the Besa River Formation (Figs. 5, 6), and that at Locality 12 this contact is gradational through about one metre.

The Pekisko is generally conformably overlain by the Clausen Formation, but north of the Clausen erosional zero-edge, it is disconformably overlain by the Fort Saint John Group of Early Cretaceous age. In most of the area, the Pekisko probably grades up into the Clausen through two metres or less; however, in the vicinity of the Home signal C.S.P. Celibeta No. 7 well (Fig. 1, Loc. 2), the transition zone is several metres thick. Toward the west, the Pekisko appears to grade laterally into the Besa River Formation.

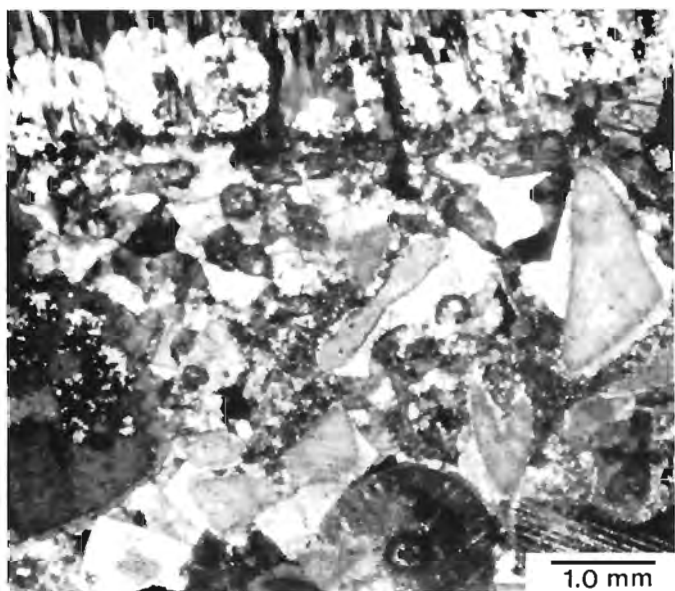


Figure 31. Photomicrograph of cherty, dolomitic bryozoan-pelmatozoan lime grainstone (GSC loc. C-52369) from the Pekisko(?) Formation at Locality 12. Pelmatozoan ossicles have monocrystalline syntaxial overgrowths. Brachiopod fragment (at top) contains fans of quartzine. ISPG 1768-39.

Because the Pekisko is mostly limestone and the basal Clausen is mainly shale, the top of the Pekisko coincides with strong inflections on gamma ray and sonic logs.

Lithology

The Pekisko consists of medium grey to light olive-grey, skeletal lime grainstone (Fig. 31) and packstone with subordinate shale. Pelmatozoan ossicles are generally the most abundant allochem, and brachiopods, bryozoans, and ostracods are moderately common. At Locality 24 and in some well sections east of the project area, some lime grainstone is oolitic, and beds of ooid lime grainstone occur locally. In the southeastern Liard Range, dolomitic and spicule-rich lime packstone is present in a unit that I tentatively assign to the Pekisko (Fig. 5).

Environmental interpretations

Because of the lithology of its strata and its spatial relationship to regional lithofacies belts, the Pekisko Formation is tentatively interpreted as having been mainly deposited on the shelf margin and slope of a carbonate buildup (ramp deposits grading into platform deposits, Fig. 87). On the interior platform, much of this unit is skeletal lime grainstone, therefore deposition in that area probably occurred mostly in the shallow-neritic zone on the shelf, where lime-mud matrix could have been removed. This conclusion is supported by the presence of abundant ooids in some beds. Moreover, limestone in the Pekisko on the platform north of latitude 60°00'N resembles Pekisko limestone in western Alberta, where much of it was deposited on high-energy shoals (Macqueen et al., 1972). On the interior platform, south of about 60°15'N, the proportion of shale in the Pekisko increases toward the east and the former strand line. This suggests that the Pekisko limestone intertongued eastward with lithofacies deposited in lower

energy shelf environments. The shallow water carbonates grade westward or basinward into spicule-rich limestone, like that in the slope facies of the Flett and Prophet formations, and then into dark-coloured, deep water Besa River strata. These interpretations are consistent with those of Bamber et al. (1984), who interpreted the Pekisko as an association of carbonate-platform lithofacies.

The ooid-bearing lime grainstone that occurs in the Pekisko Formation at Locality 24, and in some well sections east of the project area, was probably deposited on the landward part of the shelf margin (Fig. 87a). Regional studies of the Rundle Group in southwestern Alberta (Richards et al., in press; Speranza, 1984) indicate that ooids are generally rare in strata deposited on the seaward part of the shelf margin, but are commonly abundant in facies deposited on the landward part of the shelf margin.

The Pekisko Formation of the project area probably was deposited during a transgression. The presence of clean Pekisko limestone above the siliciclastic rocks of the Banff Formation suggests that sand-bearing coastal deposits were farther east during deposition of the Pekisko than during sedimentation of the uppermost Banff. Coeval deposits in the lower Clausen Formation north of 61°00'N were also deposited during a transgression. Moreover, in western Alberta, and northeastern British Columbia south of the Peace River Embayment, the lower to middle Pekisko was deposited in association with a major, regional transgression (Richards et al., in press; Illing, 1959). In these areas, Pekisko skeletal to ooid lime grainstone of shelf margin to protected shelf aspect commonly disconformably overlies restricted shelf deposits in the upper Banff.

Age

In the project area, fossils suitable for precise dating have not been collected from either the Pekisko Formation or immediately adjacent strata; consequently, the age of the Pekisko is uncertain. It is tentatively interpreted as late middle Tournaisian (Tn2) in age, but early late Tournaisian (Tn3) strata could be present because spores of middle and possibly late Tournaisian age (Tn2 to Tn3) occur in the underlying Banff Formation. Bamber and Mamet (1978, p. 4, 5) interpreted the Pekisko in the subsurface of northeastern British Columbia as mainly of middle Tournaisian (Tn2) age (Fig. 3). However, the upper Pekisko in the Carboniferous outcrop belt of northeastern British Columbia is generally of early late Tournaisian (Tn3) age (pers. comm.; Bamber and Higgins, 1981). The age of the basal Pekisko is similar throughout most of its area of distribution, but the upper Pekisko becomes progressively older toward the north and east because of depositional thinning (Figs. 3, 6; pers. comm., Bamber, 1981). Consequently, because this unit is very thin north of latitude 60°00'N, Pekisko strata of late Tournaisian (Tn3) age are probably not present in that region.

CLAUSEN FORMATION

Type section

Harker (1961, p. 3) proposed the name Clausen Formation and established its type section (Fig. 4, Jackfish Gap section; Figs. 24, 32), which is located on the west side of Yohin Ridge immediately north of Jackfish Gap (Fig. 1, Loc. 4). The locality is about 32 km west of Nahanni Butte, in the the Twisted Mountain map area (NTS 95 F/4), at latitude 61°05'54"N, and longitude 123°59'26"W, in the southwestern District of Mackenzie.

Previous work

The Clausen Formation corresponds to Patton's (1958, p. 312) Unit 2 at Jackfish Gap, and Map unit 6 of Douglas and Norris (1959, p. 10). Furthermore, it is synonymous with most of Map unit 31 of Douglas and Norris (1960, p. 30), who mapped the unit in the Virginia Falls and Sibbeston Lake map areas of southwestern District of Mackenzie.

An interval that I reassign to the Clausen Formation was included by Harker (1963, p. 47, 48, 61, 62) in the Flett Formation at Twisted and Bluefish mountains. The Clausen corresponds to the interval between 129.4 and 263.8 m in the Twisted Mountain section on Figure 4. Moreover, the unit that Harker (1963, p. 60, 61) assigned to the Clausen at Bluefish Mountain underlies instead of overlies the Yohin Formation, and it is provisionally assigned here to the Banff Formation (Fig. 4, Bluefish Mountain, 206.7–413.7 m). At Twisted Mountain, Douglas et al. (1963) and Douglas and Norris (1976c) used Harker's formational assignments. Also, the unit on the interior platform that I reassign to the Clausen (Figs. 5, 6) was included in the Flett Formation by Douglas and Norris (1976a).

Distribution

The Clausen Formation; is widely distributed in the project area (Figs. 4–6). In the Mackenzie fold belt, it outcrops in the southeastern Liard Range and in the region north of about 60°55'N. North of 60°55'N, its distribution coincides with that of the underlying Yohin Formation because the Clausen cannot be differentiated from other underlying formations where the Yohin is absent. To the south, its distribution coincides with that of the underlying Pekisko Formation. In the fold belt, the poorly exposed, recessive Clausen is preserved chiefly in several broad anticlines and synclines, and outcrops are confined to narrow belts on the limbs and noses of these structures. On the interior platform, the Clausen is a subsurface unit and is present in most of the area south of about latitude 60°35'N.

The distribution of the Clausen Formation, as discussed in this report, differs slightly from that reported by Harker (1963), Douglas et al. (1963), and Douglas and Norris (1976a, b, c). The unit that Harker (1963, p. 9), Douglas et al. (1963), and Douglas and Norris (1976b) assigned to the Clausen north of the Tlogotsho Plateau is reassigned here to the Besa River Formation. The Yohin, which defines the base of the Clausen, is absent in that area (Fig. 4). Also, the Clausen outcrops at Twisted Mountain, where it was included in the Flett Formation by Harker (1963), Douglas et al. (1963), and Douglas and Norris (1976c).

Thickness

The Clausen Formation is moderately thick (Table 1) and thins toward the east (Figs. 4–6). Its stratotype is 193.2 m thick, and at Twisted Mountain, 21.5 km northeastward, the Clausen is 134.4 m thick. Similarly, in the Texaco N.F.A. Bovie Lake J-72 well (Fig. 1, Loc. 21), the Clausen is 111.3 m thick; whereas at Locality 20, which is 20.5 km farther east, it is only 28.4 m thick.

Lithostratigraphic relationships

The Clausen Formation, which conformably overlies either the Yohin or Pekisko formations, is separated from the Besa River Formation by vertical cutoffs (Figs. 4–6). Boundaries between the Clausen and the two underlying units

are discussed in the sections describing the lithostratigraphic relationships of the Yohin and Pekisko. The Clausen is a tongue of the lithosome that includes most of the Besa River Formation. Cutoffs that separate the Clausen from that formation coincide with the western depositional limits of the Yohin and Pekisko.

Throughout most of the area, the Clausen is conformably overlain by the Prophet Formation (Figs. 4–6), but north of Twisted Mountain it is possibly overlain by the Flett Formation. The Clausen grades into the Prophet through 50 cm or more and, toward that contact, shale in the upper Clausen generally becomes calcareous and spiculitic. At the Clausen type locality (Figs. 24, 32), the base of the lowest bed of spiculite defines the Clausen/Prophet contact (Fig. 4). However, at other localities where this contact was examined, the Clausen contains widely separated intervals of spiculite, siltstone, and limestone. At those sites, the Clausen/Prophet contact is generally placed at a stratigraphic level above which spiculite and limestone constitute more than 30 per cent of the succession.

Lithology

Shale and mudstone constitute most of the Clausen Formation, but widely separated units of spiculite, limestone, and siltstone occur (Figs. 4–6, 24). In general, proportions of spiculite and limestone increase toward the top of the formation and the east. Siltstone was observed at Localities 2 and 25.

Shale (Fig. 33) and mudstone in the Clausen Formation are dark coloured, noncalcareous to calcareous, slightly pyritic, and generally sparsely fossiliferous. The shale is mostly greyish black to olive-black, whereas the mudstone is medium-dark grey. Both lithologies commonly weather moderate brown. Most of the shale splits into paper thin sheets, and the mudstone is friable to rubbly. Scattered sponge spicules and chonetid brachiopods are the main invertebrate fossils in most of the shale and mudstone, and they are generally most common near the top of the formation. Ammonites and other poorly preserved brachiopods are rare. The shale is clay-sized sediment with minor silt, whereas the mudstone is generally very silty. Semiquantitative X-ray analyses of two representative shale and mudstone samples show that quartz is the most abundant mineral present (Appendix G).

Siltstone in the Clausen Formation is sandy, calcareous to dolomitic, submature, fossiliferous subchertarenite. It is chiefly medium-dark grey, greyish orange to moderate yellowish brown weathering, and similar to siltstone in the Yohin Formation. Sponge spicules are the principal bioclasts. Quartz constitutes 88 to 92 per cent of the clasts, and chert forms 6 to 10 per cent. Other clasts include mudstone and minor mica, feldspar, and heavy minerals. Ferroan calcite and dolomite are the principal cements.

The Clausen spiculite and spicule-lime-packstone resembles that of the Prophet Formation (Figs. 36a, 44). Sponge spicules, replaced mainly by ferroan calcite and chert, are the main allochems and are commonly almost the only bioclasts. The spicules generally occur in a dark, argillaceous to siliceous and calcareous matrix, which commonly contains finely crystalline dolomite. These rocks are mostly silty, medium-dark grey, and greyish orange weathering.

Mixed-skeletal lime packstone and lime grainstone in the Clausen Formation (Fig. 34) are light olive-grey to medium-dark grey, greyish orange weathering, dolomitic, and



Figure 32. The Clausen, Prophet, and Flett formations at Jackfish Gap. Lower and upper arrows indicate the top of the type Clausen and the Prophet-Flett contact, respectively. The Prophet (127 m thick) consists of intercalated dark-shale lithofacies and spiculite and spicule-lime-packstone lithofacies. North side of a concave-upward truncation surface is evident in the Flett; view is northeastward. ISPG 798-170.

locally slightly cherty. Pelmatozoan ossicles, intraclasts, sponge spicules, and brachiopods are the most abundant allochems. The proportion of sponge spicules commonly increases upward within beds at Twisted Mountain. Bioclasts are mainly sand to granule size, fragmentary and abraded. The intraclasts, mainly skeletal lime packstone and wackestone, are irregular to tabular and range from sand size to several centimetres across. Minor quartz silt and sand occur, and microspar and pseudospar form most of the matrix. Chert, mainly microquartz, occurs as a nonselective replacement. Dolomite, which is mainly strongly ferroan, medium crystalline, and subhedral to anhedral, has locally replaced allochems and to a greater extent calcite cement and matrix in these rocks at Twisted Mountain.

Passively precipitated, sparry, calcite cement fabrics in the Clausen limestone include: monocrystalline syntaxial overgrowths on pelmatozoan fragments; pore-filling mosaics of fine to medium crystalline, subequant crystals; and fine to medium crystalline, equant to bladed, polycrystalline fringes chiefly on brachiopod material. The syntaxial overgrowths are generally most voluminous. In samples from Twisted Mountain, these overgrowths commonly comprise both early, nonferroan, and later, strongly ferroan generations. Most of these cements were probably precipitated in the meteoric-phreatic and subsurface precipitational zones of Folk (1973; 1974a, p. 45) (Fig. 19). Similar origins are proposed for the same types of cement fabrics in the Yohin and Flett formations, and reasons for favoring such environments are presented in discussions of those units.

Lithofacies

The Clausen Formation comprises a dark-shale lithofacies (Figs. 24, 33) and minor units of the lime-grainstone and packstone, the spiculite, and the siltstone

lithofacies. Toward the east, proportions of the lime-grainstone and packstone facies and the spiculite facies increase.

Dark-shale lithofacies

The Clausen dark-shale lithofacies (Figs. 24, 33), which is principally calcareous to noncalcareous shale and mudstone, is part of the shale lithosome that constitutes most of the Besa River Formation, and it occurs as eastward-thinning tongues of that lithosome. Units of other Clausen facies, particularly the spiculite lithofacies, are intercalated with the dark-shale lithofacies at most locations. Crossbedded, shallow-neritic sandstone of the Yohin Formation underlies this facies in the region east of Jackfish Gap, whereas, to the west, the Yohin graded bed lithofacies probably underlies it. On the interior platform and in the southeastern Liard Range, carbonate platform facies in the Pekisko Formation underlie the dark-shale lithofacies. The Prophet spiculite and spicule-lime-packstone lithofacies, deposited mainly on the lower slopes of carbonate buildups (mainly platform deposits, Fig. 87a), gradationally overlies this Clausen lithofacies.

Planar laminae are the principal sedimentary structures in the relatively homogeneous shale and mudstone of the dark-shale lithofacies (Fig. 33). Elliptical ironstone concretions, which locally contain well preserved ammonites (GSC loc. C-59019), are moderately common. Also, abundant masses of calcite cone-in-cone, up to 1 m across, are present in the upper Clausen at Jackfish Gap. Evidence of minor bioturbation is locally present, but *Phycodes?* sp. (GSC loc. C-74347) and *Zoophycos* sp. were the only lebensspüren observed.



Figure 33. Concretion-bearing shale of the dark-shale lithofacies, in type section of the Clausen Formation at Jackfish Gap. ISPG 1303-18.

Spiculite lithofacies

Units of spiculite lithofacies are present throughout most of the Clausen Formation on the interior platform, and they outcrop as widely separated cliffs and ledges in the Mackenzie fold belt. Toward the east, units of this facies, which are generally interbedded with the Clausen dark-shale lithofacies, commonly become more abundant. Spiculite and spicule lime packstone constitute most of the spiculite lithofacies, but minor dolostone and shale occur locally.

Units of spiculite lithofacies range in thickness from less than 0.5 to more than 20 m, are mainly thin to medium bedded (3-30 cm), and occur as westward thinning sheets. These units usually grade into underlying shale and mudstone, become more resistant and proximal in aspect upward, and have relatively abrupt tops; but some have sharp bases. Individual beds are planar to slightly wavy and have moderate lateral continuity, but their primary, internal sedimentary structures and fabrics are generally poorly preserved. Wavy to wispy, discontinuous laminae are the dominant structures within beds. An indistinct structure that resembles poorly developed, small-scale crossbedding exists in some beds. Also, thin, deformed intervals produced by soft-sediment deformation are moderately common. Most beds were intensively bioturbated, but *Zoophycos* sp. was the only ichnogenus identified.

Lime-grainstone and packstone lithofacies

The lime-grainstone and packstone lithofacies occurs as units in the lower Clausen on the interior platform and in the Twisted Mountain area (Figs. 4-6). In these areas the Clausen dark-shale lithofacies underlies and overlies these deposits. Mixed-skeletal lime grainstone (Fig. 34) and lime packstone are the main rock types, but subordinate spiculite is present in some units.

In the outcrop belt, the lime-grainstone and packstone lithofacies was examined at Twisted Mountain (Fig. 4). At that locality, it forms a sharp-based, 8 m thick, medium- and rhythmically-bedded unit in the lower Clausen. Individual beds in that unit commonly have sharp bases with load casts, crude normal grading, a resistant, unstratified to indistinctly stratified lower division, and an upper, recessive, platy division. These beds resemble some turbidites because they have a basal component and an upper component that resemble the A and D to E divisions in the standard Bouma sequence, respectively. In addition, they are similar to probable tempestites in the upper Flett Formation. The origin of these beds is discussed under environmental interpretations.

Siltstone lithofacies

The siltstone lithofacies is the least voluminous facies in the Clausen Formation. It was studied in the outcrop belt at Twisted Mountain, where it forms a moderately resistant, 4.5 m thick unit that occurs 50.1 m above the base of the Clausen and between units of dark shale (Fig. 4). Calcareous siltstone with subordinate sandstone and mudstone make up this lithofacies. Harker (1963, p. 61, Unit 27) indicated that similar deposits occur at Bluefish Mountain in a unit that I reassign to the Clausen. Minor units of this lithofacies are also present in the subsurface at Locality 25.

Poorly defined, very thin to thin (1-10 cm), wavy beds characterize the unit of siltstone lithofacies that was examined in the lower Clausen Formation at Twisted Mountain. Internally, the beds have indistinct, small-scale crossbedding and discontinuous, argillaceous partings. A predominance of small-scale crossbedding and an apparent lack of distinct grading or Bouma sequences suggest deposition by wave related processes or bottom currents, without significant fallout from suspension.

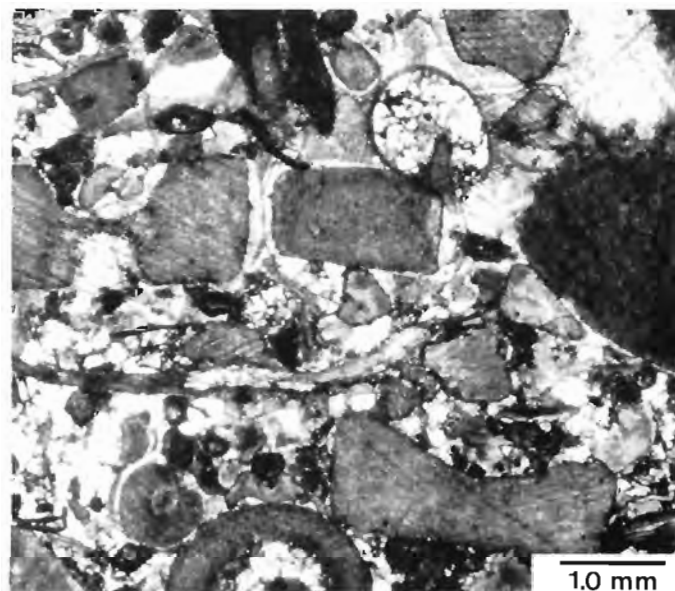


Figure 34. Photomicrograph of dolomitic pelmatozoan lime grainstone (GSC loc. C-59016) from the lower Clausen Formation at Twisted Mountain. Pelmatozoan ossicles have monocrystalline syntaxial overgrowths. ISPG 1768-48.

Environmental interpretations

Dark-shale lithofacies

Deposition in poorly oxygenated water on the eastern side of an extensive basin is suggested for most of the dark-shale lithofacies in the Clausen Formation. Byers (1977) suggested that deposits like this lithofacies commonly form in poorly oxygenated water of the dysaerobic zone (intermediate between anaerobic and well oxygenated). Bottom sediment in that zone typically lacks a calcareous epifauna, but is bioturbated by a resistant infauna dominated by vermiform organisms. Regional relationships indicate deposition of the dark-shale lithofacies as eastward thinning tongues of the basinal shale lithosome that constitutes most of the widespread Besa River Formation, which was deposited to the west at moderate depth (Pelzer, 1966, p. 306) in the axial region of a basin.

Depths at which the dark-shale lithofacies was deposited decreased eastward, but water depths probably increased throughout the area during the deposition of the thick units of this facies. Shallowing eastward, particularly during deposition of the lower Clausen Formation north of latitude 61°00'N, is indicated by a transition to lighter coloured lithologies and by increases in the proportions of siliciclastic silt, siltstone, and lime grainstone. Depths at which siliciclastic materials in the upper part of the underlying Yohin Formation were deposited also decreased toward the east. On the interior platform, easterly shallowing is indicated mainly by increases in the proportions of lime grainstone and other limestones. Shallow-neritic to possible intertidal deposits constitute much of the underlying Yohin and Pekisko formations, whereas the overlying Prophet Formation is mostly a lower-carbonate-slope lithofacies. These relationships, as well as an upward decrease in the numbers of siltstone and lime grainstone beds, suggest that the Clausen dark-shale lithofacies, and the formation as a whole, were deposited under transgressive conditions. Moreover, black shale, like that in the Clausen, is often formed during transgressions or transgressive maxima (Wetzel, 1982).

The depositional mechanism for terrigenous deposits in the dark-shale lithofacies, which has a relatively deep water aspect, is uncertain. However, for reasons similar to those given in the discussion of the dark-shale lithofacies in the Besa River Formation, most deposits in the lithofacies could be the result of deposition by dilute, gravity assisted bottom currents and hemipelagic sedimentation.

Spiculite lithofacies

Units of spiculite lithofacies are interpreted as having been deposited in moderately deep water, and some are probably related to carbonate buildups. Deposition at moderate depth is suggested by dark coloured sediment that is characteristic of deposition in the dysaerobic zone, and by the lack of fossils and primary sedimentary structures characteristic of shallow water environments. Also, Seilacher's (1967, 1978) *Zoophycos* association is present in much of this lithofacies. According to Howard (1978, p. 38, 44) and Seilacher, that association is generally typically developed in strata deposited at upper-bathyal depths. Much of the spiculite lithofacies is probably related to carbonate buildups because the resedimented bioclasts in it required a suitable provenance. Furthermore, it closely resembles lower-platform-slope lithofacies in the Prophet Formation, and on the interior platform the Clausen grades eastward into carbonate platform and ramp deposits (Figs. 6, 87).

The spiculite lithofacies possibly originated from a combination of hemipelagic sedimentation and deposition from dilute turbidity currents or similar turbid bottom currents. Deposition basinward of carbonate buildups (mainly platforms, Fig. 87a) is indicated by the spatial relationship of these deposits to regional lithofacies. A hemipelagic origin is suggested by the bioturbated, fine grained nature of much of this lithofacies. In contrast to turbidites, hemipelagites accumulate slowly and tend to be homogeneous because of bioturbation (Mutti, 1974, p. 126; Rupke and Stanley, 1974; Hesse, 1975; Rupke, 1975). However, the presence of scattered intraclasts, fragmentary macrofossils (other than spicules), and structures probably produced by traction, indicates deposition at least locally from sediment gravity flows or other currents.

Lime-grainstone and packstone lithofacies

Units of lime-grainstone and packstone lithofacies in the Bluefish-Twisted mountains region are probably erosional remnants of a carbonate buildup, possibly a platform or ramp (see Wilson, 1975, p. 21), that extended over a wider region than the Clausen Formation covers today. This is suggested by the turbidite-like beds of intraclasts and resedimented bioclasts and by their restricted distribution. Also, this limestone lithofacies in the basal Clausen is at essentially the same stratigraphic position as carbonate platform lithofacies in the Pekisko Formation on the interior platform. The Pekisko platform deposits were formerly more extensive and were possibly a source of the Clausen carbonates.

Units of lime-grainstone and packstone lithofacies in the lower Clausen Formation were probably deposited in relatively shallow water. Because these deposits are generally of proximal aspect and the stratigraphic separation between them and shallow-neritic strata in the underlying Pekisko and Yohin formations is not great, they probably would not have been deposited much below fairweather wave base.

The graded beds that occur in the lime-grainstone and packstone lithofacies at Twisted Mountain are probably tempestites. For reasons given above, these beds in the lower Clausen are interpreted as having been deposited in relatively shallow water, where storm related processes could rework the bottom sediments. These beds also closely resemble some calcareous tempestites that Aigner (1982) and others have described.

Siltstone lithofacies

The depositional mechanism and environment of the siltstone lithofacies in the lower Clausen at Twisted Mountain is uncertain. Deposition at moderate depths, possibly outer neritic, is tentatively suggested because the deposits are not of deep water aspect even though underlying and overlying units have a basinal aspect. Furthermore, these deposits resemble siltstone and sandstone units that occur in the Flett siltstone and mudstone lithofacies, and are tentatively interpreted as neritic deposits (Fig. 66a, b).

Age

The Clausen Formation is of late (Tn3) and possibly middle Tournaisian (Tn2) age (Fig. 3). Fossils suitable for precise dating were not obtained from the lower Clausen, but underlying beds in the Pekisko and uppermost Yohin formations are of middle Tournaisian (Tn2) or possibly early late Tournaisian (Tn3) age (Figs. 4-6). Palynomorphs of

probable late Tournaisian (Tn3) age occur in the middle Clausen (62.6 m above its base) at Twisted Mountain, and a similar flora is present in the middle Clausen (104.7 m above its base) at Jackfish Gap (Appendix F). The base of the overlying Prophet Formation at Twisted Mountain contains foraminifers that are of latest Tournaisian (Tn3) age and assignable to Mamet and Skipp's (1970, 1971) foraminiferal Zone 9. Also, the basal Prophet on much of the interior platform is probably of late Tournaisian (Tn3) age. Bamber and Mamet (1978, Figs. 4, 9) collected microfossils belonging to Zone 9, about 90 m above the Clausen at Jackfish Gap, but they interpreted the upper Clausen to be of early late Tournaisian (Tn3) age (zone 8).

PROPHET FORMATION

Type section

Sutherland (1958, p. 25-27) proposed the name Prophet Formation and designated its type section, which is located on Bat Creek, 8.9 km south of the Muskwa River, Trutch map area (NTS 94 G), at latitude 57°47'N, and longitude 123°37'W, in northeastern British Columbia.

The placement of the Debolt-Prophet boundary in much of northeastern British Columbia is arbitrary, because the upper part of the Prophet stratotype is equivalent to the upper Debolt Formation. Sutherland (1958, p. 25-27) subdivided the type Prophet, in ascending order, into the A, B, and C members. Unfortunately, Member C, about 45 m thick, is lithologically and stratigraphically equivalent to the upper Flett Formation of Harker (1961) and upper Debolt Formation of Macauley (1958, p. 298). Formal revision of the Prophet definition is beyond the scope of this project; however to facilitate separation of the Flett and Prophet formations in the project area, major intervals of strata that are characteristic of the Flett Formation or Member C are excluded from the Prophet in this study.

Previous work

Much of the unit I have assigned to the Prophet Formation (Figs. 2, 10, 35) was included in the Flett Formation by Harker (1961, p. 5, 6; 1963). He incorporated about 127 m of Prophet into the lower Flett type section at Jackfish Gap (Figs. 4, 24; 350.4-477.4 m). Harker's concept of the Flett was adopted by Douglas and Norris (1976a, b, c), Douglas et al. (1963), Douglas (1976), Richards (1978, p. 478), Bamber and Mamet (1978, p. 8, 9), and Bamber et al. (1980). In most of the project area, the lower one third or less of the Flett is assignable to the Prophet; however, the proportion increases westward. Near its western boundary, the entire Flett can be assigned to the Prophet.

The name Etanda Formation (Harker, 1961, p. 6) is abandoned because the type section of the Etanda comprises intervals assignable to the Prophet and Golata formations, which have priority. The Etanda type section outcrops near Etanda Lakes (Fig. 1, Loc. 8), and comprises a lower 74.2 m thick division of spiculite and dolostone with subordinate shale, and an upper 515.8 m thick division of shale and mudstone with subordinate sandstone and dolostone (Fig. 5, 0-74.2 m and 74.2-590.0 m, respectively). These two intervals are equivalent to Sutherland's (1958, p. 25-27) Prophet Formation and Halbertsma's (1959, p. 113, 114) Golata Formation, respectively.

In the Etanda Lakes area and the La Biche syncline, Harker (1961, p. 6, 7; 1963, p. 16, 17) and Douglas et al. (1963) included in the Etanda Formation strata that are assignable to the Prophet. In the same region, Douglas (1976), and Bamber et al. (1980) assigned the Etanda to the Besa River Formation.

Distribution

In the southern Mackenzie fold belt, the Prophet Formation is present in most of the project area east of the La Biche Range, and it underlies much of the Tlogotsho Plateau (Figs. 4-6). It is best exposed at the northwestern end of the Tlogotsho Plateau, where it is a cliff former (Figs. 35, 86). Elsewhere, it is generally moderately resistant to recessive and outcrops along narrow belts on the limbs of synclines and in the cores of anticlines.

Subsurface data indicate that the Prophet Formation underlies a moderately broad belt on the interior platform in the southern third of the project area (Figs. 5, 6). South of its northern, sub-Cretaceous, erosional zero-edge, which is just northeast of Locality 24, it underlies most of the platform in the project area. In addition, the Prophet is widely distributed in northeastern British Columbia (Macauley et al., 1964, p. 97, 98; Bamber et al., 1968, p. 6, 7; Bamber and Mamet, 1978, p. 8).

Thickness

North of latitude 60°00'N, the Prophet Formation is thickest in a narrow, north trending belt that is just west of the western boundary of the Flett Formation (Figs. 4, 6). This belt underlies the Tlogotsho Plateau, and to the south it is located mainly along the east side of the Kotaneelee syncline. The thickest section encountered is at Locality 18, where it is 766 m thick. Toward the southwest, it thins quite rapidly, and at Locality 19, which is 16.2 km from Locality 18, the Prophet is 90.5 m thick. The Prophet also thins relatively quickly toward the east.

Where the Flett Formation overlies the Prophet on the west side of the interior platform, the Prophet thins relatively slowly northward. For example, the Prophet is 224.6 m thick at Locality 21, but 43.5 km farther north, at Locality 25, it is 165.2 m thick. A comparable northward trend is evident where the Flett overlies the Prophet in the Mackenzie fold belt. On the interior platform, northeast of the erosional zero-edge of the overlying Flett, the Prophet thins rapidly to zero beneath the regional sub-Cretaceous disconformity.

Lithostratigraphic relationships

West of the western boundary of the Clausen Formation, the Prophet Formation conformably overlies and grades westward into the Besa River Formation (Figs. 4-6, 10). This transition begins at the base of the Prophet in the east and progresses upward toward the west. The vertical transition between the Prophet and Besa River commonly occurs through 100 m or more with spicules and spiculite in the Besa River becoming more abundant upward and toward the east. The lower boundary of the Prophet is placed at a stratigraphic level above which spiculite, siliceous spiculitic limestone, and dolostone constitute more than 30 per cent of the succession. Because chert is generally a major component in the Prophet, sonic logs commonly record a marked general decrease in interval travel time above its

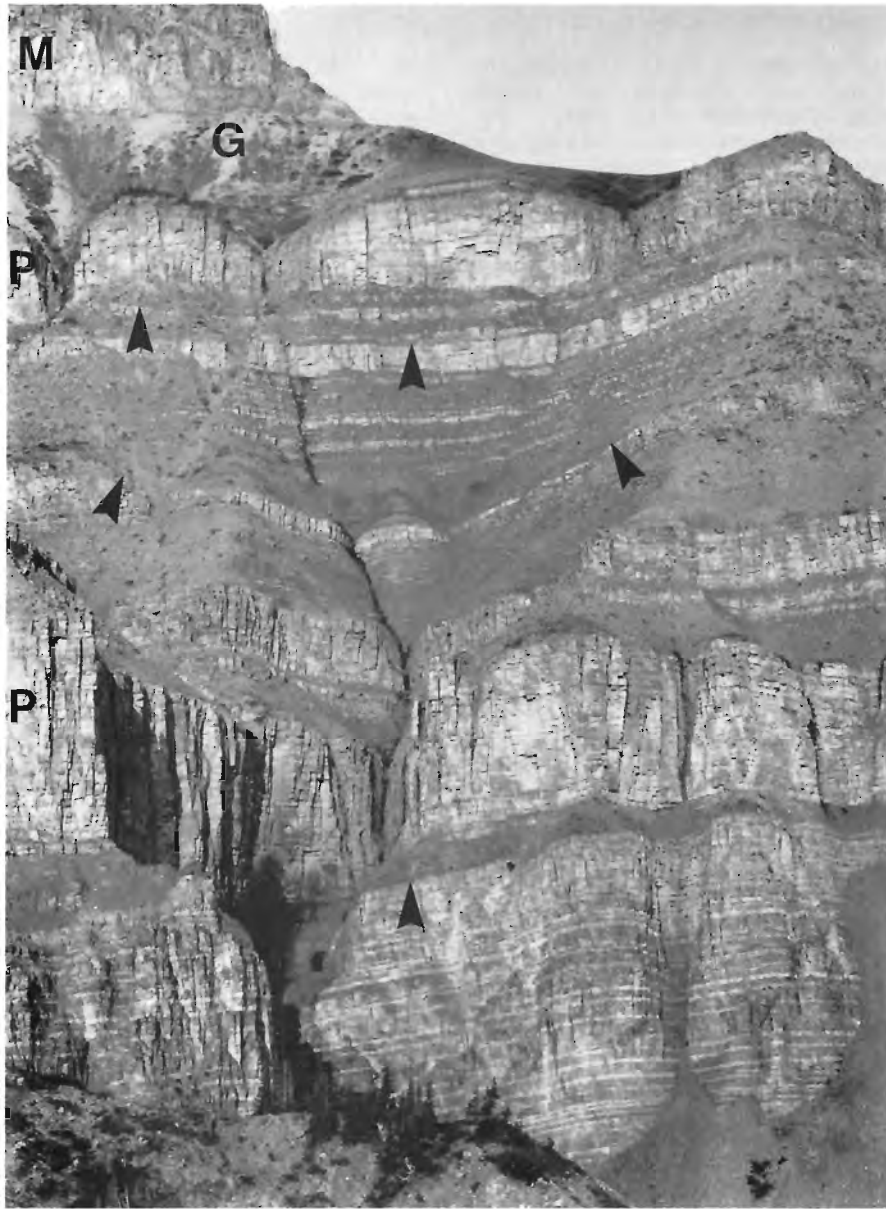


Figure 35. The Prophet (P), Golata (G), and Mattson (M) formations at Ram Creek. Upper recessive unit consists of Golata prodelta deposits (78 m thick); overlying (uppermost) cliff is Mattson deltaic sandstone. The main, lower part of the section is the Prophet Formation. Units of mixed-skeletal lime-packstone lithofacies occur in the uppermost Prophet cliff, but that formation (205 m exposed) is mainly spiculite and spicule-lime-packstone lithofacies. Large-scale truncation surfaces (arrows), and sequences that become more resistant upward, occur in the Prophet. ISPG 1756-83.

base. A corresponding decrease in radioactivity is recorded on gamma ray logs (Figs. 5, 6). Where exposed, the Prophet/Besa River contact coincides with a break in slope, because the Prophet is more resistant.

Elsewhere in the area, the Prophet Formation conformably overlies the Clausen Formation (Figs. 4-6). The Prophet/Clausen boundary is discussed in the section on the lithostratigraphic relationships of the Clausen.

Throughout much of the area in which it occurs, the Prophet Formation conformably underlies and grades eastward into the Flett Formation (Figs. 4-6). The Flett/Prophet contact becomes younger toward the west, and the uppermost Flett generally persists farthest westward. The lateral transition to the Flett, which occurs through several kilometres, is moderately well exposed along the north side of the Tlogotsho Plateau. Elsewhere, this lateral gradation occurs chiefly in the subsurface. Between the northeastern corner of the Tlogotsho Plateau and Pointed Mountain, the western limit of the Flett is in the subsurface along the east side of the Kotaneelee syncline. To the south it is in the Liard syncline. The upward transition into the Flett generally occurs through 10 m or more. A general increase in the proportions of chert, dolomite, clay- to fine silt-sized terrigenous clastics, and spicules, characterizes the Flett/Prophet gradation. Because the Prophet grades gradually into the Flett, their boundary is commonly difficult to locate.

Several criteria are used to differentiate the Prophet Formation from the Flett Formation. The Flett contains bryozoan-pelmatozoan limestone (Figs. 52b, 57) with subordinate dolostone, spicule-rich rocks, and fine grained siliciclastics. In comparison, the Prophet is chiefly spiculite (Fig. 36a), spicule-rich limestone, and shale. Chert occurs in both formations but is more abundant in the Prophet (Figs. 4-6), and most Prophet rocks are darker than those in the Flett. Sharp-based, graded laminae and thin beds (Figs. 42, 44) characterize many resistant intervals in the Prophet, whereas sharp-based, massive, ungraded to graded, and stratified beds, 10 to 50 cm thick (Figs. 58, 59a, b), constitute the majority in the lower Flett (Richards, 1983a, Pl. 22b). The Prophet/Flett contact locally coincides with a break in slope because the Flett is generally more resistant (Fig. 51). Finally, the Prophet/Flett contact is placed above a prominent shale break, which is up to 20 m thick (Figs. 5, 6) at Localities 21 and 25.

In the southeastern part of the project area, the Prophet grades eastward and upward into an unnamed formation that is here informally called Formation F. Bamber and Mamet (1978) applied the informal name "Shunda" Formation to this unnamed unit in northeastern British Columbia (Fig. 3). Only an erosional remnant of Formation F remains in the project area, where it consists of mixed-skeletal lime packstone and dolostone with subordinate shale (Figs. 5, 6). The Prophet/Formation F contact is gradational through several metres, and the transition is similar to that between the Flett and Prophet formations.

Southwest of the western depositional limit of the Flett Formation, the Golata Formation conformably overlies the Prophet (Figs. 4-6, 35). The Prophet generally grades into the Golata through 50 cm or more, and, at least locally, the boundary becomes older toward the west. The boundary is placed at a position above which shale and mudstone constitute more than 50 per cent of the succession. In outcrops this contact commonly coincides with a marked break in slope, and gamma ray well logs generally record an increase in radioactivity above it.

On the interior platform north of the erosional zero-edge of the Flett Formation, just south of Locality 24, strata of Early Cretaceous age disconformably overlie the Prophet.

Lithology

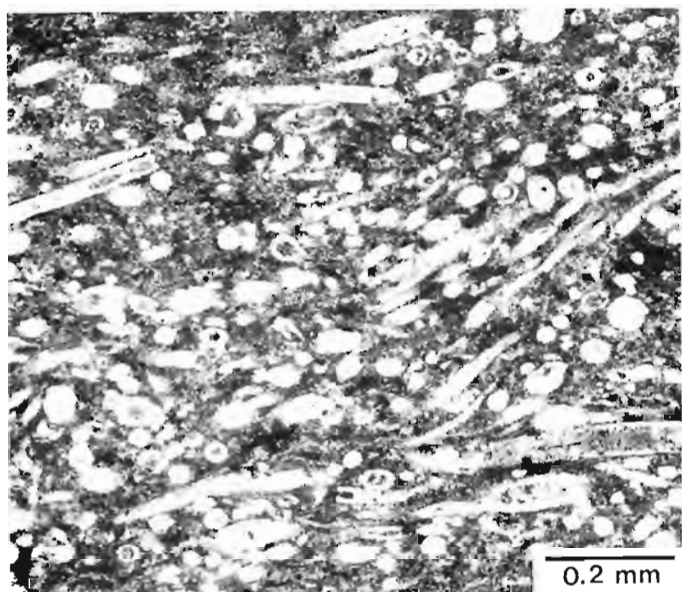
The Prophet Formation (Figs. 4-6, 35) consists of spiculite (Fig. 36a) and spicule lime packstone to wackestone with subordinate shale and mixed-skeletal lime packstone to wackestone (Fig. 36b). Minor dolostone (Fig. 36d), lime grainstone (Fig. 36c) and siltstone are also present. Spiculite and spicule lime packstone to wackestone become more abundant toward the west and the base of the Prophet, whereas mixed-skeletal limestone becomes more abundant toward the east and the upper Prophet. Shale is generally most abundant near the base of the Prophet. However, in the Mackenzie fold belt north of about latitude 60°35'N, and east of the western limit of the Flett, shale is abundant throughout most of the formation. Dolostone is locally present throughout the formation but tends to be most common near its base. Lime grainstone is locally present in the upper Prophet and was observed in the basal Prophet at Locality 20. Sandstone was observed in the upper Prophet at Localities 5 and 12.

Spiculite in the Prophet Formation is a massive to thinly laminated, cherty, sedimentary rock that is less than 50 per cent carbonate minerals by volume and has sponge spicules as its principal allochem (Fig. 36a). Quartz, mainly chert, is the most abundant mineral and forms about 48 to 93 per cent of the volume of minerals present (Appendix G). Calcite and dolomite are the other major minerals, and spiculite commonly grades into cherty limestone. At some localities, such as Ram Creek (Figs. 35, 86; Fig. 1, Loc. 6), much of this rock is essentially spiculitic chert. The spiculite is mainly dark grey to olive-black and weathers olive-grey to greyish orange.

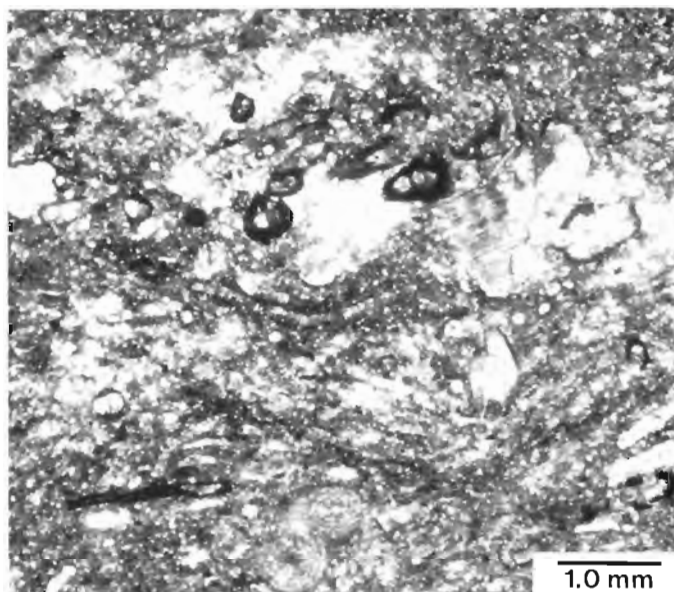
Between 80 and 99 per cent of the allochems in most spiculite are sponge spicules. Their abundance increases toward the base of the Prophet and toward the west. In most Prophet spiculite, spicules are sufficiently abundant to produce a grain-supported texture, but in many the matrix supports them. Spicules constitute greater than 30 per cent of most spiculite by volume, and locally their volume exceeds 60 per cent. In most spiculite, spicules are oriented with their long axes subparallel to the bedding as the result of compaction and depositional processes. The spiculite commonly grades into clay shale and mudstone.

In order of decreasing abundance, some or all of the following generally occur in the spiculite: pelmatozoan ossicles, bryozoans, brachiopods, and ostracods. Foraminifers, calcareous algae, fish remains, intraclasts and pellets are present in some spiculite, but are minor components. Most macrofossils are typically crushed or fragmentary and abraded.

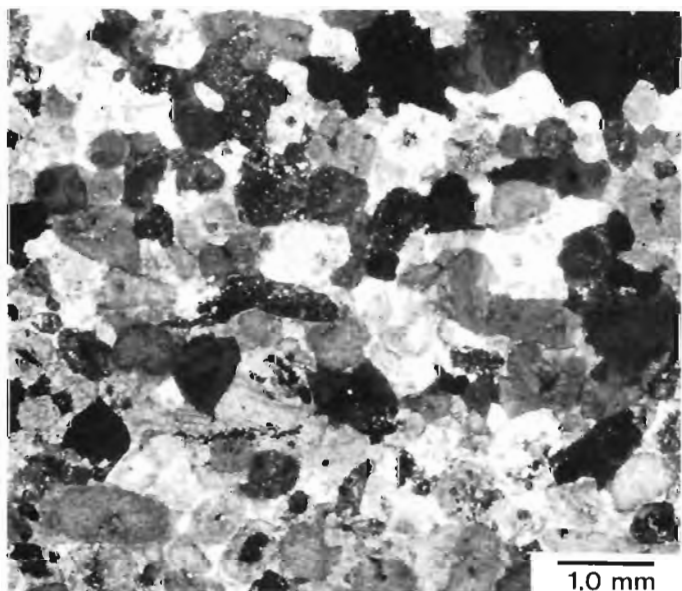
Sand, silt, and clay minerals constitute most of the terrigenous fraction in the spiculite, but mudstone intraclasts occur locally. Fine grained silt and clay, minerals that are partly replaced by chert, constitute the bulk of this fraction and the matrix in most samples. Semiquantitative X-ray analyses of nine samples (Appendix G) indicate that the matrix material is mainly quartz (chert) with subordinate clay minerals. The sand and coarse grained silt are mainly quartz and are present in most samples, but generally constitute less than 0.5 per cent of the material by volume.



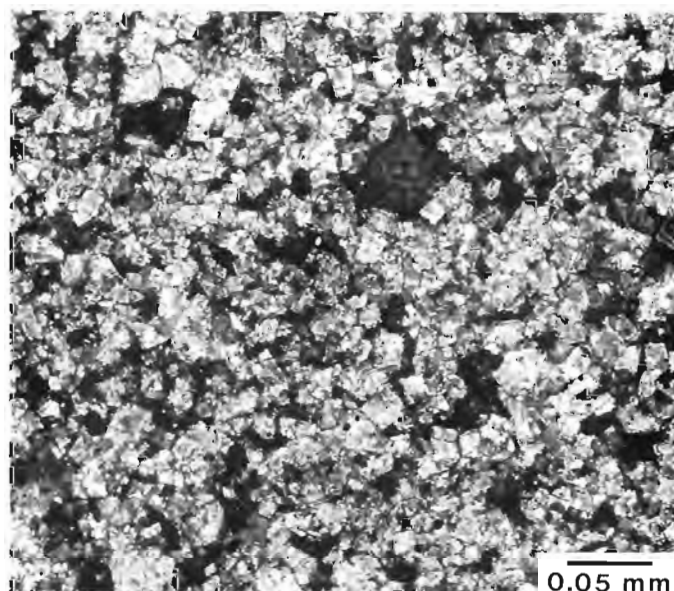
a. Cherty spiculite (GSC loc. C-58844) from the spiculite and spicule-lime-packstone lithofacies at Locality 8; taken under plane-polarized light. ISPG 1768-45.



b. Mixed-skeletal lime packstone (GSC loc. C-58960) from Locality 10. ISPG 1768-66.



c. Monocrystalline syntaxial overgrowths on pelmatozoan ossicles in pelmatozoan lime grainstone (GSC loc. C-57434F) from Locality 19. ISPG 1768-69.



d. Cherty, finely crystalline, sucrosic dolostone (GSC loc. C-58843) from Locality 8. ISPG 1768-3.

Figure 36. Photomicrographs of rocks from the Prophet Formation.

Lime packstone and wackestone in the Prophet Formation are chiefly spicule lime packstone and wackestone, but bryozoan-pelmatozoan lime packstone and wackestone are locally moderately common, and other variants occur (Fig. 36b). These limestones are chiefly olive-grey to olive-black and weather olive-grey to greyish orange. Spicules or crinoid fragments are the predominant allochems in most, and bryozoans and brachiopods are abundant in some beds. Also, foraminifers, calcareous algae, ostracods, molluscs, corals, pellets, and intraclasts (Fig. 47) are commonly present. The proportion of spicules in these limestones tends to increase toward the west, the base of the Prophet, and the tops of graded beds. Most macrofossils are fragmentary and abraded or crushed; moreover, microstylolitic contacts are common between them.

Clay, silt, sand, and mudstone intraclasts make up the terrigenous fraction in these limestones. Fine grained silt, and clay minerals, partly replaced by chert, constitute most of this fraction. Semiquantitative X-ray diffraction analyses of six representative specimens (Appendix G) indicate that this fine grained material is chiefly chalcedony or quartz and that clay minerals generally make up less than 5 per cent by volume. The sand and coarse silt are chiefly quartz and are present in most beds, although they usually constitute less than 0.5 per cent of the material by volume. Siliciclastic intraclasts of granule to pebble size are moderately common in the coarser grained limestone, but these intraclasts are relatively rare in fine grained limestone.

Lime grainstone (Figs. 36c, 39) is a minor variety of limestone in the Prophet. It is pelmatozoan and bryozoan-pelmatozoan grainstone, which weathers light greyish orange and is medium-light grey. Pelmatozoan plates are the main allochem, and locally they are almost the only allochems present. Other allochems are bryozoans, brachiopods, spicules, intraclasts, ostracods, and foraminifers. Also, shale intraclasts, up to 5 cm long, are found in some beds.

Dolostone (Fig. 36d) is a minor rock type in most of the Prophet. It is mainly sucrosic, greyish black to olive-black, and greyish orange weathering. The dolomite in it is mostly ferroan, finely crystalline, and subhedral to euhedral. Most crystals are inclusion-rich, but some are relatively inclusion-free and resemble the limpid dolomite of Folk and Land (1975, p. 65). Poorly preserved spicules are the principal allochem in most beds. Authigenic chert and cherty matrix material occur in most samples, and the dolostone commonly grades into rock that is greater than 50 per cent chert.

In the Prophet Formation, the siltstone is mainly sandy, texturally submature subchertarenite that is medium grey and weathers greyish orange to moderate yellowish brown. The sand and silt fractions are quartz with subordinate chert and mudstone rock fragments; traces of mica, feldspar, heavy minerals and opaques occur. Some beds contain fragmentary fossils, and clasts in this siltstone are generally poorly sorted. The sand clasts are chiefly subangular, but angular to very angular sand is common, and most silt is angular. Quartz and ferroan calcite are the principal cements.

Most shale and mudstone in the Prophet are siliceous to calcareous and dolomitic, slightly silty, fossiliferous, and dark grey to olive-black. The shale is chiefly clay shale that has a well developed fissility, but fissility is less well developed in the more siliceous and calcareous shale. The mudstone is friable to rubbly and platy. Semiquantitative X-ray defraction analyses (Appendix G) indicate that quartz (partly authigenic chalcedony) is the most abundant mineral and forms up to 64 per cent by volume of some samples. Clay minerals are next in abundance. Spicules are the

principal bioclasts, but pelmatozoan plates, bryozoans, brachiopods, and ostracods are locally common in the upper Prophet.

Diagenesis

Sponge spicules

Most sponge spicules in the Prophet Formation consist of authigenic chert or multicrystalline ferroan calcite (Fig. 36a), but prior to diagenesis most were probably opal. The spicules appear to be mainly monaxons, and commonly more than 50 per cent have an axial canal. According to Bergquist (1978, p. 91), the inorganic component of modern siliceous spicules is deposited around an axis of organic material, whereas an optically evident axial region is the only axial structure in calcareous spicules. Siliceous spicules are biogenic opal (opal A of Jones and Segnit, 1971) (Meyers, 1977, p. 81). Because all modern spicules that have an axial canal are opal, most spicules in the Prophet were probably opal. Spicules in the Prophet that lack a canal possibly went through a moldic stage during which the canal was destroyed. Scholle (1971, p. 243) and Meyers (1977, p. 81-84) used the same reasoning to demonstrate that chert and calcite spicules were originally opal.

Chert

Authigenic chert is a major component in Prophet Formation rocks. It is present in most beds of spiculite, limestone, and dolostone. Four varieties occur: microquartz (Folk and Weaver, 1952), length-slow chalcedony, length-fast chalcedony, and megaquartz. Michel-Lévy and Munier-Chalmas (1890, 1892) defined the three types of fibrous chert which are: chalcedonite, the length-fast variety; quartzine, a length-slow chalcedony with the C axis parallel to the fibres; and lutecite, a length-slow form with the C axis at about 30 degrees to the fibres. Chert constitutes dark grey nodules and selectively replaced matrix, carbonate cement and allochems in most Prophet rocks. In addition, much spiculite is essentially bedded chert.

Microquartz (Fig. 37), which occurs as mosaics of very fine to aphanocrystalline, anhedral, subequant crystals, is the most abundant chert in the Prophet Formation. This replacement chert occurs in most rock types, but it is most abundant in spiculite and spicule-rich lime packstone and wackestone, where it tended to preferentially replace matrix. Moreover, the chert in many spicules is also microquartz, and to varying degrees it replaced other allochems, nonferroan and ferroan calcite cement, and pseudospar. The microquartz that has replaced matrix has abundant inclusions and is pale to moderate yellowish brown in plane-polarized light, whereas that which replaced bioclasts is almost colourless.

Length-fast chalcedony or chalcedonite is probably the second most abundant chert in the Prophet and Flett formations (Fig. 53). In the Prophet, chalcedonite occurs mainly as a replacement of sponge spicules, but thin, isopachous coatings, like those found in the Flett (Fig. 53), were observed in two samples.

Length-slow chalcedony, mainly quartzine, is the least plentiful chert in the Prophet and occurs as inclusion-rich, interfering, fibrous fans (Fig. 38). This replacement chert is most common in pelmatozoan lime grainstone and packstone, where it preferentially replaced crinoid plates and thick shelled brachiopods. To a lesser extent it has replaced ferroan and nonferroan calcite cement and other bioclasts.

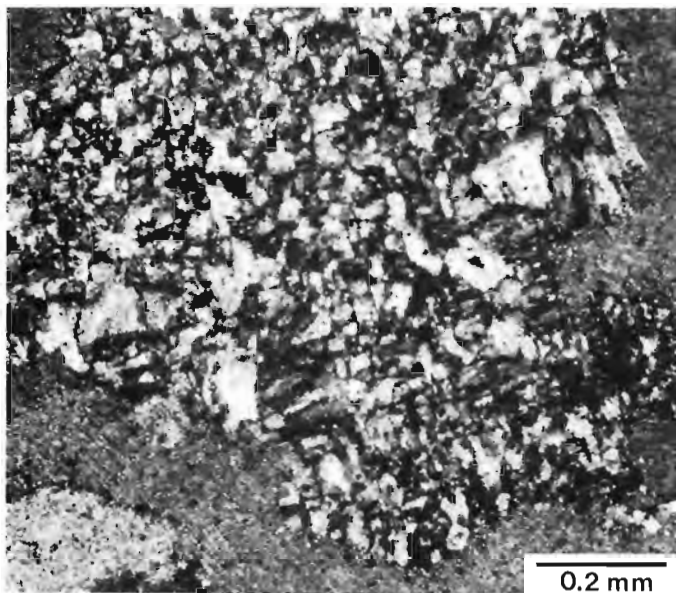


Figure 37. Photomicrograph, showing microquartz in a pelmatozoan ossicle in lime grainstone (GSC loc. C-52457), from the upper Prophet Formation at Sheaf Creek. ISPG 1768-72.

Folk and Pittman (1971) stated that length-slow chalcedony is unusual and exists almost exclusively either as a replacement of evaporites or in association with them. Because evaporites and their pseudomorphs are absent, this relationship is unlikely in the Prophet and Flett formations. Moreover, Chowns and Elkins (1974, p. 892, 897) stated that a length-slow orientation is normal. They reported that length-slow chalcedony has replaced crinoid debris and sponge spicules in the Mississippian Fort Payne and "Warsaw" formations of Tennessee.

Megaquartz in the Prophet is like that of the Flett Formation (Fig. 53). It exists as mosaics of subhedral, finely crystalline crystals that filled late voids.

Skeletal opal was probably the major source of silica for the Prophet chert. Meyers (1977) demonstrated that a strong, positive correlation exists between chert abundance and both depositional lithofacies and spicule availability in the Mississippian Lake Valley Formation of New Mexico. On the basis of this correlation and from his knowledge that silica was released from abundant spicules in that formation, he concluded that intraformational spicules were the major silica source. Similar correlations are evident in the carbonate buildup to shale basin transition in the project area (Fig. 8). Toward the basin lithofacies, the proportion of spicules and chert increases. These relationships, combined with the evidence of replacement by calcite of a large volume of spicules in the Prophet, indicate that spicules could have been the principal source of silica in the Prophet Formation.

Prophet Formation spicules were probably not the only source of silica for the chert of that formation. The diagenesis of clays and skeletal opal in the underlying Besa River Formation possibly provided much silica. This is suggested by three lines of evidence. Thick intervals of spiculite, which are essentially bedded chert, overlie or occur

in the upper Besa River at several locations (Fig. 12). The volume of chert in the Prophet exceeds that of calcite-replaced spicules because chert replaced many spicules, the volume of chert in the most abundant rock type exceeds that of calcite spicules, and chert is moderately common in Prophet rocks that contain few spicules. Finally, Pelzer (1966) determined that quartz is the main mineral in the Besa River shale and occurs chiefly as chalcedonic silica in sponge spicules, radiolarian capsules, and other shale components.

Calcite

Diagenetic calcite in the Prophet Formation formed in four basic ways: replacement of non- CaCO_3 minerals, passive precipitation into cavities, neomorphism, and displacive precipitation. In the Prophet, authigenic calcite formed by replacement of non- CaCO_3 minerals is the most abundant, whereas that produced by displacive precipitation is relatively rare. Neomorphic calcite and calcite formed by passive precipitation into voids are of intermediate importance. Both ferroan and nonferroan diagenetic calcite occur, but ferroan calcite is much more abundant, particularly in rocks other than lime grainstone and in units that are very dolomitic, argillaceous, or interbedded with shale.

Replacement calcite

Authigenic calcite produced by the replacement of non- CaCO_3 minerals is important in spiculite and most lime packstone and wackestone in the Prophet Formation. In spicule-bearing rocks, fine to medium crystalline pseudospar, which has replaced the opal in up to 98 per cent of the spicules in many samples, is commonly the most abundant calcite. Many of these spicule-rich rocks are limestone because of replacement, but they were derived from sediment that was originally less than 50 per cent CaCO_3 . The bulk of this multicrystalline calcite is ferroan, which suggests that most replacement did not occur during early diagenesis.

Passively precipitated calcite

Three morphological types of sparry calcite cement or passively precipitated calcite occur in the Prophet: monocrystalline syntaxial overgrowths (Fig. 36c), mosaics of subequant calcite that filled centers of cavities, and fringes of equant to bladed crystals (Fig. 39). Spar cement is the predominant diagenetic calcite in lime grainstone, and this calcite is moderately abundant in some coarse grained bryozoan-pelmatozoan lime packstone. However, it constitutes less than 10 per cent, by volume, of most lime packstone and wackestone, and less than 5 per cent of most spiculite.

Monocrystalline syntaxial cement, which occurs on and in pelmatozoans (Fig. 36c), is probably the most common and abundant spar cement. It occurs as overgrowths on most crinoid ossicles in lime grainstone, but in other lithologies it occurs mainly in the canal system of these bioclasts. The overgrowths in the lime grainstone are mainly nonferroan to slightly ferroan, but some consist of two or more cement generations with varying Fe^{2+} content. In other lithologies, the monocrystalline syntaxial cement is generally strongly ferroan. Relatively early to late solutions in Folk's (1973, 1974a; p. 45, 51) meteoric-phreatic and subsurface zones (Fig. 19) probably precipitated this cement. The reasons for this interpretation are similar to those given in the discussion on calcite cements in the Yohin Formation.

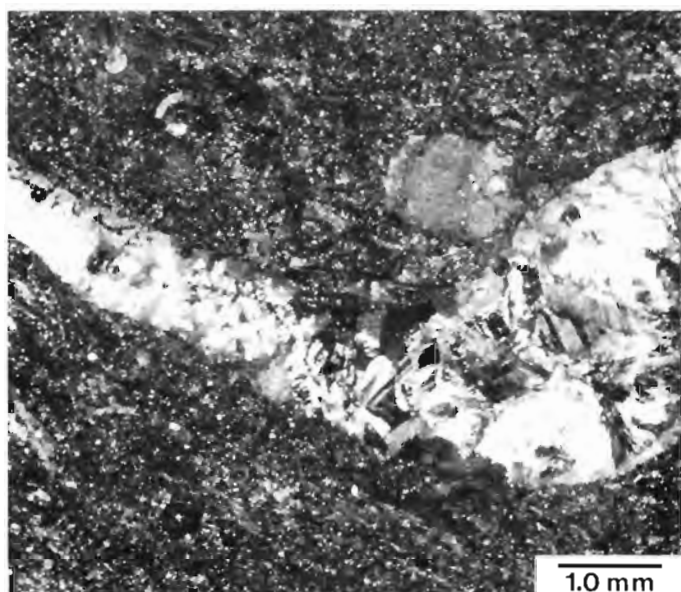


Figure 38. Photomicrograph, showing a brachiopod fragment, mainly replaced by quartzine fans, in a sample (GSC loc. C-52458) from the upper Prophet Formation at Sheaf Creek. ISPG 1768-75.

Mosaics of subequant-grained, clear, calcite crystals, like those in the Yohin Formation (Fig. 25d), either filled cavities completely or filled centers of cavities lined by other cement fabrics. The size of crystals in some mosaics increases away from pore walls, and most of this calcite is relatively inclusion free. In lime grainstone, this cement occurs intergranularly and intragranularly, but in other rock types it occurs chiefly in chambers of polycrystalline bioclasts. Most of these mosaics are interpreted as having precipitated relatively late in Folk's (1973, 1974a) meteoric-phreatic and subsurface zones, based on reasons similar to those given in the section on this cement in the Yohin Formation.

Polycrystalline fringe cement is a minor spar cement in the Prophet Formation and is the least common sparry cement fabric. It is abundant in some lime grainstone (Fig. 39), where it occurs intergranularly and intragranularly; but in other rocks it is relatively rare and occurs intragranularly only. The fringes consist of clear, equant to bladed crystals, which are mainly fine to medium crystalline and ferroan to nonferroan. Equant rhombic crystals, which are generally well developed on all allochems except pelmatozoan ossicles, are the most common. In one grainstone sample, however, they successfully competed with syntaxial overgrowths on some ossicles. Although blades occur locally on most bioclasts other than pelmatozoan ossicles, they are longest and most abundant on brachiopods, corals and bryozoans. These blades are commonly ferroan calcite and generally have sides that diverge outward. Toward the outer margins of fringes, the number of crystals generally decreases as crystal size increases.

Polycrystalline fringe cement like that in the Prophet has been produced under experimental meteoric-phreatic conditions (Badiozamani et al., 1977, p. 532-534), and it has been observed in ancient rocks by Buchbinder and Friedman (1980), Longman (1980, p. 473-477), Jacka and Brand (1977, p. 372-375), Land (1970), and others. This has generally been interpreted as an early diagenetic cement precipitated in the

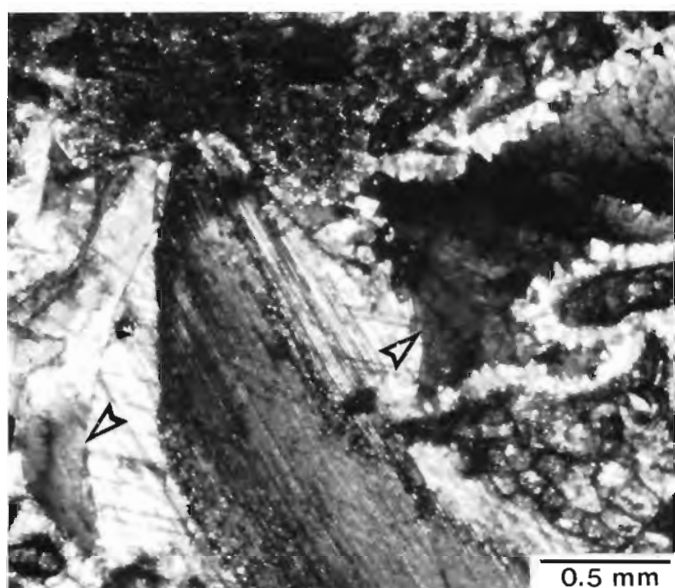


Figure 39. Photomicrograph of dolomitic bryozoan-pelmatozoan lime grainstone (GSC loc. C-74222), from the Prophet Formation at Locality 5. Shows late saddle dolomite (arrows), monocrystalline syntaxial overgrowths on pelmatozoan ossicles (centre), and equant to bladed fringes of polycrystalline, sparry calcite cement. ISPG 1768-135.

meteoric-phreatic zone, but solutions in the subsurface-mixing zone apparently can precipitate it (Buchbinder and Friedman, 1980, p. 402; Longman, 1980, p. 478). In addition, experimental work (Badiozamani et al., 1977, p. 533) suggests that connate NaCl solutions in Folk's (1973, 1974a) subsurface zone (Fig. 19) could precipitate this cement.

Neomorphic calcite

In the Prophet Formation, neomorphic calcite is a major component of some skeletal lime packstone and wackestone, but it is generally a minor variety of calcite in spiculite and other very cherty rocks. Part of the matrix calcite in some limestone is micrite, but in most it is microspar or fine to medium crystalline pseudospar. Fine to medium crystalline pseudospar, produced by degrading recrystallization of crinoid ossicles and their overgrowths, also is common in some beds. In addition, either inversion or replacement of aragonite macrofossils produced finely to very coarsely crystalline neomorphic spar, but it is not abundant. Most neomorphic calcite is slightly ferroan, which is indicative of neomorphism under reducing conditions.

Displacive calcite

Displacive sparry calcite (Fig. 40) is a minor, but locally important, diagenetic calcite in the Prophet Formation. It was observed in mixed-skeletal lime packstone and wackestone and is best developed on brachiopods and crinoid ossicles. On brachiopods it is bladed to fibrous, and on crinoids it is syntaxial and either monocrystalline or bladed. The sides of blades on crinoids are mainly subparallel, but on brachiopods they commonly diverge away from the foundations of crystals. All displacive rims and fringes were strongly ferroan, which indicates they were precipitated under reducing conditions in either the meteoric-phreatic or subsurface zones.



Figure 40. Photomicrograph, showing polycrystalline fringes of displacive calcite (arrows) on brachiopods, in cherty brachiopod lime packstone (GSC loc. C-52069), from the Prophet Formation at Jackfish Gap. ISPG 1768-84.

Dolomite

Authigenic dolomite occurs, at least in trace amounts, in most spiculite and limestone, and it constitutes between 5 and 30 per cent, by volume, of about 40 per cent of these rocks. Exceptional beds contain higher proportions of dolomite and grade into dolostone. Although some dolomite was possibly precipitated in voids as a late cement (Fig. 39), it is mainly a replacement mineral. This dolomite is mostly ferroan and stains light blue to pale blue-green when Dickson's (1965) staining technique is used.

X-ray diffraction analyses indicate that ankerite, which has physical and optical properties similar to those of dolomite, is relatively abundant in the fine grained deposits of the Prophet Formation (Appendix G). An undetermined proportion of the mineral that here is called ferroan dolomite is, therefore, ankerite.

Dolomite occurs most frequently as isolated and interfering rhombs in the cherty matrix of spiculite, lime packstone, and lime wackestone. This dolomite varies from very fine to medium crystalline, but it is chiefly finely crystalline, and the rhombs are mainly subhedral to euhedral. Rhomb outlines vary from sharp to corroded, and rhombs have straight to slightly undulose extinction. Also, some smaller rhombs closely resemble limpid dolomite that Folk and Land (1975, p. 65) have described. Although rhombs are concentrated in the matrix, they occur in dolostone intraclasts and have partly replaced some allochems, ferroan and nonferroan calcite cement, and spicules. The paragenetic relationships between dolomite and its host chert are uncertain, but the presence of some corroded and partly replaced rhombs suggests that dolomite is older.

A minor amount of dolomite commonly occurs in masses of length-slow chalcedony, which partly replaced some crinoid ossicles and less commonly other allochems and cement. This dolomite, which occurs as very fine to medium crystalline, euhedral to subhedral rhombs and subhedral

masses, is confined to the chalcedony and immediately adjacent calcite. Crystals in crinoid ossicles are oriented with respect to the crystallographic axes of the ossicles. Rhomb outlines vary from sharp to corroded, and chert appears to have partly replaced some.

Dolomite that may be a late cement (Fig. 39) is a minor component and occurs chiefly in lime grainstone. It appears to occur as a cement in voids lined by ferroan and nonferroan calcite cement, but locally it has replaced calcite cement. This dolomite occurs as finely to coarsely crystalline, subhedral crystals that have slightly undulose to sweeping-undulose extinction caused by warping of the crystal lattice. It is like baroque dolomite (Folk and Assereto, 1974, 1980) or late saddle dolomite (Radke and Mathis, 1980).

Without additional data, the mechanisms and physiochemical conditions under which dolomitization occurred in the Prophet Formation can only be speculated upon, but it is useful to demonstrate that early, surficially generated, hypersaline solutions probably did not precipitate dolomite in this unit. Until recently, the two most accepted models for dolomite formation were: formation in sabkhas and similar supratidal environments (Shinn et al., 1965; Illing et al., 1965); and formation by reflux of brines through carbonate sediment below hypersaline bodies of marine-derived water (Adams and Rhodes, 1960; Deffeyes et al., 1964, 1965).

It is unlikely that either process produced dolomite in the Prophet. Evaporites and sabkha-like deposits do not occur in either the Prophet or coeval formations of the project area. Also, it appears unlikely that the reflux mechanism would operate on a large scale because of hydrological problems (Land et al., 1975, p. 1602; Morrow, 1982b, p. 96). The presumed modern example of reflux dolomitization has been reinvestigated by Murray (1969) and Lucia (1968) and the proposed process seriously questioned. Moreover, dolomite in the Prophet and in the more proximal, correlative, Flett lithofacies generally differs markedly from most Holocene hypersaline dolomite. Crystals in Holocene hypersaline dolomite rarely exceed 5 microns and lack well developed faces (Land et al., 1975, p. 1622, 1623). In comparison, most Prophet dolomite is fine to medium crystalline and has well developed faces. Finally, the local occurrence of saddle dolomite and the high Fe^{2+} content of most dolomite present in the Prophet suggest that most dolomitization did not occur early. The presence of saddle dolomite indicates a diagenetic event in the temperature range of 60 to 150°C and most probably over 100°C (Radke and Mathis, 1980, p. 1160).

In the Prophet Formation, a positive correlation exists between the abundance of ferroan dolomite and the proximity of strata to dark shale. Moreover, this is more evident in the Flett, Golata, and Besa River formations. Dark shale units commonly enclose or occur in juxtaposition with intervals of dolostone and other dolomite-rich rocks. In addition, proceeding basinward in the Flett and Prophet, a general increase in the abundance of dolostone and dolomite occurs. This apparent correlation between dark shale and dolomite suggests a possible relationship between basinal shale and dolomitization. According to McHargue and Price (1982), similar correlations between the abundance of ferroan dolomite in strata and the proximity of the deposits to shale are evident in a variety of stratigraphic settings.

Some dolomite in the Prophet Formation possibly resulted from the dewatering of the large volumes of Carboniferous shale that are present in the project area. The compaction of fine grained sediments during burial causes the progressive expulsion of their Mg^{2+} -bearing pore water.

According to Mattes and Mountjoy (1980) and Morrow (1982b), part of the Mg^{2+} -bearing water derived from the compaction of a shale succession may pass through adjacent limestone and cause dolomitization. This mechanism, however, would probably produce only a small volume of dolomite that would occur near the shale (Morrow, 1982b, p. 97, 98).

A major proportion of the ferroan dolomite and ankerite in the Prophet possibly resulted from the diagenesis of clay minerals. In burial environments that are deeper than 2500 m, the transformation of montmorillonitic clays to illite is accompanied by the release of Si^{4+} , Fe^{2+} , Ca^{2+} and Mg^{2+} ions to pore solutions (Boles and Franks, 1979; Boles, 1981; McHargue and Price, 1982, p. 881). Pore solutions containing these ions have caused the precipitation of ankerite, ferroan dolomite and chlorite as cements in some sand/shale sequences (Boles and Franks, 1979; Boles, 1981). Also, McHargue and Price (1982, p. 881) believe that this process would result in the formation of ferroan dolomite in a limestone/shale sequence. This process would, therefore, probably have caused the precipitation of ankerite and ferroan dolomite in the Prophet.

In addition, some ferroan dolomite and ankerite in the Prophet possibly resulted from the bacterial reduction of sulphate in organic-rich sediment. Much of the fine grained, dolomite-bearing deposits in the Prophet are carbonaceous, and the presence of abundant pyrite in them suggests that sulphate-reducing bacteria were present. Dolomite is often present in organic-rich, alkaline, marine sediments (Baker and Kastner, 1981) and this type of sediment probably existed in the Prophet Formation during the relatively early stages of its diagenesis. Lippman (1973) and Morrow (1982a, p. 10) related the presence of dolomite in sediments of this type to high concentrations of CO_3^{2-} generated by the bacterial reduction of sulphate in the presence of organic material. According to McHargue and Price (1982, p. 881), ferroan dolomite and ankerite could be produced by combining the CO_3^{2-} with Ca^{2+} , Mg^{2+} and Fe^{2+} (released during clay conversion) under reducing conditions. Also, Baker and Kastner (1981, p. 215) suggested that dolomitization in the type of environment discussed above is aided by the removal of SO_4^{2-} by microbial reduction.

Part of the dolomite in the Prophet Formation is also possibly related to the formation of chert. In the Prophet, much of the abundant chert, which is commonly closely associated with dolomite, probably resulted from the transformation of biogenic opal. According to Baker and Kastner (1981, p. 215), the transformation of opal-A to opal-CT may retard $CaCO_3$ dolomitization through the formation of unidentified nuclei that contain Mg^{2+} and OH^- and enhance opal-CT formation. The common association of chert with dolomite implies that Mg^{2+} taken up by opal-CT was released when the opal was transformed to quartz (Baker and Kastner, 1981).

Pyrite

Pyrite, which is a common mineral in the Prophet Formation, exists, at least in trace amounts, in most beds. It forms between 0.2 and 1 per cent of most beds, and constitutes more than 10 per cent of some samples (Fig. 42b). This pyrite is present as framboids and very fine to medium crystalline, subhedral to euhedral crystals, which replaced bioclasts and developed interstitially. Its presence indicates that reducing conditions prevailed during much of the diagenetic history of the Prophet. Also, it suggests that sulphate-reducing bacteria were active at least during early phases of diagenesis.



Figure 41. Outcrop of normally graded, millimetre-thick spiculite laminae in the Prophet spiculite and spicule-lime-packstone lithofacies at Locality 8. ISPG 798-45.

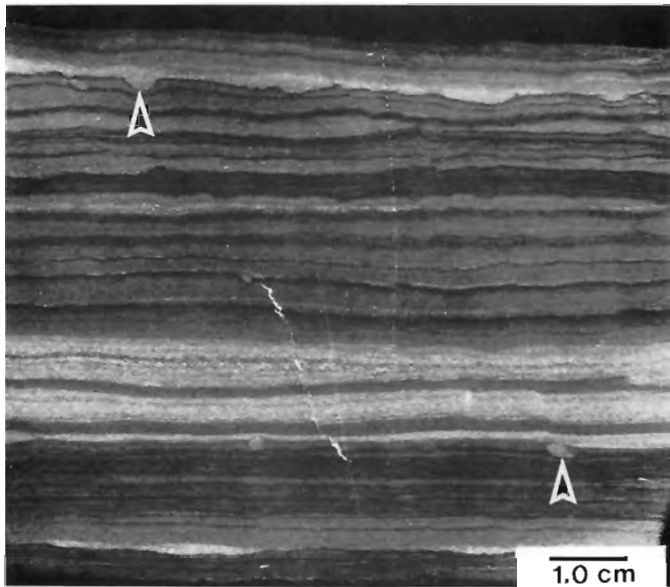
Lithofacies

A spiculite and spicule-lime-packstone lithofacies (Figs. 41, 35) and a dark-shale lithofacies constitute most of the Prophet Formation. Widely separated units of mixed-skeletal lime-packstone lithofacies (Fig. 48) also occur in some sections. Because the mixed-skeletal lime-packstone lithofacies forms a small part of the Prophet and is like the same facies in the overlying Flett Formation (which is described in detail), it is discussed briefly here.

Spiculite and spicule-lime-packstone lithofacies

The spiculite and spicule-lime-packstone lithofacies (Figs. 35, 41, 42, 86) constitutes most of the Prophet Formation. It comprises spiculite and spicule lime packstone with subordinate shale, mudstone, dolostone, siltstone, and other limestones. In most of the area, this facies grades upward and eastward into the mixed-skeletal lime-packstone lithofacies of the Flett, which was deposited mainly on a middle-slope environment (Fig. 87a). However, west of the depositional limit of the Flett Formation, this lithofacies grades into basinal-shale and prodelta deposits of the overlying Golata Formation. On the interior platform, the spiculite and spicule-lime-packstone facies generally overlies the Clausen Formation. Toward the west, the spiculite and spicule-lime-packstone lithofacies intertongues with and grades into the basinal shale of the Besa River Formation. In the Mackenzie fold belt and on the extreme western side of the interior platform, this lithofacies gradationally overlies basinal shale in the Clausen and Besa River formations.

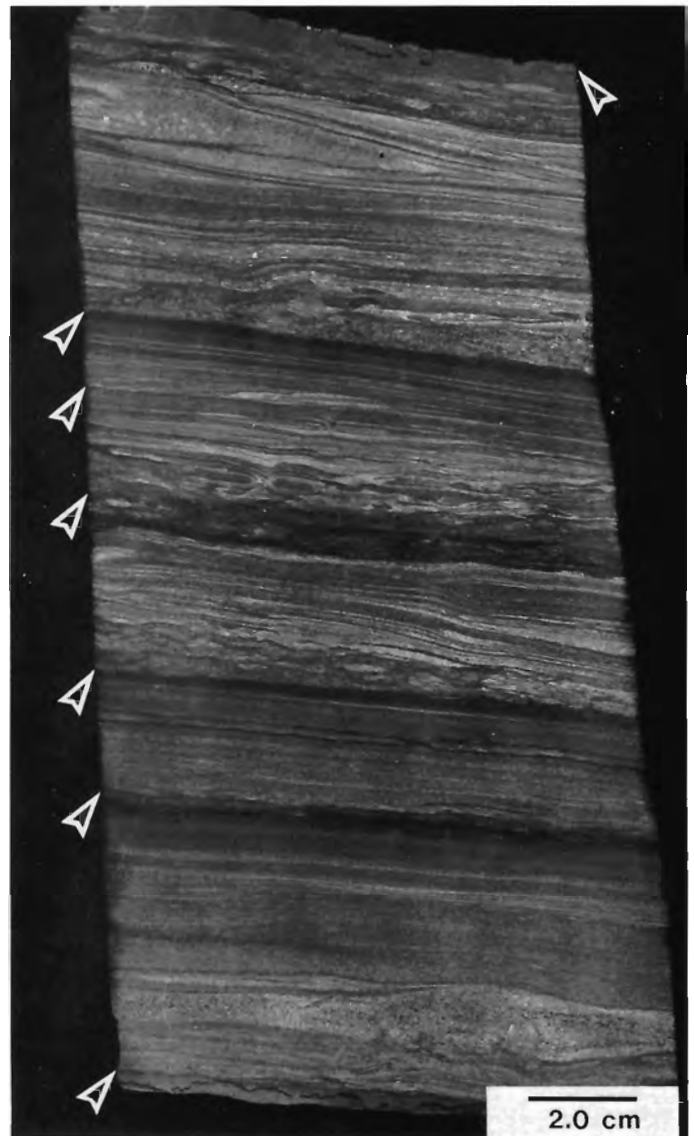
Spiculite (Fig. 36a) is the most abundant rock type in the spiculite and spicule-lime-packstone facies. It occurs throughout this lithofacies, but it becomes more abundant toward the base of the Prophet and toward the west. This rock type commonly grades into spiculitic shale, spicule lime packstone and wackestone, and dolostone.



a. Normally graded, cherty spiculite laminae, tentatively interpreted as (D, E) turbidites (GSC loc. C-57434H). Upper arrow indicates load casts; lower arrow points to possible burrow. ISPG 1766-6.



b. Proximal, pyritic, limestone and spiculite turbidite (GSC loc. C-57434K) with flute casts and the Bouma A, C, and D-E divisions. ISPG 1766-5.



c. Distal, cherty spiculite turbidites (GSC loc. C-57434D). Most have Bouma C, D, and E divisions; soft-sediment deformation is common in the C divisions. Arrows indicate tops of turbidites. ISPG 1766-4.

Figure 42. Polished slabs of turbidites from the Prophet spiculite and spicule-lime-packstone lithofacies at Locality 19.

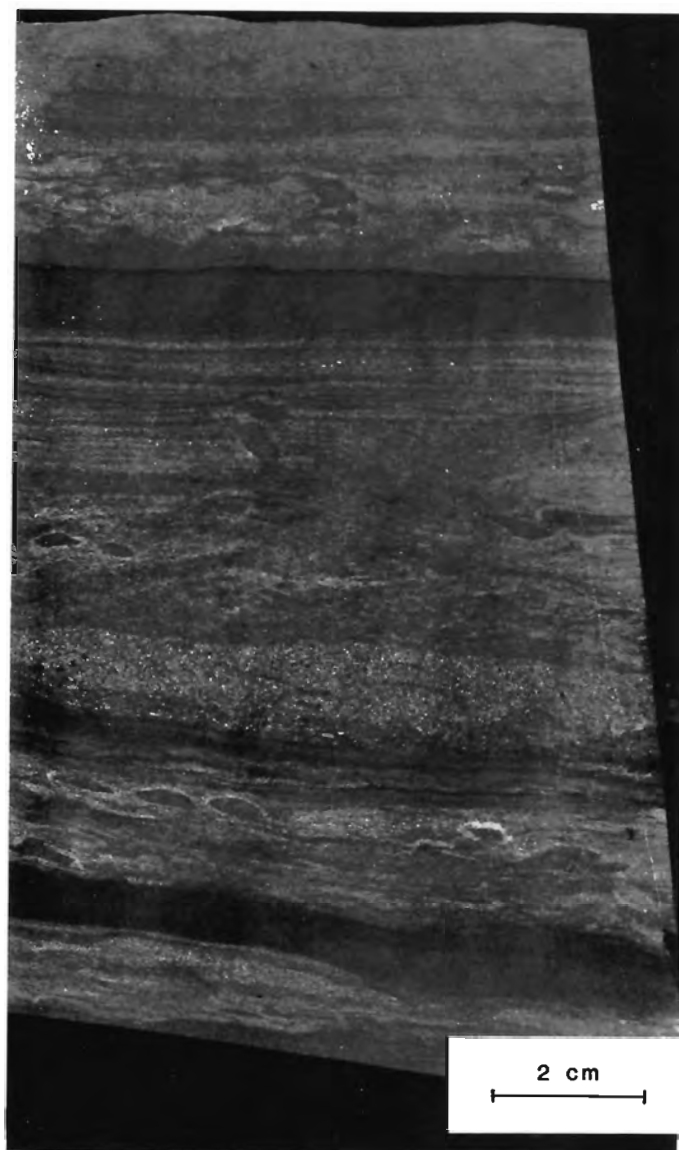
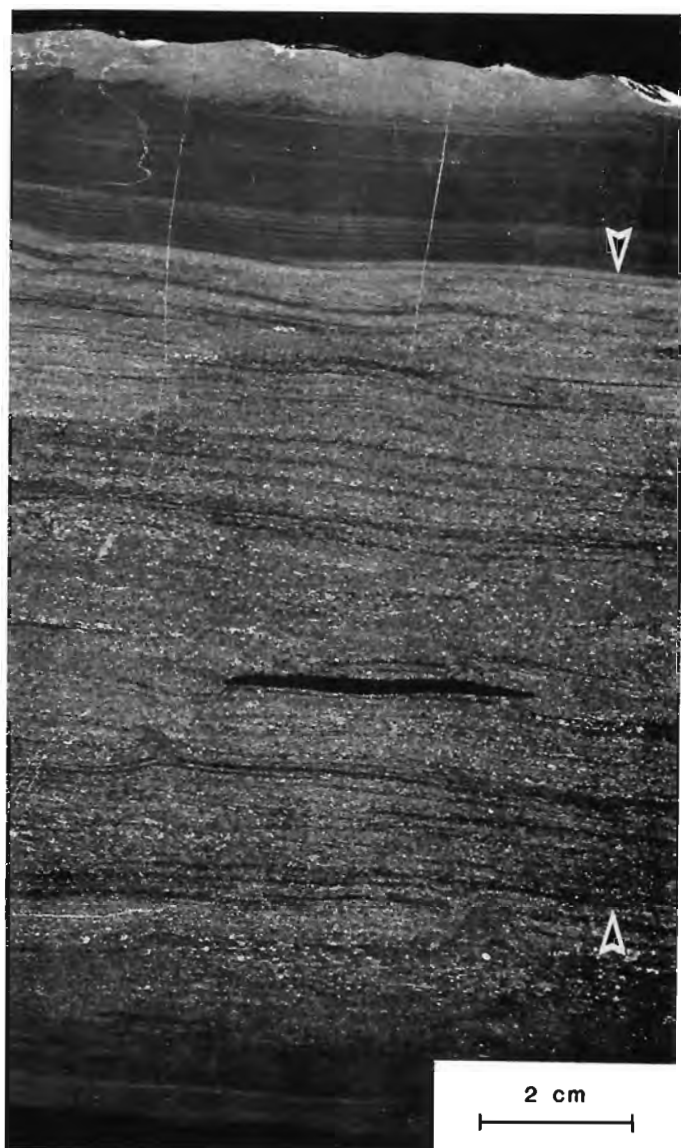
Spicule lime packstone is the predominant limestone, and spiculitic bryozoan-pelmatozoan lime packstone is the next in abundance. Skeletal lime wackestone is moderately common, but skeletal lime grainstone is a minor rock type (Fig. 36c). The proportion of limestone that has spicules for its principal allochem increases toward the west and the base of the formation, whereas the opposite applies to limestone that consists chiefly of other bioclasts.

Siliciclastic shale and mudstone, which are the next most abundant rocks types, are moderately common

throughout the spiculite and spicule-lime-packstone lithofacies. Shale and mudstone form partings and thin recessive intervals between the more resistant rocks.

Dolostone (Fig. 36d) and siltstone are relatively minor rock types. The former occurs throughout the formation, whereas siltstone occurs at a few locations just below the Prophet-Flett contact.

The resistant to moderately recessive deposits of the Prophet spiculite and spicule-lime-packstone lithofacies (Figs. 35, 41, 86) are mainly well bedded and of deeper water



a. Proximal, cherty spiculite turbidite (GSC loc. C-57434A) with the Bouma A(?), B, C, D, and E divisions. Arrows indicate base and top of the C division. ISPG 1766-2.

b. Spiculite and limestone turbidites (GSC loc. C-57434C) containing probable intraclasts and structures produced by soft-sediment deformation. ISPG 1766-1.

Figure 43. Polished slabs of turbidites from the Prophet spiculite and spicule-lime-packstone lithofacies at Locality 19.

aspect. Rhythmic bedding is common, and many beds have considerable lateral continuity. However, bedding continuity is locally interrupted by large-scale, concave-upward truncation surfaces (Figs. 77a, 85), and large-scale mound-like structures are locally present (Fig. 86). This lithofacies generally forms multibed sequences that either become more or less resistant and proximal in aspect upward (Figs. 35, 49).

Several types of deposit constitute the spiculite and spicule-lime-packstone lithofacies. Of these, beds that consist mainly of multiple, normally graded laminae (Figs. 41, 42a, 44) are probably the most widespread and volumetrically important. These laminated deposits become more abundant toward the west and the base of the Prophet. Also, they constitute most of the spiculite and spicule-lime-packstone

lithofacies near the western depositional limit of the Prophet. Sharp-based, massive to stratified, graded beds (Figs. 42b, c; 43) are common and next in abundance. In general, these sharp-based beds constitute a major proportion of the upper Prophet, and their importance in this formation increases upward and eastward. Platy, bioturbated deposits are also common in this lithofacies. They are probably slightly less voluminous than the sharp-based beds and are important in most Prophet sections that are either near or well east of the western depositional limit of the Flett. Much less abundant are massive, ungraded to poorly graded beds that have sharp bases. These massive beds occur locally in the uppermost Prophet near or east of the western depositional limit of the Flett. Deposits that were contorted prior to lithification (Figs. 83, 84) are moderately common at

Locations 8 and 19. Finally, nodular limestone (Fig. 46) is locally common in the upper Prophet in the eastern part of the Carboniferous outcrop belt.

Most sharp-based, massive to stratified graded beds in the spiculite and spicule-lime-packstone lithofacies comprise two or more components that resemble, in character and sequence, divisions A to E in the standard Bouma sequence. Also, they are associated with other deposits of deeper water aspect. These beds are, therefore, interpreted as mainly turbidites. Moreover, they are considered to be deposits of turbidity currents because they resemble sandstone and limestone turbidites described by Mutti (1977), Sanders (1965), Ricci-Lucchi (1975), and Davies (1977).

Turbidites that have Bouma A or B divisions are proximal, and those that lack these divisions are distal (Bouma and Hollister, 1973, p. 89). In the spiculite and spicule-lime-packstone lithofacies, beds that are interpreted as distal turbidites (Fig. 42c) are moderately common. Beds considered to be proximal turbidites (Figs. 42b, 43a) are more abundant, however. In general, the proportion of distal turbidites increases toward the west and the base of the Prophet.

Proximal turbidites in the spiculite and spicule-lime-packstone lithofacies vary from very thin to thick bedded (1-100 cm), but they are mainly thin to medium bedded (3-30 cm). They consist of limestone, dolostone, and spiculite but are chiefly spiculitic lime packstone. Most proximal turbidites in this lithofacies have a basal Bouma A division. Moreover, most beds that have an A division lack the B and C divisions, and turbidites with all of Bouma's (1962) divisions are rare (Fig. 43a). The A division (Fig. 42b) varies from massive to indistinctly stratified, and ungraded to distinctly graded; however, it generally has subtle grading. Grading in other divisions is also usually subtle. In contrast, well developed normal grading is generally evident between the base and tops of these turbidites (Figs. 42b, 43a). Although locally well developed, the planar stratification in the B division is frequently diffuse. Poorly developed, small-scale crossbedding dominates the Bouma C division; convoluted laminae are not common. The Bouma B and C divisions are best developed in beds that are largely spicules, but the B division is developed in some beds of fine grained, bryozoan-pelmatozoan lime packstone. Laminated, siliceous spiculite and spicule lime packstone, which commonly grade up into shale, generally constitute the D and E divisions (Fig. 43a). The D and E divisions, which are commonly difficult to separate in polished specimens, cannot be differentiated in most turbidites at the outcrop.

The proximal turbidites have sharp bases that vary from highly undulose to almost planar, but the sole marks lack diversity. Load casts are the most abundant sole marks and are most common and best developed on bases of coarse grained beds that have a basal Bouma A division and overlie shale. Load casts develop when a reversed density gradient is established while the viscosity and strength of two deposits are low enough to permit deformation (Middleton and Hampton, 1973, p. 10). Shallow scours are the next most common sole mark, whereas flute casts (Fig. 42b) are rare. Tool casts were not observed.

Grading in the proximal turbidites resembles Middleton's (1967, p. 487) distribution grading. According to Middleton, deposits that have this type of grading show a progressive shift toward finer grain sizes, for almost all percentiles of the distribution, as the distance from the base of the bed increases. Distribution grading is the most common natural type. It is produced by layer-by-layer deposition from relatively dilute turbidity currents

(Middleton and Hampton, 1973, p. 11). However, high-density flows possibly deposited the massive, ungraded, Bouma A divisions that occur in some Prophet turbidites. An important effect of higher concentration is rapid deposition. This tends to prevent segregation of grain size and suppress formation of traction-produced structures (Middleton, 1970, p. 258; 1967, p. 495).

Beds in the spiculite and spicule-lime-packstone lithofacies that are interpreted as distal turbidites (Fig. 42c) are mainly thin to very thin (1-10 cm). They are mainly spiculite and spicule lime packstone, but some beds are dolostone. Most of the beds that are interpreted as distal turbidites have a basal Bouma C division. With the exception of turbidites at Locality 19, the Bouma C division is seldom well developed. Small-scale crossbedding (Fig. 42c) is the principal structure in the C division; convoluted laminae are uncommon. The Bouma D and E divisions are difficult to separate, but the E division tends to be darker and more thinly laminated. Very thin, planar laminae constitute the D and E divisions. Toward the tops of these turbidites, laminae in the D and E divisions become thinner, darker and finer grained (Fig. 42c). The Bouma C, D, and E divisions and their component laminae have subtle normal grading. In addition, well developed normal grading, which resembles Middleton's (1967) distribution grading, is generally present between the bases and tops of these turbidites. Except at

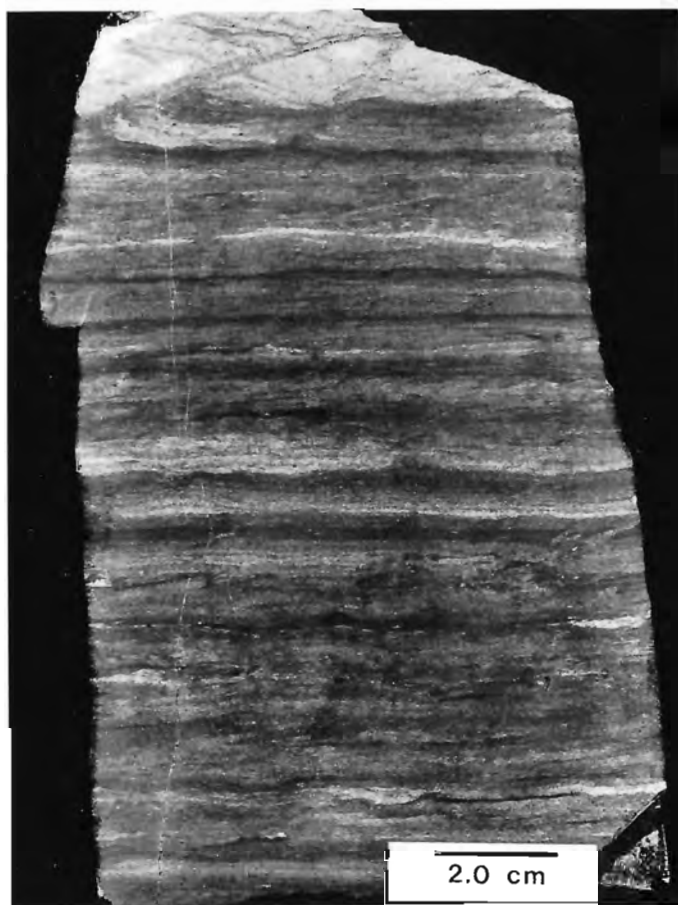


Figure 44. Polished slab of bioturbated, distal, cherty spiculite turbidites (GSC loc. C-52303), from the Prophet spiculite and spicule-lime-packstone lithofacies at Ram Creek. ISPG 1766-10.

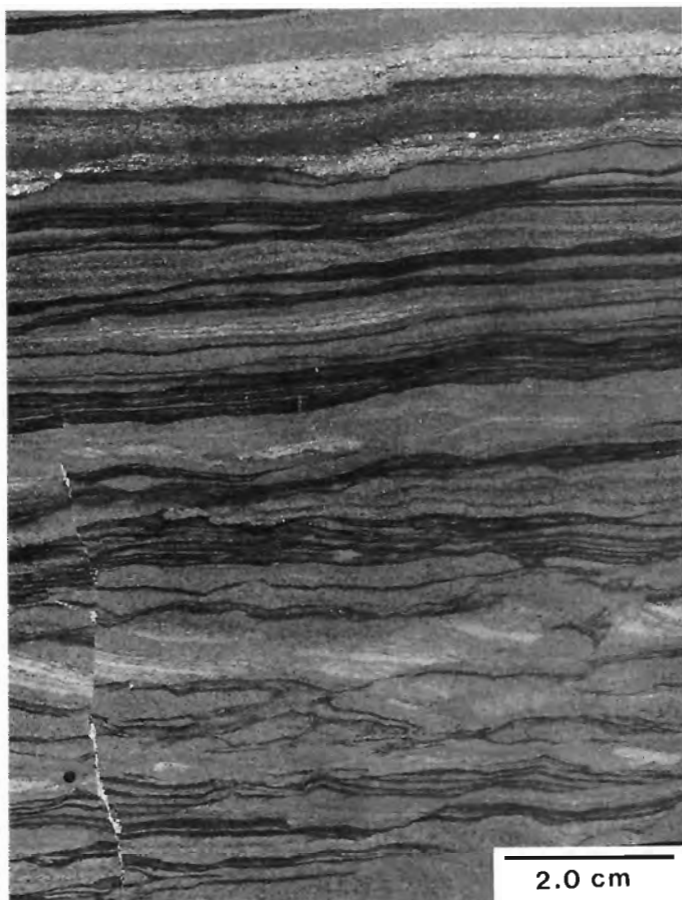


Figure 45. Polished slab of probable distal (D, E) cherty spiculite turbidites (GSC loc. C-57434F) overlying wavy, discontinuous laminae, resulting from soft-sediment deformation. Note the minor fault offsets. Sample is from the Prophet Formation at Locality 19. ISPG 1766-8.

Locality 19, evidence of bioturbation is generally common in these beds. On the bases of these turbidite beds, shallow scours and load casts are moderately common; however, neither flute nor tool casts were observed.

Beds in the spiculite and spicule-lime-packstone lithofacies that have a basal crossbedded division (Fig. 42c) are interpreted as turbidites because they correspond well with the upper part of the standard Bouma sequence. However, processes other than turbidity currents can produce similar deposits. Those processes, which include contour currents (Heezen et al., 1966) and various low density, gravity assisted suspension currents such as nepheloid-layer flow (Ewing and Thorndike, 1965; Stanley and Unrug, 1972, p. 295), probably did not produce the crossbedded deposits in the Prophet. According to Stow (1979), turbidites have distinct sequences of structures and exhibit evidence of relatively rapid deposition and burial. In contrast, contourites lack clear sequences of structures, contain irregular lag concentrations, and have features that are indicative of relatively slow accumulation. Nepheloid-layer flow deposits are not likely to show significant grading, current-ripple lamination, and scours (Shanmugam and Walker, 1978, p. 574).

Soft-sediment deformation, which possibly resulted from shearing (Fig. 43b), occurs in some of the probable turbidites described above. The deformed zones have

obliterated or distorted laminae and intraclasts that resemble pseudonodules (Macar, 1948; Skipper and Middleton, 1975, p. 1943). Skipper and Middleton (1975) described turbidites with similar deformed intervals and attributed the deformation to shearing of liquified deposits.

In Prophet beds that consist of multiple laminae, two types of laminae are present: those that are generally several millimetres thick and consist of several thinner layers (Figs. 42a, 44, 45); and millimetre-thick laminae that generally do not comprise thinner layers (Fig. 41). Most composite laminae closely resemble turbidite components that overlie the Bouma C division in Prophet turbidites described in the previous paragraphs. Toward the top of these composite laminae, the component laminae generally become thinner, darker, and finer grained (Fig. 42a). The bases of most composite laminae are sharp, and those of the millimetre-thick layers are gradational to sharp. Shallow scours and structures produced by loading (Fig. 42a) occur at the base of some composite laminae, but the bases of the millimetre-thick layers seldom have obvious sole marks. Subtle normal grading is present in most of the sharp-based, millimetre-thick laminae, and in the composite laminae. Many of the more distal occurrences of the spiculite and spicule-lime-packstone lithofacies, which are near the western depositional limit and base of the Prophet, lack obvious composite laminae. There, beds consist mainly of millimetre-thick laminae of similar aspect (Fig. 41). At most localities where these laminated deposits were studied, they contain some evidence of bioturbation (Fig. 44); but this evidence is rare to absent at Localities 8, 19, and 30, and in much of the basal Prophet at other localities (Figs. 41, 42a).

The graded laminae described above frequently form resistant beds consisting of multiple, superimposed laminae of similar thickness and aspect. These composite beds are generally between 5 and 30 cm thick and separated by thin shale partings. The beds vary in color and durability. Lighter coloured, more resistant beds appear to be slightly more dolomitic or calcareous than less resistant or darker beds. Sequences of composite beds of this type frequently form rhythmic successions of either light and dark beds (Fig. 35) or resistant and recessive beds. Rhythmic bedding of similar aspect occurs in many deeper water carbonate deposits and has been described by Smith (1977, p. 192), Bissell and Barker (1977), McIlreath and James (1978), and others.

Laminated deposits like those in the Prophet spiculite and spicule-lime-packstone facies have recently been described from several carbonate-slope successions. However, the origins of those deposits are not well understood. They have generally been interpreted as either hemipelagic deposits (Cook and Taylor, 1977, p. 79; Reinhardt, 1977, p. 104; McIlreath and James, 1978, p. 190), or turbidites (Yurewicz, 1977, p. 210; Pfeil and Reid, 1980, p. 105).

Dilute turbidity currents instead of hemipelagic sedimentation are tentatively considered to be the chief agent responsible for deposition of the graded composite laminae in the Prophet, for reasons given below. These composite laminae closely resemble Pleistocene and modern (D, E) turbidites that Stow (1979), Stow and Bowen (1980), and Chough and Hesse (1980) described. Moreover, these Prophet deposits have the same characteristics as Bouma D and E divisions in Prophet turbidites that include other divisions. The laminae are locally closely associated with deposits that are interpreted as turbidites, and they either underlie or occur basinward of Flett slope-deposits consisting largely of proximal, carbonate, sediment-gravity-flow deposits. Bioclasts in these possible (D, E) turbidites are mainly resedimented fragments of macroinvertebrates,

whereas radiolarians and other pelagic fossils are rare. Finally, the following evidence for fairly rapid deposition by currents has been observed: normal grading; sharp basal contacts, with local load casts and scours; local, incipient crosslamination; and common preservation of some primary structures in bioturbated deposits. In contrast to turbidites, which are produced by fairly rapid deposition, hemipelagic deposits are produced by slow pelagic settling (Rupke and Stanley, 1974; Hesse, 1975). Consequently, hemipelagites tend to be homogeneous because of bioturbation (Mutti, 1977, p. 124-126; Rupke, 1975; Hesse, 1975).

The origin is less certain for the simple, millimetre-thick graded laminae (Fig. 41) that are associated with the composite laminae. I tentatively interpret these millimetre-thick laminae as deposits produced by either hemipelagic sedimentation, distal turbidity currents, or a combination of these processes. In the absence of abundant infaunal organisms, hemipelagic sedimentation probably would produce laminae. However, because these laminae are associated with, and either underlie or occur basinward of turbidite-bearing lithofacies, distal turbidity currents probably formed at least some of the them. Groups of these laminae closely resemble (D, E) turbidites that Chough and Hesse (1980) illustrated. Consequently, the thin laminae are possibly components of thicker sedimentary units that resemble but are less obvious than the composite laminae discussed above.

The massive, ungraded to poorly graded beds in the upper Prophet Formation, have sharp bases, are mainly spicule-lime-packstone to wackestone, and are generally about 30 to 100 cm thick. They are similar to some graded beds in the Prophet spiculite and spicule-lime-packstone lithofacies, but the massive beds are generally thicker and have features that Middleton and Hampton (1973) considered characteristic of debris flow deposits. These characteristics include: a random fabric, poor grading if any, a high proportion of matrix, and a sharp irregular top. Some of these Prophet beds are possibly debris flow deposits; however, documented, ancient, carbonate debris flow deposits generally differ from these beds in the Prophet by being very thick, lithoclast-rich beds (see Cook et al., 1972; Davies, 1977).

Beds of syndepositionally deformed strata (Figs. 83, 84) generally form a minor proportion of the spiculite and spicule-lime-packstone lithofacies, but they are common at Localities 8 and 19. Of the Prophet sections studied, these two are farthest basinward relative to the corresponding shelf-margin deposits. The beds of deformed strata are mainly less than 2.0 m thick but range up to several metres in thickness. These deposits are characterized by chaotic bedding, detachment surfaces (Fig. 83), convoluted laminae and beds, and zones with small-scale, soft-sediment deformation (Fig. 45). Their bases are generally abrupt, and they locally overlie concave-upward truncation surfaces (Fig. 84). Overlying beds are undeformed. Because they contain numerous structures produced by soft-sediment deformation, the beds of deformed strata mainly are interpreted as slump deposits formed by the slumping of un lithified, cohesive sediment. Spiculite, spicule-lime-packstone, and dolostone constitute these slump deposits. This indicates that they resulted from the slumping of the Prophet spiculite and spicule-lime-packstone lithofacies rather than more proximal deposits.

In the spiculite and spicule-lime-packstone lithofacies, beds of nodular lime packstone and wackestone (Fig. 46) are locally common. They occur where resistant beds of spicule-lime-packstone and mixed-skeletal lime packstone are interbedded with platy, argillaceous limestone and shale in



Figure 46. Nodular, spicule lime packstone in the upper Prophet Formation at Locality 3 (scale is 15 cm long). ISPG 1764-3.

the upper Prophet. Most nodular beds are moderately recessive, rubbly weathering deposits, which generally occur between more resistant deposits; however, some of the latter are also nodular. The nodular beds are medium to very thick bedded (10 to >100 cm). Because of sedimentary boudinage in beds above and below, and load casts at the bases of overlying limestone beds, the nodular beds commonly have very irregular boundaries. The nodules, which vary from irregular and rough to ellipsoidal and relatively smooth, are commonly linked, and oriented with long axes subparallel to bedding. In some beds, the nodules closely resemble either pseudonodules described by Skipper and Middleton (1975) or ball and pillow structure. Also, some nodules have a coral or other macrofossil as a nucleus and resemble concretions. Platy, argillaceous, skeletal lime packstone and wackestone, which grade into calcareous shale, are the main rock types between nodules in the rubbly beds. Because laminae in them are generally contorted, these intervening rock types were probably compressed between the nodules.

Nodular limestone is common in deep water carbonate sequences (Mullins et al., 1980, p. 118), and several theories have been proposed to explain its origin. Suggested processes include: differential compaction and boudinage (McIlreath and James, 1978, p. 190), differential submarine cementation and subsequent resedimentation (Hopkins, 1977, p. 165, 166), and early submarine cementation (Mullins et al., 1980). Soft-sediment deformation possibly produced most nodular limestone in the Prophet spiculite and spicule-lime-packstone lithofacies because the nodules are associated with structures that appear to have been produced by this type of deformation. The other two processes possibly produced some Prophet nodular limestone, but conclusive evidence is lacking. Nodules that have macrofossils as nuclei are possibly concretions.

Platy, bioturbated deposits, which are mainly spiculite and spicule-lime-packstone, occur in much of the Prophet Formation. Because these deposits were strongly bioturbated, few primary sedimentary structures remain other than bedding, which is mainly of thin to medium thickness and relatively planar. Trace fossils present are



Figure 47. Normally graded, proximal, mixed-skeletal lime packstone turbidite in the Prophet mixed-skeletal lime-packstone lithofacies at Sheaf Creek (scale is 15 cm long). ISPG 798-115.



Figure 48. Unit of Prophet mixed-skeletal lime-packstone lithofacies 6.4 m thick. The unit becomes less resistant and finer grained upward, and comprises turbidites (Loc. 5). ISPG 1756-134.

mainly poorly preserved *Zoophycos* sp. These deposits commonly form units that are up to 42 m thick, become coarser grained and more resistant upward, and are underlain and overlain by shale and mudstone. The strongly bioturbated, fine grained character of these deposits, and their occurrence in a formation that consists mainly of deposits of deeper water aspect, suggests that they are hemipelagites. However, currents rather than pelagic settling probably deposited much of the sediment, because pelagic bioclasts are uncommon, whereas fragmented, resedimented skeletons of benthonic organisms, including scattered brachiopods and echinoderm fragments, predominate. In addition, the sharp bases of some beds suggest erosion.

Dark-shale lithofacies

The dark-shale lithofacies of the Prophet Formation occurs mainly as moderately thick, recessive intervals between units of spiculite and spicule-lime-packstone lithofacies (Fig. 32). Units of dark-shale lithofacies are generally best developed near the base of the Prophet. However, in much of the Mackenzie fold belt north of about latitude 60°35'N and east of the western depositional limit of the Flett Formation, well developed intervals of dark-shale lithofacies occur throughout the Prophet (Figs. 4-6). Intervals of this facies are eastward-thinning tongues of the shale lithosome that constitutes most of the Besa River Formation. Siliciclastic shale and mudstone are the principal rocks in this lithofacies. In order of decreasing volume, minor amounts of spiculite, spicule-lime-packstone and wackestone, dolostone, and siltstone also occur.

The dark-shale lithofacies of the Prophet resembles that of the Clausen and Besa River formations. It occurs mainly as relatively homogeneous units of shale and mudstone that are of deep water aspect. Planar laminae, which locally exhibit subtle, normal grading, are the principal sedimentary structures in the shale and mudstone. Thin, sharp-based, graded beds and laminae of other rock types, ironstone concretions, and lenses of calcite cone-in-cone are also locally present. Evidence of minor bioturbation is locally present, but identifiable lebensspuren were not observed.

Mixed-skeletal lime-packstone lithofacies

The mixed-skeletal lime-packstone lithofacies of the Prophet (Figs. 47, 48) forms resistant units, which are intercalated with units of dark-shale or spiculite and spicule-lime-packstone lithofacies. Most units of this lithofacies appear to be related to the Flett mixed-skeletal lime-packstone facies, and they generally occur as westward-thinning tongues. The mixed-skeletal lime-packstone lithofacies occurs mainly in the upper Prophet near the western depositional limit of the Flett Formation; however, it is locally present in the lower and middle Prophet, particularly on the interior platform. Mixed-skeletal lime packstone (Fig. 36b) with subordinate dolostone, lime grainstone, spicule-rich rock, and shale form this facies.

The Prophet mixed-skeletal lime-packstone lithofacies consists mainly of sharp-based, massive, ungraded to graded and stratified beds (Figs. 47, 48) of carbonates and spiculite. Because they resemble proximal turbidites in the Prophet spiculite and spicule-lime-packstone lithofacies, most of these beds are interpreted as proximal turbidites. However, some thicker massive beds are possibly of debris flow origin because they have some features that Middleton and Hampton (1973) considered characteristic of debris flow deposits. These features include: a random fabric, poor grading if any, and a sharp irregular top. Units of this lithofacies are chiefly thin to medium bedded (3-30 cm) and either become more or less resistant and proximal in aspect upward.

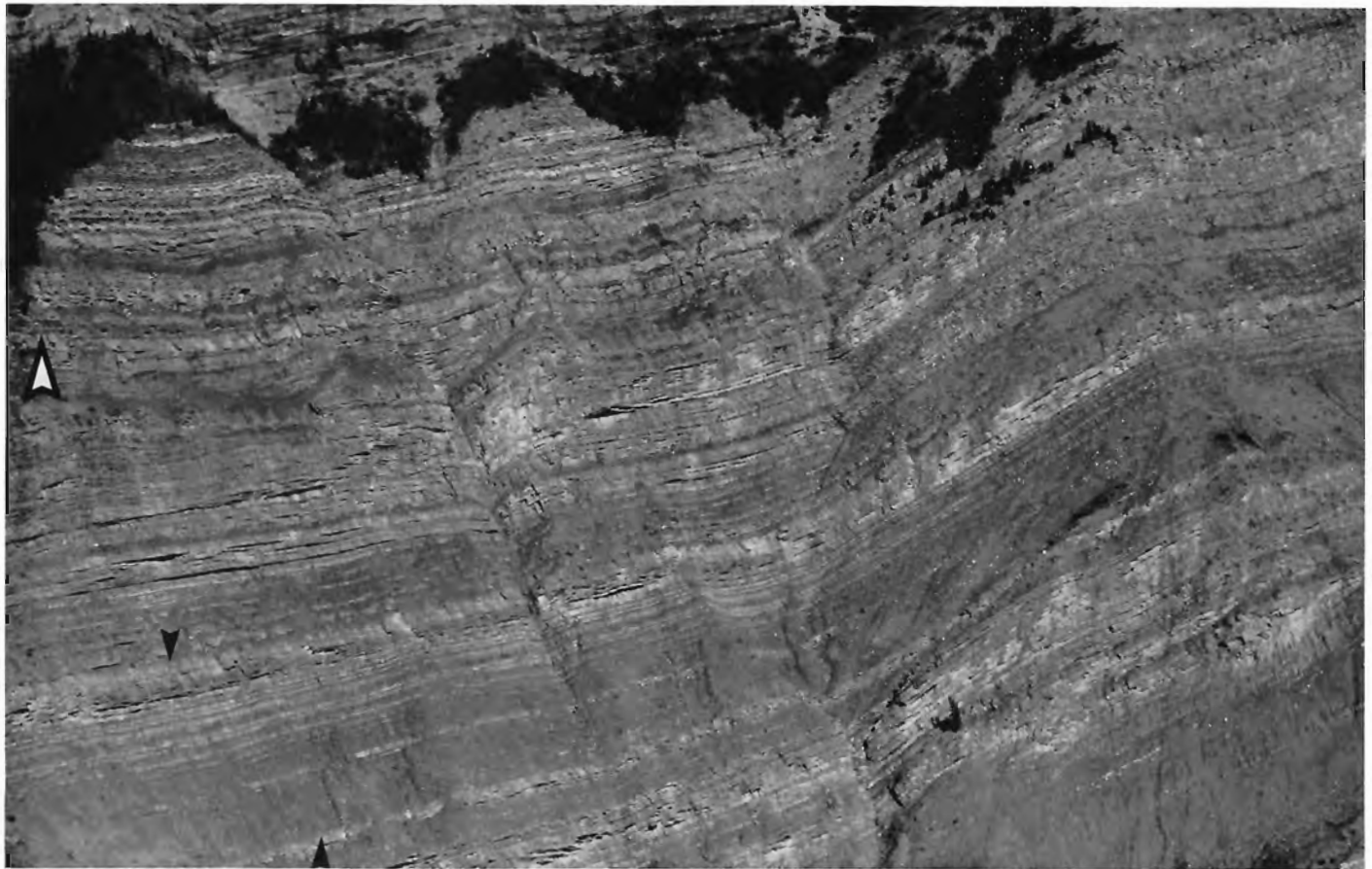


Figure 49. Multibed sequences comprising graded limestone and spiculite beds in the Flett and Prophet formations at Locality 10. Most sequences become more resistant upward. Large arrow indicates the Prophet/Flett contact; unit between small arrows is 50 m thick. ISPG 798-62.

Multibed sequences

Multibed sequences of three orders of magnitude occur between the Yohin and Golata formations. The shale of either the Clausen or upper Besa River formations, combined with the spiculite and carbonates of the Prophet and Flett formations, form a complex, progradational to aggradational megasequence. That sequence becomes, with some significant exceptions, more resistant and proximal in aspect upward (Figs. 4-6). This megasequence, which resulted from the development of at least two carbonate buildups (Fig. 50), comprises multiple, subordinate sequences (Figs. 35, 49, 70) and is called a first-order sequence here. Beds within it are grouped to form simple multibed sequences that are commonly grouped to form composites (Fig. 70). The composites are called second-order sequences, and the simple ones third-order sequences.

Two main styles of multibed sequence are present in the Prophet Formation: those that become more resistant and proximal in aspect upward, and sequences that become less resistant upward (Figs. 35, 48). Both occur as fill sequences above large-scale, concave-upward truncation surfaces, and as more widely distributed units that are traceable across extensive outcrops. At most localities, two or more superimposed sequences that have moderate lateral continuity constitute the Prophet, and the formation as a whole commonly becomes more resistant upward.

Sequences in the Prophet Formation are mostly asymmetric and become more resistant upward. Third-order sequences of this type predominate (Figs. 35, 48); however, at many localities the entire Prophet forms a second-order megasequence that becomes more resistant upward (Figs. 4-6). West of the depositional limit of the Flett Formation, the Prophet forms the top of a first-order megasequence that becomes more resistant upward. The spiculite and spicule-lime-packstone lithofacies forms most of these sequences in the Prophet but many have an upper division of that lithofacies and a lower division of dark-shale lithofacies. Also, the tops of some sequences have units of mixed-skeletal lime-packstone lithofacies (Fig. 35). The following upward changes can be observed in these sequences: sediment-gravity-flow deposits become more proximal; resistant beds become thicker and closer; the ratio of spicules to other bioclasts decreases; and the mean grain size increases. Furthermore, the abundance of carbonate minerals and limestone increases upward, whereas that of silicate minerals, spiculite, and shale decreases. Not all of these changes are evident in every sequence. Within the Prophet as a whole, this upward transition is best developed in sections that are near the western depositional limit of the Flett. To the east, these vertical changes in the Prophet are best developed in sections where the ratio of shale to other lithologies is low. Tops of these asymmetric sequences are sharp to gradational through 50 cm or more, and the recessive base of one generally overlies the resistant top of a similar underlying sequence. Where the upper contact of a sequence is sharp, a slight angular discordance of uncertain

origin may exist. For reasons given later, the basinward progradation of the lower slope on carbonate platforms (Fig. 87a), and the development of fan-like lobes on or basinward of the slope, are interpreted as being the origins of these sequences.

Sequences that become less resistant upward (Fig. 48) are relatively thin and uncommon in the Prophet, although they are relatively abundant and well developed in the Flett Formation (Figs. 51, 77b). They abruptly overlie recessive rocks and grade up into recessive strata. Deposits that are more proximal in aspect than most of the Prophet generally constitute these sequences, and they are mostly westward-thinning tongues of mixed-skeletal lime-packstone lithofacies. Probable turbidites constitute the bulk of these sequences, which become more distal upward in terms of Bouma divisions, thickness, grain size, and type of bioclast. For reasons presented later, this type of sequence is interpreted as the result of an episode of rapid progradation followed by one of progressive abandonment. Also, some are possibly channel fills.

Environmental interpretations

Spiculite and spicule-lime-packstone lithofacies

The spiculite and spicule-lime-packstone lithofacies is interpreted as having been deposited chiefly on the lower slopes of carbonate buildups (ramps grading into platforms, Fig. 87a) and as slope-related tongues in an adjacent shale basin. Slope-related tongues are mostly thin units of spiculite and spicule-lime-packstone lithofacies that are generally separated by thick units of dark shale (Figs. 4-6, 32). Thicker units of this lithofacies are considered to be lower slope deposits (Figs. 10, 35, 86). A number of criteria support the interpretation of deposition in deeper water. Much of the lithofacies is dark-coloured spiculite and spicule-rich carbonates that constitute millimetre-thick laminae and turbidites of distal aspect. Secondly, intervals of spiculite and spicule-lime-packstone lithofacies overlie and intertongue westward with basinal shale in the Besa River and Clausen formations. They also grade upward and eastward into the lighter coloured, more proximal, slope and shelf lithofacies of the Flett Formation (Figs. 50, 87a). Finally, most of this lithofacies contains an impoverished invertebrate assemblage dominated by sponge spicules and resedimented macrofossils.

The spiculite and spicule-lime-packstone lithofacies was deposited chiefly in the dysaerobic zone, but some of it originated under aerobic and some possibly in anaerobic conditions. Most of this lithofacies, particularly where the Flett overlies the Prophet, contains evidence of bioturbation but lacks remains of an indigenous calcareous epifauna. However, at Localities 8 and 19 and locally in the lower Prophet at other locations, much of this lithofacies also lacks evidence of bioturbation. In contrast, evidence of bioturbation and abundant remains of an apparently indigenous, calcareous epifauna occur locally in the spiculite and spicule-lime-packstone lithofacies of the upper Prophet in some eastern sections. According to Byers (1977), the three types of deposit mentioned above are characteristic of the dysaerobic, anaerobic, and aerobic zones, respectively.

The gradient of the lower slope cannot be determined, but it is useful to make some generalizations about this parameter. Because the lower slope was broad, up to 20 km or more across, and comprised unconsolidated, fine grained sediment, its gradient was probably low. Slump scars and slumps are locally common in distal lower slope deposits (Figs. 83, 84). This evidence of slumping indicates that the

lower slope was steep enough to be unstable, but slumping can occur on normal marine slopes with an inclination of one degree (Lewis, 1971). A gross approximation of the gradient, which is possibly a maximum, can be estimated from the amount of westward depositional thinning between the top of the Prophet Formation and underlying carbonate units of Middle Devonian age. Slope lithofacies in the Prophet, together with dark-shale lithofacies in the Besa River and Prophet formations, constitute the westward-thinning interval. The thinning in the Prophet is apparently depositional, and Pelzer (1966, p. 300-307) demonstrated that thinning in the Besa River Formation of the region is depositional. Between Localities 14 and 16, 906 m of westward thinning occurs through 17.5 km, indicating a maximum slope of 3.0 degrees. Similarly, between Localities 18 and 19, where 626 m of westward thinning occurs through 16.2 km, the estimated maximum slope is 2.2 degrees. These estimates reflect neither the effect of post-Prophet depositional compaction nor the effects of syndepositional tectonic downwarping. Because the thickness of shale is greater there, the amount of compaction was probably greater in the east. However, both estimates are probably still maximal because they do not reflect the effect of syndepositional downwarping caused by loading, which would be greatest in the east. Therefore, the true gradient may have been less than half of either estimate. On the basis of these data, the maximum mean gradient of the lower slope is tentatively interpreted as having been less than 2 degrees but greater than 0.5 degrees.

The spiculite and spicule-lime-packstone lithofacies was deposited below storm-wave base and probably in moderately deep water. Because much of this lithofacies comprises planar, millimetre-thick laminae and probable distal turbidites, which were not modified by shallow water processes, it is interpreted as having been deposited below storm-wave base. Komar (1976, p. 107) stated that storm-wave base can exceed 125 m off high-energy coasts. The slope on which the youngest units of spiculite and spicule-lime-packstone lithofacies were deposited was, at least locally, more than 18 km wide. Also, the proximal slopes, on which coeval strata in the Flett Formation were deposited, appear to have been at least 10 km wide. Sandberg and Gutschick (1979; 1980, p. 139) and Mullins and Neumann (1979, p. 185) indicated that broad carbonate slopes like those of the project area generally have mean gradients between about one and five degrees. Assuming that the upper Prophet and Flett formations were deposited on a slope that had a mean gradient of 1.5 degrees, and was about 30 km wide, water depths at the base of the slope would have been about 780 m during deposition of the upper Prophet. This estimate is possibly a minimum. Because the slope was gullied (Figs. 76, 77a) and slumps are locally common in distal-slope deposits, the slope could have exceeded two degrees.

Dark-shale lithofacies

The nature of the dark-shale lithofacies and its spatial relationship to regional facies belts, suggest deposition in moderately deep, poorly oxygenated water on the east side of an extensive basin. Most intervals of this facies are interbedded with lower slope deposits that consist of spiculite to carbonate turbidites hemipelagic deposits. Moreover, the dark-shale lithofacies occurs as eastward-thinning tongues of the shale lithosome that constitutes most of the Besa River Formation to the west. Pelzer (1966, p. 306) suggested that basinal shale, deposited at depths of 760 m or more at some locations, constitutes most of the Besa River Formation. The Prophet dark-shale lithofacies comprises shale and mudstone that are pyritic, typically lack remains of indigenous calcareous epifauna, and commonly exhibit little evidence of

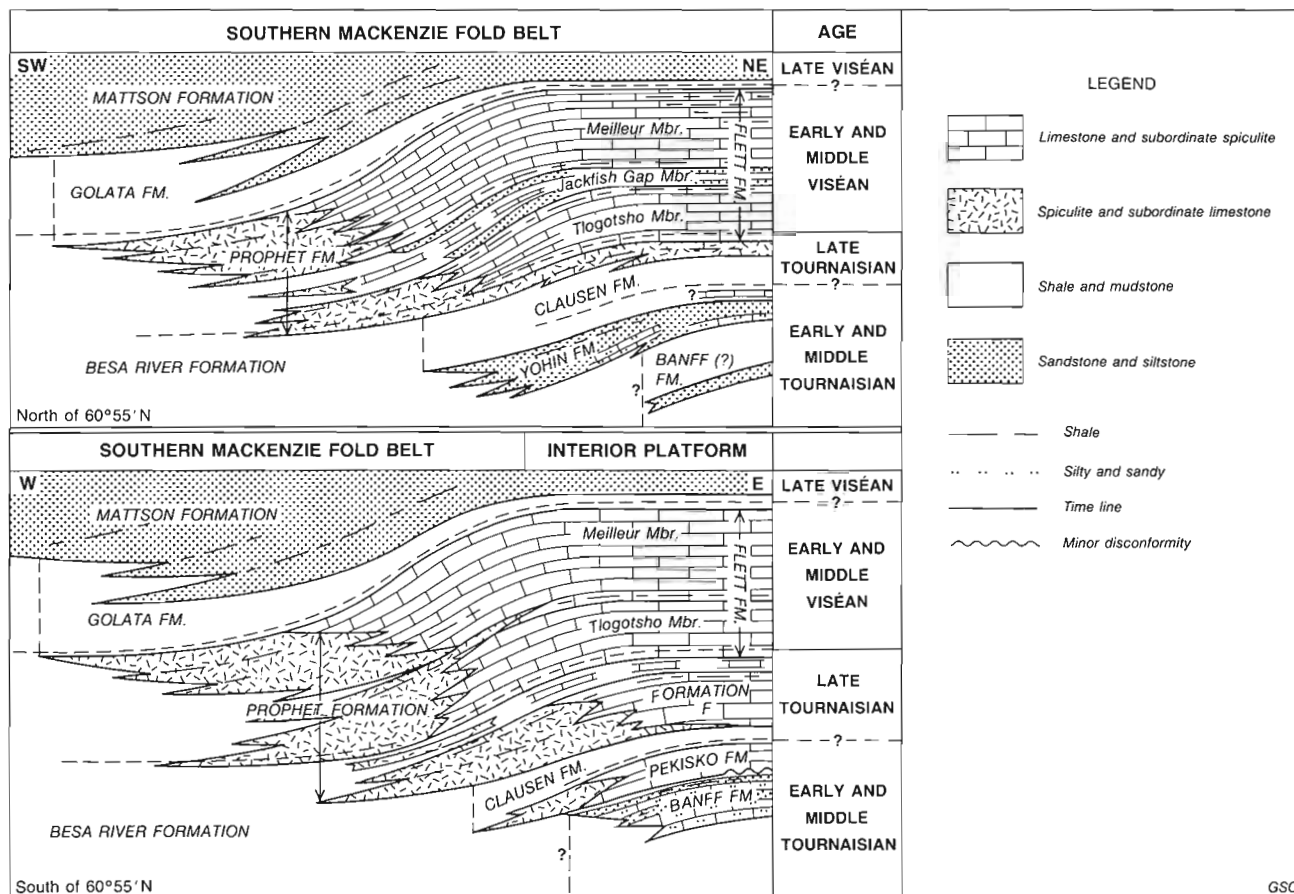


Figure 50. Schematic, restored cross-sections illustrating phases and relationships of carbonate-buildup development in study area.

bioturbation. Byers (1977) indicated that lithologies like these are commonly deposited in the poorly oxygenated water of the dysaerobic and aerobic zones. For reasons similar to those given in the discussion of the dark-shale lithofacies in the Besa River Formation, the terrigenous deposits in this facies are tentatively considered to be mainly the result of deposition from dilute, gravity-assisted bottom currents and hemipelagic sedimentation.

Mixed-skeletal lime-packstone lithofacies

Most intervals of Prophet mixed-skeletal lime-packstone lithofacies are interpreted as having been deposited on the upper parts of lower slopes on carbonate buildups (ramps grading into platforms, Fig. 87a), but some were deposited in more distal environments. This interpretation is supported by the spatial relationship of these deposits to regional lithofacies belts. Most units of this facies are intercalated with lower-slope deposits of more distal aspect, and appear to be westward-thinning tongues related to the Flett mixed-skeletal lime-packstone lithofacies. The latter is interpreted as having been deposited in middle-slope environments (Fig. 87a), for reasons given later. Intervals of Prophet mixed-skeletal lime-packstone lithofacies that are intercalated with the Prophet dark-shale lithofacies were probably deposited near the outer margin of the lower slope.

Terrigenous influx and carbonate buildup development

In the southeastern part of the project area, deposition of fine grained siliciclastics during the middle(?) to early late Tournaisian (Tn2 to Tn3) followed deposition of the Pekisko Formation and formed the Clausen Formation (Figs. 5, 6, 50). At the same time, the shale, mudstone, and siltstone of the Clausen and Besa River formations to the northwest and west were deposited. Following the initial influx, rates of terrigenous sedimentation declined in the southeastern part of the project area, and a buildup of carbonates and spiculites was deposited. The latter deposits, which are of late Tournaisian (Tn3) age, are preserved in the Prophet Formation and Formation F on the interior platform and in the eastern to central Liard Range south of about latitude 60°55'N (Figs. 5, 10, 50). To the north, deposition of the fine grained siliciclastics that constitute the Clausen continued, and a carbonate buildup was not initiated in that region until nearly the onset of Flett deposition in the latest Tournaisian (latest Tn3) (Figs. 4, 50).

Another episode of terrigenous sedimentation is recorded in the uppermost Prophet Formation on the interior platform and in the Mackenzie fold belt east of the western Liard Range (Fig. 1, Loc. 12 and eastward). This event, which occurred in the late Tournaisian (Tn3; middle to late foraminiferal zone 9), terminated a second phase of carbonate buildup development. At this time, the fine grained siliciclastics in the uppermost Prophet on the interior platform were deposited. These deposits, which are

commonly of basinal aspect, form a unit that is 15 to 20 m thick and consists mainly of shale, mudstone, spiculite, and argillaceous limestone (Fig. 5, Loc. 25; Fig. 6, Loc. 21). A lithologically similar but commonly thicker unit forms the uppermost Prophet in part of the eastern and central Liard Range. The terrigenous deposition interrupted carbonate sedimentation in the region and followed the second phase of Carboniferous carbonate buildup development (Fig. 50). When the deposition of shale and mudstone ceased, carbonate sedimentation resumed, and deposition of the carbonates that are preserved in the overlying Flett and coeval components of the Prophet proceeded.

The first episode of terrigenous deposition discussed above coincided with a major transgression in the project area. In the southeastern part of the project area, the transgression started during deposition of the carbonates in the Pekisko Formation and continued while the overlying shales in the Clausen and basal Prophet were deposited. This transgression resulted in a marked increase in water depths in the area. The latter interpretation is supported by the presence of a thick succession of shale and spicule-rich rocks that are of moderately deep water aspect and overlie the shallow water carbonates of the Pekisko (Fig. 5, Loc. 24; Fig. 6, Locs. 20, 21; Fig. 50). In the northwestern part of the project area, the transgression is recorded by the basinal shales of the lower Clausen Formation, which overlie neritic sandstone of the Yohin Formation (Fig. 4, Locs. 2-4).

Subsequent to the first period of terrigenous sedimentation and the transgression discussed above, carbonates and spiculites of late Tournaisian (Tn3) age were deposited in the southeastern part of the project area. These deposits, which are preserved as a carbonate buildup (mainly platform deposits) in the Prophet Formation and Formation F (Fig. 5, Locs. 24, 25; Fig. 5, Locs. 20, 21; Fig. 50), were deposited under shallowing-upward conditions. Evidence for this interpretation is provided by the Prophet Formation and Formation F, which form a sequence that grades upward from basinal shale and spiculite to coarse grained skeletal carbonates that are of relatively shallow water aspect. Also, the gamma ray and sonic log profiles for the Prophet/Formation F interval in this area are characteristic of progradational or shallowing-upward successions.

The second episode of terrigenous deposition that is discussed above also coincides with a transgression in the project area. This interpretation is supported by the presence in the upper Prophet of an interval of upper Tournaisian (Tn3; middle to upper zone 9) basinal shale and spicule-rich rocks that abruptly overlie deposits of more shallow water aspect (Fig. 50, interior platform south of latitude 60°55'N). A well developed hiatal surface (Frazer, 1974) underlies the terrigenous deposits (Fig. 5, Loc. 25 at 2208 ft/673 m; Fig. 6, Loc. 21 at 2405 ft/733 m). According to Frazer (1974) these surfaces commonly develop during transgressions. Also, at the same time, the initial phase of a major regional transgression occurred south of the project area. That event resulted in deposition of open-marine grainstone of the lower Turner Valley Formation above restricted-shelf deposits of the Shunda Formation (Macqueen et al., 1972; Richards et al., in press).

Age

Microfossils collected from the Prophet, Flett, and Besa River formations (Appendices A, E) indicate that the Prophet ranges in age from middle(?) Tournaisian to latest middle Viséan (Tn2 to V2).

In most of the area, the age of the basal Prophet is uncertain because fossils with narrow stratigraphic ranges are rare in both the lower Prophet and underlying strata; moreover, fossils were not collected from the Prophet on the interior platform. Foraminifers and calcareous algae assignable to foraminiferal zone 9 (Mamet and Skipp, 1970, 1971), of latest Tournaisian (Tn3) age, were identified in samples from the base of the Prophet at Twisted Mountain. Because palynomorphs of probable late Tournaisian (Tn3) age (Appendix E) are present 133 m below the Prophet at the north end of the Flett anticline (Fig. 1, Loc. 11), the basal Prophet in the eastern Liard Range and on much of the platform is probably also of late Tournaisian age.

The uppermost Prophet Formation ranges in age from latest Tournaisian (Tn3; foraminiferal zone 9) to latest middle Viséan (V2; latest zone 13). In most of the project area east of the Tlogotsho Plateau and the western Liard Range, the base of the overlying Flett Formation is of latest Tournaisian age (Tn3; late zone 9). To the west, the Prophet-Flett contact becomes younger, and immediately west of the western depositional limit of the Flett, the uppermost Prophet is of latest middle Viséan age (V2; latest zone 13).

FLETT FORMATION

Type section

Harker (1961, p. 4) proposed the name Flett Formation and designated its type section (Fig. 4, Jackfish Gap section; Figs. 24, 51), which outcrops on the west side of Yohin Ridge immediately north of Jackfish Gap (Fig. 1, Loc. 4). He included 604.1 m (1982 ft) of strata in this section. The locality is about 32 km west of Nahanni Butte in the Twisted Mountain map area (NTS 95 F/4), at latitude 61°05'54"N, and longitude 123°59'26"W.

In this report, the definition of the Flett Formation is restricted, and only 347.3 m of strata are included in its stratotype. The restricted type section corresponds to the interval between 477.4 and 824.7 m in the Jackfish Gap sections on Figures 4 and 24. The Flett is redefined here because Harker (1961, p. 4; 1963, p. 10, 36, 37, units 1-16) included in the lower part of its stratotype a unit that is stratigraphically and lithologically equivalent to the Prophet Formation of Sutherland (1958, p. 25-27). It is further restricted because Harker (1961, p. 4; 1963, p. 33, units 91-94) included at the top of the Flett type section a unit (Fig. 71) that is stratigraphically and lithologically equivalent to the Golata Formation of Halbertsma (1959, p. 113, 114).

The base of a resistant limestone unit, which is approximately 40 m thick and about 127 m above the former lower boundary stratotype, defines the lower boundary of the restricted Flett type section (Fig. 51). This boundary coincides with a marked break in slope caused by an abrupt change in the proportions of rock types present. Shale with subordinate spiculite and skeletal lime packstone constitute the Prophet Formation, whereas the lower Flett is mostly skeletal lime packstone (Figs. 24, 51, 52a).

The upper boundary of the restricted Flett type section is about 8 m below the position specified as the upper boundary stratotype by Harker (1961, p. 4; 1963). A moderately abrupt lithological change defines the new boundary (Fig. 71). Dolostone and limestone with subordinate shale form the uppermost Flett, and the overlying, recessive Golata Formation is shale with subordinate dolostone and minor argillaceous sandstone.



Figure 51. Type sections of the Flett Formation (347 m thick) and the Tlogotsho, Jackfish Gap, and Meilleur members at Jackfish Gap. From the base upward, large arrows indicate the following contacts:

1. Prophet Formation and Tlogotsho Member
2. Tlogotsho and Jackfish Gap members
3. Jackfish Gap and Meilleur members
4. Meilleur Member and Golata Formation

The Tlogotsho is a multibed sequence that becomes less resistant upward and has large-scale, concave-upward truncation surfaces (small arrows). ISPG 798-171.

The name Flett Formation (Harker, 1961, p. 4) is possibly a junior synonym of Debolt Formation (Macauley, 1958, p. 298) (Fig. 3), but resolution of this problem will require considerable regional work. In much of northeastern British Columbia, a unit that has been assigned to the Debolt Formation (Macauley et al., 1964, p. 97, 98; Bamber and Mamet, 1978, p. 6) appears to be equivalent to the redefined Flett Formation. However, neither the Flett nor much of the Debolt in northeastern British Columbia closely resembles the type Debolt, which is in the Peace River area of Alberta. Also, regional studies of the Lower Carboniferous in British Columbia and western Alberta (Richards et al., in press) suggest that the type Debolt consists of strata that are lithologically and stratigraphically equivalent to the Turner Valley and Mount Head formations (Fig. 3) of Douglas (1958).

Previous work

The redefined Flett Formation corresponds with most of the upper two thirds of the following units in southwestern District of Mackenzie: Patton's (1958, p. 312-319) Unit 3 at Jackfish Gap, Unit 7 of Douglas and Norris (1959) in the Fort

Liard and La Biche map areas (95B and 95C), Unit 32 of Douglas and Norris (1960) in the Virginia Falls and Sibbeston Lake map areas (95F and 95G), and the Flett Formation of Harker (1963). Also, the restricted Flett corresponds to most of the upper two thirds of the Flett Formation on geological maps by Douglas et al. (1963), Douglas and Norris (1976a, b, c), and Douglas (1976). Richards (1978, p. 478), Bamber and Mamet (1978), and Bamber et al. (1980, p. 12, 13) used the name Flett in the same way as Harker (1963).

Distribution

The Flett Formation has a moderately wide distribution in the project area. In the southern Mackenzie fold belt south of the Tlogotsho Plateau, this unit occurs mainly east of the Kotaneelee syncline and Pointed Mountain anticline. To the north, it underlies much of the north side of the Tlogotsho Plateau and the fold belt to the northeast. In the fold belt, this moderately resistant unit outcrops chiefly along narrow belts on the limbs and noses of several broad synclines and anticlines between latitudes 60°22'N and 61°30'N. East of the Mackenzie fold belt and north of

60°00'N, the Flett is present on the interior platform south of about 60°45'N, where it is mainly a subsurface unit. On the interior platform south of Pointed Mountain, the Flett probably does not occur much west of about longitude 123°50'W, but control in that area is meagre. Also, much of the unit that has been called Debolt Formation in northeastern British Columbia (Macauley et al., 1964, p. 97, 98; Bamber and Mamet, 1978, p. 6) is possibly assignable to the Flett.

Thickness

The thickness of the Flett Formation is moderately variable (Table 1, Figs. 4-6). Where strata of Early Carboniferous age conformably overlie it, the Flett generally thins toward the west. For example, at Jackfish Gap it is 347.3 m thick and thins quite rapidly to 234.0 m at Locality 5, which is 8.5 km to the west. Similar but less pronounced trends occur to the south between the western Liard Range and the interior platform. The thickest known section is at Locality 3, where the Flett is more than 358 m thick. In the southern half of the project area, it is probably thickest on the west side of the interior platform. On the platform, north and east of the erosional zero-edge of the overlying Mattson Formation, the Flett thins fairly rapidly to zero beneath a regional unconformity.

Lithostratigraphic relationships

At Twisted Mountain and southward, the Flett Formation generally conformably overlies and grades westward into the Prophet Formation (Figs. 4-6), but north of Twisted Mountain it possibly overlies the Clausen Formation. Toward the west, the Flett/Prophet contact becomes younger, and eventually the entire Flett grades into the Prophet. The characteristics of the Flett/Prophet transition are given in the discussion on the lithostratigraphic relationships of the Prophet. The Flett probably locally overlies Formation F on the interior platform, but their contact was not examined.

In the project area, the Flett Formation is overlain by the Golata Formation, Lower Cretaceous Fort Saint John Group, and Permian strata (Figs. 4-6). The Golata (Fig. 71) conformably overlies the Flett in the Mackenzie fold belt and on the interior platform west of the erosional zero-edge of the Mattson Formation. Eastward and northward from the Mattson zero-edge, the Golata thins rapidly to zero. Beyond the erosional zero-edge of the Golata, the Flett in turn thins quite rapidly beneath sub-Permian and sub-Cretaceous regional unconformities.

The Flett/Golata contact is mainly abrupt, but locally it is gradational through an interval of less than one metre. It is placed at a stratigraphic position above which carbonates constitute less than 50 per cent of the succession. Toward this contact, the proportion of shale in the underlying Flett, which comprises interbedded carbonates and shale, increases rapidly. Because the Golata is chiefly shale, this contact is readily located in well sections by using gamma ray and sonic logs.

Members

At Jackfish Gap the Flett Formation is herein formally subdivided into three members that are named, in ascending order, the Tlogotsho, Jackfish Gap and Meilleur members (Figs. 2, 3, 24, 51). The thicknesses of these members at selected localities are listed in Table 1. The distributions of

the Tlogotsho and Meilleur members are similar and generally coincide with that of the Flett in the region east of the northeastern corner of the Tlogotsho Plateau and the westernmost Liard Range. To the west, where the Flett generally cannot be subdivided, only strata equivalent to the Meilleur Member occur. The Jackfish Gap Member is confined to the Mackenzie fold belt and the region that is north of about latitude 60°55'N and east of the western two thirds of the Tlogotsho Plateau. South of 60°55'N, the Flett deposits that are equivalent in age to those in the Jackfish Gap Member are included in the Tlogotsho Member. Because regional unconformities cut progressively downward into the Flett toward the east and north, only the Tlogotsho Member is preserved farthest eastward on the interior platform (Figs. 5, 6).

Tlogotsho Member

The name Tlogotsho Member is proposed for the lower 130.9 m of the Flett Formation at Jackfish Gap (Figs. 4, 24; 477.4-608.3 m) and is derived from the Tlogotsho Plateau, which is 8 km to the southwest. North of approximately 60°55'N, the base of this member is resistant and cliff forming, but the overlying deposits in the Tlogotsho become progressively less resistant upward because the proportion of limestone decreases. To the south, the Tlogotsho is mainly resistant and cliff forming but has some moderately thick recessive units. The Tlogotsho (Figs. 32, 51) consists of well bedded mixed-skeletal lime packstone with subordinate grainstone, crystalline limestone, shale and mudstone. Minor lime wackestone, spiculite, and dolostone also occur. In the Carboniferous outcrop belt, most limestone in this member is rhythmically bedded, but units of crossbedded limestone are locally present.

The Tlogotsho Member, which conformably overlies the Prophet Formation, is conformably overlain by the Jackfish Gap Member in the Mackenzie fold belt north of about latitude 60°55'N, and by the Meilleur Member elsewhere (Figs. 4-6). Contacts between the Tlogotsho and both overlying members are clearly defined, with minor gradation through 10 cm or more. The base of a unit of siltstone and sandstone defines the Tlogotsho/Jackfish Gap contact. To the southeast, the recessive basal deposits of the Meilleur mark the Tlogotsho/Meilleur contact (Figs. 5, 6). The base of the Meilleur Member marks a position above which the Flett generally becomes more resistant upward; moreover, the lower proportion of lime grainstone in the Tlogotsho distinguishes it from the overlying member. In subsurface sections, the lower radioactivity of strata in the uppermost Tlogotsho serves to differentiate them from those in the basal Meilleur. Also, the gamma ray and sonic log profiles of the Tlogotsho are more deeply serrated than those of the Meilleur.

The thickness of the Tlogotsho Member is moderately variable (Figs. 4-6, Table 1). In the west, it thins rapidly toward its western depositional limit, and in the east its thickness diminishes rapidly eastward below the Cretaceous. South of about latitude 60°55'N, the Tlogotsho is locally thicker than it is to the north because it includes strata that are equivalent in age to the Jackfish Gap Member (Fig. 3).

Jackfish Gap Member

The name Jackfish Gap Member is proposed for the interval from 130.9 to 210.9 m above the base of the Flett Formation at Jackfish Gap (Figs. 4, and 24 at 608.3-688.3 m, 51, 67) and is derived from Jackfish Gap, which is a narrow valley. The type section consists of a lower 18.0 m

thick unit of planar-laminated to crossbedded siltstone and sandstone; a recessive middle 45.2 m thick unit of shale and mudstone, with subordinate rhythmically bedded limestone; and an upper 21.2 m thick interval that is mainly crossbedded siltstone and sandstone. At most other localities, this member consists of either the upper siltstone and sandstone unit or three units that are similar to those in the type section. At the type locality and most other localities, the Jackfish Gap Member gradationally overlies the Tlogotsho Member and conformably underlies the Meilleur Member. The thickness of the Jackfish Gap Member is moderately variable (Table 1; Figs. 4-6).

Meilleur Member

The name Meilleur Member is proposed for the unit from 210.9 to 347.3 m above the base of the Flett Formation at Jackfish Gap (Figs. 4 and 24 at 688.3-824.7 m, 51). This name is derived from the Meilleur River, a large stream west of the Tlogotsho Plateau. The Meilleur Member (Fig. 51), which is the most resistant member in the Flett, is rhythmically bedded to crossbedded lime grainstone and packstone with subordinate dolostone, shale, and mudstone.

The Meilleur Member conformably overlies either the Jackfish Gap or Tlogotsho members and is either conformably overlain by the Golata Formation or disconformably overlain by the Permian and Cretaceous. At its type locality and elsewhere north of about latitude 60°55'N, the Meilleur passes into the underlying Jackfish Gap through 10 cm or less; but to the south, where the latter is not developed, it conformably overlies the Tlogotsho.

The thickness of the Meilleur Member is moderately variable (Table 1, Figs. 4-6). In the west, it generally thins slowly toward its western depositional limit, but in the east it thins rapidly eastward below the Permian and Cretaceous.

Lithology

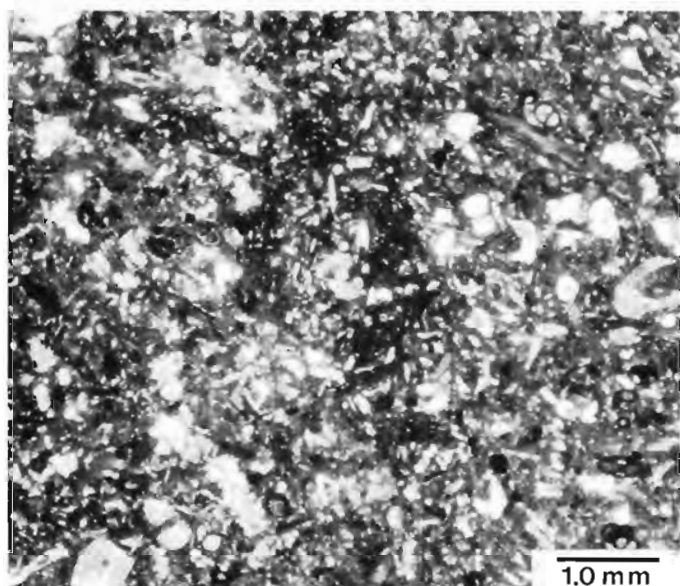
The Flett Formation comprises lime packstone and grainstone with subordinate lime wackestone, dolostone, spiculite, siltstone, sandstone, shale, and mudstone (Figs. 4-6, 24). Lime packstone (Fig. 52a) and wackestone become more abundant toward the west. They generally constitute most of the Tlogotsho Member west of the eastern Liard Range, most limestone beds in the Jackfish Gap Member, most of the Meilleur Member west of the Liard Range, and part of the lower Meilleur Member in the east. In contrast, lime grainstone (Fig. 52b) becomes more abundant toward the east. Lime grainstone forms much of the Tlogotsho in the eastern Liard Range and in the subsurface to the east. It also constitutes most of the upper one half or more of the Meilleur in the Liard Range and Jackfish Gap area and a major proportion of the Meilleur on the interior platform. Dolostone (Fig. 52c) is a minor rock type in most of the Flett, but it is commonly the main types in the upper one to four metres of the Meilleur. Spiculite, which becomes more abundant toward the west, is common in the upper part of the graded beds in much of the Flett. Also, beds of spiculite are locally common in the basal Meilleur and in western occurrences of the Flett. Spiculite in the Flett is like that described from the Prophet Formation (Fig. 36a); consequently it is not described again here. Sandstone (Fig. 52d) and siltstone appear to occur only in the Jackfish Gap Member, where they are major rock types. In the Flett, the volume of shale and mudstone increases toward the northeast. Shale (Fig. 68) and mudstone, which are present in much of the Flett as thin partings to beds that are several metres thick, are most abundant in the upper Tlogotsho north of about latitude 60°55'N, in the Jackfish Gap, and the basal and upper Meilleur.

Lime packstone and wackestone in the Flett Formation are chiefly bryozoan-pelmatozoan lime packstone and wackestone, but pelmatozoan-spicule lime packstone and wackestone are quite common, and other variants are present (Fig. 52a). These limestones are mainly olive-grey to olive-black and weather light olive-grey. Pelmatozoan ossicles, bryozoans, and spicules are generally the principal allochems, but brachiopods, foraminifers, pellets, and intraclasts are present and locally predominate. Calcareous algae, ostracods, molluscs, and corals occur, but are seldom abundant. For reasons given in the discussion on spicule diagenesis in the Prophet Formation, most spicules are interpreted as having been opal originally. Spicules are most abundant in the lime packstone and wackestone of the mixed-skeletal lime-packstone lithofacies and the spiculite and spicule-lime-packstone lithofacies. In these rocks, they constitute more than 90 per cent of the bioclasts in some beds. Spicules, which are generally most abundant in recessive units, become more plentiful toward the west and the tops of graded beds. Proportions of other allochems are highest in resistant units and generally increase toward the east and top of the Flett Formation. Although most allochems are of silt to small-pebble size, coarser material, which includes brachiopods, corals, bryozoans, and intraclasts, is moderately common. Well preserved microfossils are relatively common, and well preserved macrofossils exist in some beds; however, most macrofossils are fragmentary, crushed, and abraded because of transportation, compaction, and pressure solution.

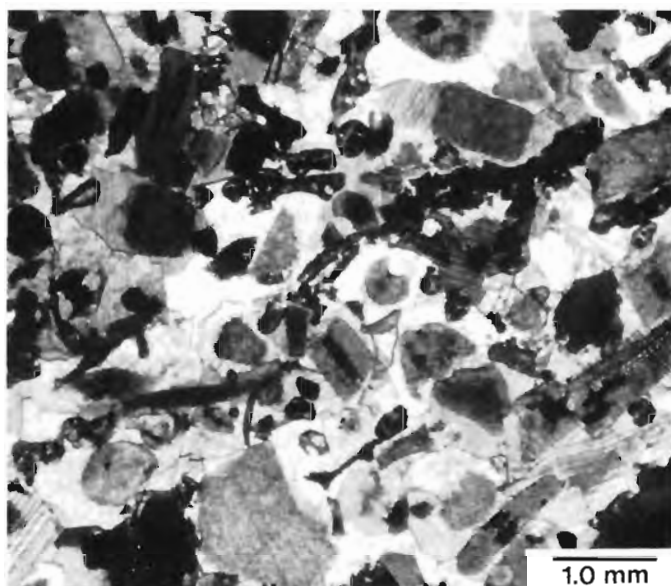
Sand and silt, and siliceous, clay-sized matrix material (Appendix G) are the main terrigenous components in the lime packstone and wackestone, but granule- to pebble-sized intraclasts of mudstone and shale are locally common in sharp-based beds. The sand and silt material is mainly quartz and is present in most beds; however it typically constitutes less than 0.5 per cent by volume. Fine grained siliciclastic matrix is common in the upper parts of sharp-based, massive and ungraded to graded and stratified limestone beds.

Lime grainstone in the Flett Formation is chiefly bryozoan-pelmatozoan lime grainstone (Fig. 52b) but brachiopod (Fig. 54), and pelmatozoan-bryozoan lime grainstone are moderately common. These grainstones are olive-grey to light olive-grey and weather light olive-grey. In order of decreasing abundance, the principal allochems are pelmatozoan ossicles, bryozoans, and brachiopods. Intraclasts, foraminifers, calcareous algae, and ostracods are moderately common, but they are seldom the main allochems. Spicules, corals, molluscs, and pellets are minor components. Ooids occur locally in the lime grainstone of the Meilleur Member at Locality 21 on the interior platform, but were not observed elsewhere. In general, foraminifers and calcareous algae become more abundant toward the east and top of the Flett; bryozoans and pelmatozoans are common in most lime grainstone of the formation. Spicules become more abundant toward the west and the base of the Flett. Although present in most beds, brachiopods are seldom abundant, but in some thick deposits of lime-grainstone lithofacies at Locality 13 they are almost the only allochems present. Many microfossils are moderately well preserved, whereas macrofossils seldom are. Largely because of transportation, most macrofossils are of sand to small-pebble size, fragmentary and abraded. Coarser material, which includes intraclasts, and fragments of brachiopods and corals, is moderately common in many beds. Scattered quartz silt and sand occur in most beds but generally constitutes less than 0.5 per cent of these beds.

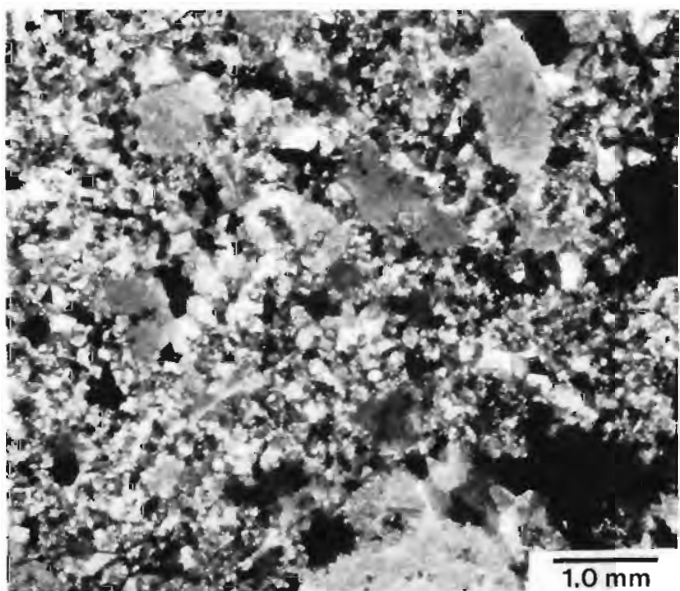
The dolostone at the top of the Flett Formation (Fig. 52c) is fossiliferous and comprises finely to very coarsely crystalline, anhedral to subhedral crystals. This



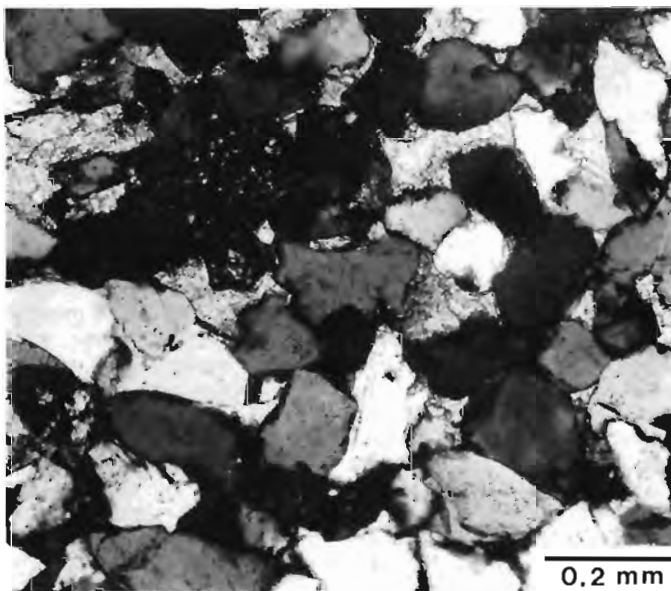
a. Mixed-skeletal lime packstone (GSC loc. C-74264) from Locality 5. ISPG 1768-57.



b. Bryozoan-pelmatozoan lime grainstone (GSC loc. C-52139), from the upper Flett Formation at Jackfish Gap. Pelmatozoan ossicles have monocrystalline syntaxial overgrowths. ISPG 1768-54.



c. Finely to coarsely crystalline, fossiliferous, ferroan, dolostone (GSC loc. C-74269); from the uppermost Flett Formation at Locality 5. ISPG 1768-96.



d. Fine sandstone: calcareous, submature subchertarenite (GSC loc. C-52529); from the Jackfish Gap Member at Jackfish Gap. ISPG 1768-150.

Figure 52. Photomicrographs of Flett rock types.

dolostone is chiefly olive-grey to light olive-grey and weathers yellowish orange. Pelmatozoan ossicles and bryozoans are the principal allochems; scattered brachiopods, intraclasts, ostracods, and corals also occur. Most bioclasts are fragmentary, abraded, and of sand to granule size. Although part of some invertebrates are calcite, dolomite has completely replaced the majority. Minor siliciclastic sand,

silt, silicified mudstone intraclasts, and glauconite are present, but they generally constitute less than one per cent of the rock by volume.

Elsewhere in the Flett Formation, the dolostone is mainly a dark, siliceous, sucrosic rock similar to most dolostone in the Prophet Formation (Fig. 36d), and consists

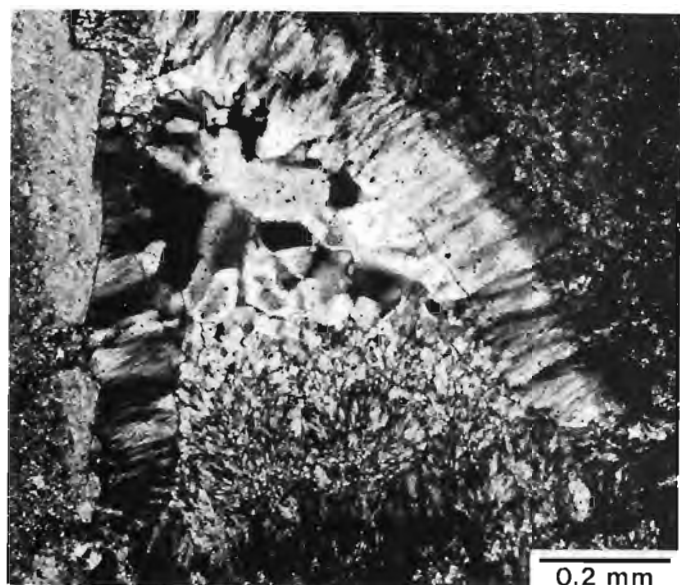


Figure 53. Photomicrograph, showing chalcidonite (fibrous chert), megaquartz (near centre), and microquartz with calcite (upper right), in chert nodule (GSC loc. C-52142) from the upper Flett Formation at Jackfish Gap. ISPG 1768-81.

chiefly of finely crystalline, subhedral to euhedral rhombs of ferroan dolomite. The allochems present include those that occur in the dolostone described in the previous paragraph; sponge spicules are also common and locally predominate. Fine grained, siliciclastic matrix and minor quartz silt and sand constitute the terrigenous fraction. This dolostone is mainly olive-black to olive-grey and weathers greyish orange.

The siltstone and sandstone in the Flett Formation are mainly siliceous to calcareous, submature subchertarenite (Fig. 52d). The sandstone is mainly very fine to fine grained. Both lithologies are olive-grey to medium light grey and weather greyish orange to moderate brown. The sorting of the clasts is mainly moderate to poor, and these rock types vary from texturally immature to mature, although they are chiefly submature. Fine to coarse sand sized clasts of quartz and chert are mainly subangular to subrounded. In this size range, angular to very angular clasts are moderately common, and rounded to well rounded clasts occur but are not common. In contrast, most clasts in the finer grained fractions are subangular to angular. Quartz and strongly ferroan calcite are the principal cements; minor dolomite is present in some samples. Calcite commonly partially replaced quartz overgrowths and clasts, and in some samples clasts float in calcite.

The mean percentages of clast types in 10 sandstone samples are: quartz 86.7 ± 3.2 , chert rock fragments 8.8 ± 2.5 , other rock fragments (mudstone and subordinate metamorphic rocks) 3.2 ± 1.9 , feldspar 0.2 ± 0.2 , nonopaque heavy minerals (mainly tourmaline, zircon, and sphene) 0.3 ± 0.3 , micas 0.5 ± 0.4 , and opaques 0.3 ± 0.3 (Appendix F). Mean percentages of the types of quartz grains in five sandstone samples are: clasts with straight extinction 63.2 ± 4.9 , clasts with undulose extinction ($>5^\circ$) 31.8 ± 3.8 , polycrystalline clasts with two to three units 1.4 ± 0.6 , and polycrystalline clasts with more than three units 3.7 ± 1.0 . These two analyses are based on 500 and 400 counts per thin section, respectively. Mica is a minor component in the sandstone and is concentrated on bedding planes, whereas it

is moderately abundant in siltstone. Minor glauconite and phosphates occur in a few samples, and fragmentary invertebrate fossils and carbonized plant fragments are common to rare.

In the Flett Formation, the shale (Fig. 68) and mudstone are calcareous to noncalcareous, commonly fossiliferous, and medium-dark grey to greyish black. Most mudstone is very calcareous, and commonly grades into very argillaceous limestone. The former is difficult to distinguish from the latter without X-ray diffraction analyses. Although the shale is mainly calcareous, noncalcareous shale is quite common, particularly in the upper 10 to 50 m of the Flett. The slightly calcareous to noncalcareous shale can be split into paper-thin sheets. Fissility is less well developed in the more calcareous shale, which commonly grades into friable to platy mudstone. Semiquantitative X-ray analyses indicated that quartz is the principal mineral in the shale and that quartz and calcite are the main minerals in the mudstone (Appendix G). Well preserved to fragmentary and abraded microfossils and macrofossils are common in the calcareous shale and mudstone, but bioclasts are relatively rare in noncalcareous lithologies.

Diagenesis

Chert

Authigenic chert is a major component in the spiculite, limestone, and dolostone of the Flett Formation. It occurs in most beds; however, chert is generally less abundant than in the Prophet Formation. Four chert fabrics are present: microquartz; chalcidonite or length-fast chalcedony; quartzine or length-slow chalcedony; and megaquartz. Some chert cement is present, but it is less common than replacement chert. The replacement chert has almost completely replaced some beds, but it most commonly occurs as isolated, greyish black to light grey nodules, and as a partial replacement of matrix, calcite cement, and allochems. In general, chert is least abundant in the lime grainstone and most plentiful in the spiculite and dark, spicule-rich lime packstone and wackestone.

Microquartz (Fig. 53) is the most abundant chert fabric. It occurs as mosaics of very fine to aphanocrystalline, subequant, anhedral grains. This replacement chert most commonly replaced matrix, particularly the clay-sized siliciclastics that occur in most spiculite and spicule-rich limestone. Microquartz is also the principal mineral in most nodules and beds of chert. Moreover, it largely replaced sediment in the upper, fine grained component of many graded beds in some western occurrences of the Flett. Microquartz replaced both ferroan and nonferroan calcite cement, and is the most abundant chert in pseudomorphs of bioclasts. The chert in most of the sponge spicules appears to be microquartz, but chalcidonite replaced some spicules in most samples.

Chalcidonite (Fig. 53) is the second most abundant type of chert in the Flett Formation, but it is much less abundant than microquartz. This length-fast chalcedony occurs most commonly in sponge spicules. The greatest volume of chalcidonite occurs as botryoidal, isopachous coatings on bioclasts and as cement in lime grainstone. Isopachous chalcidonite frequently appears to have lined or filled cavities, where it is commonly overlain by sparry calcite cement or other chert fabrics. The substrate of the isopachous chalcidonite is generally a corrosion surface. Length-fast chalcedony, which also exists as spherulites and fibrous fans, is the second most abundant chert in most nodules and predominates in some.

Folk and Pittman (1971, p. 1050) and Meyers (1977, p. 89) suggested that chalcedony almost always occurs as a cavity filling instead of as a replacement mineral. However, part of the chalcedony in the Flett is possibly a replacement mineral. Evidence for a possible replacement origin includes: spherulites in the walls of a few bioclasts; abundant, well developed examples of surfaces that are convex into adjacent calcite; isopachous coatings developed between pelmatozoan fragments and their probable monocrySTALLINE syntaxial overgrowths; oriented, apparent islands of host calcite in chalcedony; chert cutting across twin planes in calcite; and a substrate that is commonly a corrosion surface.

Length-slow chalcedony, mainly quartzine, is common in pelmatozoan-rich limestone and dolostone, but is relatively minor volumetrically. This replacement chert is like that in the Prophet Formation (Fig. 38) and occurs as interfering fans and irregular masses, which commonly have a poikilotopic texture. It replaced crinoid ossicles and less commonly brachiopods, nonferroan and ferroan calcite cement, and pseudospar. According to Folk and Pittman (1971), length-slow chalcedony exists almost exclusively either as a replacement of evaporites or in association with them. This is probably not true in the Flett and Prophet formations of the project area, because evaporites and related lithofacies are absent from both units.

Megaquartz (Fig. 53) is relatively rare in the Flett and exists chiefly as isolated euhedra and mosaics of fine to medium crystalline, subhedral crystals. It is most common as a late void filling, and also occurs in bioclasts, some chert nodules, and in interstices between bioclasts.

For reasons given in the discussion on chert in the Prophet Formation, a main source of silica in chert of the Flett and Prophet formations is considered to have been biogenic opal, particularly that of spicules. This interpretation is in agreement with Meyers and James (1978) and Chown and Elkins (1974).

Most chert nodules and masses in the carbonates of the Flett Formation appear to have formed relatively early during the diagenetic and compactional histories of the formation. The interpretation is supported by the moderately common occurrence of compaction-deformed laminae around chert nodules and masses. The deformation indicates that the chert developed prior to the cementation and much of the compaction of the enclosing sediment. Also, microstylolitic allochem contacts, which frequently develop during advanced stages of compaction in noncemented sediment, are commonly much less abundant in the chert nodules and masses than in the surrounding grain-supported carbonates. This indicates that the chert formed prior to most microstylolite development.

Petrographic evidence suggests, however, that some chert in the Flett Formation is not of early diagenetic origin. At least some first-generation, nonferroan to slightly ferroan, calcite cement is older than the chert fabrics observed, because chert either precipitated on or partly replaced those cements in some samples. For reasons given in the next section, the first-generation calcite cement that is associated with the chert is not syndepositional-marine cement. In addition, microquartz and chalcedony locally partly replaced later ferroan and nonferroan calcite cement.

Calcite

Authigenic calcite in the Flett Formation formed in four basic ways: passive precipitation into cavities; displacive precipitation; neomorphism; and replacement of

non-CaCO₃ minerals. Neomorphic calcite is the most widespread and abundant, whereas sparry-calcite cement produced by passive precipitation is second. Replacive calcite is probably slightly less plentiful than cement. Displacive calcite, although relatively common in some lime packstone and wackestone, is a minor component by volume. Because the displacive calcite in the Flett is similar to that in the Prophet Formation, it is not discussed further. Using Dickson's (1965) staining technique for carbonate thin sections, it was determined that ferroan and nonferroan, authigenic calcite occur in subequal proportions.

Three main morphologic types of sparry calcite cement or passively precipitated calcite occur in the Flett Formation: monocrySTALLINE syntaxial overgrowths (Fig. 52b); pore-filling mosaics of subequant crystals (Fig. 54); and polycrySTALLINE fringes of equant to bladed crystals (Figs. 55, 56). These are the principal types of authigenic calcite in lime grainstone, and they are moderately abundant in some coarser grained lime packstone. However, they are relatively minor components in other rock types.

In the Flett Formation, monocrySTALLINE syntaxial cement, which occurs on pelmatozoan ossicles and in their canal systems, is the most common and volumetrically abundant sparry calcite cement (Fig. 52b). Where pelmatozoan fragments are the principal allochems in lime grainstone, their overgrowths occupy most interstitial space; volumes of other calcite-cement fabrics are small. Moreover, many of these overgrowths enveloped adjacent polycrySTALLINE bioclasts, thereby producing crystals with a poikilotopic texture. The monocrySTALLINE syntaxial overgrowths are generally relatively clear, and lack evidence of probable acicular calcite and aragonite precursors like those discussed by Kendall and Tucker (1971, 1973), Davies (1977), Lohmann and Meyers (1977), and Mazzullo (1980). These overgrowths vary from nonferroan to strongly ferroan, and Dickson's (1965) staining technique revealed that they commonly consist of two or more generations. Where two or more generations are present, the mole percent of Fe²⁺ is generally lowest in the first generation. In some, however, it is highest in the first generation. In others, ferroan and nonferroan generations alternate, thereby indicating fluctuations between oxidizing and reducing conditions in their precipitational environments.

Solutions in Folk's (1973; 1974a, p. 45, 51) meteoric-phreatic and subsurface zones, instead of in the vadose and marine-phreatic zones (Fig. 19), probably precipitated the monocrySTALLINE syntaxial overgrowths. Reasons for this interpretation are similar to those given in the discussion of the sparry calcite cement in the Yohin Formation. This interpretation is consistent with Longman (1980, p. 477), Meyers (1974; 1978, p. 379), Meyers and Lohmann (1978, p. 477) and Richter and Füchtbauer (1978). During the Carboniferous, vadose processes probably could not have affected much of the Flett in the project area, because this formation and the overlying Golata Formation lack intraformational unconformities. Also, supratidal deposits were not observed in either formation.

Mosaics of subequant-grained, clear calcite (Fig. 54) are the second most widespread and abundant form of passively precipitated calcite in the Flett Formation. This fabric occurs intergranularly and intragranularly, and it overlies older cements or cavity walls directly. These mosaics comprise finely to very coarsely crystalline, subhedral crystals that commonly become larger away from pore walls and vary from nonferroan to strongly ferroan. These mosaics are interpreted as having been precipitated relatively late in Folk's (1973; 1974, p. 45) meteoric-phreatic and subsurface zones for reasons similar to those given in the discussion of this fabric in the Yohin.

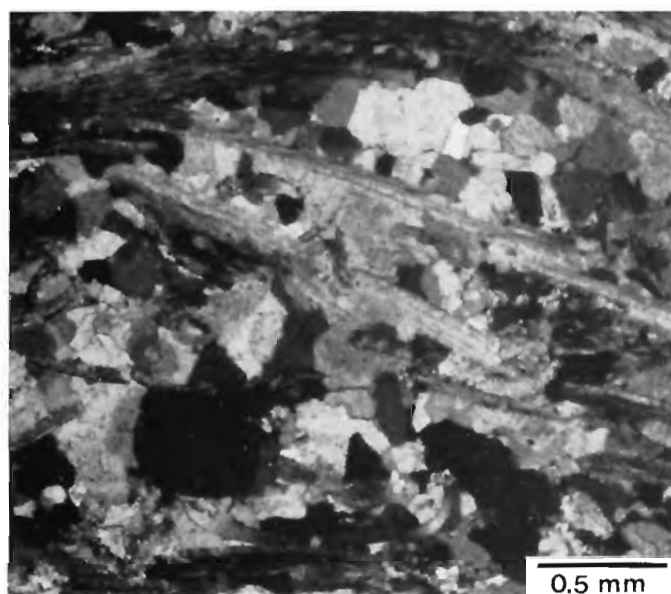


Figure 54. Photomicrograph of brachiopod lime grainstone (GSC loc. C-52341) from the Tlogotsho Member of the Flett at Locality 13. Blocky mosaics are the main sparry calcite cement. ISPG 1768-142.

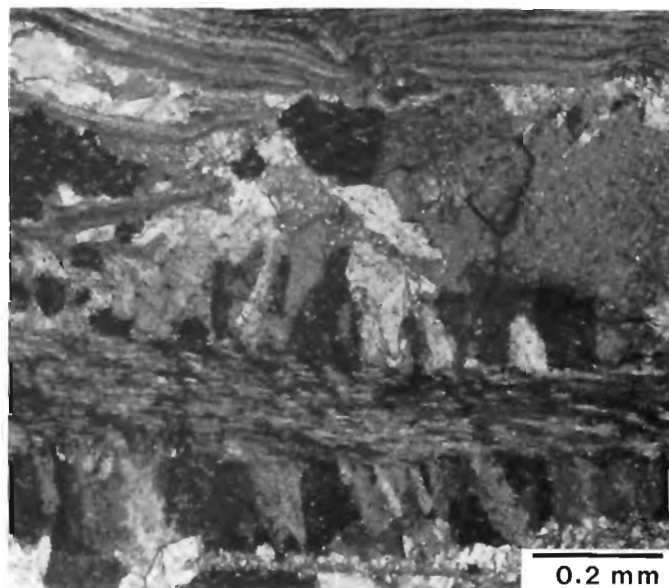


Figure 55. Photomicrograph, showing fringes of bladed, polycrystalline, sparry calcite cement, on brachiopods in lime grainstone (GSC loc. C-52346); from the Tlogotsho Member of the Flett Formation at Locality 13. ISPG 1768-160.

Polycrystalline fringe cement (Figs. 55, 56) is relatively common in the Flett Formation, but it is the least volumetrically abundant of the three main cement fabrics present. It occurs both intergranularly and intragranularly in about 98 per cent of the lime grainstone, and intragranularly in about 20 per cent of the other limestones. Equant to subequant, epitaxial crystals predominate in most fringes, but blades exist on some allochems in many samples. Most fringe crystals are clear and fine to medium crystalline. Blades either predominate or are as common as equant crystals in about five per cent of the lime grainstone beds; mainly beds in which brachiopods are the principal bioclasts. Only two specimens were observed in which blades were present on a major proportion of most other bioclasts. In those two samples, the fringe cement was strongly ferroan and did not occur on echinoderms. Blades generally have length-to-width ratios that are less than 4:1. However, they are fiber-like in two dimensions on some brachiopods, and most tend to be relatively wide (>0.02 mm). The blades have subparallel to divergent sides, and commonly occur in bundles that superficially resemble Bathurst's (1959, p. 11; 1971, p. 26-427) radiaxial-fibrous mosaic. Blades commonly increase in size while decreasing in number away from their foundations. The fringes occur as coatings of variable thickness on allochems, and opposing fringes commonly interlock. These fringes, which are substrate specific to some extent, were not observed on echinoderm ossicles, and they are generally best developed on brachiopods. Fringe cement in the Flett is mainly nonferroan, but ferroan, equant to bladed, polycrystalline fringes are moderately common.

Most polycrystalline fringe cement in the Flett Formation probably precipitated relatively early in Folk's (1973; 1974a, p. 45) meteoric-phreatic or shallow-subsurface zones instead of in marine-phreatic, vadose, or deep-sub-surface environments (Fig. 19). This interpretation is based on reasons similar to those given in the discussion on the sparry-calcite cement of the Yohin Formation. This interpretation is compatible with the work of Longman (1980), Badiozamani et al. (1977) and Richter and Füchtbauer (1978).

Neomorphic calcite, which occurs in allochems and matrix, is a major component of most lime packstone and wackestone in the Flett Formation, but it is a relatively minor component in other rock types. Microspar and pseudospar produced by the recrystallization of lime mud are the main neomorphic calcites, but fine to medium crystalline pseudospar produced by degrading recrystallization of echinoderm debris and spar cement is locally abundant. In comparison, micrite and pseudospar formed by inversion of aragonite skeletons are relatively minor. Most micrite has recrystallized to microspar and finely crystalline pseudospar (0.03-0.062 mm), but medium crystalline pseudospar (0.062-0.25 mm) is locally common. These neomorphic calcites are chiefly nonferroan to slightly ferroan. At some locations, neomorphism, together with the replacement of non- CaCO_3 minerals by calcite, transformed about 10 to 15 per cent of the Flett lime packstone and wackestone into finely crystalline limestone. In these limestones, carbonate allochems are mainly pseudomorphs, which consist of neomorphic and replacement pseudospar.

Authigenic calcite, produced by replacement of opal sponge spicules, is volumetrically abundant in spicule-rich rocks. Where spicules are the principal allochem, fine to coarse crystalline pseudospar that replaced spicule opal commonly constitutes more than half of the calcite present. Most of the replacement calcite is ferroan and multi-crystalline, and the spicules are commonly visible only in thin sections that were stained for ferroan calcite.

Dolomite

Dolomite in the dolostone of the uppermost Flett Formation is mainly a nonselective replacement mineral. It is chiefly medium to coarsely crystalline, although crystals range from very fine to very coarse (Fig. 52c). Generally, the dolomite that has replaced bioclasts is coarser than that which has replaced calcite cement and matrix. Many crinoid ossicles and their overgrowths are single dolomite crystals.

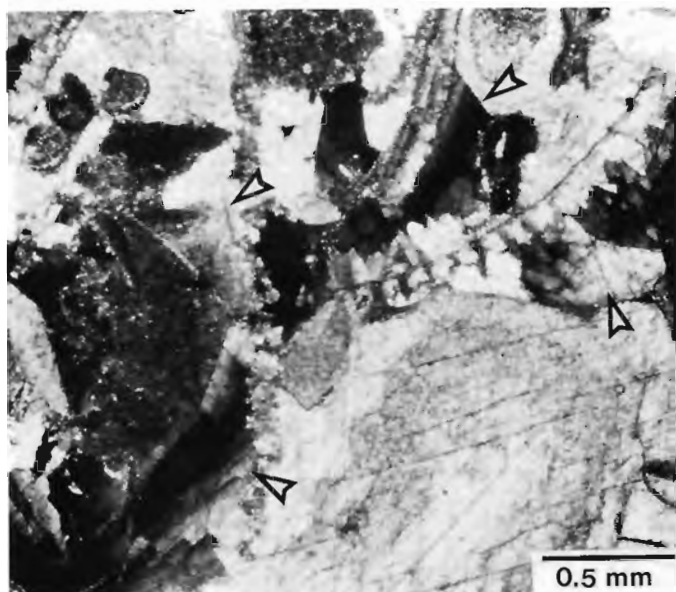


Figure 56. Photomicrograph, showing late saddle dolomite (arrows) that has undulose extinction; in skeletal lime grainstone (GSC loc. C-59058) from the Meilleur Member of the Flett at Twisted Mountain. A brachiopod shell (upper right) displays bladed, polycrystalline, calcite fringe cement; pelmatozoan fragments have monocrystalline syntaxial overgrowths. ISPG 1768-108.

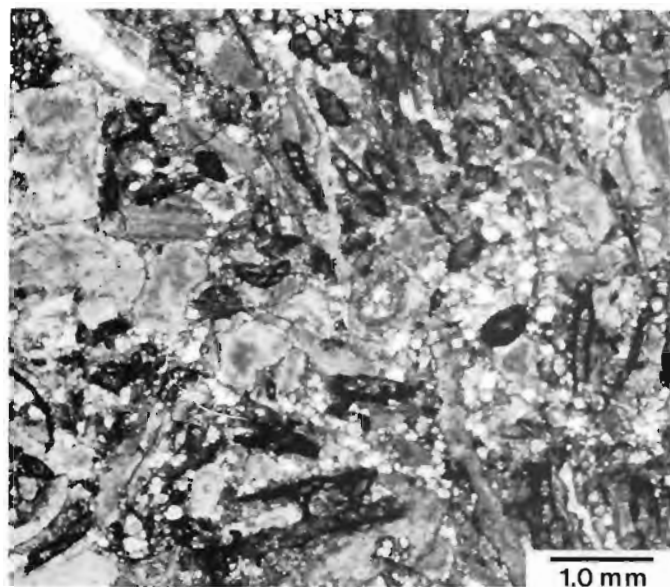


Figure 57. Photomicrograph, showing rhombs of ferroan dolomite (very light grey) in cherty, dolomitic bryozoan-pelmatozoan lime grainstone (GSC loc. C-74266); from the upper Flett Formation at Locality 5. ISPG 1768-105.

Crystals in the dolostone generally have compromise boundaries, and they are chiefly subhedral, cloudy, and strongly ferroan. Many crystals have slightly undulose extinction and are possibly the saddle dolomite of Radke and Mathis (1980). In the dolostone, the extent to which dolomitization went to completion increases toward the Debolt-Golata contact.

In addition to its occurrence in dolostone, dolomite is present in about 35 per cent of the limestone samples; furthermore, much of the limestone in the uppermost Flett Formation is greater than 30 per cent dolomite and grades into dolostone. Most of the dolomite is strongly ferroan, but nonferroan dolomite is moderately common. This mineral occurs mostly as a replacement of matrix, allochems, and cement; but some dolomite that was possibly passively precipitated occurs in lime grainstone (Fig. 56).

X-ray diffraction analyses indicate that ankerite, which has physical and optical properties similar to those of dolomite, is relatively common in the fine grained deposits of the Flett Formation (Appendix G). An undetermined proportion of the mineral that is called ferroan dolomite here, is, therefore, ankerite.

In the Flett Formation, dolomite has three principal modes of occurrence in rocks other than dolostone. It is probably most widespread and abundant as isolated and interfering, euhedral to subhedral, very fine to medium crystalline rhombs in fine grained siliciclastics; and in the matrix, cement, bioclasts, and intraclasts of limestone (Fig. 57). This type of dolomite is commonly closely associated with microquartz, and some of it is possibly saddle dolomite, because it has a slightly undulose extinction. Dolomite also occurs commonly as euhedral to subhedral crystals that occur in length-slow chalcedony that has partly replaced pelmatozoan fragments. Finally, very coarse to medium crystalline, subhedral saddle dolomite (Fig. 56), with



Figure 58. Outcrop of normally graded, proximal (Bouma A, D-E) limestone and spiculite turbidite in the Flett mixed-skeletal lime-packstone lithofacies at Sheaf Creek. Upper fine grained part of the bed was bioturbated (scale is 15 cm long). ISPG 798-109.

a sweeping undulose extinction, locally occurs in lime grainstone as a replacement mineral and possibly as a late void filling.

The paragenetic relationships between dolomite (or ankerite) and calcite in the Flett Formation are similar to those in the Prophet Formation, and indicate that some dolomitization occurred after the host sediment was at least partly lithified. The three types of dolomite occurrence described above are at least partly younger than the monocrystalline syntaxial overgrowths, polycrystalline fringe cements, and much of the late, blocky, calcite spar cement. Evidence for the replacement of calcite cement by dolomite includes: crosscutting relationships, apparent islands of calcite cement in dolomite, dolomite surfaces concave into the host calcite, remnant cement fabrics, and the occurrence of ideomorphic dolomite crystals in calcite cement. These paragenetic relationships were determined by examining dolomitic lime grainstone and calcareous dolostone from the uppermost Meilleur Member, but relationships may differ elsewhere. The local occurrence of saddle dolomite and the high Fe^{2+} content of most dolomite in the Flett also suggest that most dolomitization did not occur early. According to Radke and Mathis (1980, p. 1160) saddle dolomite indicates a diagenetic event in the temperature range of 60° to 150°C and most probably over 100°C.

For reasons given in the discussion on authigenic dolomite in the Prophet Formation, early, surficially generated hypersaline solutions probably did not precipitate dolomite and ankerite in the Flett Formation. Moreover, it appears improbable that most dolomitization occurred relatively early in the subsurface-mixing zone (Fig. 19) by the process that Folk and Land (1975) advocated, because most of the dolomite (or ankerite) is ferroan. Dolomite that formed in the mixing zone should have a nonferroan composition because it generally forms under oxidizing conditions (McHargue and Price, 1982, p. 878).

The dolomite and ankerite in the Flett Formation probably had origins similar to those of these minerals in the Prophet Formation, because in both formations these minerals are similar in aspect and occur in similar physical settings. In the discussion about dolomite in the Prophet, it was suggested that dolomite could have resulted from dewatering of shale, diagenesis of clays, bacterial reduction of sulphate in organic-rich sediment, and the formation of chert.

Other authigenic minerals

In addition to the minerals discussed above, pyrite, plagioclase, glauconite, siderite, and phosphates are present as authigenic minerals. Pyrite occurs in trace amounts in most samples and is similar to pyrite in the Prophet Formation. Equant to lath-shaped euhedra of fine to medium crystalline plagioclase constitute between 0.1 and 9 per cent of the material present in 60 to 75 per cent of the lime packstone and wackestone, but plagioclase is not common in other rocks. Siderite is common in concretions, which occur in some shale beds, but it is rare in most limestones. Glauconite is confined to limestone and dolostone at the top of the Meilleur Member, and phosphates were common only in one dolostone sample from the top of the Flett.

Lithofacies

In the project area, a mixed-skeletal lime-packstone lithofacies and a lime-grainstone lithofacies constitute most of the Flett Formation (Figs. 62-64, 76). In addition, a

siltstone and sandstone lithofacies (Fig. 66) and a shale and mudstone lithofacies (Fig. 68) are important in much of the Flett. Intervals of spicule-lime-packstone lithofacies are locally present at some localities as well.

Well core is not available from the Flett Formation in the subsurface on the interior platform. The characteristics of the bedding and sedimentary structures in the Flett lithofacies of that area are, therefore, unknown.

Mixed-skeletal lime-packstone lithofacies

Rocks of the resistant mixed-skeletal lime-packstone lithofacies (Figs. 76, 79) constitute more of the Flett Formation than those of the other main lithofacies. In the Mackenzie fold belt, the mixed-skeletal lime-packstone lithofacies forms most of the Tlogotsho Member, much of the Meilleur Member, and most limestone beds in the Jackfish Gap Member. It also makes up much of the Tlogotsho and Meilleur on the interior platform.

The mixed-skeletal lime-packstone lithofacies commonly overlies and grades westward into the Prophet spiculite and spicule-lime-packstone lithofacies which may be intercalated with the Prophet dark-shale lithofacies. South of approximately latitude 60°55'N, it is also locally intercalated with the Flett spicule-lime-packstone lithofacies. Contacts between intervals of the mixed-skeletal lime-packstone lithofacies and intervals of these other facies vary from abrupt to gradational through several metres. In addition to being mainly mixed-skeletal lime-packstone, this lithofacies differs from the spiculite and spicule-lime-packstone lithofacies by being much less siliceous and generally thicker bedded.

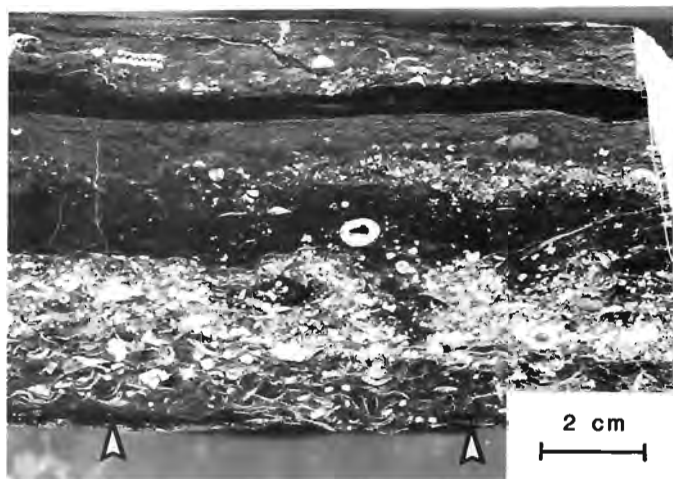
Units of mixed-skeletal lime-packstone lithofacies commonly grade upward and eastward into the lime-grainstone lithofacies of the Flett; however, in the upper Flett, west of the depositional limit of the grainstone lithofacies, the dark-shale, sandstone, and dolostone lithofacies in the Golata Formation gradationally overlie this lithofacies (Figs. 4-6). Contacts between units of the mixed-skeletal lime-packstone lithofacies and the lime-grainstone lithofacies vary from abrupt to gradational through one metre or more. The contact with the Golata is generally abrupt to gradational through less than one metre. This lithofacies differs from the lime-grainstone facies, consisting mainly of dark, rhythmically bedded lime packstone instead of massive to crossbedded, light coloured lime grainstone.

Throughout much of the Flett Formation, multibed units of the mixed-skeletal lime-packstone lithofacies are underlain and overlain by beds of the shale and mudstone lithofacies. In addition, beds of mixed-skeletal lime-packstone lithofacies are commonly rhythmically interbedded with those of the shale and mudstone lithofacies in the Jackfish Gap Member, uppermost Tlogotsho Member, and basal Meilleur Member. Contacts between these two lithofacies vary from abrupt to gradational through one metre or more.

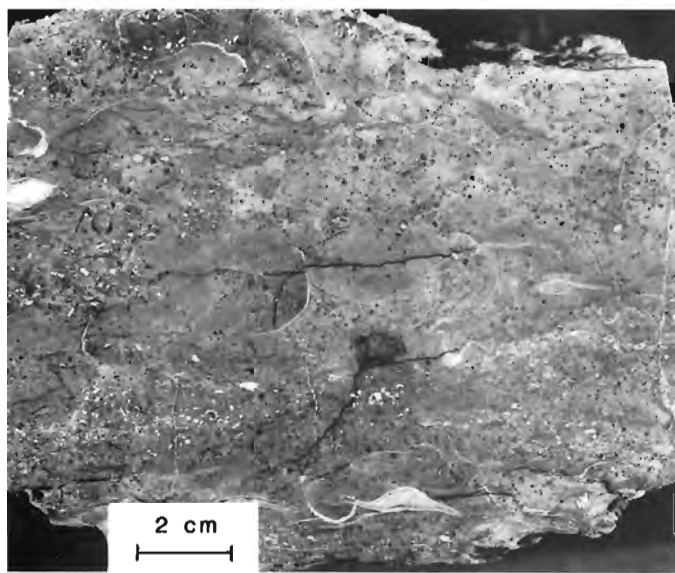
Mixed-skeletal lime packstone (Fig. 52a) is the main limestone in the mixed-skeletal lime-packstone lithofacies and predominates in most units. In order of decreasing abundance, crystalline limestone, lime grainstone, and lime wackestone also occur. Lime grainstone becomes more abundant eastward in the Flett Formation as a whole and upward within the Meilleur Member. When present in this lithofacies of the Tlogotsho Member, lime grainstone is most abundant in its lower two thirds. Crystalline limestone and lime wackestone occur chiefly in recessive intervals that



a. Massive, ungraded limestone bed with sharp top and bottom; interpreted as either a proximal turbidite or a thin debris flow bed; outcrops at Jackfish Gap. ISPG 1756-157.



b. Polished slab of limestone and spiculite turbidites (GSC loc. C-74256) from Locality 5. Lower, completely preserved turbidite has Bouma A, D, and E divisions and overlies the E division of another turbidite (arrows). ISPG 1766-11.



c. Polished sample (GSC loc. C-52095) from the lower three quarters of a massive and ungraded limestone bed in the lower Flett Formation at Jackfish Gap. Specimen has a chaotic fabric and is possibly from a thin debris flow bed. ISPG 1766-13.

Figure 59. Examples of beds from the Flett mixed-skeletal lime-packstone lithofacies.

contain high proportions of shale and mudstone. These recessive intervals are best developed in the upper Tlogotsho Member, the Jackfish Gap Member, and in the basal Meilleur Member.

Shale and mudstone are moderately abundant in the mixed-skeletal lime-packstone lithofacies, and minor dolostone and spiculite occur. Within this lithofacies, the shale and mudstone occur mainly as laminae and thin beds, and become more abundant northeastward. Their abundance also increases upward in the Tlogotsho Member and downward in the Meilleur Member. In this lithofacies, shale and mudstone are the most abundant in the region northeast of Jackfish Gap and least abundant in the southern Liard Range and in the subsurface on the interior platform. Dolostone and spiculite are locally present throughout this lithofacies, but dolostone is most plentiful in the upper one to three metres of the Flett.

In the outcrop belt, sharp-based, massive to stratified and ungraded to graded beds (Figs. 58, 59, 79) constitute most of the mixed-skeletal lime-packstone lithofacies, but nodular limestone (Fig. 60), minor deformed deposits, and platy bioturbated deposits are also present. The deposits in this lithofacies generally resemble deep water deposits. They are chiefly well bedded and form intervals of rhythmically interbedded, resistant and recessive strata (Figs. 70, 79). Most beds have considerable lateral continuity; however, the bedding continuity is commonly interrupted by large-scale concave-upward truncation surfaces. For reasons given later, these discontinuities (Figs. 76, 79a, 81) are interpreted as mainly erosional surfaces of submarine channels. Finally, this lithofacies forms multibed sequences that either become more resistant and proximal in aspect upward or less resistant and less proximal in aspect upward (Fig. 70).

Most of the sharp-based, massive to stratified and ungraded to graded beds in the mixed-skeletal lime-packstone lithofacies can be discussed reasonably well by referring to the Bouma sequence. These deposits, which resemble some sediment-gravity-flow deposits described by Middleton and Hampton (1973) and others, vary from laminated to very thick bedded (1 to >100 cm), but are mostly medium bedded (10 to 30 cm). Most comprise limestone with subordinate spiculite and fine grained siliciclastics (Figs. 58, 59). Although some beds have a basal division that resembles the Bouma B division, most start with an A-like division and lack



Figure 60. Nodular lime grainstone and lime packstone in the Flett mixed-skeletal lime-packstone lithofacies at Sheaf Creek. The light coloured bed (2 m thick) is a possible debris flow deposit, with a chaotic internal fabric and an undulous top. ISPG 1756-56.



Figure 62. Fining- and thinning-upward sequence of Flett lime-grainstone lithofacies in the upper Meilleur Member at Jackfish Gap. Overlying recessive unit is Flett shale and mudstone lithofacies. Person (centre left) indicates scale. ISPG 1303-5.



Figure 61. *Zoophycos* sp. on slab of limestone from the Flett mixed-skeletal lime-packstone lithofacies at Sheaf Creek. ISPG 1756-60.

components that resemble B and C divisions. Most beds have an upper argillaceous component that resembles the Bouma D and E divisions. Beds exhibiting components that correspond to all five divisions of the standard Bouma sequence were not observed. In much of the mixed-skeletal lime-packstone lithofacies, these sharp-based beds are generally closely spaced, and, in units that consist of them, the ratio of resistant to recessive rock types is commonly high (Fig. 79). Most beds have distinct normal grading, but this is commonly



Figure 63. Hummocky crossbedding in bryozoan-pelmatozoan lime grainstone of the Flett lime-grainstone lithofacies, upper Jackfish Gap Member, Locality 3. The limestone abruptly overlies crossbedded sandstone (below hammer). ISPG 1756-72.

evident only in the finer grained upper parts of the beds. Within individual divisions, grading varies from marked to nonevident. Sole marks are commonly present on the bases of these beds and are mainly casts of shallow scours, which are locally more than 20 cm across, and load casts.

The component that corresponds to the Bouma A division varies from massive to crudely stratified and ungraded to distinctly graded. Contacts between this division and overlying divisions vary from gradational to sharp (Figs. 58; 59a, b). Normal grading, which resembles Middleton's (1967, p. 487) distribution grading, is the most common type in this division. However, both inverse and combinations of inverse and normal grading occur in a few beds. About 20 to 30 per cent of the beds have a distinctly graded component that corresponds to the A division, but, in most beds, grading in this component is either nonevident or subtle. Toward the east, the proportion of beds that have a distinctly graded A-like division decreases. Moreover, grading in this division is generally best developed near its top and in thin to medium bedded deposits that consist of relatively coarse grained mixed-skeletal lime-packstone and grainstone. Grading is least distinct in spicule-rich rocks. In some beds, the component that resembles the Bouma A division has a chaotic fabric (Fig. 59c) in which vague, intraclast-like components are common. Weathered beds of the latter type tend to have a nodular appearance. Distinct intraclasts, similar to those that occur in some proximal turbidites in the Prophet Formation (Fig. 47), are also common in the A-like division of many beds. In some beds, the element that corresponds to the A division is crudely stratified because of oriented allochems and vertical variations in grain size.

Components corresponding to the Bouma B and C divisions are less common in the sharp-based graded beds of the Flett mixed-skeletal lime-packstone lithofacies than in those of the Prophet Formation. The B-like division, which resembles the B division in the Prophet turbidites, is characterized by diffuse planar laminae. Poorly defined, small-scale crossbedding appears to predominate in the C-like division. Because of bioturbation and soft-sediment deformation related to the deposition of overlying deposits, the component that resembles the C division is generally poorly preserved and difficult to differentiate from overlying divisions in these beds.

Divisions corresponding to Bouma D and E divisions cannot be separated at most outcrops and are generally difficult to separate in polished slabs (Fig. 59b). Laminae in these divisions are mainly diffuse and poorly preserved. The laminae are commonly wavy because the tops of underlying divisions are seldom planar, and soft-sediment deformation produced by the loading of overlying beds is commonly marked. The component that resembles the D-E division generally has normal grading, becomes darker and more argillaceous upward, is mainly recessive and platy, and locally has autochthonous, colonial corals on top of it.

Turbidity currents rather than grain flows, fluidized flows, or debris flows probably produced most of the beds that are described above. Most have the following attributes of turbidity currents deposits: two or more components that correspond to divisions of the standard Bouma sequence; normal grading; and sharp bases with sole marks. The surface on which these beds were deposited appears to have been a broad, gentle slope (Fig. 8). Consequently, it is improbable that any of these beds are grain-flow deposits. Subaqueous grain flows require slopes that are at or above the static angle of repose, and they cannot account for the formation of thick sedimentary units (Lowe, 1976, p. 198; Middleton and Hampton, 1973, 1976). The principal objection for fluidized

flows as a mechanism is that most beds in the mixed-skeletal lime-packstone lithofacies are relatively thin. According to Middleton and Hampton (1973, 1976), the excess pore pressure required by fluidized flows is rapidly dissipated by loss of pore fluids from thin beds. Moreover, fluidized-sediment flow deposits are characterized by sharp bases and tops, dish structures, deformed laminae, and by a lack of normal traction structures and generally grading (Middleton and Hampton, 1973, 1976). A debris flow origin appears to be unlikely for most beds because deposits produced by that process are typically massive, have poor grading if any, and have sharp upper and lower contacts (Middleton and Hampton, 1973). Beds that have an ungraded or chaotic basal division (Figs. 59a, c; 60) are, however, possibly debris flow deposits. Some of the sharp-based, massive to internally stratified beds discussed above are possibly tempestites, because they are closely associated with relatively shallow water deposits. In addition, they resemble some limestone tempestites, that have been described by Aigner (1982) and by others. This hypothesis is discussed later in the section about environmental interpretations.

Beds of nodular limestone are moderately common in the mixed-skeletal lime-packstone lithofacies (Fig. 60). Because similar deposits have already been described above from the Prophet Formation (Fig. 46), in which they are commonly better developed, the nodular limestone is not described again here. For reasons given in the discussion of the Prophet nodular limestone, a reasonable interpretation is that soft-sediment deformation produced most of these deposits in the Flett and Prophet formations.

Evidence of bioturbation (Fig. 61) is present in much of the mixed-skeletal lime-packstone lithofacies, particularly in the fine grained, spicule-rich limestone. In turbidite-like beds it is particularly common above the massive basal division. Bioturbation accounts for the typical absence of well preserved, primary sedimentary structures in the upper



Figure 64. Closely spaced graded beds in the Flett lime-grainstone lithofacies of the Meilleur Member at Jackfish Gap (scale is 15 cm long). Beds, mostly lime grainstone, have subtle normal grading and are tentatively interpreted as storm deposits (tempestites). ISPG 1756-167.

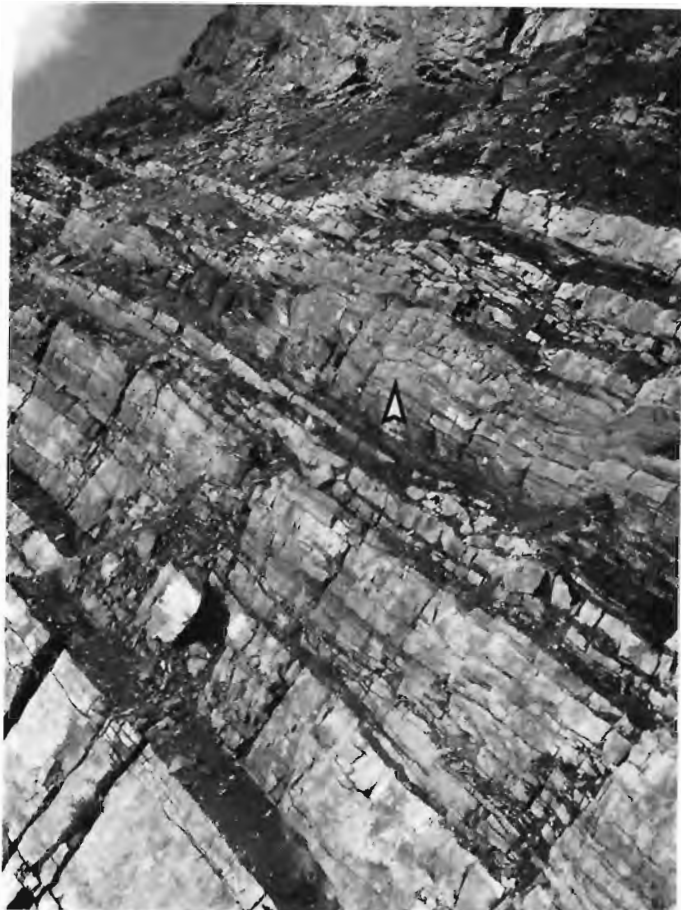


Figure 65. Dolostone, dolomitic lime grainstone, and shale in the lime-grainstone lithofacies of the uppermost Flett Formation at Jackfish Gap. Note bedding irregularity and local occurrence of probable hummocky crossbedding (arrow). Recessive unit below uppermost cliff is the Golata Formation (8 m thick). ISPG 1756-175.

part of these beds. *Zoophycos* sp. (GSC loc. C-59031; Fig. 61), the most common ichnogenus, is pervasive enough in many beds to produce internal stratification and a platy fissility. The trace fossil assemblage is assignable to Seilacher's (1967, 1978) *Zoophycos* association, which is generally best developed in strata deposited in a bathyal slope setting (Howard, 1978, p. 38-41).

Lime-grainstone lithofacies

The lime-grainstone lithofacies (Figs. 62-65) occurs chiefly in the Meilleur Member, but it is locally present in the Tlogotsho Member. An important, isolated outcrop of this lithofacies also is present in the middle of the Jackfish Gap Member at Locality 3 (Fig. 63). In the Meilleur, this facies is best developed in the southeastern Liard Range and the subsurface on the interior platform. It occurs chiefly in the upper two thirds or less of the Meilleur in the Mackenzie fold belt, and units of it generally thin westward in that member. Units of this lithofacies are locally present in the Tlogotsho Member in the southeastern Liard Range (Fig. 1, Loc. 13) and on the interior platform.

The lime-grainstone lithofacies overlies and grades westward into the mixed-skeletal lime-packstone lithofacies and also is overlain by this lithofacies in the Tlogotsho Member. West of the eastern, erosional zero-edge of the Mattson Formation, the dark-shale, sandstone, and dolostone lithofacies of the Golata Formation generally gradationally overlie the lime-grainstone lithofacies of the Meilleur.

Intervals of lime-grainstone lithofacies are locally in contact with those of the shale and mudstone lithofacies (Fig. 68). These latter, which occur as beds that range in thickness from less than 10 cm to more than 2 m, are locally associated with the lime-grainstone lithofacies of the upper Meilleur Member. In that member, the shale and mudstone lithofacies becomes more abundant toward the northeast. In the middle of the Jackfish Gap Member at Locality 3, a deposit of lime-grainstone lithofacies (Fig. 63), which abruptly overlies crossbedded sandstone, is abruptly overlain by the shale and mudstone lithofacies.

Mixed-skeletal limestone with subordinate dolostone and minor shale constitute most of the lime-grainstone lithofacies. Skeletal lime grainstone is the most abundant limestone (Figs. 52b, 54), and is followed by skeletal lime packstone. In addition, ooid-skeletal lime grainstone is present in the upper Meilleur Member at Locality 21. Dolostone, which occurs in the upper two to four metres of the Meilleur Member, is commonly the main rock type at that stratigraphic level (Fig. 52c), but it was not observed elsewhere. Shale occurs locally as partings.

The lime-grainstone lithofacies, which is mainly resistant and cliff forming (Fig. 62), consists chiefly of crossbedded carbonates (Fig. 63) and sharp-based, massive to stratified, and ungraded to graded limestone and dolostone beds. In much of the Mackenzie fold belt, sharp-based deposits (Fig. 64) are more abundant than crossbedded strata. Sharp-based beds become more abundant westward, and constitute the bulk of the lime-grainstone lithofacies in the western Liard Range and in the region that is west of Locality 3. A 60 cm thick, fenestrate-bryozoan biostrome (Heckel, 1974, p. 98), which is exposed for several metres along strike and consists of bryozoan bafflestone, is associated with the sharp-based deposits at Jackfish Gap. Similar biostromes were not observed elsewhere. The lime-grainstone lithofacies is poorly developed at Twisted Mountain, where the proportion of intercalated units of shale lithofacies (Fig. 68) is high. Elsewhere, interbeds of the shale and mudstone lithofacies are less abundant. Bedding is generally less regular than in the mixed-skeletal lime-packstone lithofacies, and both lensing and marked lateral variations in bed thickness are common (Fig. 65). Also, large-scale, concave-upward truncation surfaces locally interrupt bedding continuity in intervals that consist mainly of the sharp-based deposits (Fig. 70). Deposits that constitute the lime-grainstone lithofacies commonly form multibed sequences, which become either more or less resistant upward (Fig. 62).

The sharp-based, massive to stratified, and ungraded to graded beds in the lime-grainstone lithofacies are very thin to very thick bedded (1.0 to >100 cm, but most are between 10 and 30 cm thick). A lower component, which is ungraded or subtly graded and massive to crudely stratified, constitutes the bulk of most beds (Fig. 64). Other beds have a resistant basal part that has diffuse, planar laminae and is ungraded or subtly graded. Beds that contain both a massive basal division and an overlying planar-laminated division were not observed. Intraclast-bearing skeletal lime grainstone, packstone, and dolostone constitute the resistant parts of these deposits, but lime grainstone predominates. Recessive layers, chiefly between 0.5 and 10 cm thick, abruptly to

gradationally overlie the resistant divisions. In order of decreasing abundance, the recessive units comprise argillaceous carbonates, shale, mudstone, and spiculite. A few recessive intervals contain poorly developed crossbedding, but most are characterized by wavy to contorted laminae. The bases of these beds are erosional, vary from almost planar to highly undulose, and generally have load casts and casts of scours. Because of soft-sediment deformation, the upper surfaces of the resistant parts of these beds are generally undulose to irregular. Amalgamation and lensing of beds is locally common. Evidence of bioturbation is minimal, and identifiable lebensspuren were not observed.

The sharp-based, massive to stratified beds described above resemble turbidites, but it is possible that they were not deposited by density currents. They are possibly turbidites because they generally have the following: two or more divisions that correspond reasonably well to those in the standard Bouma sequence; sharp bases with sole marks; and normal grading. However, they also resemble some storm deposits or tempestites, particularly those with a massive or planar-stratified basal component, that were described by Johnson (1978, p. 251, 252), Kumar and Sanders (1976), Nelson (1982), Aigner (1982), and others. The possibility that these sharp-based beds in the lime-grainstone lithofacies are of storm origin and formed in relatively shallow water is discussed further in the section about environmental interpretation.

The crossbedded carbonates of the lime-grainstone lithofacies (Fig. 63) were not extensively studied and were examined chiefly at Localities 2, 3, and 13. In the outcrop belt, these crossbedded deposits are thickest and best developed in the southeastern Liard Range. Also, throughout the project area, the proportion of the lime-grainstone lithofacies that consists of these deposits appears to increase eastward. These deposits are mainly light olive-grey bryozoan-pelmatozoan lime grainstone with subordinate brachiopod lime grainstone and fossiliferous dolostone. The brachiopod lime grainstone (Fig. 54) was observed at Locality 13 in the southeastern Liard Range. There, it appears to form low brachiopod banks or biostromes, which are up to two metres or more thick. Dolostone intraclasts are locally abundant in the crossbedded lime grainstone and dolostone, and most beds consist largely of sand- to granule-sized clasts. These deposits, which are medium to very thick bedded, are commonly cliff forming. Bedding surfaces are generally sharp and undulose, and beds are commonly not very continuous laterally because of lensing. The crossbedding appears to be mainly poorly defined medium- to large-scale trough crossbedding. However, hummocky crossbedding, which is formed by strong surges generated by storm waves (Harms, 1975b, p. 88; Hamblin and Walker, 1979, p. 108), is well developed in a unit of lime-grainstone lithofacies that occurs in the Jackfish Gap Member at Locality 3 (Fig. 63). Hummocky crossbedding is also locally present in the Meilleur Member (Fig. 65), and small-scale crossbedding occurs locally as well. In the southern Liard Range, the crossbedded carbonates of the lime-grainstone lithofacies are generally intercalated with units of mixed-skeletal lime-packstone lithofacies, but in the northern part of the project area, the intervening deposits are mainly shale and mudstone lithofacies. In the upper Meilleur Member at Locality 13, the crossbedded lime grainstone is associated with a bed of lime-grainstone lithofacies that is about two metres thick and contains abundant, colonial rugose corals; organic reefs were not observed.

Siltstone and sandstone lithofacies

The siltstone and sandstone lithofacies (Fig. 66), which comprises sandy siltstone and very fine to fine grained

sandstone (Fig. 52d) with subordinate shale and minor sandy limestone, is present only in the Jackfish Gap Member (Fig. 67). At most localities, this lithofacies forms approximately the lower and upper third of the Jackfish Gap Member. However, it forms all of the member at Locality 5 and is present in the middle Jackfish Gap at Locality 3. Most units of the siltstone and sandstone lithofacies gradationally overlie beds of the shale and mudstone lithofacies and are abruptly to gradationally overlain by them as well.

The siltstone and sandstone lithofacies occurs mainly as recessive to moderately resistant coarsening-upward sequences that range in thickness from less than 1 m to more than 10 m (Fig. 66a). Most of the sequences grade upward from silty shale and mudstone to crossbedded, sandy siltstone and sandstone. The thicker sequences commonly contain two or more subordinate sequences that also coarsen upward.

Units of siltstone and sandstone lithofacies are mainly laminated to thin bedded and contain abundant current-produced structures (Fig. 66b, c). These deposits were studied between Twisted Mountain and the northeastern corner of the Tlogotsho Plateau, and do not differ appreciably between those localities. Most beds and laminae of siltstone and sandstone are internally stratified and comprise either individual or superimposed sets of ripple-crossbedded clastics. Because of lensing and marked variations in thickness, the bedding in these cross-stratified deposits is extremely irregular. Mudstone drapes or flasers, containing abundant, carbonized plant fragments and mica, commonly accentuate laminae. Other beds consist, in whole or in part, of a division that comprises planar laminated very fine grained sandstone (Fig. 66b). The presence of planar stratification in very fine grained sandstone indicates deposition under lower-flow-regimen conditions (Southard, 1975). These planar-stratified divisions are either gradationally overlain by ripple-crossbedded deposits or are abruptly overlain by other beds. Some internally stratified beds are composites produced by amalgamation, and along strike they commonly split into thinner sedimentation units separated by mudstone. Less commonly, beds have a sharp-based, massive to indistinctly stratified basal division that has crude normal grading. Also, near the top of the Jackfish Gap Member in the Flett type section, sandstone containing medium- to large-scale trough and tabular(?) crossbedding is locally present (Fig. 66c). Granule- to pebble-sized mudstone intraclasts occur in many beds, either as isolated clasts or as lag deposits. Soles of the beds are generally sharp and undulose, but sole marks other than dish-like scours and trace fossils are uncommon.

Shallow scours, which are up to several metres across and resemble erosion surfaces of minor submarine channels, occur locally in intervals of the siltstone and sandstone lithofacies. The only scour that was examined in detail is present in the upper Jackfish Gap Member at Locality 4. This structure, which is several metres across, is overlain by a fining-upward fill sequence containing medium-scale trough crossbedding overlain by small-scale crossbedding. A 90 cm thick set of crossbeds that resemble epsilon crossbedding occurs above the south side of the scour as well. The foresets in the latter dip toward the axis of the scour.

Lebensspuren are locally common in the siltstone and sandstone units. The assemblage present is much more diverse than that in the associated limestone beds, where *Zoophycos* sp. was the only ichnogenus identified. The common ichnogenes in the siliciclastics include *Asterosoma* sp. (GSC locs. C-47931, C-58521; Richards, 1983a, Pl. 28a), *Conostychus* sp. (GSC locs. C-47931, C-52242), *Locheia* sp. (GSC locs. C-52242, C-58521), *Stelloglyphus* sp. (GSC loc. C-58521), *Zoophycos* sp. (GSC loc. C-74240), *Chondrites* sp. (GSC loc. C-52242), and *Scalarituba* sp. (GSC



a. Coarsening-upward sequences of siltstone, sandstone and shale (below trees) at Locality 3. Lowest cliff is 11 m high and gradationally overlies the Flett shale and mudstone lithofacies. ISPG 1303-33.



b. Small-scale crossbedding, planar stratification, and lenticular to flaser bedding in probable neritic siltstone, sandstone, and shale at Locality 3 (scale is 15 cm long). ISPG 1303-31.



c. Medium- and small-scale crossbedding in probable shallow-neritic sandstone at Jackfish Gap (scale is 15 cm long). ISPG 1756-146.

Figure 66. The siltstone and sandstone lithofacies in the upper Jackfish Gap Member of the Flett Formation.

loc. C-58521). Because it contains at least three ichnogen-
era that occur in more than one association, this assemblage is not readily assignable to Seilacher's (1967, 1978) trace fossil associations. However, at most localities the presence of abundant *Asterosoma* sp., *Conostychus* sp., and *Locheia* sp. indicates affinities with his *Cruziana* association.

Traction currents and wave controlled processes probably produced most of the siltstone and sandstone deposits that occur in the siltstone and mudstone lithofacies. The presence of medium- to large-scale trough and tabular(?) crossbedding indicates deposition by traction currents. According to Harms (1975a), migrating dunes form trough crossbedding, whereas tabular sets are deposited by migrating sand waves. Some of the deposits that contain small-scale crossbedding were probably deposited by wave related processes, because they have features that de Raaf et al. (1977) considered useful for identifying wave deposited strata. These features include: crosslaminae that are commonly strongly tangential toward the lower set boundary; lower boundaries of sets that are commonly scooped and undulatory; crosslamination that locally has a bidirectional character; swollen, lens-like sets; and a tendency toward the superposition of lenses.

The sandstone and siltstone beds that contain a massive to indistinctly stratified basal division are probably storm deposits or tempestites. Also, the sharp-based beds that have a planar-laminated division overlain by a ripple-crossbedded division are probably tempestites. These deposits are similar to some turbidities; however, they more closely resemble shallow water, storm generated, sheet sandstones described by Johnson (1978, p. 251, 252) and are closely associated with probable wave formed structures.

Some of the broad, shallow scours are probably erosion surfaces of channels. They have a channel-like configuration, and at least some are overlain by fill sequences that closely resemble channel fills.

Shale and mudstone lithofacies

The shale and mudstone lithofacies is best developed north of approximately latitude 60°55'N. There, it commonly constitutes a major part of the upper Tlogotsho Member, the middle Jackfish Gap Member (Fig. 67), and the lower Meilleur Member. In the same region, it is also locally common and well developed in the upper Meilleur (Fig. 68), in which it



Figure 67. Type section of the Jackfish Gap Member (arrows indicate boundaries) of the Flett Formation at Locality 4. Upper and lower cliffs comprise the siltstone and sandstone lithofacies; recessive intervals below and above the lower cliff comprise the shale and mudstone lithofacies, intercalated with beds of mixed-skeletal lime-packstone lithofacies. ISPG 1281-25.

becomes more abundant toward the northeast. South of 60°55'N, the shale and mudstone lithofacies occurs mainly in the middle Tlogotsho and the basal and uppermost Meilleur.

In the Tlogotsho Member, Jackfish Gap Member, and lower Meilleur Member, the shale and mudstone lithofacies is commonly intercalated with deposits of the mixed-skeletal lime-packstone lithofacies. It also commonly underlies and overlies the intervals of siltstone and sandstone lithofacies that occur in the Jackfish Gap. In the upper Meilleur, the shale and mudstone lithofacies generally overlies and underlies units of lime-grainstone lithofacies. South of approximately 60°55'N, this lithofacies is locally intercalated with the Flett spiculite and spicule-lime-packstone lithofacies in the lower Meilleur. Contacts between the shale and mudstone lithofacies and the other four Flett lithofacies vary from abrupt to gradational through several metres and are described in sections dealing with these other four lithofacies.

Olive-black to greyish black shale and mudstone, with minor limestone, sandstone, and siltstone constitute the shale and mudstone lithofacies. In the upper Meilleur Member, the shale is generally noncalcareous to slightly calcareous, very



Figure 68. Upper Meilleur Member at Jackfish Gap showing bed of Flett shale and mudstone lithofacies (below arrow) overlain by mudstone and nodular limestone. Hammer (arrow) indicates scale. ISPG 1303-8.



Figure 69. Rhythmically interbedded, resistant (spicule lime packstone) and recessive (spiculite) beds in spicule-lime-packstone lithofacies of the Flett Formation at Locality 12. ISPG 1756-41.



Figure 70. Type section of the Meilleur Member, Jackfish Gap. Simple and composite multibed limestone sequences that become more resistant and coarser grained upward. Upper and lower arrows indicate base and top of the Meilleur Member, respectively. A large-scale truncation surface, overlain by lime grainstone and interpreted as the erosion surface of a submarine channel, is indicated by the middle arrow. The lower two thirds of the Meilleur are mixed-skeletal lime-packstone lithofacies. ISPG 1281-16.

fissile, and sparsely fossiliferous. Elsewhere, both the shale and the mudstone are generally calcareous, silty, friable, and moderately fossiliferous.

Units of shale and mudstone lithofacies resemble those of the dark-shale lithofacies of the Besa River, Clausen and Prophet formations, and they are possibly of similar origin. These units of fine grained siliciclastics vary from several centimetres to several metres in thickness and were observed only at weathered outcrops. The main primary sedimentary structures present are vague laminae and minor soft-sediment deformation, which occurred in occasional intervals containing numerous nodule-like structures of limestone. The nodule-like structures resemble those in the mixed-skeletal lime-packstone lithofacies and are possibly of similar origin. Locally, lenses and laminae of siltstone and sandstone are present, and some thin beds and lenses of limestone occur. Scattered and locally concentrated, resedimented to autochthonous invertebrate fossils are locally common. They include relatively well preserved to fragmentary, abraded, and crushed specimens.

Spicule-lime-packstone lithofacies

The spicule-lime-packstone lithofacies (Fig. 69) is a relatively minor facies, occurring chiefly in the basal

Meilleur Member of the southern Liard Range. In that area, it is generally abruptly to gradationally overlain and underlain by deposits of either the Flett mixed-skeletal lime-packstone lithofacies or the shale and mudstone lithofacies. Spicule lime packstone and wackestone with subordinate spiculite and very calcareous mudstone constitute this facies.

The spicule-lime-packstone lithofacies consists mainly of rhythmically interbedded, recessive to moderately resistant beds (Fig. 69), occurring in multibed sequence that become more resistant upward. Beds in this facies are mainly of medium thickness (10-30 cm) and have moderate to great lateral continuity. Evidence of sedimentary boudinage is moderately common in some units, however. The bases of some resistant beds are sharp, but, more commonly, resistant beds appear to grade into underlying and overlying recessive deposits through 15 cm or more. Most of the resistant and recessive beds have both diffuse internal stratification and subplanar laminae. Other resistant beds appear to be mainly massive. Invertebrate fossils, other than sponge spicules, are generally rare, and evidence of bioturbation varies from rare to moderately common.

In general, the deposits described above closely resemble those in the spiculite and spicule-lime-packstone lithofacies of the Prophet Formation. They are, therefore, tentatively interpreted as having been deposited by similar

mechanisms. The Prophet deposits are interpreted as having been formed mainly by hemipelagic processes and by turbidity currents.

Multibed sequences

In the discussion on multibed sequences in the Prophet Formation, it was pointed out that sequences in three orders of magnitude constitute the Lower Carboniferous between the Yohin and Golata formations. That interval consists of the Besa River, Clausen, Prophet, and Flett formations, which together constitute a first-order megasequence with the Flett at the top. With some exceptions, this megasequence becomes coarser grained and more resistant and proximal in aspect upward.

Beds in the Flett Formation occur in simple multibed units called third-order sequences, which are commonly grouped to form composite second-order sequences (Figs. 51, 70). The second-order sequences are generally between 25 and 30 m thick, but locally exceed 200 m. At most locations, the Flett comprises two or more superimposed, laterally continuous second-order sequences. Three styles of third- and second-order sequence occur in the Flett:

1. Those that become more resistant and coarser grained upward (Fig. 70)
2. Those that become finer grained and less resistant upward (Fig. 51)
3. Symmetrical sequences that are coarsest and most resistant near their middles (Fig. 81).

Of these, the first is most abundant and the third is the least abundant. Sequences that become less resistant upward are moderately common, but many overlie large-scale concave-upward truncation surfaces, which resemble erosion surfaces of submarine channels. The origins of the three styles of multibed sequence and the truncation surfaces are discussed below, after the discussion on the Golata Formation.

In first- and second-order asymmetric sequences that become more resistant upward and consist mainly of carbonates, the deposits tend to become more proximal in aspect toward the top. A similar transition is also well developed from the base to the top of the Meilleur Member and in the Flett Formation west of the depositional limits of the Tlogotsho and Jackfish Gap members. In order of decreasing importance, the principal upward changes are: beds and Bouma divisions comprising resistant lithologies become thicker and closer; sediment-gravity-flow deposits become more proximal in aspect; within successive resistant beds, proportions of siliciclastics and carbonate matrix decrease; the proportion of spicules decreases, whereas that of other bioclasts increases; the proportion of lime grainstone increases; lateral continuity of beds decreases; and medium- to large-scale crossbedding becomes more common. Not all of these changes are evident in every sequence. Moreover, they are most pronounced in those that contain two or more lithofacies, in second-order sequences, and within the Meilleur Member. Boundaries of these sequences can be sharp, but more commonly the resistant top of a sequence grades into the recessive base of an overlying one through 50 cm or more. When present, large-scale truncation surfaces occur mainly in the upper part of the thicker sequences.

Laterally continuous, asymmetric sequences that become less resistant upward and consist mainly of carbonates generally have abrupt bases. They are commonly

thick, second-order sequences (Figs. 32, 51, 77b) comprising several subordinates. Most subordinate sequences are asymmetric, and the basal one is generally the most resistant. Second-order sequences that become less resistant upward generally abruptly overlie poorly developed sequences that become more resistant upward. Moreover, the second-order sequences tend to grade basinward into units that become more resistant upward and shelfward into symmetrical sequences. Large-scale, concave-upward truncation surfaces are common in the second-order and thicker third-order sequences, particularly near their bases. Also, the sharp bases of some sequences are possibly truncation surfaces. At Jackfish Gap (Figs. 4, 51) and to the northeast, the Tlogotsho Member is an excellent example of a second-order sequence that becomes less resistant upward.

Both third- and second-order symmetrical sequences occur, and the latter may consist of both asymmetric and symmetric subsequences. Between the base and resistant middle of symmetrical sequences, the same upward trends that occur in the sequences that become more resistant upward are evident. Conversely, from the middle to the top of symmetric sequences, the upward trends resemble those of asymmetric sequences that become less resistant upward. When present, large-scale truncation surfaces occur mainly in the resistant, proximal, central parts of these sequences (Fig. 81).

One of the best examples of a symmetrical sequence is a thick, second-order sequence that includes the basal Meilleur Member, the Tlogotsho Member, the Prophet Formation, and either the Clausen or upper Besa River Formation. This sequence is well developed in much of the project area that is east of the Flett anticline and south of about latitude 60°35'N (Fig. 5, southern Liard Range section). Another example, which excludes the Meilleur, is well developed at the northern end of the Mattson anticline (Fig. 4).

Environmental interpretations

Mixed-skeletal lime-packstone lithofacies

The mixed-skeletal lime-packstone lithofacies is interpreted as having been deposited mainly between the lower and upper slope environments of westward-prograding carbonate buildups (ramps grading into platforms, Fig. 87). A middle slope depositional environment is indicated by the spatial relationship of this facies to other lithofacies, its lithology, and the type of deposits present. In most of the project area, this lithofacies overlies and grades westward into either lower slope deposits or intervals of intercalated lower slope and basinal deposits. Carbonate lithofacies that were deposited in upper slope and shelf margin environments commonly overlie or grade westward into the mixed-skeletal lime-packstone lithofacies. This lithofacies comprises dark-coloured, matrix- and commonly spicule-rich rock types that occur mainly in rhythmically bedded, locally channelized, proximal, sediment-gravity-flow deposits. Deposits of this type are characteristic of the intermediate slope on many platforms (Wilson, 1975, p. 25-28; Davies, 1977; Schlager and Chermak, 1979; Yurewicz, 1977; Gutschick et al., 1980; and others).

At least locally, the middle slope appears to have had two topographic subdivisions that occurred as broad belts subparallel to the shelf margin. The upper belt probably had the steepest gradient, and it was incised by channels, which ran subperpendicular to the shelf margin and extended onto the upper slope. This belt is represented by deposits of the mixed-skeletal lime-packstone lithofacies that contain

abundant concave-upward discontinuities. At its lower end, the upper belt terminated at the broad zone of locally channelled, relatively small, coalesced fans and fan-like lobes that formed the lower belt. The upper part of the lower belt is represented by deposits of the Flett and Prophet mixed-skeletal lime-packstone lithofacies, characterized by multibed sequences that become more resistant upward and lack abundant concave-upward truncation surfaces. In comparison, the distal part of the lower belt is represented by the Prophet spiculite and spicule-lime-packstone lithofacies, which generally lacks abundant concave-upward discontinuities. Spatial relationships between multibed Flett and Prophet sequences, with or without abundant concave-upward discontinuities, provide the evidence for this interpretation. The upper, channelled belt resembled the gullied slope in the Tongue of the Ocean in the Bahamas, whereas the lower belt resembled the corresponding basin margin setting that is basinward of that slope (see Schlager and Chermak, 1979, p. 204; Hook and Schlager, 1980). The gradient of the upper, channelled belt on the middle slope was probably steeper than the gradient of the lower belt because that, according to Schlager and Chermak (1979, p. 204), is the situation in the Bahamas. Moreover, basinward of the uppermost slope, carbonate slopes generally have a concave-upward longitudinal profile (Fig. 87) on which gradients decrease basinward in response to decreased rates of sedimentation (Meissner, 1972; Wilson, 1975).

Segments of the middle slope appear to have lacked abundant channels. Thick intervals of the mixed-skeletal lime-packstone lithofacies that lack abundant concave-upward discontinuities represent these parts of the slope. In areas without channels, the region basinward of the uppermost slope was possibly a simple carbonate wedge, with a concave-upward longitudinal profile lacking discrete topographic subdivisions. Most documented ancient carbonate slopes appear to have been like this, and are represented by relatively simple progradational sequences that become progressively more proximal in aspect upward.

The gradient of the middle slope was probably low, and intermediate between those of the uppermost and lowermost slopes, but it is possible only to speculate about the mean gradient. Because the middle slope was broad, from 10 to 20 km or more across, and consisted mainly of relatively fine grained, unconsolidated sediment, its gradient must have been low. The work by Sandberg and Gutschick (1980, p. 139) on carbonate slope deposits of Mississippian age in the western United States, and that of Mullins and Neuman (1979, p. 185) on modern Bahamian carbonate slopes, suggest that broad carbonate slopes generally have mean gradients of one to five degrees or slightly less.

Most units of the mixed-skeletal lime-packstone lithofacies were deposited below storm wave base and probably at moderate depth in the aerobic zone. Deposition below storm wave base is indicated by the abundance of sediment-gravity-flow deposits that were not reworked by waves. Also, beds that resemble turbidites are preserved in the more proximal lime-grainstone lithofacies. On high-energy coasts, storm wave base can exceed 125 m (Komar, 1976, p. 107). The trace fossil assemblage present also suggests deposition at moderate depth. Seilacher's (1967, 1978) *Zoophycos* association (Fig. 61) is well developed in much of this lithofacies. According to Howard (1978, p. 38, 44) and Seilacher, that association is generally typically developed in strata deposited at upper-bathyal depths. Deposition at moderate depth is also indicated by spatial relationships between this facies and other lithofacies. The mixed-skeletal lime-packstone lithofacies grades basinward into the Prophet spiculite and spicule-lime-packstone lithofacies, which appears to have been deposited

at depths of several hundred metres. Finally, abundant evidence of bioturbation and the common occurrence of autochthonous, benthonic macrofossils is indicative of deposition under aerobic conditions.

Like the beds that resemble turbidites and occur in the Yohin graded-bed lithofacies of the Bluefish-Twisted mountains region, it is possible that many sharp-based graded beds in some intervals of mixed-skeletal lime-packstone lithofacies are tempestites. The tempestites would have been produced in relatively shallow water by storms, rather than in moderately deep water by turbidity currents generated on slopes by slumping or by other processes. Beds that are possibly tempestites occur mainly in the following occurrences of the mixed-skeletal lime-packstone lithofacies: those that are intercalated with crossbedded lime grainstone at Locality 13; those that are present in the Jackfish Gap Member; and those that occur in the upper Meilleur Member at Locality 2. Deposition by storm processes in relatively shallow water is suggested mainly by the close proximity of the sharp-based beds to strata that have been deposited above to slightly below wave base. The latter contain wave-formed crossbedding, hummocky crossbedding, and medium- to large-scale trough crossbedding. Also, the sharp-based beds in these occurrences are similar to tempestites described by Aigner (1982) and to probable tempestites in the Yohin Formation.

Some intervals of mixed-skeletal lime-packstone lithofacies may have been deposited on the protected shelves of platforms (Fig. 87a). Occurrences of this lithofacies that are possibly protected shelf deposits include: those associated with crossbedded lime grainstone at Locality 13; most intervals in the Tlogotsho and Meilleur members at Localities 21 and 26; and much of the strata in the upper Meilleur northeast of Locality 4. This interpretation is based mainly on spatial relationships, which suggest that the deposits at these localities may have been deposited between the shelf-margin sand belt and the restricted shelf (Fig. 87a). Studies of protected shelf deposits in the Rundle Group of western Alberta (Richards et al., in press) indicate that these deposits commonly consist of sharp-based, graded beds that closely resemble some of those in the mixed-skeletal lime-packstone lithofacies of the Flett Formation.

Lime-grainstone lithofacies

The lime-grainstone lithofacies is interpreted as having been deposited mainly in carbonate-platform environments ranging from upper slope to shelf margin (Fig. 87a). The deposits constituting this facies represent these two major environments but are not readily separable. The principal problem entails determining the location of the shelf-slope break because the strata, and to some extent the sedimentary structures, are similar in both environments. Also, neither a sharp break in slope nor shallow water, organic reefs appear to be present.

Intervals of lime-grainstone lithofacies consisting chiefly of graded beds that resemble turbidites, were probably deposited on the upper slope (Fig. 87a). These deposits appear to correspond approximately with the periplatform talus in McIlreath and James's (1978, p. 196) model for a depositional carbonate margin dominated by shallow water, lime sands. Deposition on the upper slope is indicated chiefly by the close proximity of these deposits to crossbedded limestone of probable shallow water origin and to underlying middle slope deposits. The predominance of light coloured lime grainstone that is relatively mature texturally also suggests deposition on the upper slope. Because clean lime sands consisting largely of fragmented

and abraded bioclasts are produced chiefly in shallow, high-energy environments, the shelf-margin environments would have supplied most of the lime sand in the grainstone. Many of the beds that resemble turbidites are probably tempestites (for reasons similar to those given in the section dealing with the origin of the sharp-based beds that occur in the mixed-skeletal lime-packstone lithofacies), and are associated with relatively shallow water deposits.

Parts of the lime-grainstone lithofacies, which consist mostly of crossbedded limestone and dolostone, were probably deposited mainly on the shelf margin. The presence of medium- to large-scale crossbedding in beds of clean lime sand is indicative of deposition in a regimen dominated by wave- and tide-controlled processes. Because these crossbedded deposits overlie and grade basinward into deposits that resemble turbidites, they were probably deposited in a belt of shelf-margin sands, rather than environments situated closer to the shoreline. However, some of the crossbedded carbonates may have been deposited slightly basinward of the shelf-slope break, because tide- and wave-controlled processes generally affect sedimentation on the upper slope (see Wilson, 1975, p. 26, 27). The crossbedded carbonates would, therefore, be slope deposits.

Components of the lime-grainstone lithofacies that were deposited on the upper slope would probably have been deposited on a gentle gradient at moderate to shallow depths. The following evidence indicates that the gradient of the upper slope was relatively low: the absence of steeply inclined foresets of the type observed by Davies (1977) in upper slope deposits of the Sverdrup basin; the absence of paleoscarpments; and the fact that the lithofacies belt is relatively broad. However, the upper slope probably had a convex-upward longitudinal profile and a slightly steeper gradient than the middle to lower slope because this is typical of most carbonate slopes. Deposition at moderate depths is suggested for many of the upper slope deposits because turbidite-like beds, which were not significantly reworked by shallow water processes, predominate. However, the crossbedded deposits must have been deposited near to or well above wave base.

The ooid-skeletal lime grainstone that occurs in the upper Meilleur Member at Locality 21 was probably deposited on the landward part of the shelf margin (Fig. 87a). Regional studies of the Rundle Group of southwestern Alberta (Richards et al., in press) indicate that ooids are generally rare in strata deposited on the seaward part of the shelf margin, but are commonly abundant in shoreline facies deposited on the landward part.

Siltstone and sandstone lithofacies

The siltstone and sandstone lithofacies in the upper Jackfish Gap Member at Locality 4, and occurrences of this facies to the east, are interpreted as having been deposited mainly in environments ranging from slightly below to well above fairweather wave base. Deposition in relatively shallow water is indicated by the common occurrence of coarsening-upward sequences (Fig. 66a) that were deposited under shallowing-upward conditions, and which contain abundant crossbeds formed by traction currents (Fig. 66b, c) and waves. These sequences closely resemble shallowing-upward intervals that occur in the crossbedded-sandstone lithofacies of the Yohin Formation and are interpreted as shallow-sublittoral deposits. Sequences like these in the Flett may develop in both the shallow-neritic and intertidal zone. However, it is improbable that the siltstone and sandstone lithofacies was deposited in the intertidal zone because evidence of emergence has not been observed, and it

is closely associated only with offshore-marine facies. Deposition at relatively shallow depths also is indicated by the trace fossils present. Trace fossils that are probably assignable to Seilacher's (1967, 1978) *Cruziana* association, which is diagnostic of neritic shelf strata, are locally abundant. The presence of some turbidite-like storm deposits that have not been reworked by waves suggests parts of this lithofacies were deposited at moderate water depths (just below to slightly above storm wave base).

In contrast, the siltstone and sandstone lithofacies in the lower part of the Jackfish Gap Member at Locality 4, and occurrences of this facies to the west (Fig. 4), were probably mainly deposited in moderately deep water (well below wave base). This is suggested by the relationship of these deposits to other facies and by the sedimentary structures present. These occurrences of the siltstone and sandstone lithofacies are underlain and overlain by deposits that appear to have been deposited in moderately deep water, slope and basin environments. Small-scale, current crossbeds and low-amplitude current ripples are the main primary sedimentary structures present. Wave-formed structures and medium- to large-scale crossbeds are absent. Also, Seilacher's (1967, 1978) *Zoophycos* association, which typically occurs in strata deposited at upper bathyal depths (Seilacher, 1978; Howard, 1978), is locally well developed.

The siltstone and sandstone lithofacies is interpreted as having been deposited on a shelf or slope that had a very low gradient. North of approximately latitude 60°55'N, this facies and associated deposits in the Jackfish Gap Member and uppermost Tlogotsho Member conformably overlie carbonates deposited on a southwest-dipping slope that had a gradient of one to five degrees. The characteristics of the siltstone and sandstone lithofacies change slowly between Twisted Mountain and Locality 6, about 30 km basinward. Therefore, the gradient of the depositional surface must have remained low during the deposition of this facies.

Shale and mudstone lithofacies

Deposition in low-energy marine environments at water depths ranging from near to well below fairweather wave base is suggested for the shale and mudstone lithofacies. Intervals of this facies in the upper Meilleur Member were probably deposited mainly in relatively shallow water, because they are associated with units of lime-grainstone lithofacies comprising tempestites and shallow water, crossbedded carbonates. Also, deposits of shale and mudstone lithofacies that occur with the shallow-neritic siltstone and sandstone lithofacies must have been deposited near fairweather wave base. Beds of shale and mudstone lithofacies that are interbedded with those of the mixed-skeletal lime-packstone lithofacies in the upper Tlogotsho Member, Jackfish Gap Member, and lower Meilleur Member were deposited at slightly greater depths. This is indicated by their association with beds of the latter facies that are interpreted as either turbidites or storm beds deposited below fairweather wave base. They are also similar to and contiguous with units of Prophet dark-shale lithofacies, which is a basin facies. Deposition in relatively deep water is suggested for beds of shale and mudstone lithofacies that occur with the Flett spicule-lime-packstone lithofacies in the southern Liard Range. The latter facies, which closely resemble the deep water deposits in the spiculite and spicule-lime-packstone lithofacies of the Prophet Formation, is interpreted as consisting of turbidites and hemipelagites deposited well below wave base.

Intervals of the shale and mudstone lithofacies that are intercalated with those of the lime-grainstone lithofacies in the uppermost Meilleur Member are interpreted as precursors of the prodelta deposits constituting most of the overlying Golata Formation (Fig. 71). This is supported by the similarity between the shale in the uppermost Meilleur and that in the Golata and by the upward increase in the abundance of shale. Moreover, the proportion of shale in the uppermost Meilleur increases toward the north and northeast, the probable direction from which siliciclastics in the Golata were derived.

Spicule-lime-packstone lithofacies

The spicule-lime-packstone lithofacies is interpreted as having been deposited in relatively deep water. This is indicated mainly by its resemblance to the Prophet spiculite and spicule-lime-packstone lithofacies, which is interpreted to have been deposited in a lower-slope setting (Fig. 87a) in moderately deep water. Also, units of spicule-lime-packstone lithofacies commonly underlie units of the Flett mixed-skeletal lime-packstone lithofacies. The latter was probably deposited mainly on a middle-slope setting.

Carbonate buildup development and terrigenous influx

During the latest Tournaisian to latest middle Viséan (Tn3 to V2; late zone 9 to latest zone 13), two carbonate buildups developed north of approximately latitude 60°55'N while one formed to the south (Fig. 50). Remnants of these buildups (ramp deposits grading into platform deposits) consist of the slope to shelf-margin deposits of the Flett Formation and correlative lower slope deposits of the Prophet Formation (Fig. 87a). The two buildups in the north, which are preserved in the Tlogotsho and Meilleur members, are separated by a thick interval dominated by terrigenous clastics (Fig. 4). Two main episodes of terrigenous deposition and several changes in water depths influenced the development of the buildups.

Deposition of the resistant carbonate buildup deposits that generally constitute the lower Tlogotsho Member (Figs. 4-6, 51) followed the initial phase of a major regional transgression. The initial phase of that transgression resulted in the deposition of dark, shale-rich deposits that are of latest Tournaisian (Tn3) age, and which are preserved in the uppermost Prophet Formation in much of the eastern half of the project area (Fig. 5, Loc. 25; Fig. 6, Loc. 21). The carbonate buildup deposits in the lower Tlogotsho rapidly prograded westward beyond the underlying carbonate buildups of Tournaisian age.

Water depths possibly increased in the area during the early Viséan (V1; middle to late zone 10) subsequent to deposition of the lower Tlogotsho Member. This is suggested by an upward increase in the abundance of spicule-rich, recessive, argillaceous rocks in the upper half of the Tlogotsho north of about 60°55'N (Figs. 4, 51). To the south, similar trends are locally evident in Tlogotsho deposits that are approximately the same age as those in the north (see Fig. 5, Loc. 13, 163-215 m).

North of approximately latitude 60°55'N, a major break in carbonate buildup development and a decrease in water depth are recorded by the lithofacies in the uppermost Tlogotsho Member and in the overlying Jackfish Gap Member. The siltstone and sandstone lithofacies, together with the shale and mudstone lithofacies constitute a major part of this interval (Figs. 66, 67). These deposits, of early to middle Viséan age (V1 to V2; latest zone 10? to the 12/13 boundary),

form a blanket over the underlying carbonate buildup deposits. A decrease in water depth is indicated by the presence of the siltstone and sandstone lithofacies above deeper water deposits. The siltstone and sandstone lithofacies contains crossbedded shallow-neritic deposits (Fig. 66b, c), and generally constitutes the upper and lower parts of the Jackfish Gap Member. Most of the underlying Tlogotsho Member consists of the rhythmically bedded deposits of the mixed-skeletal lime-packstone lithofacies, which are interpreted as having been deposited on a carbonate slope below wave base. Moreover, the units of siltstone and sandstone lithofacies that form the lower and upper Jackfish Gap appear to have been deposited contemporaneously with the Wileman and Salter members, respectively (Fig. 3). Data provided by Macqueen and Bamber (1968) indicate that the Wileman and Salter were deposited during marked regional regressions.

During deposition of the siliciclastics of the Jackfish Gap Member, deposition of carbonate buildup deposits continued in the southern part of the project area. In that region, the shallow water, crossbedded lime grainstone that occurs in the middle to upper Tlogotsho Member at Locality 13 (Fig. 5) was deposited. Lime grainstone, of probable shallow water origin, was observed at a similar stratigraphic position at Locality 21 as well (Fig. 6). At Locality 13, the presence of the lime grainstone, immediately above shale and rhythmically bedded strata deposited in moderately deep water, indicates that water depths also decreased substantially in the southern part of the project area at this time.

A major transgression occurred in the project area after deposition of the Jackfish Gap Member and during the middle Viséan (V2; 12/13 boundary to early zone 13). North of about latitude 60°55'N, this transgression is indicated by the rapid transition from shallow-neritic sandstone in the Jackfish Gap Member to the moderately deep water deposits of the overlying Meilleur Member. In that area, the shale and



Figure 71. The dark-shale lithofacies and the dolostone lithofacies (light beds) in the Golata Formation (arrows indicate boundaries) at Locality 4; note wedging of dolostone beds. Overlying resistant beds are delta-front sandstone of the Mattson Formation. ISPG 1303-10.

mudstone lithofacies and the mixed-skeletal lime-packstone lithofacies constitute the lower Meilleur. To the south, similar evidence for this transgression is present in the upper Tlogotsho Member and basal Meilleur. For example, at Locality 13, the shallow water, crossbedded lime grainstone in the upper Tlogotsho passes up into deposits of the spicule-lime-packstone and the shale and mudstone lithofacies in the basal Meilleur. These last two facies are interpreted as having been deposited in moderately deep water. Additional evidence for a major transgression at this time is present in the Loomis Member in southwestern Alberta (Fig. 3). The Loomis, which comprises skeletal and ooid lime grainstone deposited in shelf-margin to protected-shelf environments (Fig. 87a), abruptly overlies restricted-shelf deposits. This member was deposited during a major regional transgression (Richards et al., in press). As a consequence of the transgression, the development of another carbonate buildup was initiated in the northern part of the project area. In the southern part of the project area, carbonate production continued but in deeper water than before.

Subsequent to the initial phase of the transgression, discussed above, the carbonate buildup deposits in the Meilleur Member were deposited under shallowing-upward conditions. Shallowing upward is indicated by an upward transition from the slope deposits of the mixed-skeletal lime-packstone lithofacies to the shelf-margin and possible open-shelf deposits of the lime-grainstone lithofacies. The formation of these carbonate buildup deposits was terminated by the deposition of the basal siliciclastics of the Golata Formation (Figs. 35, 71), which are of latest middle Viséan (V2; latest zone 13) age or slightly younger.

Alternating periods of siliciclastic and carbonate-platform deposition occurred in the project area during the early to late Viséan (V1 to early V3). This style of cyclic sedimentation was common in the past (Meissner, 1972; Wilson, 1975, p. 42, 43). It resulted from changes in the proximity of the siliciclastic shoreline deposits in response to fluctuations in sea level, changes in basin-subsidence rates, and uplift of the source areas for terrigenous clastics (Rose, 1976, p. 451-453). According to Rose (1976) and Wilson (1975), when the shoreline is far from the carbonate-shelf margin, the shelf and slope are generally protected from terrigenous influx and the progradation and aggradation of carbonate platforms occurs. However, when the siliciclastic shoreline deposits are close to the shelf margin, siliciclastics are transported across the shelf and bypass the shelf margin, thereby reducing platform relief and terminating its development.

Age

Microfossils and rugose corals collected from the Flett Formation (Appendices A, B) indicate an age range from latest Tournaisian (Tn3; late foraminiferal zone 9 of Mamet and Skipp, 1970, 1971) to latest middle Viséan (V2; latest zone 13) or possibly younger (Figs. 3-6). The base of the Flett, which is diachronous, ranges in age from latest Tournaisian (Tn3; late zone 9) in the east, to latest middle Viséan (V2; zone 13) in the west. Throughout the project area, the uppermost Flett contains a foraminiferal assemblage that is of latest middle Viséan (V2; latest zone 13) age or possibly slightly younger. At Jackfish Gap, Bamber and Mamet (1978, Fig. 9) questionably assigned an early late Viséan age (V3; early zone 14) to the interval that I reassign to the Golata and upper four metres of the Flett. Their age assignment was based on the presence of the corals *Ekvasophyllum inclinatum?* and *Zophriphyllum?* in strata assigned to the Golata here.

The top of the Tlogotsho Member is diachronous. North of approximately latitude 60°55'N, where it is conformably overlain by the Jackfish Gap Member, the uppermost Tlogotsho is of early Viséan (V1; early zone 11) age. To the south, the upper Tlogotsho includes strata that are equivalent in age to the Jackfish Gap and, in this area, the upper boundary of the Tlogotsho is of middle Viséan (V2; 12/13 boundary) age.

The top of the Jackfish Gap member and the base of the Meilleur Member are of middle Viséan (V2; 12/13 boundary) age.

GOLATA FORMATION

Type section

Halbertsma (1959, p. 113) proposed the name Golata Formation and designated its type section, which is between 1322.2 and 1375.3 m (4338 and 4512 ft) in the Imperial Belloy No. 12-14 (12-14-78-1W6) well, Peace River area, Alberta.

Previous work

In the project area, the Golata Formation, or parts of it, have been variously included in the Flett, Etanda, and Besa River formations (Fig. 2). Strata that I reassign to the Golata were included by Harker (1961, 1963) in the Flett Formation at its type locality (Fig. 1, Loc. 4) and elsewhere in southwestern District of Mackenzie. Douglas et al. (1963), Douglas et al. (1970, p. 418), Douglas and Norris (1976a, b, c), Douglas (1976), Bamber and Mamet (1978, p. 8, 9), and Bamber et al. (1980, p. 12) followed Harker's usage of the Flett.

The Golata Formation corresponds to Harker's (1961, p. 6, 7; 1963, p. 16, 17) upper Etanda Formation at Etanda Lakes (Fig. 1, Loc. 8) and in the La Biche syncline to the south. In the same region, Douglas (1976) and Bamber et al. (1980) assigned the Etanda to the Besa River Formation and included the Golata and Prophet Formation in its upper part.

Distribution

The Golata Formation (Figs. 35, 71) is widely distributed in the project area, occurring in the Mackenzie fold belt and on the interior platform (Figs. 5, 6). Moreover, it is widely distributed in northeastern British Columbia and the Peace River area of Alberta (Halbertsma, 1959; Macauley et al., 1964, p. 98-100). Its distribution north of latitude 60°00'N is controlled chiefly by that of the Prophet and Mattson formations. Because the Golata is thin and easily eroded, it is preserved only where it is overlain by the Mattson. West of the western depositional limit of the underlying Prophet, the Golata cannot be differentiated from the Besa River Formation.

In the project area, the Golata is present between latitudes 60°00'N and 61°27'N, and occurs principally within the District of Mackenzie. Outcrops are confined to the southern Mackenzie fold belt between 60°27'N and 61°27'N, and at most localities this formation is recessive and poorly exposed. South of Etanda Lakes (Fig. 1, Loc. 8), the western boundary of the Golata is probably in the La Biche syncline. This boundary extends northward from the Etanda Lakes area to the northwestern corner of the Tlogotsho Plateau. East of the Mackenzie fold belt, the Golata is restricted to the southwestern side of the interior platform, where it has essentially the same distribution as the Mattson (Fig. 1).

Thickness

The thickness of the Golata Formation is moderately variable (Table 1). In much of the region, its thickness is less than 20 m and varies erratically, but near the Prophet-Flett boundary it begins to increase progressively and quite rapidly toward the west and southwest (Figs. 5, 6). For example, near the Prophet-Flett boundary at Locality 5, the Golata overlies the Flett Formation and is 8.5 m thick. In comparison, at Etanda Lakes, 27.5 km southwestward (Fig. 1, Loc. 8), it overlies the Prophet Formation and is 515.8 m thick. On the interior platform, east of the erosional zero-edge of the overlying Mattson Formation, the Golata thins rapidly to zero beneath a regional unconformity. South of the project area, thickness trends in the Golata are similar to those in the project area. Its stratotype is 53 m thick (Halbertsma, 1959, p. 113; Macauley et al., 1964, p. 100).

Lithostratigraphic relationships

The Golata Formation conformably overlies either the Flett or Prophet formations (Figs. 35, 71) and is separated from the Besa River Formation by an arbitrary cutoff, which coincides with the western depositional limit of the Prophet. Boundaries between the Golata and the two underlying formations are discussed in sections about the lithostratigraphic relationships of the Flett and Prophet. In the project area, the Golata is a tongue of the thick shale lithosome that constitutes most of the Besa River Formation.

Throughout most of the project area, the Mattson Formation conformably overlies the Golata Formation (Fig. 71), but immediately east of the Mattson erosional zero-edge on the interior platform, Permian strata overlie the Golata (Figs. 5, 6). The Golata grades upward into the Mattson, and toward the west the boundary between these formations becomes younger, because the Mattson sandstone grades laterally into the shale and mudstone of the Golata. Their boundary is defined by the base of the lowest major sandstone unit above which sandstone constitutes greater than 25 per cent of the succession. Proportions of silt, sand, and sandstone increase toward the top of the Golata, which grades upward into the Mattson through 50 cm or more. In the outcrop belt, this contact generally coincides with a prominent break in slope because the Mattson is resistant and the Golata is very recessive. Above the Golata/Mattson contact, gamma ray logs generally record a marked decrease in radioactivity that corresponds to a decrease in interval travel times on sonic logs (Fig. 5).

Lithology

The Golata Formation comprises shale and mudstone with subordinate dolostone and sandstone (Figs. 4-6, 71, 72). Minor dolomitic limestone, spiculite, and siltstone are locally present as well. In most of this formation, shale is more abundant than mudstone; however, at localities where the Golata overlies the Flett Formation, mudstone commonly predominates in its upper part. To the west, in parts of sections where sandstone is moderately common, mudstone is also more abundant than shale. Dolostone is present at most localities, but it generally becomes less abundant toward the west. At some localities, where the Golata overlies the Flett, dolostone is locally present throughout the Golata. To the west, however, dolostone occurs mainly in the lower part of the formation. East of the western depositional limit of the Flett (Fig. 89), sandstone is generally a minor rock type occurring in the uppermost Golata. To the west, sandstone is commonly abundant in the middle to upper Golata. Sandstone is more abundant in the west because the sandstone in the

lower Mattson of that region passes rapidly westward into the shale and mudstone of the upper Golata, and numerous minor tongues of the sandstone extend into the Golata.

Shale and mudstone in the Golata Formation are chiefly greyish black to olive-black, moderate brown weathering, and sparsely fossiliferous. Most of the shale has a well developed fissility and commonly splits into paper-thin sheets. The mudstone is friable and commonly grades into muddy sandstone and siltstone. Sponge spicules and fragmentary pelmatozoans and bryozoans are the main macrofossils. They become less abundant upward in the Golata, and spicules were not observed in intervals that consist of sandstone interbedded with shale and mudstone. Semiquantitative X-ray diffraction analyses of five representative shale and mudstone samples (Appendix G) indicate that quartz is the most abundant mineral, forming up to 76 per cent of some samples. Also, some of the shale and mudstone is slightly calcareous and most of it is dolomitic to ankeritic.

East of the western depositional limit of the Flett Formation (Fig. 89), most dolostone in the Golata Formation is fossiliferous, light olive-grey to olive-black, dark yellowish orange weathering, and slightly cherty. Pelmatzoan fragments and bryozoans are the main allochems. Brachiopods, intraclasts, ostracods, molluscs, and corals also occur but never predominate. Most bioclasts are of sand to granule size and fragmented to abraded. Precursor textures are generally poorly preserved, but all samples examined have a grain-supported texture and are either dolomitized lime grainstone or packstone. In addition to allochems, siliciclastic mudstone intraclasts are common in some beds (Fig. 74), and siliciclastic silt and sand constitute between 0.1 and 5 per cent of most beds by volume. Most dolostone is noncalcareous to slightly calcareous, but locally it grades into very dolomitic limestone.

The dolostone that occurs in the Golata west of the Flett Formation is mostly uniformly sucrosic, slightly fossiliferous or unfossiliferous, olive-grey to olive-black, and greyish orange weathering. Sponge spicules are the main allochem, but intraclasts and fragmentary brachiopods, pelmatozoans, bryozoans, and ostracods are moderately common in some beds. This dolostone is slightly silty, generally has some dark siliceous matrix, locally grades into spiculite, and is commonly slightly calcareous.

Sandstone and siltstone in the Golata Formation are siliceous to dolomitic, submature quartzarenite (Fig. 72) and muddy, immature quartzarenite, both of which are mainly light grey to light olive-grey and weather moderate yellowish brown. The sandstone is mainly fine to very fine grained, and the sorting of the clasts in the sandstone and the siltstone varies from moderate to poor but is mainly poor. Some greyish black mud matrix is generally present, and commonly the sandstone and siltstone grade into mudstone. The fine to coarse sand-sized quartz clasts are mainly subangular to subrounded, but round and very angular to angular clasts are moderately common. Quartz is the principal cement, but trace quantities of ferroan dolomite (possibly ankerite) occur in many of these rocks. A few beds are very dolomitic.

The mean percentages of clast types in two sandstone samples from the Golata at Etanda Lakes are: quartz 96.7 ± 2.1 , chert rock fragments 0.4 ± 0.3 , other rock fragments (mainly siltstone) 1.7 ± 2.1 , feldspar 0.3 ± 0.1 , nonopaque heavy minerals (mainly tourmaline, zircon, and sphene) 0.3 ± 0.1 , micas 0.3 ± 0.1 , and opaques 0.3 ± 0.1 (Appendix F). Mean percentages of the types of quartz grains in the same two samples are: clasts with straight extinction 55.3 ± 14 , clasts with undulose extinction ($>5^\circ$) 43.3 ± 2.1 , polycrystalline clasts with two to three units 0.4 ± 0.2 , and

polycrystalline clasts with more than three units 1.1 ± 0.5 . These analyses are based on 500 and 400 counts per thin section, respectively. Although mica is a minor accessory in these samples, it is common on some partings and in muddy sandstone. In addition to the components listed above, carbonized plant fragments are common to rare. The clast composition of the Golata sandstone is essentially the same as that of sandstone in correlative beds in the lower Mattson Formation.

Diagenesis

Chert

Authigenic chert is an important component in some spiculite and is present in most dolostone beds. The chert comprises microquartz, quartzine, chalcedonite, and megaquartz. Microquartz is most abundant, whereas the other minerals are generally minor constituents. The microquartz, which is like that in the Flett and Prophet formations, selectively replaced allochems and matrix. Chert nodules formed of microquartz are locally present as well. Biogenic opal is interpreted as having been the major source of silica in the chert, for the same reasons given in the discussion on diagenetic chert in the Prophet Formation.

Dolomite

Most dolomite in Golata sections that overlie the Flett Formation is medium to coarsely crystalline and ferroan. The surfaces of contact between crystals are mainly compromise boundaries, and crystals are chiefly subhedral. Many crystals have a slightly undulous extinction, and some of these are possibly saddle dolomite. Individual crystals commonly have inclusion-rich cores and clear rims. According to Land (1980, p. 99), crystal zoning of this type is common and suggests that more than one episode of dolomitization occurred. This dolomite is present as a nonselective replacement of allochems, cement, and matrix. In most samples, dolomitization went almost to completion.

In sections of the Golata that overlie the Prophet Formation, dolomite occurs as a nonselective replacement. It is strongly ferroan, very finely to finely crystalline, subhedral to euhedral, and contains numerous dark inclusions.

In addition to its occurrence in dolostone, authigenic dolomite occurs in much of the spiculite, shale, mudstone, and limestone. Dolomite occurs in the last four rock types chiefly as a nonselective replacement of matrix, allochems, and calcite cement. All dolomite observed in these rocks is strongly ferroan and occurs mostly as finely crystalline, subhedral to euhedral, isolated and interfering rhombs. Some of the more finely crystalline rhombs are limpid, but most are inclusion rich.

The mineral that is called dolomite in the preceding paragraphs may be mainly ankerite, because it contains abundant Fe^{2+} . Also, X-ray diffraction analyses indicate that ankerite is the main carbonate mineral in at least some of the shale and mudstone (Appendix G).

The dolomite and ankerite in the Golata and Prophet formations probably originated in a similar way, because in both formations these minerals are similar in aspect and occur in similar settings. In the discussion about the origin of dolomite in the Prophet, it was suggested that dolomite and ankerite could have resulted from the dewatering of shale, diagenesis of clays, bacterial reduction of sulphate in organic-rich sediment, and the formation of chert.

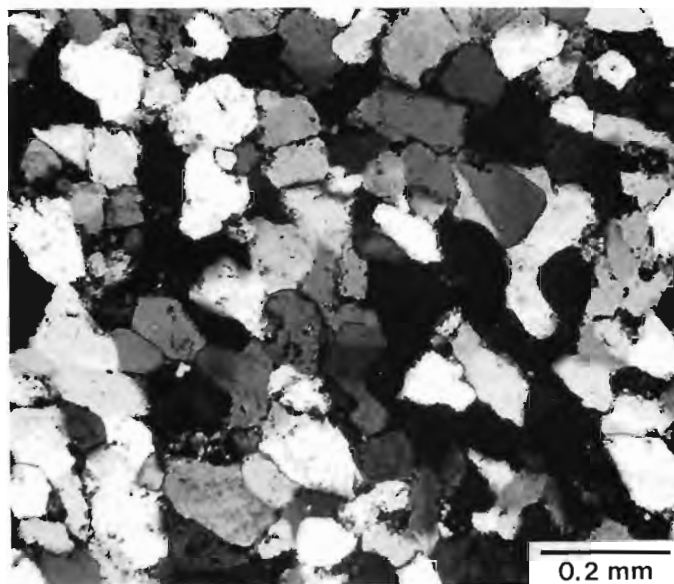


Figure 72. Photomicrograph of very fine sandstone (siliceous, submature quartzarenite; GSC loc. C-58871); from the Golata Formation at Locality 8. ISPG 2026-8.

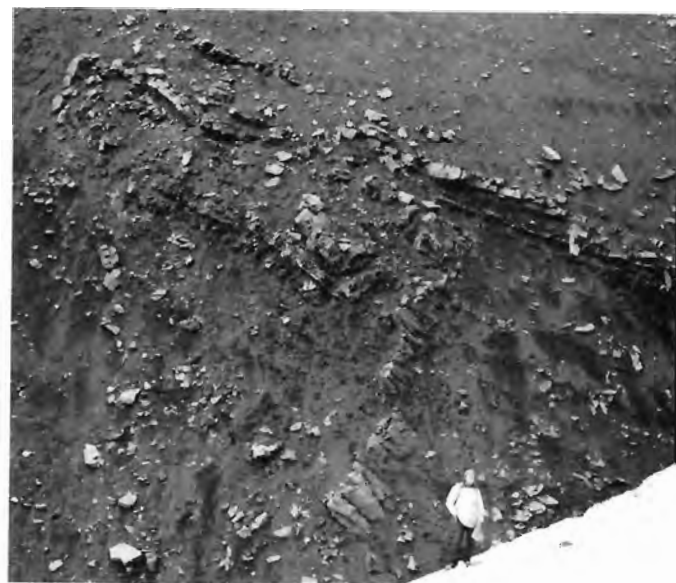


Figure 73. Slump deposit comprising the dark-shale and the sandstone lithofacies of the upper Golata Formation at Locality 8. ISPG 798-52.

Other authigenic minerals

Diagenetic calcite, together with minor pyrite, phosphates, glauconite, and plagioclase occur in Golata rocks. Diagenetic calcite is either absent from or a minor component in most samples and occurs most commonly as a replacement of sponge spicules. Both neomorphic and passively precipitated calcite are relatively rare, and most authigenic calcite present is strongly ferroan. In most samples, pyrite framboids and isolated very fine to medium crystals occur at least in trace amounts. In some dolostone

beds that occur in sections overlying the Flett Formation, phosphates are present as rounded, fine to medium sand-sized clasts, which are locally concentrated into laminae. Phosphates generally constitutes less than 0.2 per cent of the volume of these beds, but locally it exceeds 2 per cent. Both glauconite and plagioclase generally occur in trace amounts, but feldspar is locally moderately abundant.

Lithofacies

In the project area, a dark-shale lithofacies constitutes most of the Golata Formation (Figs. 35, 71, 73). In addition, a dolostone lithofacies (Fig. 71) and a sandstone lithofacies (Fig. 73) constitute significant proportions of the Golata at several localities. Intervals of spiculite lithofacies are present at some localities as well. The latter lithofacies is discussed briefly here because it is a minor facies examined only at Locality 8 (Fig. 5) and is similar to the laminated deposits in the spiculite and spicule-lime-packstone lithofacies of the Prophet Formation.

Dark-shale lithofacies

The dark-shale lithofacies comprises greyish black to olive-black shale and mudstone with minor lenses and laminae of other rock types. It is commonly intercalated with the other lithofacies of the Golata Formation (Figs. 71, 73). The association of lithofacies is transitional between the carbonate buildup facies in the underlying Flett and Prophet formations and overlying delta-slope and delta-front facies in the Mattson Formation (Figs. 4-6). Also, intervals of the dark-shale lithofacies are extensions of the prodelta and basinal shales that constitute most of the upper Besa River Formation to the west. Near the western depositional limit of the Prophet, the dark-shale lithofacies both overlies and passes eastward into the upper Prophet (Fig. 5, Loc. 8; Fig. 6, Locs. 18, 19). At most localities to the east, this facies overlies but does not intertongue with the carbonates of the Prophet and Flett.

Beds of the dark-shale lithofacies are recessive, relatively homogeneous, and generally contain few prominent sedimentary structures and macrofossils. Indistinct, millimetre-thick, subplanar laminae are the most common sedimentary structure. Ellipsoidal ironstone concretions, which generally lack macrofossils and are mainly 5 to 20 cm long, are locally common in some beds of shale and mudstone that are not closely associated with sandstone. In addition, two sandstone dykes, with the same lithology as the sandstone of the upper Golata, were observed in the dark-shale lithofacies between 265 and 295 m at Locality 8. Fenestrate bryozoans and pelmatozoan fragments, occurring in lenses and as isolated specimens, are locally abundant in beds of dark-shale lithofacies that overlie the Flett Formation. To the west, however, macrofossils are generally rare. Evidence of bioturbation was not observed in deposits of this facies but is locally present in the associated sandstone deposits of the Golata and basal Mattson Formation.

Intervals of penecontemporaneously deformed deposits consisting of dark-shale lithofacies associated with the sandstone lithofacies are moderately common in the upper Golata Formation at Locality 8 (Fig. 73). These intervals range in thickness from less than 50 cm to several metres. The deformed deposits are characterized by beds and laminae that were contorted while soft. Also, deformation probably occurred prior to the deposition of immediately overlying beds, because the latter are parallel to beds that underlie the deformed strata. The intervals containing these deformed strata are interpreted as syndepositional slump deposits because they formed prior to lithification.



Figure 74. Normally graded, turbidite-like dolostone bed of probable storm origin, in the dolostone lithofacies of the Golata Formation at Jackfish Gap (scale is 15 cm long). ISPG 1756-177.



Figure 75. Convoluted dolostone laminae in a slump deposit of the Golata dolostone lithofacies at Locality 8 (scale is 15 cm long). ISPG 798-47.

Dolostone lithofacies

The dolostone lithofacies of the Golata Formation comprises dolostone with minor dolomitic limestone and shale partings. Its distribution in the Golata coincides with that of dolostone, which is discussed in the section dealing with lithology (Figs. 4-6). At most localities, deposits of the dolostone lithofacies are intercalated with those of the dark-shale lithofacies (Fig. 71). However, at Locality 14, it is also closely associated with the sandstone lithofacies. Near the

western depositional limit of the underlying Prophet Formation, the dolostone lithofacies locally grades into the spiculite lithofacies (Fig. 5, Loc. 8).

The moderately resistant deposits of the dolostone lithofacies are mainly thin to medium bedded (3–30 cm). Some beds of this lithofacies have large-scale crossbedding; however, most beds resemble some turbidites and tempestites (Fig. 74). Beds displaying planar to convoluted laminae are locally present as well (Fig. 75).

Dolostone beds with large- to medium-scale crossbedding are locally present in the dolostone lithofacies, where it overlies the Flett lime-grainstone lithofacies. The best examples observed are at Twisted Mountain, where tabular crossbedding exists in sets that are up to 20 cm thick and enclosed by silty shale. The foresets in these beds dip westward or basinward, which indicates off-shelf transport by traction currents. Elsewhere, hummocky crossbedding is locally present. Other beds, which are associated with the crossbedded dolostone, contain numerous, dark grey, argillaceous flasers; but the flasers are generally not associated with well developed crossbedding.

The dolostone beds that resemble turbidites and tempestites have sharp bases with load casts and casts of shallow scours. Lensing and wedging of these beds is locally evident (Fig. 71), and their lateral continuity is generally not great. Most of these dolostone beds have either a massive to crudely stratified basal division or one characterized by planar stratification (Fig. 74). The upper parts of these beds grade into laminated, argillaceous dolostone and shale. Both the beds and their divisions vary from ungraded to distinctly graded.

At Locality 8, most beds of the dolostone lithofacies comprise planar laminae, but structures produced by soft-sediment deformation were observed in one bed (Fig. 75). The deposits of the spiculite lithofacies, which are associated with the dolostone facies at this locality, are of similar aspect. Laminae in these beds commonly have subtle normal grading and sharp bases. Moreover, they resemble laminae in the Prophet (Fig. 41), which are tentatively interpreted as either distal turbidites or hemipelagic deposits. In one dolostone bed at Locality 8, the laminae were contorted during syndepositional slumping (Fig. 75).

Sandstone lithofacies

The sandstone lithofacies, which comprises sandstone with subordinate siltstone and minor shale, is generally intercalated with the deposits of the dark-shale lithofacies (Figs. 4–6). At Locality 14, it is also closely associated with the dolostone lithofacies of the Golata. Above the Flett Formation, the sandstone lithofacies generally occurs only in the uppermost Golata. To the west, this facies occurs mainly in the middle to upper Golata. Most intervals of the sandstone lithofacies are actually minor tongues that extend into the Golata from the sandstone-dominated Mattson Formation (Figs. 5, 6).

Deposits of the sandstone lithofacies are mainly thin to medium bedded (3–30 cm), but very thick sandstone beds (>100 cm) are locally present. Bioturbated deposits and beds resembling turbidites and some tempestites constitute most of this facies. In the upper Golata, at Locality 8, some beds of the lithofacies occur with those of the dark-shale lithofacies in syndepositional slump deposits (Fig. 73). Also, a thick bed, which resembles a debris flow deposit, is present between 476 and 482 m at Locality 8.

The highly bioturbated beds of the sandstone lithofacies occur chiefly at the top of thin intervals of this lithofacies situated between the Flett and Mattson formations. These deposits, which are mainly muddy, bioturbated sandstone and siltstone, have gradational bases. Thicker units of this type form thin, poorly developed, coarsening-upward sequences, similar to those that constitute most of the overlying Mattson delta-front deposits.

The sandstone beds and laminae, which resemble turbidites and some tempestites, occur chiefly in intervals of the Golata sandstone lithofacies that are west of the depositional limit of the Flett Formation. Reconnaissance work and examination of subsurface logs and samples suggest that these beds and laminae are widely distributed in that region, but they were examined in outcrop only at Etanda Lakes. At Etanda Lakes, sharp-based beds resembling proximal and distal sandstone turbidites occur, but the latter appear to predominate. A component that is similar to the C Bouma division is commonly well developed at this locality and is characterized by convoluted laminae and small-scale crossbedding. Tabular to contorted mudstone intraclasts are common in the basal massive division of some beds, and most beds and laminae have subtle normal grading. Load casts and casts of shallow scours are the most common sole marks. Some of these beds at Locality 8 were deformed while soft (Fig. 73).

The thick bed that occurs at Etanda Lakes and resembles a debris bed has a chaotic internal structure. Both its upper and lower surfaces are sharp. Also, large-scale ball and pillow structure (Richards, 1983a, Plate 32c), load casts, and flame structure are present at its base.

Environmental interpretations

Deposition in a prodelta setting is suggested for intervals of the Golata dark-shale, dolostone, and sandstone lithofacies that were deposited subsequent to the Flett and Prophet formations. According to Fisher et al. (1969, p. 8), prodelta facies represent the first terrigenous sediment introduced into a depositional basin by an advancing delta. This is the depositional significance of most of the Golata dark-shale lithofacies, which occurs between carbonate buildup facies in the underlying Flett and Prophet formations, and between delta deposits in the overlying Mattson Formation (Fig. 7). The dark-shale lithofacies is mainly dark coloured, sparsely fossiliferous shale and mudstone with minor amounts of other rock types. According to Fisher et al. (1969, p. 18, 19), this is characteristic of prodelta deposits. Episodic, local proliferation of invertebrates and the subsequent resedimentation of their skeletons probably produced the beds of dolostone lithofacies that are commonly intercalated with the prodelta deposits of the dark-shale lithofacies. Most beds of the Golata sandstone lithofacies are interpreted as minor tongues of delta-slope and delta-front deposits because they generally extend into the dark-shale lithofacies from the Mattson, and resemble the delta-front to delta-slope deposits of the basal Mattson.

The deposits discussed above are interpreted as having been deposited partly on a slope and at depths ranging from slightly above to well below wave base. Much of these lithofacies were deposited on a gentle slope underlain in part by carbonate-slope deposits (Fig. 7). However, the presence of slump deposits in the upper Golata at Etanda Lakes indicates that the slope was at least locally steep enough to cause instability in the sediment deposited on it. Units of Golata lithofacies that immediately underlie crossbedded Mattson delta-front deposits, overlie the shallow water, Flett lime-grainstone facies, or contain dolostone beds with

hummocky and medium- to large-scale tabular crossbedding, were probably deposited at relatively shallow depths. Hummocky crossbedding is generally interpreted to result from strong storm-generated surges in neritic environments (Harms, 1975b, p. 88; Hamblin and Walker, 1979, p. 1681; Hunter and Clifton, 1982). Tabular crossbedding is common in shallow neritic environments, where it is produced by migrating sand waves (Spearing, 1975; Johnson, 1978).

Some dolostone beds that resemble turbidites and occur in the Golata above the Flett Formation are possibly turbidites, but most are probably better classified as storm deposits or tempestites (Fig. 74). They are similar to probable storm deposits in the Flett and Yohin formations. Also, they could be of storm origin because they resemble some storm beds that Aigner (1982) described, and they are situated near shallow water facies. Most intervals that contain these beds are underlain by relatively shallow water, crossbedded lime grainstone in the Flett, and are overlain by the crossbedded to highly bioturbated delta-front sandstone of the Mattson Formation.

Most sharp-based, graded sandstone beds in the upper Golata Formation at Etanda Lakes are interpreted as turbidites. They have the characteristics of turbidites but also resemble some tempestites. These beds are probably turbidites rather than tempestites, however, because they accumulated in a moderately deep water environment along with slump and debris flow deposits.

The prodelta and associated terrigenous deposits in the Golata record the early phase of an episode of siliciclastic sedimentation, during which a major regional regression occurred. During the deposition of these deposits in the lower Golata, water depths possibly increased slightly. This is suggested by the presence of the black, prodelta shale and mudstone of the Golata, above crossbedded, shallow water carbonates in the upper part of the underlying Flett Formation. However, the occurrence of a thick shallowing-upward succession of delta-slope to delta-plain deposits in the overlying Mattson Formation indicates that a major regression occurred subsequent to this. During the regression, fluvial deposits and coal beds formed as far west as Tika Creek (Fig. 1, Loc. 9).

Intervals of the Golata dark-shale lithofacies, that appear to have been deposited contemporaneously with the upper Prophet Formation in the western part of the project area (Fig. 5, Loc. 8; Fig. 6, Loc. 19), probably formed in a moderately deep water, basin setting. Unlike the deposits of the Golata dark-shale lithofacies discussed above, these siliciclastics are not prodelta deposits that intertongue eastward with a deltaic succession. Instead, they intertongue landward with the hemipelagites and distal turbidites of the western Prophet. The latter were deposited in moderately deep water on the lower part of a carbonate slope. These deposits of dark-shale lithofacies are locally interbedded with the Golata spiculite lithofacies, which is of moderately deep water aspect. Also, they occur as eastward-thinning tongues of the shale lithosome that constitutes most of the Besa River Formation to the west. Pelzer (1966, p. 306) suggested that basinal shale deposited at moderate depths, over 760 m at some locations, constitutes most of the Besa River. The dark-shale lithofacies comprises thinly laminated rocks that are dark coloured and pyritic, generally lack remains of autochthonous benthonic macrofauna, and exhibit little evidence of bioturbation. According to Wilson (1975, p. 354, 355), such features typify deposits of quiet-water basinal settings. Byers (1977) indicated that strata of this type are commonly deposited in the poorly oxygenated water of the dysaerobic and anaerobic zones in stratified basins.

Age

Palynomorphs and foraminifers collected from the Golata Formation and adjacent formations (Appendix A; Richards, 1983a, Appendix D), indicate that the Golata in the project area ranges in age from latest middle Viséan (V2; late foraminiferal zone 13 of Mamet and Skipp, 1970, 1971) to early late Viséan (V3).

In most of the project area, the basal Golata is probably of latest middle Viséan (V2; latest zone 13) age or possibly slightly younger. Foraminifers of this age occur in the uppermost beds of the underlying Flett at all sampled locations. However, Bamber and Mamet (1978, Fig. 9) questionably assigned an early late Viséan age (V3; early foraminiferal zone 14) to the upper 12 m of the Flett at Jackfish Gap, which includes the interval 1 reassign to the Golata. Their assignment was based chiefly on the presence of the corals *Ekvasophyllum inclinatum* and *Zophriphyllum*?. No microfossils of unequivocal early late Viséan (V3) age were collected from either the Golata or underlying Flett and Prophet during the present investigation. At Locality 8, the basal Golata is probably slightly older than it is to the east, because the lower 288 m of the Golata at that locality appears to have been deposited contemporaneously with the upper Prophet to the east (Fig. 5). The basal Golata is younger at some localities south of the project area, and underlying strata in northeastern British Columbia contain foraminifers of early late Viséan (V3; early foraminiferal zone 14) age (Bamber and Mamet, 1978, Fig. 4).

The age of the uppermost Golata Formation, which is of early late(?) Viséan (V3) age or possibly slightly older, is less precisely established than the age of its base. On the basis of corals, and as discussed in the previous paragraph, Bamber and Mamet (1978, Figs. 4, 9) questionably assigned an early late Viséan (V3; early zone 14) age to the base of the overlying Mattson Formation at Jackfish Gap. Palynomorphs assignable to the *Rotaspora* assemblage (Braman and Hills, 1977), of middle to late Viséan (V2 to V3) age, occur in all sampled intervals of the Golata and lowermost Mattson that overlie the Flett. However, at Locality 8, where the Golata overlies the Prophet Formation, palynomorphs that are assignable to the younger *Densospora* assemblage (Braman and Hills, 1977), of late Viséan (V3) age, occur in the upper Golata and lower Mattson (Richards, 1983a). At Jackfish Gap, the lowest established occurrence of the *Densospora* assemblage is 230 m above the base of the Mattson (Barss, pers. comm., 1977), thereby indicating that the uppermost Golata becomes younger westward. The upper boundary of the Golata also becomes younger toward the south (Bamber and Mamet, 1978, Fig. 4).

CONCAVE-UPWARD TRUNCATION SURFACES

Distribution and general characteristics

Large-scale, concave-upward truncation surfaces occur in the Yohin, Prophet, and Flett formations (Fig. 76). Most of these discordances are similar to erosion surfaces of submarine channels (Figs. 70, 76, 79-81). However, the Prophet locally has some truncation surfaces that have the characteristics of slump scars (Figs. 83, 84), and others that resemble channels but are associated with deposits of uncertain origin (Figs. 85, 86). Slumps occur locally in the Golata Formation, but they do not overlie well developed concave-upward discontinuities. Truncation surfaces similar to those in the project area have been reported from numerous, ancient, carbonate-slope and siliciclastic submarine-fan deposits (Davies and Nassichuk, 1975; Davies,

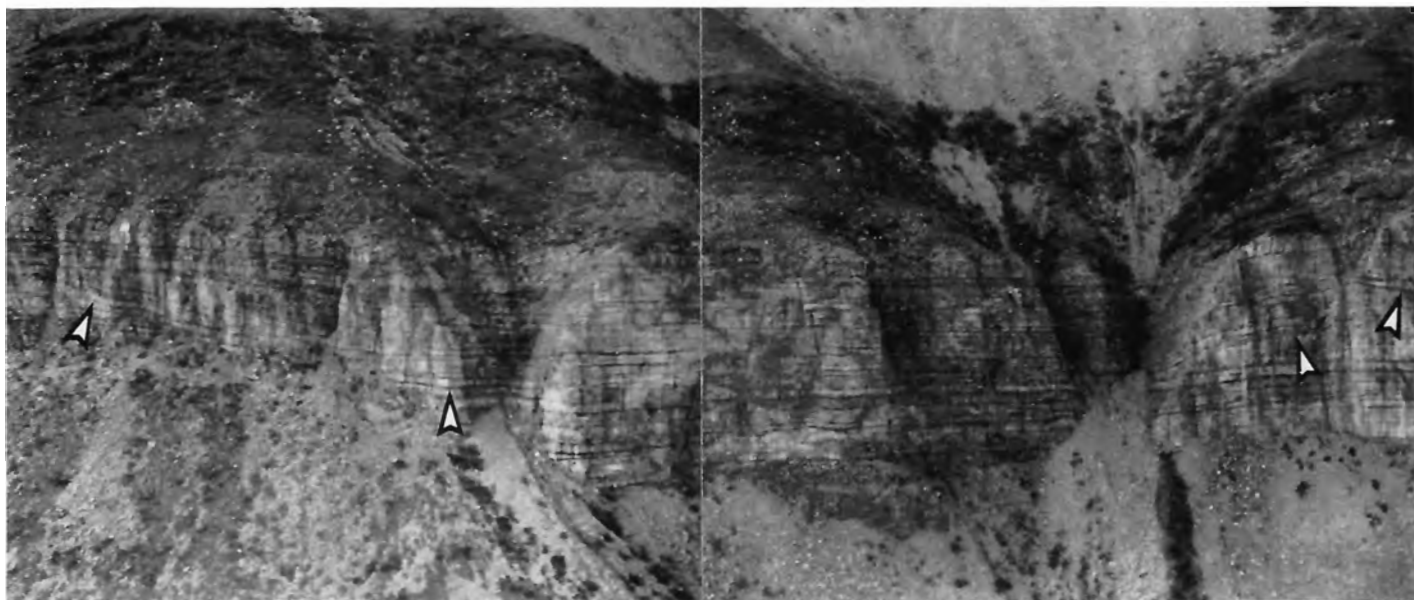


Figure 76. The Flett mixed-skeletal lime-packstone lithofacies at Sheaf Creek, showing two, large-scale, concave-upward truncation surfaces (arrows) in a 45 m thick fining-upward unit. Nesting of truncation surfaces is evident above the main discontinuity. Unit mainly consists of proximal turbidites; direction of view is toward the southwest or basinward. ISPG 710-33, 34, 35, 36.

1977; Harms, 1974; McIlreath, 1977; Walker, 1975). Furthermore, examples have been reported from suspected shelf deposits (Clari and Ghibaudo, 1979; Kennedy and Juignet, 1974). However, origins of these structures, particularly those in carbonate strata, remain somewhat controversial. They generally have been interpreted as either gravity-slide megastructures (Davies and Nassichuk, 1975; Davies, 1977; McIlreath, 1977, p. 122; Kennedy and Juignet, 1974; Clari and Ghibaudo, 1979) or erosion surfaces of submarine channels (Middleton, 1963, p. 1918; Harms, 1974; Jacka et al., 1972; Harms and Pray, 1974; Newell et al., 1953, p. 91; Richards, 1978). The objectives of this section are: to discuss the distribution of the truncation surfaces in the project area; to describe the structures and their fill sequences; and to demonstrate that most are erosion surfaces of submarine channels overlain by sediment-gravity-flow deposits. Their relationship to the evolution of carbonate slopes in the region is discussed in the following section.

Large-scale truncation surfaces are more abundant in the Flett Formation than in the Yohin and Prophet formations. Although they are mostly in the resistant mixed-skeletal lime-packstone lithofacies of the Flett (Figs. 76, 78, 79), they also occur locally in the lime-grainstone lithofacies (Fig. 70). The mixed-skeletal lime-packstone facies is interpreted as having been deposited mainly on the middle part of a slope, and the lime-grainstone facies in the upper-slope to shelf-margin environments (Fig. 87a). At most localities, these discontinuities in the Flett are most common in the basal Tlogotsho and Meilleur members, but at the northwestern corner of the Tlogotsho Plateau they are generally abundant throughout most of the Flett Formation.

In the Prophet Formation, large-scale truncation surfaces are locally common (Figs. 77a, 85). They occur mainly near or west of the western depositional limit of the Flett in resistant units of the spiculite and spicule-lime-packstone lithofacies that were deposited on the lower part of a carbonate slope (Fig. 87a). In the outcrop belt, truncation surfaces are most common in the Prophet at the

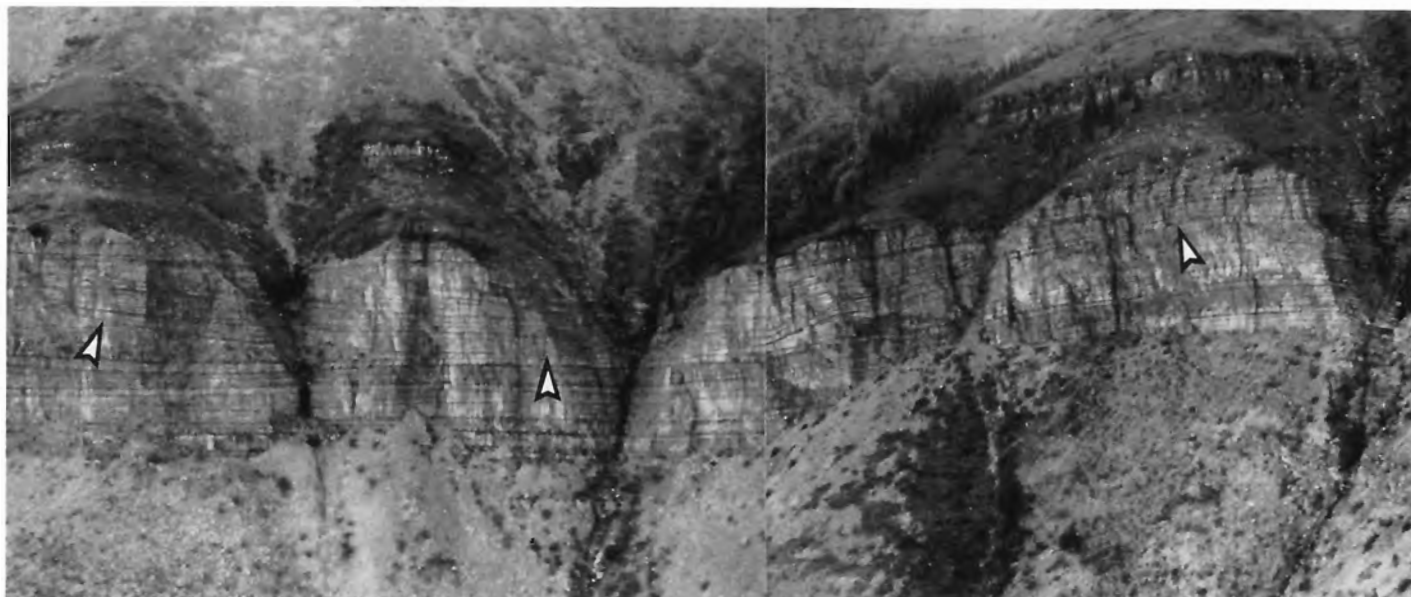
northwestern corner of the Tlogotsho Plateau (Fig. 1, Loc. 6) and at Locality 8. Well developed truncation surfaces were not observed in Prophet sections that have a high proportion of basal shale, and appear to be absent from most of the Liard Range.

Large-scale, concave-upward truncation surfaces were observed in the Yohin Formation only near Jackfish Gap (Fig. 1, Locs. 4, 30). In that area, they occur in siltstone and sandstone of the Yohin graded bed lithofacies, which is interpreted as having been deposited on a slope or submarine-fan complex in moderately deep water (Fig. 80).

The truncation surfaces in the Yohin, Prophet, and Flett occur mainly in multibed sequences that have moderate lateral continuity. Three main types of sequence, consisting mostly of sediment-gravity-flow deposits, occur:

1. Those that become more resistant and proximal in aspect upward (Fig. 77a)
2. Those that become less resistant and proximal upward (Figs. 51, 80)
3. Symmetrical sequences that are most resistant near their middle parts (Fig. 81).

As already mentioned, these sequences commonly comprise two or more subordinates. Truncation surfaces occur principally in the resistant upper half of sequences that become more resistant upward, the lower resistant half of ones that become less resistant upward, and near the middle of symmetrical sequences. In the Flett, discontinuities occur in all three types of sequence, but they are most abundant in symmetrical ones and those that become less resistant upward. This also appears to be true in the Yohin (Fig. 80). In the Prophet, truncation surfaces were observed mainly in sequences that become more resistant upward.



Most of the large-scale truncation surfaces appear to be elongate, and are exposed mainly in outcrops cut perpendicular to their long axes. They appear as two-dimensional, concave-upward traces, generally with a pronounced angular relationship to underlying beds (Fig. 79b). Associated with the concave-upward traces at some locations are subplanar erosion surfaces (Fig. 80, lowest arrow) that lack a pronounced angular relationship with underlying beds, at least over the distance of an outcrop. Some of these surfaces possibly represent sections that were cut subparallel to the long axes of broad truncation surfaces. The long axes of the truncation surfaces appear to be subperpendicular to the depositional strike of the host formations.

Submarine channels and fills

Truncation surfaces resembling erosion surfaces of submarine channels or gullies are symmetric to asymmetric, concave-upward surfaces ranging from about 2 m across and less than 50 cm deep to over 100 m across and more than 30 m deep (Fig. 76). Broader discontinuities occur at some localities, but they are incompletely exposed. Most truncation surfaces are greater than 10 m across, and the smaller structures generally occur in fill sequences or as irregularities in the major surfaces. Both sides of the U-shaped discontinuities (Figs. 76, 77a) are commonly preserved. However, in depositional sequences that contain multiple structures, generally only the youngest truncation surfaces are relatively complete. From inflection points that are about halfway up the sides of the truncation surfaces, apparent dips of opposing walls generally decrease toward the axis of the structures, and in some structures the floor in the axial region is essentially planar and subparallel to underlying beds. In an upward direction, their upper walls either terminate abruptly against younger truncation surfaces and beds, or flatten out to become subparallel with beds that are adjacent to the structure (Figs. 79, 80). The discontinuities are commonly stacked within individual depositional sequences (Figs. 77b, 80); in addition, they are commonly nested within individual fill sequences (Figs. 76, 81, 82). Where the truncation surfaces are nested in fill sequences, evidence for the lateral migration of successive surfaces is locally present (Fig. 81).

From a distance, the truncation surfaces that resemble submarine channels appear to be simple, smoothly curved surfaces, but closer examination reveals that they are more complex. Most surfaces are generally undulous (Figs. 76, 78) because of terraces, shallow scours, and, rarely, minor soft-sediment deformation. Also, the walls of the structures are not always simple, continuous surfaces produced by one sedimentary event. Instead, some are discontinuous surfaces produced by many episodes of erosion and deposition.

With the exception of truncation surfaces that resemble slump scars, medium- to large-scale soft-sediment deformation is uncommon in strata immediately below the discordances. In the Prophet and Yohin formations, syndepositional soft-sediment deformation was not observed in the footwalls of truncation surfaces resembling channels, but two examples were seen in the Flett Formation. In one of these examples, thickening and slight warping of beds is present to a depth of about one metre below the discontinuity. The origin of this deformation, which appears to be the result of compression, is uncertain, and the structure may be a slump scar. In the other Flett example, at Sheaf Creek (Fig. 1, Loc. 7), there is minor folding and overlapping of broken beds to a depth of about 2 to 5 m below the walls of a truncation surface. Because fold axes in the latter example are subparallel to the long axis of the truncation structure rather than perpendicular to it, the deformation structures possibly originated from sidewall instability and movement of wall deposits toward the axis of the floor. Tensional features such as fissured and folded zones, which commonly exist upslope of the main glide plane of slump scars (Dingle, 1977, p. 296; Lewis, 1971, p. 100), are not associated with the suspected channels.

These discontinuities resemble erosion surfaces of submarine channels more closely than they do slump scars. Their U-shaped, concave-upward surfaces are like the cross-sectional profiles of many submarine channels (see Nelson and Kulm, 1973, p. 42; Walker, 1975; Normark, 1970, 1974; Stanley and Unrug, 1972; Hook and Schlager, 1980) and differ from the steep, listric curves that characterize slump scars in longitudinal profile (see Dingle, 1977, p. 296; Davies and Nassichuk, 1975, p. 231). Moreover, these truncation

surfaces are not associated with the tensional structures that generally occur with slump scars. Some truncation surfaces are relatively smooth, but most are slightly irregular and have shallow scours and terrace-like features characteristic of submarine channels. In contrast, the principal glide planes of slumps are generally smooth curves (Dingle, 1977, p. 296). Truncation surfaces that are interpreted as relict submarine channels are commonly stacked and nested, in a manner commonly observed in such channels (Walker, 1975; Ricci-Lucchi, 1975; Carter and Lindqvist, 1975). It is improbable that most superimposed discontinuities are either subsidiary glide planes in slumps (see Dingle, 1977; p. 296, 297), or glide planes of stacked slides like those observed by McIlreath (1977, p. 122) in the Cambrian Boundary limestone of British Columbia. This conclusion is supported by the absence of large-scale tensional and compressional deformation from overlying fill sequences, and by the fact that sediment-gravity-flows produced most fills. Finally, the size of the truncation surfaces is compatible with the interpretation that they resemble channels, because modern, deep-sea channels are commonly more than 10 km wide (Nelson and Kulm, 1973; Normark, 1974; Hook and Schlager, 1980).

Constructional, levee-like, depositional features flank several concave-upward truncation surfaces in the Flett and Yohin formations (Figs. 76, 79a, 80), but well developed examples were not observed in the Prophet Formation. The levee-like features are broad, convex-upward sediment packages consisting mainly of turbidites, and some of the beds in them can usually be traced laterally into adjacent, related fill sequences. Beds within these levee-like packages are thinner than those above the associated discordances. Although these constructional features occur on both sides of some truncation surfaces, they are generally best developed and most common on the right side (looking basinward). In comparison, the left walls generally appear to be erosion surfaces across which beds cannot be traced (Fig. 79). The distribution of the levee-like features is possibly a consequence of the Coriolis effect. Nelson and Kulm (1973, p. 44) stated that submarine fan-valley systems more frequently shift to the left, and levees are best developed on their right side (looking downstream) in the northern hemisphere.

Two types of fill sequence overlie the truncation surfaces that resemble submarine-channel erosion surfaces:

1. Sequences that record two or more main episodes of deposition and erosion (Figs. 76, 81, 82)
2. Those that record one principal episode of deposition (Figs. 70, 77a, 80).

Of these, the first is more common. Although fill sequences recording more than one episode occur locally in the Yohin and Prophet formations, they are much more common in the Flett Formation. In comparison, fills that record only one episode are common in all three formations. Both types of fill sequence are multibedded and consist mainly of beds resembling turbidites. These fills are generally either coarser grained and more proximal in aspect or the same as the footwall deposits of the discordance, but some fills are of more distal aspect than the underlying deposits. Finally, these fills either grade upward into overlying nonchannelled deposits (Fig. 80) or are abruptly overlain by younger strata.

Thin drapes consisting of medium to dark grey, laminated, argillaceous and spiculitic sediment overlie some truncation surfaces. The presence of these drapes indicates that a significant time interval elapsed between the erosion and filling of some truncation structures. Moreover, if en masse transport of the overlying fill sequence had produced the truncation surfaces, drapes would not occur.

The following three bedding styles occur in the fill sequences:

1. Beds that conform to the truncation surfaces
2. Inclined beds resembling foresets
3. Planar beds that are subparallel to beds below the discontinuities.

According to Reineck and Singh (1975, p. 63) and McKee (1957), the same three types of bedding are characteristic of channel fills. In fill sequences with the first two styles of bedding, a flattening upward of bed surfaces occurs, particularly in the upper half of the fills. Reineck and Singh (1975, p. 63) stated that this flattening trend occurs in most channel fills.

Numerous examples of fill sequences comprising beds that conform to the shape of truncation surfaces occur in the Yohin, Flett, and Prophet formations (Figs. 76, 77b, 80). This type of bedding usually forms in completely submerged channels (Reineck and Singh, 1975, p. 63). Such beds in the Yohin are proximal to distal sandstone and siltstone turbidites. Those in the Flett are chiefly proximal, limestone turbidites. In the Prophet, these fills consist mainly of spicule-rich beds and laminae that are probably distal turbidites, but some contain proximal turbidites, and others are mostly laminae of possible hemipelagic origin. In fills that consist mainly of proximal limestone and spiculite turbidites, beds tend to be thickest above the axial region of the truncation surface. Where they onlap the walls of the truncation surfaces, these proximal beds commonly thin gradually to zero. Consequently, the walls are progressively onlapped by younger beds toward their tops. Harms (1974), Jacka et al. (1972), Mutti (1977), and others have illustrated examples of this style of bedding in submarine channel fills.

Three examples of fills with inclined foreset-like beds were observed in the Flett Formation (Fig. 81), but this bedding style was not observed in the Yohin. In the Prophet Formation, this style of bedding was observed above one truncation surface that is of uncertain origin. In the Flett, these fills consist chiefly of proximal, limestone turbidites, and the foreset-like beds occur as concave-upward to slightly convex-upward packages of strata that are commonly separated by minor discontinuities. The beds appear to have aggraded from right to left (looking basinward). Reineck and Singh (1975, p. 63) suggested that diagonally passing currents produce this style of bedding in channels.

The only observed fill sequence with a significant proportion of beds that are subparallel to underlying beds occurs in the Yohin Formation near Jackfish Gap (Fig. 82). At this locality, sandstone beds in the lower half of the fill are subhorizontal and parallel to strata beneath the related truncation surface. Harms (1974) observed similar bedding in some sandstone submarine channel fills in the Permian Brushy Canyon Formation of western Texas. Beds in the upper half of the Yohin fill sequence conform to the outline of the depression.

Fills, above discontinuities that are similar to erosion scars of channels, commonly become slightly less resistant and proximal upward (Fig. 80). Toward the top of a fill sequence, the sediment becomes finer grained, and the turbidites become somewhat less proximal in aspect. Also, resistant beds commonly become thinner, and proportions of recessive argillaceous and spiculitic rocks increase. Similarly, in sequences that contain stacked truncation surfaces and fills, the lowest fills are generally the most resistant and proximal in aspect. However, these trends are generally subtle, because thick bedded, conglomeratic, basal

lag deposits are absent, and in some fills either distinct vertical trends are absent or a coarsening- and thickening-upward trend occurs. Fining- and thinning-upward trends are common in siliciclastic turbidite, submarine channel fills (Mutti and Ghibaudo, 1972; Ricci-Lucchi, 1975; Mutti, 1977; Walker and Mutti, 1973).

Evidence of medium-scale, soft-sediment deformation is locally present in some fills. This includes minor folds, and structures produced by sedimentary boudinage (Fig. 77b).

Several features, discussed above, indicate that multiple sediment-gravity-flows, rather than the emplacement of large-scale slumps, produced the fill sequences above truncation surfaces that resemble submarine channels. Constructional levee-like deposits, which are related to the fill deposits, flank some truncation surfaces. Most beds in the fills are probable sediment-gravity-flow deposits rather than slump deposits. The fill deposits have bedding that is characteristic of channel fills; moreover, fining- and thinning-upward sequences, characteristic of channel fills, overlie many discordances. Finally, a significant interval of time elapsed between the erosion and the filling of some truncation structures. This suggests that the processes that formed the discontinuities may have differed from those that deposited the fills.

Processes other than slumping and debris flow probably produced most of the structures resembling submarine-channel erosion surfaces. Several criteria that were discussed above support this. Many discontinuities, particularly those with both walls preserved, lack the geometry of typical slump glide planes. The soft-sediment deformation and tensional structures that commonly occur in the footwalls of slump scars, and in strata situated up slope are generally absent. No large-scale slumps, thick debris flow deposits, or olistostromes overlie these intraformational truncation surfaces. Finally, large-scale slumps, olistostromes, and thick debris flow deposits consisting of Flett and Yohin rocks were not observed in the project area, and slumps comprising Prophet strata are common at only two localities. Above modern slump glide planes or scars, slumps are almost always present; moreover, related slump and thick debris flow deposits are generally present downslope (Prior et al., 1979; Prior and Coleman, 1980; Dingle, 1977, 1980; Field and Clarke, 1979; Lewis, 1971).

The truncation surfaces, which are similar to the erosion surfaces of submarine channels, are chiefly the result of episodic erosion, and powerful turbidity currents appear to have been the principal erosive agent. Although a combination of deposition and erosion probably formed most of the truncation surfaces, a single major episode of erosion possibly produced some. In addition, either one main period of filling, or at least two episodes of aggradation separated by one of erosion, produced the fill sequences above the principal truncation surfaces. Turbidity currents possibly eroded the truncation surfaces because a major proportion of the beds in the fill sequences are probably proximal turbidites. Moreover, turbidity currents are the main channel-forming agent in modern, deep water, terrigenous environments (Nelson and Kulm, 1973), and, according to Hook and Schlager (1980), they probably produced the gullies on the modern, submarine carbonate slopes of the Bahamas. The apparent episodic nature of the erosional events suggests that the channels in the project area were produced by different processes than the fills. However, I am unaware of documented processes other than sediment-gravity-flows that could produce these discontinuities. Other bottom currents, commonly tidally induced, occur in modern submarine

canyons and fan valleys, but most appear to be relatively weak currents (Shepard and Marshall, 1978; Keller and Shepard, 1978; Nelson and Kulm, 1973; p. 61, 62).

Slump scars

Large-scale truncation surfaces that resemble scars produced by slumping, are relatively uncommon and were observed only in the Prophet Formation. Two variations of these truncation surfaces were observed: listric glide planes (Fig. 83); and undulose, concave-upward discontinuities that resemble cross-sections of channel erosion surfaces (Fig. 84). Most of these surfaces, particularly the slump glide planes, are relatively small-scale features about 3 to 10 m across, but an incompletely exposed large-scale slump occurs near the Etanda Lakes section (Fig. 1, Loc. 8). Evidence of syndepositional, soft-sediment deformation occurs in both the footwall and hanging wall of the discontinuities, but it is most pronounced in the hanging wall. Shale, dolostone, and spiculite constitute the footwall deposits; the hanging wall deposits are mainly dolostone and spiculite.

These discontinuities in the Prophet Formation are interpreted as slump scars because they are associated with abundant soft-sediment deformation. Also, the listric discontinuities appear to be longitudinal profiles of minor slump glide planes similar to those described by Dingle (1977) and Lewis (1971). The concave-upward, channel-like discontinuities are either sections cut perpendicular to the longitudinal profile of slump glide planes, or scars produced by sliding of slump-derived material.

Truncation surfaces of undetermined origin

Two large-scale truncation surfaces (Figs. 35, 85) of undetermined origin occur in the Prophet Formation at Ram Creek (Fig. 1, Loc. 6). Similar structures are preserved between that locality and Sheaf Creek (Fig. 1, Loc. 7) to the west, but they are less well exposed and were not examined in detail. Separating the two discontinuities at Ram Creek is a large-scale mound-like structure (Fig. 86) that resembles submarine foreslope hills on the Fraser delta (Tiffen et al., 1971), and deep-sea sediment waves described by Damuth (1975, p. 28). Similar convex-upward features separate the other discontinuities to the west. Tiffen et al. (1971) attributed the foreslope hills and intervening troughs to downslope sliding of soft sediment. Deep-sea sediment waves are generally interpreted as depositional structures produced by contour or turbidity currents (Stow and Lovell, 1979, p. 260). Multiple, spicule-rich, graded laminae (Fig. 44), which are possibly distal turbidites, constitute individual beds in the mound-like structures. These beds are subparallel to the truncation surfaces, but some younger beds on the flanks of the convex-upward features are truncated. Only the truncation surface and fill sequence on the west side of the Ram Creek mound-like structure is well exposed (Fig. 85). This discordance is a large-scale, channel-like structure that is more than 300 m across and terraced on its west side. The overlying fill sequence consists of possible distal turbidites, lacks slump deposits, and records one cycle of deposition. The western fill sequence at Ram Creek is unusual, because beds within it prograded well beyond the west side of the truncation structure. Also, the structure in this fill resembles slope-foreset bedding more closely than bedding produced by turbidity currents confined to a channel. The truncation surfaces at Ram Creek are partly the product of erosion that occurred after the intervening mound-like structure developed, but their origin is possibly linked in part with that of the convex-upward feature.



a. Concave-upward discontinuities (arrows) in Prophet sequences that become more resistant upward (Loc. 6). Fill above lower surface records one main episode of deposition. Upper cliff is 20 m high. ISPG 798-87.

Figure 77. Large-scale truncation surfaces and sequences.

ORIGIN OF MULTIBED CARBONATE-BEARING SEQUENCES

Asymmetric progradational sequences

Numerous multibed sequences that become more resistant and proximal in aspect upward (Figs. 49, 70, 77a) occur in the Flett, Prophet and Besa River formations. Many of these are progradational to aggradational units that appear to have resulted chiefly from deposition basinward of submarine channels. Three lines of evidence support this interpretation. This type of sequence is common in submarine siliciclastic fans. In the fans, they generally resulted from progradation and aggradation of fan-like lobes basinward of channels (Mutti and Ricci-Lucchi, 1972; Mutti, 1974, 1977; Ricci-Lucchi, 1975). Secondly, the discovery in the Bahamas of modern, gullied carbonate slopes with related progradational fans at their bases (Hook and Schlager, 1980; Schlager and Chermak, 1979, p. 204, 205; Mullins and Neuman, 1979, p. 183) indicates that processes like those on siliciclastic fans operate on some carbonate slopes. The third and principal evidence for my interpretation is the common occurrence of probable submarine channel surfaces in much of the Flett and Prophet slope lithofacies (Figs. 76, 77, 79). These discontinuities in the Flett and Prophet are present in

the upper part of some multibed sequences that become more resistant upward. Also, discontinuities are common in the more proximal slope deposits that occur in the other types of sequences. Truncation surfaces in the upper parts of some progradational to aggradational Flett and Prophet sequences (Fig. 77a) probably resulted from channel progradation subsequent to deposition of related nonchannelled strata.

The asymmetric Flett, Prophet, and Besa River sequences discussed above are interpreted as deposits of progradational fans or fan-like lobes. Their similarity to fan deposits on some modern carbonate slopes and to lobe deposits of siliciclastic fans supports this interpretation. The proximal deposits of these progradational to aggradational sequences occur chiefly in the middle slope deposits of the Flett, whereas distal equivalents are mainly in the Prophet lower slope deposits and basinal Besa River strata (Fig. 87).

Many of the multibed sequences that become more resistant upward and occur in the Flett, Prophet and Besa River formations were probably produced by the progradation and aggradation of carbonate slope-deposits that were not deposited basinward of channels. This is suggested by the fact that channel-like truncation surfaces are not common in the proximal carbonate lithofacies of the Flett and Prophet



b. Stacked discontinuities (large arrows) in fining- and thinning-upward Flett sequence (Loc. 7). Some basal beds are mainly lime grainstone; remainder of sequence is spiculite and lime packstone grading upward into shale. Soft-sediment deformation occurs above discontinuity in centre. Small arrows indicate base and top of sequence. Central cliff is 43 m high. ISPG 798-95.

at all locations. Moreover, most documented ancient carbonate slope-successions apparently lack evidence of abundant channels. They developed chiefly from deposition by sediment-gravity-flows that were not confined to channels (see Schlager and Chermak, 1979, p. 204).

Asymmetric abandonment sequences

An initial period of rapid sedimentation and progradation, followed by one in which carbonate sedimentation rates declined, produced many extensive Flett and Prophet multibed sequences that become less proximal and less resistant upward (Fig. 51). These sequences, which consist mainly of carbonate slope-lithofacies, are common in the Flett Formation and occur locally in the Prophet Formation. Truncation surfaces, interpreted as channel erosion surfaces (Figs. 51, 76, 77b), are common in the basal parts of many deposits of this type. The presence of these discontinuities indicates that deposition of their host deposits was related to the progradation of slope channel systems. Because basal channelled strata in these sequences commonly abruptly overlie deposits of distal aspect, channel migration was probably rapid. Thick sequences that become less resistant upward and contain truncation surfaces, generally

correlate basinward with progradational sequences that are interpreted as developing basinward of channels. This spatial relationship provides additional support for the interpretation that rapid progradation of channelled slope deposits produced the discontinuity-bearing part of many sequences. Some sequences that contain abundant channel erosion surfaces become slightly less resistant and proximal in aspect upward, because of vertical trends in probable channel fills. Because gradual channel abandonment produces similar trends in channel fills on siliciclastic submarine fans (Fig. 80; Ricci-Lucchi, 1975; Mutti, 1977), it could have caused these trends in Flett and Prophet channel fills. Thick, composite sequences become less resistant and more distal upward as a consequence of vertical trends in probable channel fills near their bases. Also, these upward trends occur because less resistant and more distal subsequences, which resemble those deposited basinward of channels, occur above the basal, channelled strata.

Some asymmetric sequences that consist of carbonate buildup deposits and become less resistant and more distal in aspect upward, appear to lack large-scale truncation surfaces. The origins of these sequences, which are locally present in the Flett, Prophet, Clausen and Pekisko formations, are uncertain. Comparison with sequences

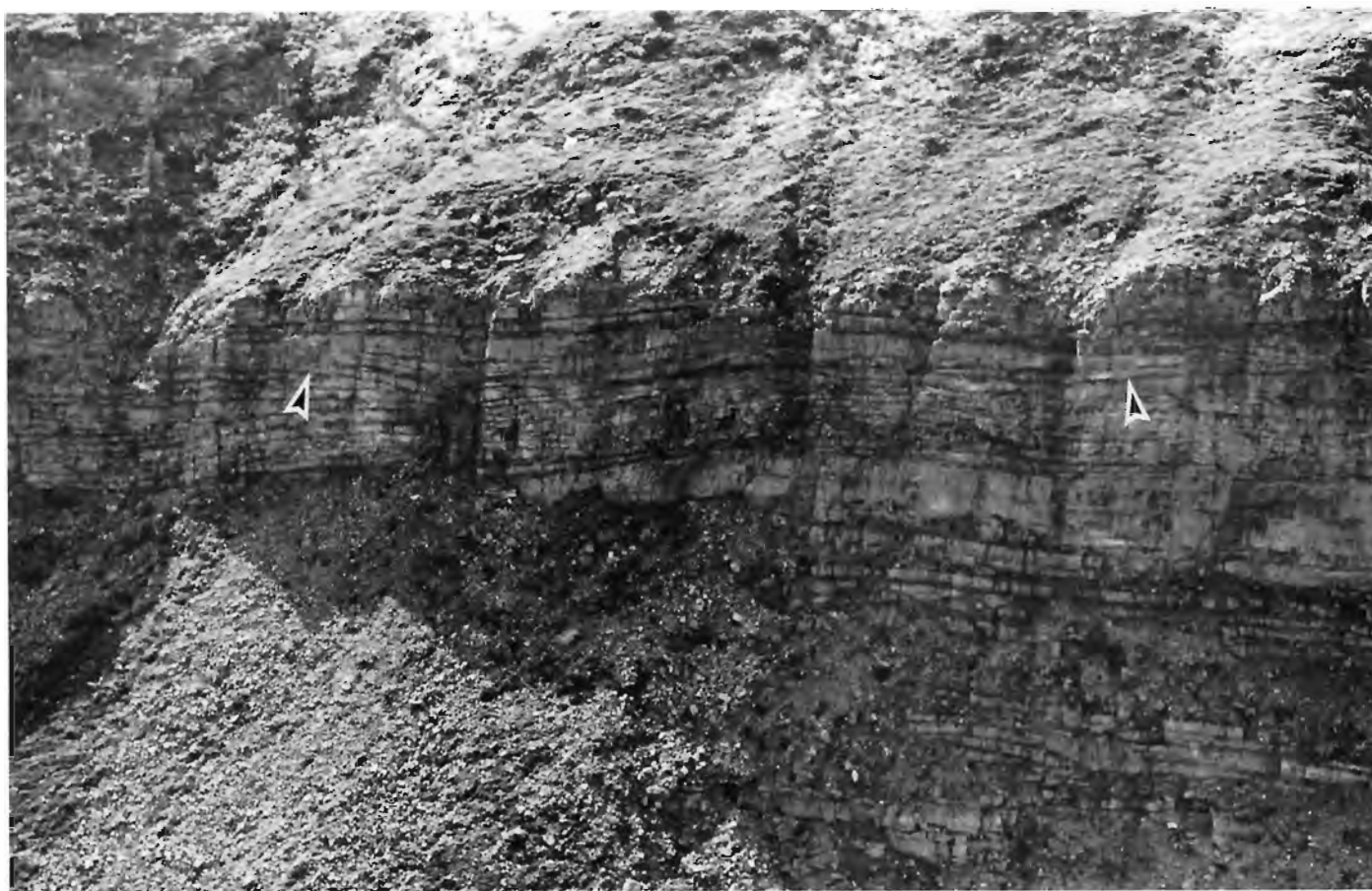


Figure 78. A large-scale, undulous, concave-upward truncation surface (arrows) in Flett mixed-skeletal lime-packstone lithofacies near Sheaf Creek. Cliff is 10 m (left) to 30 m (right) high. ISPG 798-102.

discussed above suggests that an initial episode of rapid aggradation and progradation of platform strata produced the resistant bases. The less resistant upper parts apparently were produced during a subsequent period, in which rates of carbonate deposition steadily declined. However, some of these asymmetric sequences are possibly submarine channel fills exposed in outcrops cut subparallel to their depositional strikes.

Symmetric sequences

An episode of gradual progradation and aggradation, together with a subsequent period of declining carbonate deposition rates are considered to have produced symmetrical multibed sequences that contain carbonate buildup and related facies. These sequences occur mainly in the Flett Formation (Fig. 81). However, the best developed example is a thick composite sequence that consists of the Prophet Formation, the Tlogotsho and basal Meilleur Member of the Flett, and, commonly, either the upper Besa River or Clausen Formation. This composite is well developed on the interior platform and in much of the eastern and central Liard Range (Figs. 5, 6). A similar sequence, which does not include the Meilleur, is also well developed at the northern end of the Mattson anticline (Fig. 4). The basal, nonchannelled parts of the symmetrical sequences resemble asymmetric Flett and Prophet sequences that become more resistant upward. Therefore, the basal part of the symmetrical sequences probably resulted from progradation and aggradation of

strata deposited on either nonchannelled slopes or on parts of fans situated basinward of gullied slopes. Intervals that contain probable channel fills resemble basal portions of asymmetric Flett sequences that become less resistant upward. Consequently, the progradation of proximal channelled slope deposits over nonchannelled, more distal slope facies, probably formed the middle part of the symmetrical sequences. The upper part of the symmetrical sequences has the same characteristics, and evidence of deposition under conditions of waning sedimentation rates, as the tops of asymmetric Flett sequences that become less resistant upward.

CARBONATE BUILDUPS

Style of buildup

In the project area, the carbonate buildups of Carboniferous age are tentatively interpreted as mainly poorly developed platforms; however, some carbonate ramp deposits are probably present in the buildups (Fig. 87). According to Wilson (1975, p. 21), carbonate platforms are large buildups that have a more or less horizontal top and relatively abrupt shelf margins, where sediment deposited in high-energy environments occurs. On platforms, the shelf margin is separated from the main shoreline by a broad, relatively low-energy, protected-shelf environment, where carbonates are deposited in the neritic and intertidal zones

(Fig. 87a). In contrast, carbonate ramps are, according to Wilson (1975, p. 21), large buildups that prograde away from positive areas and down gentle regional slopes. Also, ramps lack an obvious break in slope, and facies on them occur as wide, irregular belts with the highest energy deposits close to the shore (Fig. 87b).

The interpretation that the carbonates in the project area are mainly platform deposits is based mainly on the following evidence. Most of the high-energy, shallow water, lime grainstones in the Pekisko and Flett formations appear to have been deposited in shelf-margin environments. In addition, some of the mixed-skeletal lime-packstone lithofacies in the Flett may have been deposited on the protected shelf. The latter is suggested mainly by the spatial relationship between some occurrences of the lime-grainstone lithofacies and the mixed-skeletal lime-packstone lithofacies in the Flett. In the Flett Formation, a well developed slope facies dominated by relatively coarse grained allochthonous deposits can be differentiated from a shallow water belt of shelf-margin lime grainstone. On carbonate ramps, a shelf slope break is generally not evident. Also, slope deposits on ramps tend to be fine grained and consist mainly of pelagic to hemipelagic carbonates and shales (James and Mountjoy, 1983, p. 201). Carbonates that are the same age as those in the project area occur in the Rundle Group south of the Peace River Embayment, and are mainly platform deposits (Bamber et al., 1980; Speranza, 1984; Richards et al., in press). The Rundle Group between the Peace River Embayment and the project area may comprise mainly carbonate-platform deposits as well. Unfortunately, little is known about the style of buildup present in that region. Finally, ramps generally evolve rapidly into platforms (Wilson, 1975, p. 21), so that ramp deposits are less abundant than those of platforms. All of the platforms in the study area are, however, considered to be poorly developed because they are relatively thin, commonly grade into ramps, and generally include abundant siliciclastics.

In the project area, carbonates that were deposited either during or immediately after major transgressions are probably ramp deposits. According to James and Mountjoy (1983, p. 194, 195), after a major transgression, the shelf of a carbonate platform is covered by relatively deep water and is below the zone in which carbonate sediments form rapidly. In such cases, the shelf slope break is only an inherited morphological feature that generally lacks a specific facies. Moreover, the style of shelf present is similar to that of a carbonate ramp. Ramp deposits that resulted from major transgressions are probably present in the basal Pekisko Formation, the basal Meilleur Member, and in the lower and uppermost Prophet Formation on the interior platform.

Also, ramp deposits probably occur at some localities where abundant terrigenous clastics are present in the carbonate buildups. The influx of these clastics would have prevented development of the shelf-margin environment that is characteristic of the platforms. Probable ramp deposits resulting from this influx occur in the middle to upper Tlogotsho Member of the Flett at Locality 4 and northeast of it.

Shelf-margin characteristics

On carbonate platforms, slope sedimentation is a function of the abruptness of the platform-to-basin transition and the characteristics of the shelf margin (McIlreath and James 1978, p. 195). According to McIlreath and James, the two basic types of platform-shelf margin are bypass and depositional margins. Either a belt of shallow water carbonate sand or a shallow water reef is present on both

types of shelf margin. Bypass margins are at the tops of submarine escarpments where carbonate sediment is transported directly from the shelf to deep water, thereby bypassing much of the slope. In comparison, platforms that have depositional margins generally have slopes with low gradients where carbonate sediment is deposited at various depths.

In the project area, the carbonate platforms of Carboniferous age had depositional shelf margins with shallow water sand belts (Fig. 87a). The platform facies of the area appear to lack evidence of submarine escarpments and thick, very coarse grained, rudaceous deposits. According to McIlreath and James (1978, p. 191, 192), coarse grained rudites generally occur in slope deposits related to bypass margins. Also, reefs and reef related deposits were not observed in the project area. In contrast, the slope lithofacies form broad belts, which consist chiefly of granule- to silt-sized sediment. This indicates that the paleoslopes had low gradients and were underlain by sediment wedges, which consisted mainly of lime sand and lime silt (Fig. 87a). Moreover, Flett and Prophet slope lithofacies grade eastward into shallow water strata that were probably deposited in shelf-margin sand belts. Platforms that had depositional margins with shelf-margin sand belts have been reported in the Carboniferous Lisburne Group of Alaska (Wood and Armstrong, 1975, p. 10, 11), and in the Carboniferous of the western United States (Sandberg and Gutschick, 1980; Gutschick et al., 1980).

Effects of terrigenous input

In the project area, terrigenous influx had a major effect on the development of carbonate platforms and their constituent multibed sequences. According to Wilson (1975, p. 42, 43), terrigenous influx onto a carbonate platform commonly terminates or slows carbonate production and rates of platform progradation and aggradation. Evidence for this in the project area is provided by the progressive upward increase in the proportions of siliciclastics in the upper part of some second-order symmetrical sequences, and in asymmetric sequences that become less resistant upward. In addition, siliciclastics abruptly overlie some asymmetric, progradational to aggradational, second-order sequences such as the Meilleur Member of the Flett Formation (Figs. 4-6, 71). This indicates that major, relatively sudden influxes of terrigenous clastics periodically terminated the development of platforms or their components.

PROVENANCE OF SILICICLASTICS

Golata, upper Besa River, and Mattson formations

Most sandstone and siltstone in the Golata and upper Besa River formations are interpreted as having the same northern provenance as the clastics constituting deltaic and related lithofacies in the lower two thirds of the Mattson Formation. The following interpretations are derived largely from the study of the Mattson.

In all three intervals, the clast composition of the sandstone and the characteristics of the quartz clasts indicate that sandstone and sand-bearing rocks provided most of the clasts. The sandstone is mainly quartzarenite, so that a high proportion of the sand in the Golata, upper Besa River, and lower two thirds of the Mattson is stable quartz (Appendix F; Richards et al., in press). In contrast, heavy minerals and feldspar are minor components, mafic silicate minerals other than biotite were not observed, and igneous or



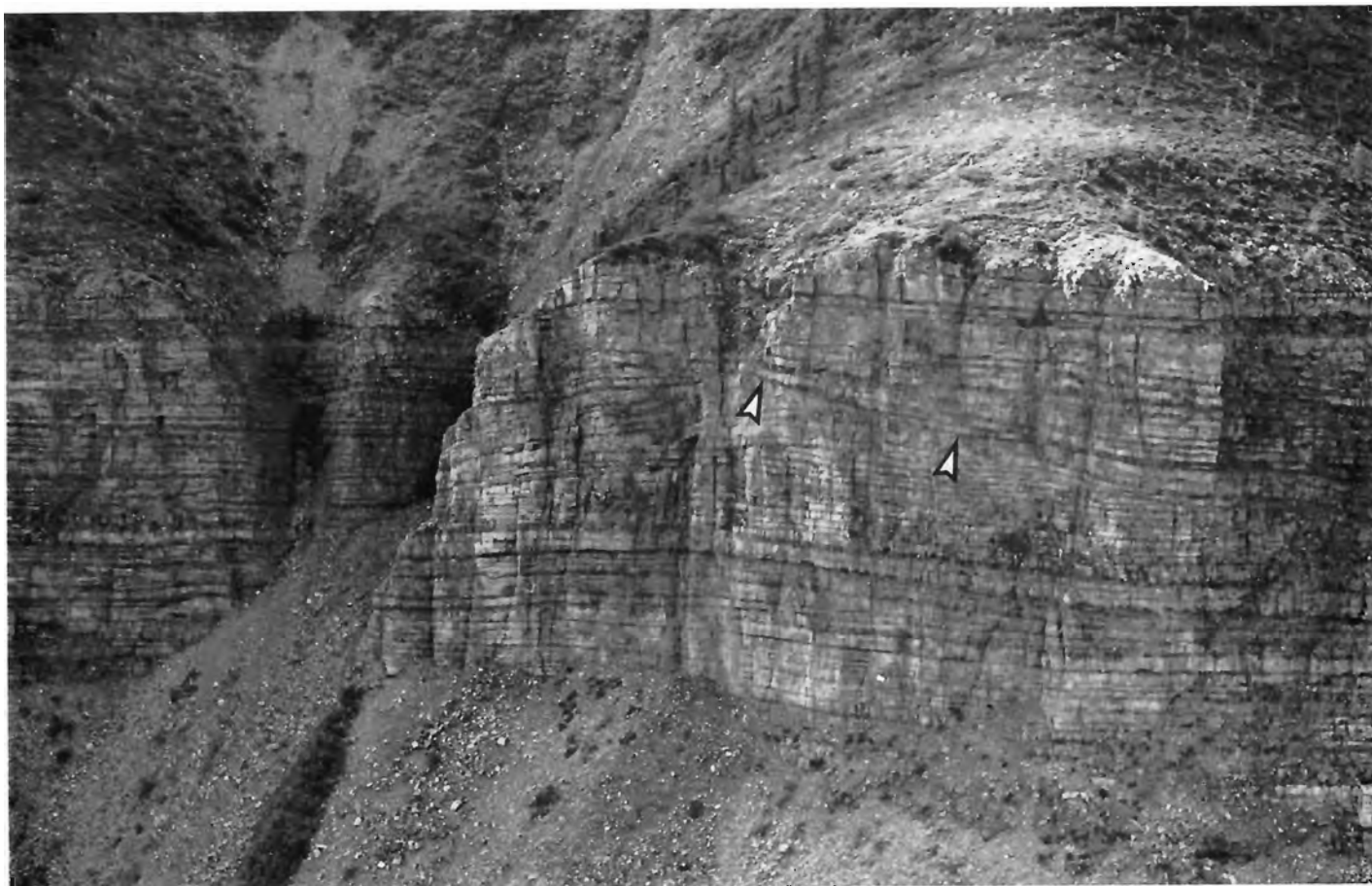
a. Levee-like deposits on the right-hand, or northwest, side of the discontinuity. ISPG 798-96.

Figure 79. Margins of the concave-upward discontinuity shown on the right-hand side of Figure 76 (45 m high cliff of Flett mixed-skeletal lime-packstone lithofacies). Direction of view is southwestward or basinward.

metamorphic rocks fragments are rare. If a major proportion of the grains were first-cycle clasts from igneous and metamorphic rocks, heavy minerals and unstable components would probably be more abundant. Furthermore, the scarcity of chert rock fragments suggests that chert-bearing carbonate rocks and bedded chert were minor sources. Intensive, prolonged weathering of igneous and metamorphic rocks in areas with relatively low relief can produce sand that is mainly quartz, but the compositional maturity of sand in these three intervals probably did not result from this. In contrast, erosion in the source area must have been relatively rapid because the Mattson is thick (Table 1) and was deposited quite rapidly. The fine sand-sized and coarser quartz clasts are mainly subangular to subrounded, and rounded clasts are moderately common in the Mattson. Because quartz sand does not round rapidly (Pettijohn et al., 1972, p. 83), most clasts probably went through more than one sedimentary cycle. According to Basu et al. (1975), the ratio of sand-sized quartz clasts that have undulatory extinction (extinction angle $>5^\circ$) to those with non-undulatory extinction (extinction angle $<5^\circ$) is potentially useful in provenance interpretation. This ratio in quartzarenite from the project area (Appendix F) suggests that metamorphic and igneous rocks each provided significant proportions of the quartz sand. However, for reasons given above, most clasts are probably not first cycle. Moreover, the ratio of polycrystalline quartz, derived largely from igneous and low-

grade metamorphic rock, to monocrystalline quartz grains is very low. This also suggests that most of the quartz has been through more than one sedimentary cycle. Because polycrystalline quartz breaks down to monocrystalline quartz, the ratio of polycrystalline to monocrystalline quartz decreases with the effective residence time of a population of clasts in the sedimentary mill (Basu et al., 1975, p. 882).

Sedimentary rocks in a distant fold belt, rather than in a local source area or the Canadian Shield, probably provided most of the terrigenous clasts in the Golata Formation, upper Besa River Formation, and Mattson Formation. The Mattson deltas are mainly of the high constructional type. According to Fisher et al. (1969, p. 30), large fluvial systems that extend inland about 1600 to 3200 km generally supply the sediment for such systems. Because the Mattson is thick (up to 1400 m) and widely distributed in northeastern British Columbia and in the project area, a major, elevated source area was required. Moreover, rivers that deposit large volumes of sediment at or near their mouths commonly have headwaters in elevated fold belts (Miall, 1977b, p. 3). The region near the project area lacks evidence of extensive sand-rich deposits of early to middle Paleozoic age, that could have been subaerially exposed during the Early Carboniferous. Finally, sand-bearing rocks of Proterozoic age are common in the Canadian Shield east and northeast of the project area, but that vast, tectonically stable region



b. Pronounced angular relationship between the truncation surface (arrows) and underlying beds on the left-hand, or southeast, side of the structure. ISPG 798-99.

provides no evidence of elevated fold belts or other major uplifts during the Carboniferous.

A northern, dominantly sedimentary provenance is suggested for most terrigenous sand and silt in the Golata, upper Besa River, and Mattson. Sedimentary strata in the Arctic Archipelago and northwestern District of Mackenzie probably supplied much of the silt and sand in these units. During the Late Devonian to Early Carboniferous Ellesmerian Orogeny (Thorsteinsson and Tozer, 1970, p. 551), a thick, widespread succession of Middle to Upper Devonian sandstone, in the Franklinian geosyncline and adjacent areas to the south, was uplifted and deformed (Embry and Klovan, 1976, p. 612; Trettin, 1973, p. 68, 69; Bell, 1973). During this orogeny, older sedimentary strata and subordinate igneous and metamorphic rocks in that region were also involved. The Sverdrup Basin started to develop across part of the orogenic belt in Viséan time. However, most of the extensive area affected by the Ellesmerian Orogeny remained subaerially exposed throughout the Viséan and Serpukhovian (Nassichuk, 1975, p. 23; Thorsteinsson, 1974, p. 17-23; Thorsteinsson and Tozer, 1970, p. 566-571; Trettin, 1973, p. 658-669), providing a potential source of terrigenous clastics. Moreover, during the formation of Sverdrup Basin, the terrane immediately to the south was probably uplifted and could have been a major source of siliciclastics (Embry, pers. comm., 1984).

Preliminary paleocurrent data from the Mattson (Fig. 88), and spatial relationships between delta plain and marine lithofacies in that formation, suggest that terrigenous clastics in the Mattson and Golata came from the north or northeast. Moreover, the basal Golata becomes younger toward the south and southeast, and the age of the basal Mattson decreases toward the west and southwest. This indicates that the siliciclastics prograded southward and westward.

Thick, widespread deposits of Tournaisian to Serpukhovian age, derived mainly from the northeast, are present in northern Yukon Territory (Graham, 1973; Bamber and Waterhouse, 1971). Their presence provides additional support for the hypothesis that a major source existed north of the project area and shed large volumes of siliciclastics.

Formations between the Exshaw and Golata formations

A northern, dominantly sedimentary provenance also is suggested for the terrigenous sand and silt that occur in the succession between the Exshaw and Golata formations (Figs. 2, 3). Shale and mudstone occur throughout most of this interval, but the following interpretations are based mainly on data from siltstone and sandstone that occur in the



Figure 80. Large-scale truncation surfaces (arrows) and related fills in fining-upward sequence of Yohin graded-bed lithofacies (Loc. 29). Deposits are siltstone with subordinate sandstone; discontinuities are interpreted as erosion surfaces of submarine channels. ISPG 798-139.

Banff and Yohin formations, and in the Jackfish Gap Member of the Flett Formation. The siltstone and sandstone in those units is mainly subchertarenite.

The clast composition of sandstone and siltstone in the Banff, Yohin, and Jackfish Gap, together with the characteristics of quartz grains in these rocks, suggest that sedimentary rocks provided most of the clasts. However, low-grade metasediments possibly provided a significant proportion of the grains. Most sand and silt in these rocks are stable quartz and chert (Appendix F). If a major proportion of the grains were first-cycle clasts from igneous and metamorphic rocks, heavy minerals and unstable components would probably be more abundant. The fine sand-sized and coarser quartz clasts are chiefly subangular to subrounded. Because quartz sand grains do not round rapidly, many of these clasts probably have been through more than one sedimentary cycle. Polycrystalline quartz clasts that have more than three units are moderately common, particularly in the Yohin Formation. Many of these polycrystalline grains probably came from well cemented siltstone or low-grade metasediments, because the ratio of polycrystalline to monocrystalline quartz in sandstone that consists mainly of multicycle quartz is generally low.

The Ellesmerian fold belt in the Arctic Archipelago and adjacent uplifted areas to the south probably supplied a major part of the terrigenous clastics to the interval between the

Exshaw and Golata formations. The Yukon fold belt, which developed in northern Yukon Territory during the Ellesmerian Orogeny (Bell, 1974), was possibly an important source as well. A lack of other suitable source areas, and the distribution of siliciclastics in strata of earliest Tournaisian to latest middle Viséan (Tn1a to V2) age support this interpretation. In the project area, a consistent northward to northeastward increase in the volume and coarseness of terrigenous clastics is evident. This is most marked in the Flett Formation and at the stratigraphic levels of the Banff and Clausen formations. According to Macauley et al. (1964), similar northward trends are evident on most of the western Canadian interior platform south and southeast of the project area. Moreover, thick, widespread, siliciclastic deposits of middle to early late Viséan (V2 to V3) age, derived mainly from the northeast, unconformably overlie older rocks in northern Yukon Territory (Bamber and Waterhouse, 1971). The great volume of sediment involved, particularly in the Banff Formation, required a major, elevated source area. The Yukon and Ellesmerian fold belts consist of mainly sedimentary strata and low grade metasediments (Trettin, 1973; Bell, 1973; Embry and Klovan, 1976, p. 612, 613). These fold belts, therefore, would have been a suitable source area.

The Canadian Shield was probably subaerially exposed during the Early Carboniferous. It may have been, therefore, a source area for a small proportion of the terrigenous clastics in the Lower Carboniferous of the project area.



Figure 81. West sides of nested truncation surfaces in a unit of Flett mixed-skeletal lime-packstone lithofacies at Locality 5. Beds resembling foresets occur between the two main discontinuities (arrows), which are broad, concave-upward surfaces. Surfaces are in the proximal, middle part of a symmetrical sequence near the base of the Meilleur Member. Central cliff is 24 m high. ISPG 1756-120.

PALEOGEOGRAPHY

In the project area, strata of latest Devonian and Carboniferous age were deposited mainly in a broad, northwest trending, trough-shaped basin produced by subsidence of the western side of the ancestral North American plate (Richards et al., in press). Douglas et al. (1970, p. 411, 413) called the part of this basin that occurs north of the Peace River Embayment the Liard Trough. The eastern hinge for this trough was probably a broad belt, because abrupt basinward or westward thickening of the uppermost Devonian and Carboniferous is not evident in the project area or the region to the south. An extensive shallow sea apparently covered the cratonic platform east of the trough, and its eastern shoreline was probably well east of the subcrop erosional zero-edge of the Carboniferous (Douglas et al., 1970, p. 413). West of the former trough, the present day Canadian Cordillera is mainly a collage of allochthonous terranes, which coalesced with one another and the western margin of the North American plate, mainly in the Mesozoic (Monger and Price, 1979). The trough resulted from the subsidence of miogeoclinal terrane in the Late Devonian (Monger and Price, 1979, p. 784), which continued to subside throughout the Early Carboniferous. According to Monger and Price, the tectonic significance of the

subsidence that occurred at this time is not clear. Only remnants of the Carboniferous remain in the project area. Consequently, the geometry of the trough and the location of its eastern hinge line in this area can only be speculated upon.

In the project area, the shelf margin formed a broad embayment that opened toward the southwest. South of the project area and north of the Peace River Embayment, the transitional belt of platform-slope carbonates between the shelf and shale basin has a north or north-northwest trend (Bamber et al., 1980, Fig. 1). However, in the northern half of the project area, this trend curves toward the west, thus defining a former embayment. The shape of this embayment is best indicated by the western depositional limit of units of the Flett mixed-skeletal lime-packstone lithofacies that are of latest middle Viséan (V2) age (Fig. 89). That limit marks the western extent of the Flett Formation and facies that were deposited on a middle slope setting (Fig. 87a). Moreover, the embayment appears to have had a similar outline during deposition of the lower Flett in the early Viséan (V1), and the deposition of the Yohin and upper Banff formations in the middle Tournaisian (Tn2). Because the major lithofacies belts bend toward the west in the northern half of the project area, the hinge line of the Liard Trough possibly had a similar trend.

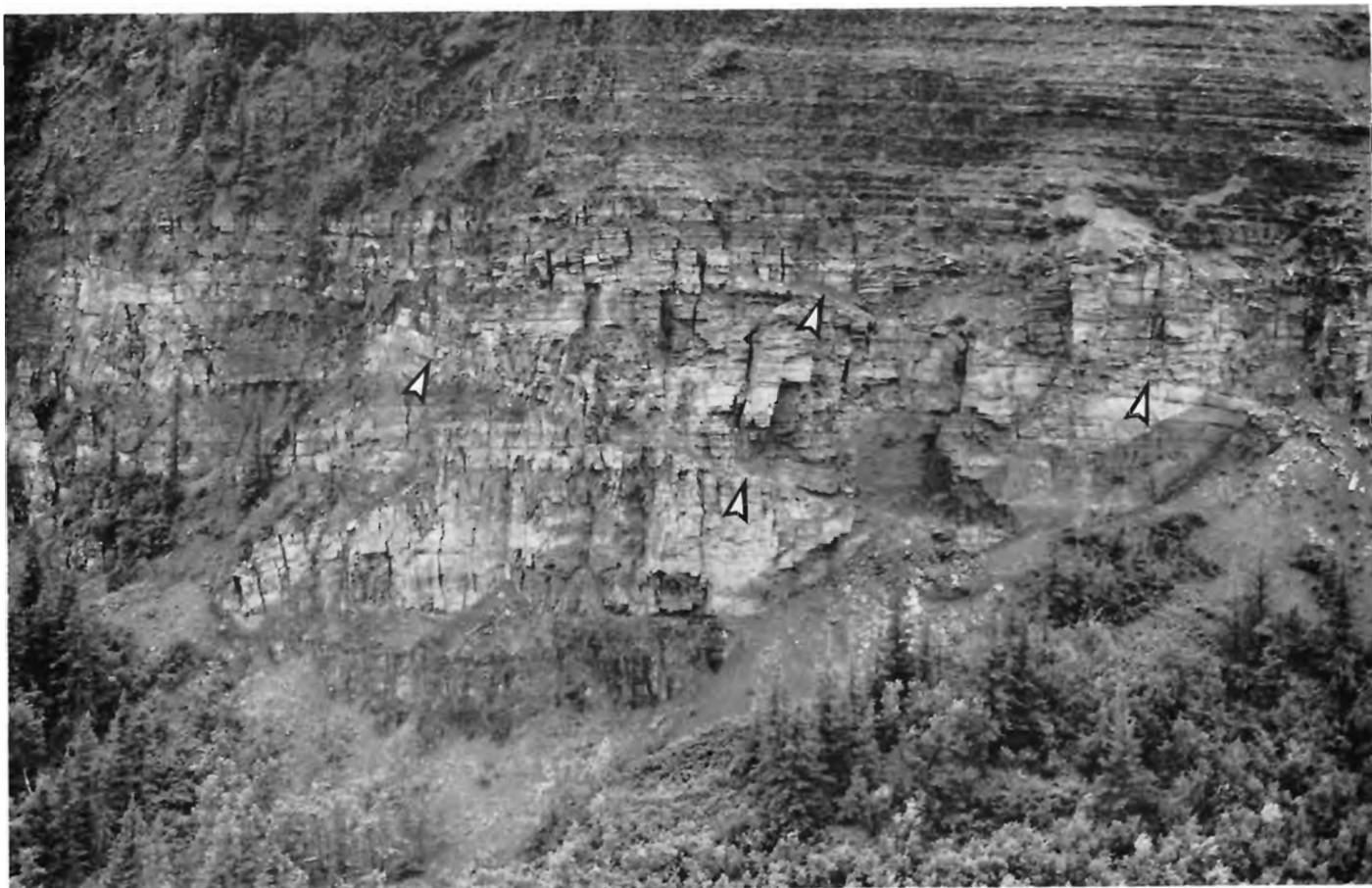


Figure 82. Large-scale truncation surfaces or paleochannels (arrows), in a siltstone and sandstone, fining-upward sequence of the Yohin graded-bed lithofacies (Loc. 29). Beds in lower part of the channel fills are subparallel to strata below the discontinuities. ISPG 798-142.

DEPOSITIONAL SUMMARY

Uppermost Devonian and Lower Carboniferous strata in the project area were mainly deposited during a series of progradational to aggradational depositional episodes, with each major regressive unit prograding farther westward than its predecessor. With possible minor exceptions, the region appears to have subsided at a moderate rate from the latest Devonian (Tn1a) to early Serpukhovian. During this time, deposition occurred under the influence of variable rates of terrigenous influx from the north. Terrigenous influx was greatest during the early Tournaisian to late middle Tournaisian (late Tn1b to Tn2), and in the late Viséan (V3) to early Serpukhovian.

Early Tournaisian to late middle Tournaisian (Tn1a to Tn2)

In the project area, there was a general shallowing-upward trend during most of the early Tournaisian to late middle Tournaisian (Tn1a to Tn2), although periods of transgression possibly occurred and global sea level rose. Shale and mudstone of early Tournaisian (Tn1a and early Tn1b) age in the basal Banff Formation, and in coeval intervals to the west and north, may have been deposited during a regional transgression that started during deposition of the Upper Devonian Exshaw Formation. However, during

deposition of the lower to middle Tournaisian (upper Tn1b to Tn2) Yohin Formation, and underlying strata of early Tournaisian (early to late Tn1b) age in the Besa River and Banff(?) formations, there was an upward trend from deposition of siliciclastic basinal mud to the formation of crossbedded sandstone on a shallow-neritic shelf. Similarly, the lower Banff on the interior platform is mainly lower Tournaisian (Tn1) shale and mudstone, resulting from sedimentation in moderately deep water, whereas the upper Banff contains middle Tournaisian (Tn2) shallow marine limestone and sandstone. This shoaling-upward probably resulted mainly from the abundant influx of northerly derived terrigenous clastics from the recently elevated Ellesmerian orogen and adjacent uplifted areas. Reduced subsidence rates in the basin were possibly a factor as well. Intertidal to supratidal lithofacies of middle Tournaisian (Tn2) age do not appear to be preserved in the Yohin and upper Banff in the project area or the region to the east. Nevertheless, considerable regression probably occurred east of the present erosional zero-edge of the upper Banff during deposition of these intervals. The Yohin and upper Banff are of regressive aspect, and evidence of marked regression is preserved in the upper Banff over wide areas in western Alberta (Morin, 1981; Richards et al., in press; Chatellier, 1983). During deposition of the Yohin and upper Banff, dark muds of the Besa River Formation were deposited to the west. Minor eustatic oscillations in sea level probably occurred in the Tournaisian (Ramsbottom, 1973); however, global sea level apparently rose slowly throughout most of this time (Vail et al., 1977b).



Figure 83. Dolostone and spiculite slump deposit in the Prophet spiculite and spicule-lime-packstone lithofacies at Locality 8. Arrow points to minor glide plane; divisions on the Jacob's staff are 50 cm long. ISPG 798-43.



Figure 84. Dolostone and spiculite slump deposits in the Prophet spiculite and spicule-lime-packstone lithofacies at Locality 8. Upper slump mass overlies a concave-upward truncation surface (arrow). Divisions on Jacob's staff are 50 cm long. ISPG 798-42.



Figure 85. Large-scale channel-like structure (see also Figure 86) (arrows), in the Prophet spiculite and spicule-lime-packstone lithofacies at Ram Creek. ISPG 798-83.

During the early Tournaisian to late middle Tournaisian (Tn1 to Tn2), major carbonate buildups did not develop in the project area or toward the east. Carbonate beds separated by siliciclastics were deposited, however, and are preserved in the upper Banff Formation on the interior platform, and locally in the Yohin Formation.

Latest middle and late Tournaisian (Tn2 and Tn3)

During the latest middle and late Tournaisian (Tn2 and Tn3; late foraminiferal zone 7 to late zone 9), carbonates, spiculite, and shale of the Besa River, Pekisko, Clausen, and



Figure 86. Large-scale, mound-like structure (arrows) in the Prophet spiculite and spicule-lime-packstone lithofacies (Loc. 6). ISPG 798-84.

Prophet formations and Formation F were deposited (Figs. 2-6, 50). At this time, essentially continuous marine sedimentation probably occurred throughout the project area. Deposition took place during a period of rising global sea level, followed by a global highstand from approximately late Tournaisian to early Viséan (Tn3 to V1) (Vail et al., 1977b). Rates of terrigenous influx were generally lower than in the early Tournaisian to late middle Tournaisian (Tn1 to Tn2), and, with minor local exceptions, deposition of terrigenous sand and silt ceased. However, south of about latitude 60°55'N and east of the western Liard Range, significant volumes of mud, preserved in the Clausen and Prophet, were periodically deposited. To the west and north, where the Clausen and Besa River formations are preserved, deposition of dark mud was essentially continuous. Two carbonate buildups, consisting of platform deposits and subordinate ramp deposits (Fig. 87), developed and prograded westward into a deeper water shale basin (Fig. 50), but only erosional remnants of these buildups remain.

The oldest of the carbonate buildups constitutes the Pekisko Formation (Figs. 5, 6, 50). Because of terrigenous influx, this buildup is poorly developed and relatively thin in the project area. During its formation, siliciclastic mud, preserved as shale and mudstone in the Clausen and Besa River formations, was deposited in deeper water to the west and northwest. The Pekisko and correlative strata to the west and north were deposited during a period of increasing regional water depth, and either a major transgression or

onlap of coastal deposits occurred. The following evidence supports this interpretation:

1. The Clausen lithofacies are of deeper water aspect than those in the upper Yohin Formation
2. Correlative, widespread platform limestone in the basal Pekisko Formation in northeastern British Columbia and southwestern Alberta was deposited during a major transgression (Illing, 1959; Richards et al., in press)
3. The deposition of clean limestone above the siliciclastics of the Banff Formation suggests that sand-bearing coastal lithofacies were farther eastward than during deposition of the uppermost Banff.

A subsequent rapid increase in water depth terminated growth of this buildup and resulted in deposition of the shale-rich Clausen Formation in moderately deep water.

The youngest of the carbonate buildups that developed during latest middle and late Tournaisian time (Tn2 and Tn3) is chiefly an association of aggradational to progradational platform and ramp lithofacies. Remains of it appear to be mainly platform-slope deposits that are preserved in the lower Prophet Formation and coeval Formation F on the southwestern side of the interior platform, and in the eastern to central Liard Range south of about latitude 60°55'N (Figs. 5, 6, 10, 50). It is more widely distributed and better

developed than the underlying buildup in the Pekisko, and it prograded several kilometres farther westward. Following the increase in water depth and episode of terrigenous sedimentation that terminated the underlying buildup, the rate of carbonate production increased gradually and the aggradation and progradation of this second buildup proceeded. To the north and west, however, deposition of the fine grained basinal siliciclastics of the Clausen and Besa River formations continued. In these areas, the construction of a carbonate buildup was not initiated until the latest Tournaisian (Tn3; late zone 9). Some onlap of coastal lithofacies possibly occurred during the growth of this second buildup because global sea level was rising slowly at this time (Vail et al., 1977b). This buildup was, however, deposited under shallowing-upward conditions and shorelines in the region probably advanced basinward during most of its development. At this time, in northeastern British Columbia and western Alberta, the shoreline advanced many kilometres westward during deposition of evaporites and other restricted shelf lithofacies (Fig. 87a) in the Shunda Formation (Macqueen et al., 1972, p. 22-25; Bamber et al., 1980; Richards et al., in press).

During the late Tournaisian (Tn3; late zone 9), growth of the second carbonate buildup was terminated by the early phase of a transgression and by a resulting episode of terrigenous sedimentation (Fig. 50). At this time, a shale-rich unit, which is widely distributed in the uppermost Prophet on the interior platform, was deposited in moderately deep water (Fig. 5, Loc. 25; Fig. 6, Loc. 2). The transgression in the project area appears to have coincided with one that occurred in southwestern Alberta and resulted in deposition of open-marine grainstone of the lower Turner Valley Formation (Fig. 3) above restricted-shelf deposits in the Shunda Formation. A marked, eustatic rise in global sea level, which occurred during the latest Tournaisian (Tn3; Sandberg and Gutschick, 1980, p. 142), possibly caused the transgression.

Latest Tournaisian through latest middle Viséan (Tn3 to V2)

During the latest Tournaisian through latest middle Viséan (Tn3 to V2; latest zone 9 to latest zone 13), marine sedimentation was essentially continuous, and two carbonate buildups developed north of about latitude 60°55'N, while one formed to the south (Fig. 50). The buildups are mainly carbonate platform deposits (Fig. 87a); however, some carbonate ramp deposits (Fig. 87b) are present. Middle-slope deposits in the Tlogotsho Member of the Flett Formation and coeval lower-slope facies in the Prophet Formation constitute most of the older of the two northern buildups. The younger of the northern buildups consist mainly of slope, shelf-margin, and possible protected-shelf deposits in the Meilleur Member of the Flett, and correlative lower-slope facies in the Prophet. Remnants of the southern buildup comprise slope, shelf-margin, and possible protected-shelf deposits in the Flett, and correlative lower-slope deposits in the Prophet (Figs. 4-6). These buildups are the most widely distributed, thickest, and best developed carbonate buildups of Carboniferous age in the project area. They prograded several kilometres farther westward than the underlying upper Tournaisian (Tn3) buildup in the Prophet Formation and Formation F. Moreover, the younger of the two northern buildups and upper part of the southern buildup prograded farthest westward into the shale basin. The platforms that developed at this time had depositional shelf margins covered by broad belts of shallow water, carbonate sands (Fig. 87a).

Numerous submarine channels, which directed carbonate sediment basinward to be deposited on submarine fans and fan-like lobes on carbonate slopes, developed on the

gentle slopes of the platforms. Similar channelled slopes were possibly present on underlying buildups, but they have not been identified.

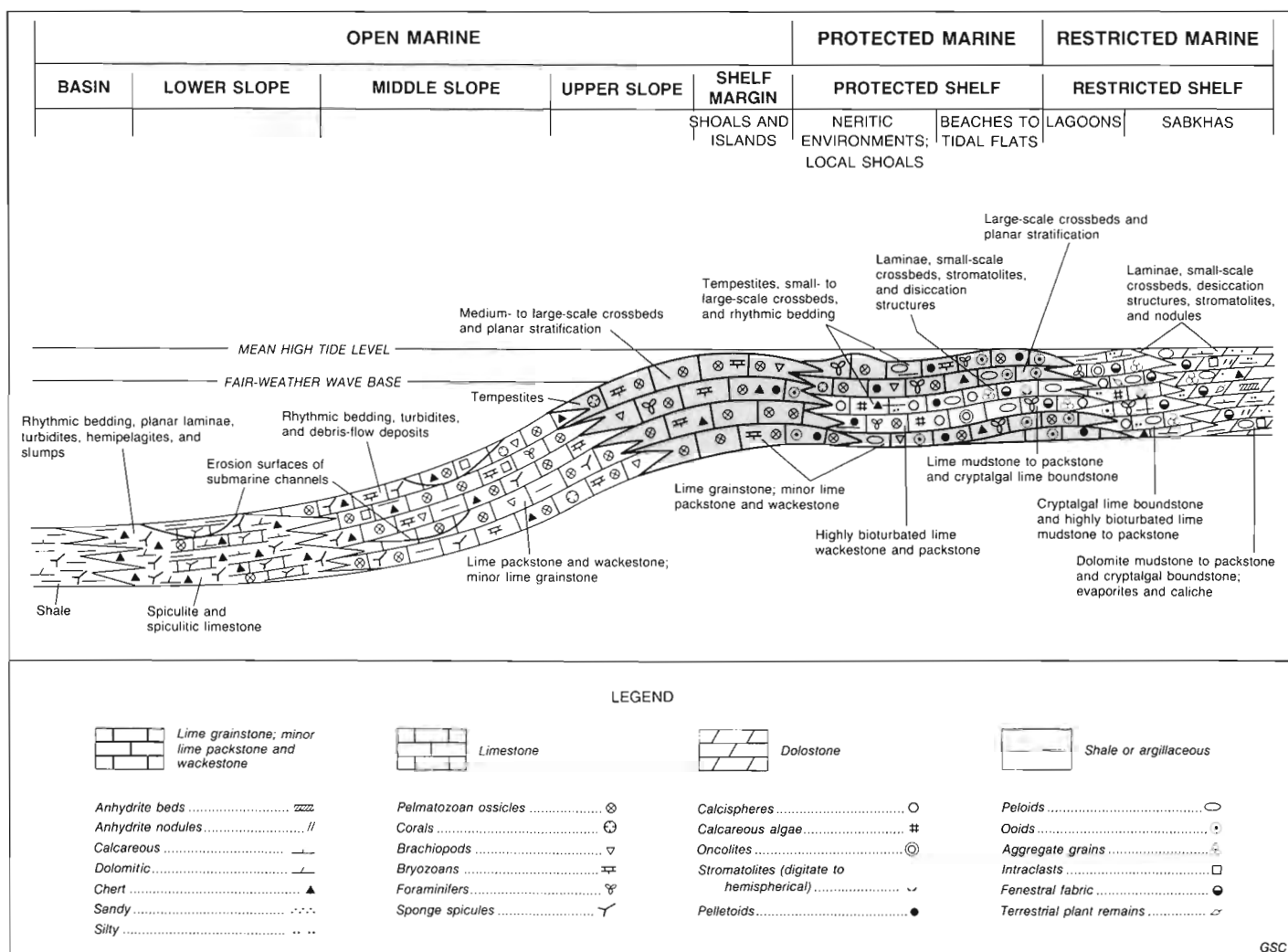
Influx of northerly derived siliciclastics affected platform development throughout most of the latest Tournaisian to latest middle Viséan (Tn3 to V2), but with one notable exception, terrigenous influx was generally lower than at other times in the Early Carboniferous. The volume of terrigenous clastics increased gradually toward the north and northeast. In addition, dark shale of the Besa River was deposited to the west in a moderately deep, starved basin. A major episode of terrigenous influx terminated development of the lower buildup in the north, but platform aggradation and progradation continued to the south (Fig. 50). North of about latitude 60°55'N, this episode, which occurred during the early to middle Viséan (V1 to V2; late zone 10 to latest zone 12), resulted in deposition of the sandstone, siltstone, shale, and mudstone in the Jackfish Gap and upper Tlogotsho members of the Flett Formation (Figs. 4-6). The amount and coarseness of sediment deposited generally increased toward the north and northeast. Following the relatively abrupt cessation of this influx, a second buildup consisting of platform deposits with subordinate ramp deposits was initiated in the north and platform growth continued in the south.

Several important fluctuations in regional water depths influenced development of the carbonate buildups during latest Tournaisian to latest middle Viséan time (Tn3 through V2; latest zone 9 to latest zone 13). Some of these can be correlated with transgressions and regressions recorded by strata in southwestern Alberta.

Deposition of the resistant carbonate buildup deposits in the lower Tlogotsho Member of the Flett (Figs. 4-6, 32, 51) followed the initial phase of a transgression that began in latest Tournaisian (Tn3; latest zone 9) time. Subsequent to the formation of these deposits of latest Tournaisian to early Viséan age (Tn3 to V2; latest zone 9 to middle? Zone 10), water depths appear to have increased slightly during early Viséan time (V1; middle? to late zone 10). This is mainly suggested by an upward increase in the abundance of spicule-rich, and recessive argillaceous rocks in the upper half of the Tlogotsho north of about 60°55'N, and by similar trends in the middle Tlogotsho to the south.

During early to middle Viséan time (V1 to V2; latest (zone 10? to the 12/13 boundary), there was a major break in carbonate buildup development north of approximately latitude 60°55'N. This break, which coincided with a decrease in water depth, is recorded by the terrigenous facies in the uppermost Tlogotsho Member and in the overlying Jackfish Gap Member. Units of shallow-neritic sandstone and siltstone, which constitute the lower and upper Jackfish Gap, appear to have been deposited contemporaneously with the Wileman and Salter members, respectively (Fig. 3). The Wileman and Salter, which occur in southwestern Alberta, were deposited during regional regressions (Macqueen and Bamber, 1968; Richards et al., in press). During deposition of the siliciclastics in the Jackfish Gap, deposition of the carbonate buildup deposits in the middle to upper Tlogotsho and in the Prophet Formation continued to the south. In the middle to upper Tlogotsho of the southern Liard Range (Fig. 5, Loc. 13), the presence of shallow-neritic lime grainstone above moderately deep water strata indicates that substantial shallowing also occurred in the southern part of the project area.

A major transgression influenced carbonate sedimentation during the middle Viséan (V2; 12/13 boundary to early zone 13). North of approximately latitude 60°55'N, this transgression is represented by the rapid transition from



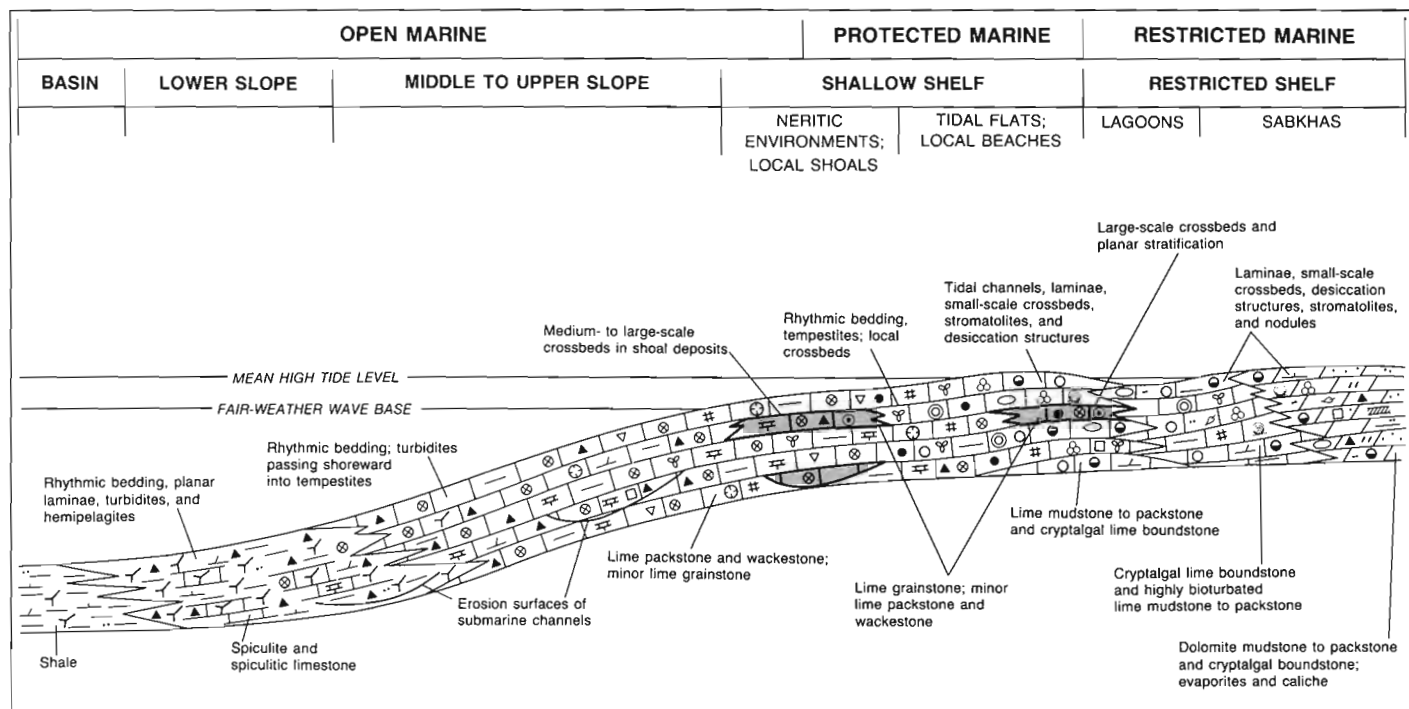
- a. Generalized depositional model of a carbonate platform with a depositional shelf margin covered by shallow water carbonate sands. Characteristics of basin and slope deposits are based mainly on the present study; those of the shelf are based mainly on regional studies of the Lower Carboniferous in southwestern Alberta (Richards et al., in press).

Figure 87. Generalized depositional models.

shallow-neritic sandstone in the Jackfish Gap Member to moderately deep water limestone and shale in the overlying lower Meilleur Member (Figs. 51, 70). In the southern Liard Range (Fig. 5, Loc. 13), the shallow-neritic, shelf-margin lime grainstone in the upper Tlogotsho Member grades up into shale and spicule-rich deposits in the basal Meilleur that were deposited in moderately deep water. As a consequence of this transgression, development of the younger of the two Carboniferous carbonate buildups in the northern part of the area was initiated (Fig. 50). In the southern part of the project area, carbonate buildup development continued, but in deeper water than before. At this time, in southwestern Alberta, the open-marine skeletal and ooid lime grainstones in the lower Loomis Member (Fig. 3), which abruptly overlies restricted-shelf deposits (Fig. 87a) in the Salter Member, were deposited during a major transgression (Macqueen and Bamber, 1968; Richards et al., in press). Subsequent to the initial phase of the transgression in middle Viséan (V2; 12/13 boundary to early zone 13) time, progradational carbonate

buildup facies in the Meilleur, and in correlative parts of the Prophet Formation, were deposited under shallowing-upward conditions.

The considerable regression that generally occurs during progradational to aggradational episodes on carbonate platforms probably occurred on platforms in the project area during the latest Tournaisian to latest middle Viséan (Tn3 to V2; latest zone 9 to latest zone 13). Supratidal deposits of this age have not been identified in remnants of these platforms. The presence in the Flett Formation, however, of widely distributed, shallow water, shelf-margin deposits, above moderately deep water lithofacies, indicates that regression occurred. In addition, coeval strata in the Debolt Formation of northwestern Alberta and northeastern British Columbia contain evidence of marked regression during the middle to early late Viséan (V2 to V3) (see Macauley, 1958; Macauley et al., 1964).



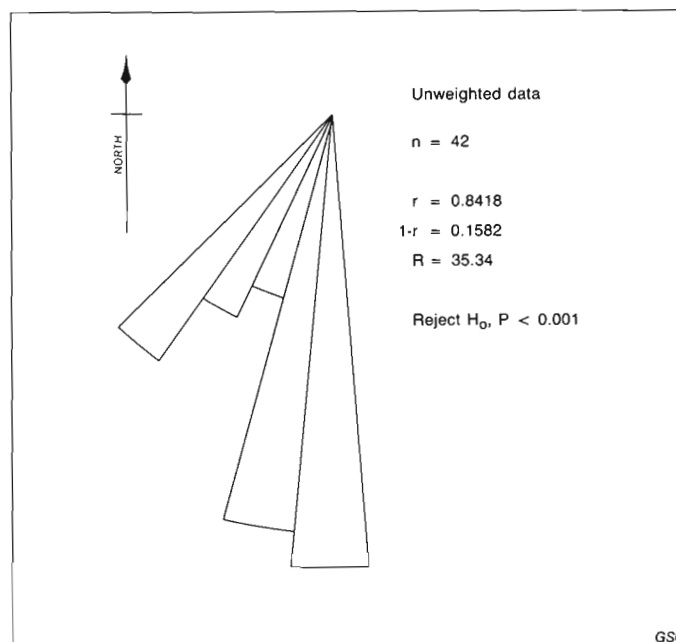
GSC

b. Generalized depositional model of a carbonate ramp of Early Carboniferous age. Characteristics of the basin and slope deposits are based partly on the present study; those of the shallow shelf and restricted shelf are based on regional studies of the Lower Carboniferous of the Western Canada sedimentary basin (Richards et al., in press).

Figure 87 (cont.)

Figure 88. Rose diagram of paleocurrents, based on large-scale trough and tabular crossbedding in fluvial lithofacies of the middle Mattson Formation near Jackfish Gap. Symbols used are: n = number of observations, r = a measure of concentration, $1 - r$ = the angular dispersion, R = Rayleigh's R , H_0 = null hypothesis, H_A = alternate hypothesis, and P = probability. Equations for circular distributions given by Zar (1974, p. 313-317) and ungrouped data are used for calculations. Rayleigh's significance test is used; the testing considers:

1. H_0 (the population angles are randomly distributed), versus
2. H_A (the angles are not randomly distributed).



GSC

Latest middle Viséan (V2) to early Serpukhovian

During the latest middle Viséan (V2; latest zone 13), influx of northerly derived terrigenous clastics terminated carbonate buildup development in the region, and initiated a period of regressive deltaic sedimentation that continued into early Serpukhovian time. During the initial phase of this period, deposition of dark mud in prodelta settings

predominated. This produced the Golata Formation (Figs. 35, 71) in the east and the upper Besa River Formation to the west (Fig. 50). Deposition of the sandstone-rich delta deposits of the Mattson Formation commenced in the northeast during the earliest late Viséan (V3; zone 14) and possibly the latest middle Viséan (V2; latest zone 13).

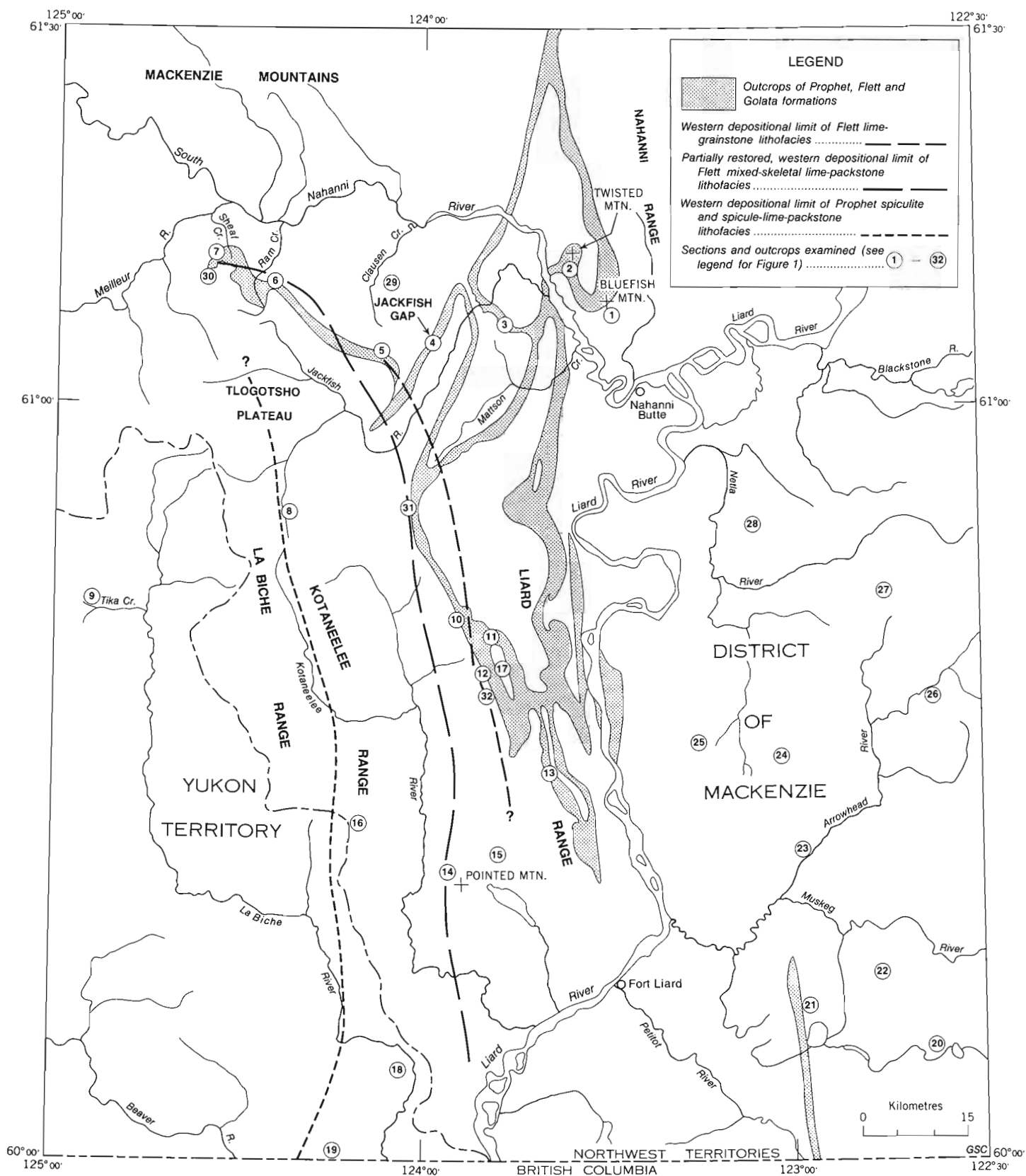


Figure 89. Map of the project area, showing approximate western depositional limits of the Flett lime-grainstone, and mixed-skeletal lime-packstone lithofacies, and the Prophet spiculite and spicule-lime-packstone lithofacies. Limits are for deposits of latest middle Viséan (V2) age.

Subsequently, the Mattson delta-slope and delta-front facies gradually prograded southwestward over the prodelta deposits and were followed by delta plain and various other delta related facies. A major regression occurred, and during the late Viséan (V3), coal and fluvial facies were deposited at least as far west as Tika Creek (Fig. 1, Loc. 9). Although it is mainly a progradational formation, the Mattson was deposited during multiple transgressive-regressive episodes.

Uplift in northern source areas, rather than either a major, sudden, eustatic drop in sea level or uplift within the project area, is interpreted as being the principal cause of this massive terrigenous influx. Thick, widespread, progradational-aggradational coastal successions like the Mattson Formation are deposited mainly under conditions of rising relative sea level. In comparison, a non-depositional hiatus is commonly caused by a stillstand, and during lowstands the shallow shelf is generally bypassed and exposed to subaerial erosion (Vail et al., 1977a). However, during the late Viséan (V3) and early Serpukhovian there were probably numerous minor oscillations in global sea level (Ramsbottom, 1973) that may have influenced deposition of the Mattson.

REFERENCES

- Adams, J.E. and Rhodes, M.L.
1960: Dolomitization by seepage refluxion; American Association of Petroleum Geologists, Bulletin, v. 44, p. 1912-1920.
- Aigner, T.
1982: Calcareous tempestites: storm-dominated stratification in upper Muschelkalk limestones (Middle Trias, S.W.-Germany); in *Cyclic and event stratification*, G. Einsele and A. Seilacher (eds.); Springer-Verlag, New York, p. 180-207.
- Anderton, R.
1976: Tidal-shelf sedimentation: an example from the Scottish Dalradian; *Sedimentology*, v. 23, p. 429-458.
- Badiozamani, K., Mackenzie, F.T., and Thorstenson, D.C.
1977: Experimental carbonate cementation: salinity, temperature and vadose-phreatic effects; *Journal of Sedimentary Petrology*, v. 47, p. 529-542.
- Baker, P.A. and Kastner, M.
1981: Constraints on the formation of sedimentary dolomite; *Science*, v. 213, p. 214-216.
- Bamber, E.W., Macqueen, R.W., and Richards, B.C.
1980: Facies relationships at the Mississippian carbonate platform margin, Western Canada; Geological Survey of Canada, Open File 674.
1984: Facies relationships at the Mississippian carbonate platform margin, western Canada; in *Part 3: Sedimentology and Geochemistry*, E.S. Belt and R.W. Macqueen (eds.); *Neuvième Congrès International de Stratigraphie et de Géologie du Carbonifère*, 1979; *Compte-Rendu*, v. 3, p. 461-478.
- Bamber, E.W. and Mamet, B.L.
1978: Carboniferous biostratigraphy and correlation, northeastern British Columbia and southwestern District of Mackenzie; Geological Survey of Canada, Bulletin 266.
- Bamber, E.W., Taylor, G.C., and Procter, R.M.
1968: Carboniferous and Permian stratigraphy of northeastern British Columbia; Geological Survey of Canada, Paper 68-15.
- Bamber, E.W. and Waterhouse, J.B.
1971: Carboniferous and Permian stratigraphy and paleontology, northern Yukon Territory, Canada; *Bulletin of Canadian Petroleum Geology*, v. 19, p. 29-250.
- Bassett, H.G. and Stout, J.G.
1967: Devonian of Western Canada; in *International Symposium on the Devonian System*, Calgary, 1967, D.H. Oswald (ed.); Alberta Society of Petroleum Geologists, v. 1, p. 717-752.
- Basu, A., Young, S.W., Suttner, L.J., James, W.C., and Mack, G.H.
1975: Re-evaluation of the use of undulatory extinction and polycrystallinity in detrital quartz for provenance interpretation; *Journal of Sedimentary Petrology*, v. 45, p. 873-882.
- Bathurst, R.G.C.
1959: The cavernous structure of some Mississippian *Stromatactis* reefs in Lancashire, England; *Journal of Geology*, v. 67, p. 506-521.
1971: Carbonate sediments and their diagenesis; Elsevier, New York, 620 p.
- Bell, J.S.
1973: Late-Paleozoic orogeny in the northern Yukon; in *Canadian Arctic Geology*, J.D. Aitken and D.J. Glass (eds.); Geological Association of Canada-Canadian Society of Petroleum Geologists Symposium, Saskatoon, Saskatchewan, 1973, p. 23-28.
- Bergquist, P.R.
1978: *Sponges*; University of California Press, Berkeley, Los Angeles, 268 p.
- Bissell, H.J. and Barker, Holly K.
1977: Deep-water limestones of the Great Blue Formation (Mississippian) in the eastern part of the Cordilleran miogeosyncline in Utah; in *Deep-water Carbonate Environments*, H.E. Cook and P. Enos (eds.); Society of Economic Paleontologists and Mineralogists, Special Publication no. 25, p. 171-186.
- Boles, J.R.
1981: Clay diagenesis and effects on sandstone cementation (case histories from the Gulf Coast Tertiary); in *Clays and the Resource Geologist*; F.J. Longstaffe (ed.); Mineralogical Association of Canada, Short Course Handbook, v. 7, p. 148-168.
- Boles, J.R. and Franks, S.G.
1979: Clay diagenesis in Wilcox sandstone of southwest Texas; implications of smectite diagenesis on sandstone cementation; *Journal of Sedimentary Petrology*, v. 49, p. 55-70.
- Bouma, A.H.
1962: *Sedimentology of Some Flysch Deposits: A Graphic Approach to Facies Interpretation*; Elsevier Publishing Co., Amsterdam, 168 p.

- Bouma, A.H. and Hollister, C.D.
1973: Deep ocean basin sedimentation; in *Turbidites and Deep Water Sedimentation*; Society of Economic Paleontologists and Mineralogists, Pacific Section, short course, Anaheim, 1973, p. 79-118.
- Braman, D.R.
1976: Palynology and Paleoecology of the Mattson Formation, Northwest Canada; unpublished Master of Science thesis, Department of Geology, University of Calgary, 140 p.
- Braman, D.R. and Hills, L.V.
1977: Palynology and paleoecology of Mattson Formation, northwest Canada; *Bulletin of Canadian Petroleum Geology*, v. 25, p. 582-630.
- Buchbinder, L.G. and Friedman, G.M.
1980: Vadose, phreatic, and marine diagenesis of Pleistocene-Holocene carbonates in a borehole: Mediterranean coast of Israel; *Journal of Sedimentary Petrology*, v. 50, p. 395-408.
- Byers, C.W.
1977: Biofacies patterns in euxinic basins: a general model; in *Deep-water Carbonate Environments*, H.E. Cook and P. Enos (eds.); Society of Economic Paleontologists and Mineralogists, Special Publication no. 25, p. 5-17.
- Campbell, C.V.
1971: Depositional model-Upper Cretaceous Gallup beach shoreline, Ship Rock area, northwestern New Mexico; *Journal of Sedimentary Petrology*, v. 41, p. 395-409.
- Carter, Robert M. and Lindqvist, Jon K.
1975: Sealers Bay submarine fan complex, Oligocene, southern New Zealand; *Sedimentology*, v. 22, p. 465-483.
- Chatellier, J.Y.
1983: Sedimentology of the Mississippian Banff Formation in Southwestern Alberta Mountains and Plains; unpublished Masters thesis, University of Calgary, 159 p.
- Chough, S.K. and Hesse, R.
1980: The northwest Atlantic mid-ocean channel of the Labrador Sea: III. Head spill vs. body spill deposits from turbidity currents on natural levees; *Journal of Sedimentary Petrology*, v. 50, p. 227-234.
- Chowns, T.M. and Elkins, J.E.
1974: The origin of quartz geodes and cauliflower cherts through the silicification of anhydrite nodules; *Journal of Sedimentary Petrology*, v. 44, p. 885-903.
- Clari, P. and Ghibaudo, G.
1979: Multiple slump scars in the Tortonian type area (Piedmont basin, northwestern Italy); *Sedimentology*, v. 26, p. 719-730.
- Clayton, G., Coquel, R., Doubinger, J., Gueinn, K.J., Loboziak, S., Owens, B., and Streel, M.
1977: Carboniferous miospores of western Europe: illustration and zonation; *Mededelingen Rijks Geologische Dienst*, v. 29, p. 1-71.
- Clifton, H.E.
1969: Beach lamination: nature and origin; *Marine Geology*, v. 7, p. 553-559.
- Clifton, H.E., Hunter, R.E., and Phillips, R.L.
1971: Depositional structures and processes in the non-barred, high energy nearshore; *Journal of Sedimentary Petrology*, v. 41, p. 651-670.
- Collinson, C., Scott, A.J., and Rexroad, C.B.
1962: Six charts showing biostratigraphic zones and correlations based on conodonts from the Devonian and Mississippian rocks of the upper Mississippi Valley; *Illinois Geological Survey, Circular 328*, 32 p.
- Cook, H.E., McDaniel, P.N., Mountjoy, E.W., and Pray, L.C.
1972: Allochthonous carbonate debris flows at Devonian bank ('Reef') margins Alberta, Canada; *Bulletin of Canadian Petroleum Geology*, v. 20, p. 439-497.
- Cook, H.E. and Taylor, M.E.
1977: Comparison of continental slope and shelf environments in the Upper Cambrian and lowest Ordovician of Nevada; in *Deep-water Carbonate Environments*, H.E. Cook and P. Enos (eds.); Society of Economic Paleontologists and Mineralogists, Special Publication no. 25, p. 51-81.
- Cotter, E.
1966: Limestone diagenesis and dolomitization in Mississippian carbonate banks in Montana; *Journal of Sedimentary Petrology*, v. 36, p. 764-774.
- Damuth, J.E.
1975: Echo character of the western equatorial Atlantic floor and its relationship to the dispersal and distribution of terrigenous sediments; *Marine Geology*, v. 18, p. 17-45.
- Davidson-Arnott, R.G.D. and Greenwood, B.
1976: Facies relationships on a barred coast, Kouchibouguac Bay, New Brunswick, Canada; in *Beach and nearshore sedimentation*, R.A. Davis Jr. and R.L. Ethington (eds.); Society of Economic Paleontologists and Mineralogists, Special Publication no. 24, p. 149-168.
- Davies, G.R.
1977: Turbidites, debris sheets, and truncation structures in Upper Paleozoic deep-water carbonates of the Sverdrup basin, Arctic Archipelago; in *Deep-water Carbonate Environments*, H.E. Cook and P. Enos (eds.); Society of Economic Paleontologists and Mineralogists, Special Publication no. 25, p. 221-247.
- Davies, G.R. and Nassichuk, W.W.
1975: Gravity-slide megastructures in deep-water carbonates of the Pennsylvanian-Permian Hare Fiord Formation of Ellesmere Island; *Geological Survey of Canada, Paper 75-1, Part B*, p. 50-232.
- Deffeyes, K.S., Lucia, F.J., and Weyl, P.K.
1964: Dolomitization: observations on the island of Bonaire, Netherlands Antilles; *Science*, v. 143, p. 678-679.

- 1965: Dolomitization of Recent and Plio-Pleistocene sediments by marine evaporite waters on Bonaire, Netherlands Antilles; in *Dolomitization and Limestone Diagenesis, a Symposium*, L.C. Pray and R.C. Murray (eds.); Society of Economic Paleontologists and Mineralogists, Special Publication no. 13, p. 112-123.
- Dickson, J.A.D.
1965: A modified staining technique for carbonates in thin section; *Nature*, v. 205, p. 587.
- Dingle, R.V.
1977: The anatomy of a large submarine slump on a sheared continental margin (S.E. Africa); *Geological Society of London, Journal*, v. 134, p. 293-310.
1980: Large allochthonous sediment masses and their role in the construction of the continental slope and rise off southwestern Africa; *Marine Geology*, v. 37, p. 333-354.
- Douglas, R.J.W.
1958: Mount Head map area, Alberta; Geological Survey of Canada, Memoir 291.
1976: Geology - La Biche River, District of Mackenzie; Geological Survey of Canada, Map 1380A.
- Douglas, R.J.W., Gabrielse, H., Wheeler, J.O., Stott, D.F., and Belyea, H.R.
1970: Geology of Western Canada; in *Geology and Economic Minerals of Canada*, R.J.W. Douglas (ed.); Geological Survey of Canada, Economic Geology Report No. 1, p. 366-488.
- Douglas, R.J.W., Harker, P., and Norris, D.K.
1963: Geology southern Mackenzie Mountains area Yukon Territory and District of Mackenzie; Geological Survey of Canada, Map 1141A.
- Douglas, R.J.W. and Norris, D.K.
1959: Fort Liard and La Biche map-areas, Northwest Territories and Yukon; Geological Survey of Canada, Paper 59-6.
1960: Virginia Falls and Sibbeston Lake map-areas, Northwest Territories 95F and 95G; Geological Survey of Canada Paper 60-19.
1976a: Geology-Fort Liard, District of Mackenzie; Geological Survey of Canada, Map 1379A.
1976b: Geology-Virginia Falls, District of Mackenzie; Geological Survey of Canada, Map 1378A.
1976c: Geology-Sibbeston Lake, District of Mackenzie; Geological Survey of Canada, Map 1377A.
- Dunham, R.J.
1962: Classification of carbonate rocks according to depositional texture; in *Classification of Carbonate Rocks*, W.E. Ham (ed.); American Association of Petroleum Geologists, Memoir 1, p. 108-121.
1971: Meniscus cement; in *Carbonate Cements*, P.O. Bricker (ed.); Johns Hopkins University Studies in Geology, No. 19, p. 297-300.
- Elliott, T.
1978a: Deltas; in *Sedimentary Environments and Facies*, H.G. Reading (ed.); Elsevier, New York, p. 97-142.
1978b: Clastic shorelines; in *Sedimentary Environments and Facies*, H.G. Reading (ed.); Elsevier, New York, p. 143-177.
- Embry, A. and Klován, J.E.
1976: The Middle-Upper Devonian clastic wedge of the Franklinian geosyncline; *Bulletin of Canadian Petroleum Geology*, v. 24, p. 485-639.
- Epstein, A.G., Epstein, J.B., and Harris, L.D.
1977: Conodont color alteration - an index to organic metamorphism; United States Geological Survey, Professional Paper 995, 27 p.
- Evamy, B.D.
1967: The precipitational environment and correlation of some calcite cements deduced from artificial staining; *Journal of Sedimentary Petrology*, v. 39, p. 787-821.
- Ewing, M. and Thorndike, E.M.
1965: Suspended matter in deep ocean water; *Science*, v. 147, p. 1291-1294.
- Field, M.E. and Clarke, S.H. Jr.
1979: Small-scale slumps and slides and their significance for basin slope processes, southern California borderland; in *Geology of Continental Slopes*, L.J. Doyle and O.H. Pilkey (eds.); Society of Economic Paleontologists and Mineralogists, Special Publication no. 27, p. 223-230.
- Fisher, W.L., Brown, L.F., Scott, A.J., and McGowen, J.H.
1969: Delta systems in the exploration for oil and gas; Bureau of Economic Geology, University of Texas, Austin, 212 p.
- Folk, R.L.
1965: Some aspects of recrystallization in ancient limestones; in *Dolomitization and Limestone Diagenesis, a Symposium*, L.C. Pray and R.C. Murray (eds.); Society of Economic Paleontologists and Mineralogists, Special Publication no. 13, p. 14-48.
1973: Carbonate petrography in the post-Sorbian age; in *Evolving Concepts in Sedimentology*, R.N. Ginsburg (ed.); Johns Hopkins University, Studies in Geology, no. 21, p. 118-158.
1974a: The natural history of crystalline calcium carbonate: effect of magnesium content and salinity; *Journal of Sedimentary Petrology*, v. 44, p. 40-53.
1974b: Petrology of sedimentary rocks; Hemphill Co., Austin, Texas, 182 p.
- Folk, R.L. and Assereto, R.
1974: Giant aragonite rays and baroque white dolomite in tepee fillings, Triassic of Lombardy, Italy; American Association of Petroleum Geologists, Abstracts with programs, Annual Meeting, San Antonio, p. 34-35.

- 1980: Diagenetic fabrics of aragonite, calcite, and dolomite in an ancient peritidal-spelean environment: Triassic Calcare Rosso, Lombardia, Italy; *Journal of Sedimentary Petrology*, v. 50, p. 371-394.
- Folk, R.L. and Land, L.S.
1975: Mg/Ca ratio and salinity: two controls over crystallization of dolomite; *American Association of Petroleum Geologists, Bulletin*, v. 59, p. 60-68.
- Folk, R.L. and Pittman, J.S.
1971: Length-slow chalcedony: a new testament for vanished evaporites; *Journal of Sedimentary Petrology*, v. 41, p. 1045-1058.
- Folk, R.L. and Weaver, C.E.
1952: A study of the texture and composition of chert; *American Journal of Science*, v. 250, p. 498-510.
- Frazer, D.E.
1974: Depositional episodes: their relationship to the Quaternary stratigraphic framework in the northwestern portion of the Gulf Basin; Bureau of Economic Geology, the University of Texas at Austin, Geological Circular 74-1, 28 p.
- Friedman, G.M. and Kolesar, P.T. Jr.
1971: Fresh-water carbonate cements; in *Carbonate Cements*, P.O. Bricker (ed.); Johns Hopkins University, Studies in Geology, no. 19, p. 122-123.
- Galloway, W.E.
1975: Process framework for describing the morphologic and stratigraphic evolution of deltaic depositional systems; in *Deltas, Models for Exploration*, M.L. Broussard (ed.); Houston Geological Society, Houston, p. 87-98.
- Graham, A.D.
1973: Carboniferous and Permian stratigraphy, southern Eagle Plain, Yukon Territory, Canada; in *Canadian Arctic Geology*, J.D. Aitken and D.J. Glass (eds.); Geological Association of Canada-Canadian Society of Petroleum Geologists Symposium, Saskatoon, Saskatchewan, 1973, p. 159-180.
- Griffin, D.L.
1967: Devonian of northeastern British Columbia; in *International Symposium on the Devonian System*, Calgary, 1967, D.H. Oswald (ed.); Alberta Society of Petroleum Geologists, v. 1, p. 803-826.
- Gutschick, R.C., Sandberg, C.A., and Sando, W.J.
1980: Mississippian shelf margin and carbonate platform from Montana to Nevada; in *Paleozoic Paleogeography of the West-Central United States*, Rocky Mountain Paleogeography Symposium I, T.D. Fouch and E.R. Magathan (eds.); Rocky Mountain Section, Society of Economic Paleontologists and Mineralogists, p. 111-128.
- Hacquebard, P.A. and Barss, M.S.
1957: A Carboniferous spore assemblage in coal from the South Nahanni River area, Northwest Territories; *Geological Survey of Canada, Bulletin* 40.
- Hage, C.O.
1945: Geological reconnaissance along lower Liard River, British Columbia, Yukon and Northwest Territories; *Geological Survey of Canada, Paper* 45-22.
- Halbertsma, H.L.
1959: Nomenclature of Upper Carboniferous and Permian strata in the subsurface of the Peace River area; *Journal of the Alberta Society of Petroleum Geologists*, v. 7, p. 109-118.
- Hamblin, A.P. and Walker, R.G.
1979: Storm-dominated shallow marine deposits: the Fernie-Kootenay (Jurassic) transition, southern Rocky Mountains; *Canadian Journal of Earth Sciences*, v. 16, p. 1673-1690.
- Harker, P.
1961: Summary of Carboniferous and Permian formations, southwestern District of Mackenzie; *Geological Survey of Canada, Paper* 61-1.
- 1963: Carboniferous and Permian rocks, southwestern District of Mackenzie; *Geological Survey of Canada, Bulletin* 95.
- Harms, J.C.
1974: Brushy Canyon Formation, Texas: a deeper-water density current deposit; *Geological Society of America, Bulletin*, v. 85, p. 1763-1784.
- 1975a: Stratification produced by migrating bed forms; in *Depositional Environments as Interpreted from Primary Sedimentary Structures and Stratification Sequences*; Society of Economic Paleontologists and Mineralogists, short course no. 2, Dallas, p. 45-61.
- 1975b: Stratification and sequence in prograding shoreline deposits; in *Depositional Environments as Interpreted from Primary Sedimentary Structures and Stratification Sequences*; Society of Economic Paleontologists and Mineralogists, short course no. 2, Dallas, p. 81-102.
- Harms, J.C. and Pray, L.C.
1974: Erosion and deposition along the mid-Permian intracratonic basin margin, Guadalupe Mountains, Texas; in *Modern and Ancient Geosynclinal Sedimentation*, R.H. Dott, Jr. and R.H. Shaver (eds.); Society of Economic Paleontologists and Mineralogists, Special Publication no. 19, p. 37.
- Hayes, M.O.
1967: Hurricanes as geological agents - case studies of hurricanes Carla, 1961 and Cindy, 1963; Bureau of Economic Geology, University of Texas at Austin, Report of Investigations no. 61, 56 p.
- Heckel, P.H.
1974: Carbonate buildups in the geologic record: a review; in *Reefs in Time and Space*, L.F. Laporte (ed.); Society of Economic Paleontologists and Mineralogists, Special Publication no. 18, p. 90-154.
- Heezen, B.C., Hollister, C.D., and Ruddiman, W.T.
1966: Shaping of the continental rise by deep geostrophic contour currents; *Science*, v. 152, p. 502-508.

- Hesse, R.
1975: Turbiditic and non-turbiditic mudstone of Cretaceous flysch sections of the East Alps and other basins; *Sedimentology*, v. 22, p. 387-416.
- Hook, R.L. and Schlager, W.
1980: Geomorphic evolution of the Tongue of the Ocean and the Providence channels, Bahamas; *Marine Geology*, v. 35, p. 343-366.
- Hopkins, J.C.
1977: Production of foreslope breccia by differential submarine cementation and downslope displacement of carbonate sands, Miette and Ancient Wall buildups, Devonian, Canada; in *Deep-Water Carbonate Environments*, H.E. Cook and P. Enos (eds.); Society of Economic Paleontologists and Mineralogists, Special Publication no. 25, p. 155-170.
- Howard, J.D.
1972: Trace fossils as criteria for recognizing shorelines in stratigraphic records; in *Recognition of Ancient Sedimentary Environments*, J.K. Rigby and Wm. K. Hamblin (eds.); Society of Economic Paleontologists and Mineralogists, Special Publication no. 16, p. 215-225.
1978: Sedimentology and trace fossils; in *Trace Fossil Concepts*, P.B. Bason (ed.); Society of Economic Paleontologists and Mineralogists, short course no. 5, Oklahoma City, p. 13-47.
- Hume, G.S.
1923: A Kinderhook fauna; *American Journal of Science*, series 5, v. 6, p. 48-52.
- Hunter, R.E. and Clifton, H.E.
1982: Cyclic deposits and hummocky cross-stratification of probable storm origin in Upper Cretaceous rocks of the Cape Sebastian area, southwestern Oregon; *Journal of Sedimentary Petrology*, v. 52, p. 127-143.
- Illing, L.V.
1959: Cyclic carbonate sedimentation of the Mississippian at Moose Dome, southeast Alberta; *Alberta Society of Petroleum Geologists, Ninth Annual Field Conference Guidebook*, p. 37-52.
- Illing, L.V., Wells, A.J., and Taylor, J.C.M.
1965: Penecontemporary dolomite in the Persian Gulf; in *Dolomitization and Limestone Diagenesis*, a Symposium, L.C. Pray and R.C. Murray (eds.); Society of Economic Paleontologists and Mineralogists, Special Publication no. 13, p. 89-111.
- Jacka, A.D. and Brand, J.P.
1977: Biofacies and development and differential occlusion of porosity in a Lower Cretaceous (Edwards) reef; *Journal of Sedimentary Petrology*, v. 47, p. 366-381.
- Jacka, A.D., Thomas, C.M., Beck, R.H., Williams, K.W., and Harrison, S.C.
1972: Guadalupian depositional cycles of the Delaware basin and northwest shelf; in *Cyclic Sedimentation in the Permian Basin*, J.G. Elam and S. Chuber (eds.); West Texas Geological Society, p. 151-202.
- James, H.P., Ginsburg, R.H., Marszalek, D.S., and Choquette, P.W.
1976: Facies and fabric specificity of early subsea cements in shallow Belize (British Honduras) reef; *Journal of Sedimentary Petrology*, v. 46, p. 523-544.
- James, N.P. and Mountjoy, E.W.
1983: Shelf-slope break in fossil carbonate platforms: an overview; in *The Shelf-Break: Critical Interface on Continental Margins*, D.J. Stanley and G.T. Moore (eds.); Society of Economic Paleontologists and Mineralogists, Special Publication no. 33, p. 189-206.
- Jenkyns, H.C.
1978: Pelagic environments; in *Sedimentary Environments and Facies*, H.G. Reading (ed.); Elsevier, New York, p. 314-371.
- Johnson, H.D.
1978: Shallow siliciclastic seas; in *Sedimentary Environments and Facies*, H.G. Reading (ed.); Elsevier, New York, p. 207-258.
- Jones, J.B. and Segnit, E.R.
1971: The nature of opal; I. Nomenclature and constituent phases; *Geological Society of Australia, Journal*, v. 18, p. 57-67.
- Jopling, A.W. and Walker, R.G.
1968: Morphology and origin of ripple drift cross-lamination with examples from the Pleistocene of Massachusetts; *Journal of Sedimentary Petrology*, v. 38, p. 971-984.
- Keller, G.H. and Shepard, F.P.
1978: Currents and sedimentary processes in submarine canyons off the northeast United States; in *Sedimentation in Submarine Canyons, Fans, and Trenches*, D.J. Stanley and G. Kelling (eds.); Dowden, Hutchinson, and Ross Inc., Stroudsburg, Pennsylvania, p. 15-32.
- Kendall, A.C. and Tucker, M.E.
1971: Radial fibrous calcite as a replacement after syn-sedimentary cement; *Nature: Physical Science*, v. 232, p. 62-63.
1973: Radial fibrous calcite: a replacement after acicular carbonate; *Sedimentology*, v. 20, p. 365-389.
- Kennedy, W.J. and Juignet, P.
1974: Carbonate banks and slump beds in the Upper Cretaceous (Upper Turonian-Santonian) of Haute Normandie, France; *Sedimentology*, v. 21, p. 1-42.
- Kidd, F.A.
1963: The Besa River Formation; *Bulletin of Canadian Petroleum Geology*, v. 11, p. 369-372.
- Kindle, E.M.
1924: Standard Paleozoic section of Rocky Mountains near Banff, Alberta; *Pan-American Geologist*, v. 42, p. 113-124.
- Komar, P.D.
1976: The transport of cohesionless sediments on continental shelves; in *Marine Sediment Transport and Environmental management*, D.J. Stanley and D.J.P. Swift (eds.); John Wiley and Son, New York, p. 107-125.

- Kumar, N. and Sanders, J.E.
1976: Characteristics of shoreface storm deposits: modern and ancient examples; *Journal of Sedimentary Petrology*, v. 46, p. 145-162.
- Land, L.S.
1970: Phreatic versus vadose meteoric diagenesis of limestones: evidence from fossil water table; *Sedimentology*, v. 14, p. 175-185.
1980: The isotopic and trace element geochemistry of dolomite: the state of the art; in *Concepts and Models of Dolomitization*, D.H. Zenger and R.L. Ethington (eds.); *Society of Economic Paleontologists and Mineralogists, Special Publication no. 28*, p. 87-110.
- Land, L.S., Salem, M.R.I., and Morrow, D.W.
1975: Paleohydrology of ancient dolomites: geochemical evidence; *American Association of Petroleum Geologists, Bulletin*, v. 59, p. 1602-1625.
- Lewis, K.B.
1971: Slumping on a continental slope inclined at 1° - 4° ; *Sedimentology*, v. 16, p. 97-110.
- Lippman, F.
1973: *Sedimentary Carbonate Minerals*; Springer-Verlag, New York, 228 p.
- Lohmann, K.C. and Meyers, W.J.
1977: Microdolomite inclusions in cloudy prismatic calcites: a proposed criterion for former high-magnesium calcites; *Journal of Sedimentary Petrology*, v. 47, p. 1078-1088.
- Longman, M.W.
1980: Carbonate diagenetic textures from nearshore diagenetic environments; *American Association of Petroleum Geologists, Bulletin*, v. 64, p. 461-487.
- Loucks, R.G.
1977: Porosity development and distribution in shoal-water carbonate complexes - subsurface Pearsall Formation (Lower Cretaceous), south Texas; in *Cretaceous Carbonates of Texas and Mexico, Applications to Subsurface Exploration*, D.G. Bebout and R.G. Loucks (eds.); *Bureau of Economic Geology, the University of Texas at Austin, Report of Investigations no. 89*, p. 97-126.
- Lowe, D.R.
1976: Grain flow and grain flow deposits; *Journal of Sedimentary Petrology*, v. 46, p. 188-199.
1979: Sediment gravity flows: II. Depositional models with special reference to the deposits of high-density turbidity currents; *Journal of Sedimentary Petrology*, v. 52, p. 279-297.
- Lucia, F.J.
1968: Recent sediments and diagenesis of south Bonaire, Netherlands Antilles; *Journal of Sedimentary Petrology*, v. 38, p. 845-858.
- Macar, P.
1948: Les pseudonodules du Fammenian et leur origine; *Société Géologique de Belgique, Annales*, v. 72, p. 47-74.
- Macauley, G.
1958: Late Paleozoic of Peace River area, Alberta; in *Jurassic and Carboniferous of Western Canada*, A.J. Goodman (ed.); *American Association of Petroleum Geologists, Allan Memorial Volume*, p. 289-308.
- Macauley, G., Penner, D.G., Procter, R.M., and Tisdall, W.H.
1964: Carboniferous; in *Geological History of Western Canada*, R.G. McCrossan and R.P. Glaister (eds.); *Alberta Society of Petroleum Geologists*, p. 89-102.
- Macqueen, R.W. and Bamber, E.W.
1967: Stratigraphy of Banff Formation and lower Rundle Group (Mississippian), southwestern Alberta; *Geological Survey of Canada, Paper 67-47*.
1968: Stratigraphy and facies relationships of the Upper Mississippian Mount Head Formation, Rocky Mountains and Foothills, southwestern Alberta; *Bulletin of Canadian Petroleum Geology*, v. 16, p. 225-287.
- Macqueen, R.W., Bamber, E.W., and Mamet, B.L.
1972: Lower Carboniferous stratigraphy and sedimentology of the southern Canadian Rocky Mountains; 24th International Geological Congress, Montreal, Quebec Guidebook, 62 p.
- Macqueen, R.W. and Sandberg, C.A.
1970: Stratigraphy, age, and interregional correlation of the Exshaw Formation, Alberta Rocky Mountains; *Bulletin of Canadian Petroleum Geology*, v. 18, p. 32-66.
- Mamet, B.L. and Skipp, B.A.
1970a: Preliminary foraminiferal correlations of early Carboniferous strata in the North American cordillera; in *Colloque sur la Stratigraphie du Carbonifère, Les Congrès et Colloques de l'université de Liège*, v. 55, p. 327-348.
1971b: Lower Carboniferous calcareous foraminifera: preliminary zonation and stratigraphic implications for the Mississippian of North America; in *Sixième Congrès International, de Stratigraphie et de Géologie du Carbonifère, Sheffield 1967, Compte Rendu*, v. 3, p. 1129-1146.
- Mattes, B.W. and Mountjoy, E.W.
1980: Burial dolomitization of the Upper Devonian Miette buildup, Jasper National Park, Alberta; in *Concepts and Models of Dolomitizations*, D.H. Zenger and J.B. Dunham (eds.); *Society of Economic Paleontologists and Mineralogists, Special Publication No. 28*, p. 259-297.
- Mazzullo, S.J.
1980: Calcite pseudospar replacive of marine acicular aragonite, and implications for aragonite cement diagenesis; *Journal of Sedimentary Petrology*, v. 50, p. 409-422.
- McConnell, R.G.
1891: Report on an exploration in the Yukon and Mackenzie basins, Northwest Territories; *Geological Survey of Canada, Annual Report 1888-1889*, v. 4, Part D.

- McHargue, T.R. and Price, R.C.
1982: Dolomite from clay in argillaceous or shale-associated marine carbonates; *Journal of Sedimentary Petrology*, v. 52, p. 873-886.
- McIlreath, I.A.
1977: Accumulation of a Middle Cambrian deep-water limestone debris apron adjacent to a vertical, submarine carbonate escarpment, southern Rocky Mountains, Canada; in *Deep-Water Carbonate Environments*, H.E. Cook and P. Enos (eds.); Society of Economic Paleontologists and Mineralogists, Special Publication no. 25, p. 113-124.
- McIlreath, I.A. and James, N.P.
1978: Facies models: B. Carbonate slopes; *Geoscience Canada*, v. 5, p. 189-199.
- McKee, E.D.
1957: Flume experiments on the production of stratification and cross-stratification; *Journal of Sedimentary Petrology*, v. 27, p. 129-134.
- Meissner, Fred F.
1972: Cyclic sedimentation in Middle Permian strata of the Permian basin, West Texas and New Mexico; in *Cyclic Sedimentation in the Permian Basin*, J.G. Elam and S. Chuber (eds.); West Texas Geological Society, p. 203-232.
- Meyers, W.J.
1974: Carbonate cement stratigraphy of the Lake Valley Formation (Mississippian) Sacramento Mountains, New Mexico; *Journal of Sedimentary Petrology*, v. 44, p. 837-861.
1977: Chertification in the Mississippian Lake Valley Formation, Sacramento Mountains, New Mexico; *Sedimentology*, v. 24, p. 75-105.
1978: Carbonate cements; their regional distribution and interpretation in Mississippian limestones of southwestern New Mexico; *Sedimentology*, v. 25, p. 371-400.
- Meyers, W.J. and James, A.T.
1978: Stable isotopes of cherts and carbonate cements in the Lake Valley Formation (Mississippian), Sacramento Mountains, New Mexico; *Sedimentology*, v. 25, p. 105-124.
- Meyers, W.J. and Lohmann, K.C.
1978: Microdolomite-rich syntaxial cements: proposed meteoric-marine mixing zone phreatic cements from Mississippian limestones, New Mexico; *Journal of Sedimentary Petrology*, v. 48, p. 475-488.
- Miall, A.D.
1977a: A review of the braided river depositional environment; *Earth Science Reviews*, v. 13, p. 1-62.
1977b: Sedimentation and tectonics; in *Fluvial Sedimentology*; Canadian Society of Petroleum Geologists, Lecture Series Notes, Calgary, p. 1-19.
- Michel-Lévy, A. and Munier-Chalmas
1890: Sur de nouvelles formes de silice cristallisée; *Comptes-rendus, Académie des Sciences, Paris*, v. 110, p. 649-652.
- 1892: Mémoire sur les diverses formes affectées par le réseau élémentaire du quartz; *Bulletin, Société française de minéralogie et de cristallographie*, v. 15, p. 159-190.
- Middleton, G.V.
1963: Facies variation in Mississippian of Elbow Valley area, Alberta, Canada; *American Association of Petroleum Geologists, Bulletin*, v. 47, p. 1813-1827.
1967: Experiments on density and turbidity currents. III. Deposition of sediment; *Canadian Journal of Earth Sciences*, v. 4, p. 475-505.
1970: Experimental studies related to problems of flysch Sedimentation, in *Flysch Sedimentology In North America*, J. Lajoie (ed.); Geological Association of Canada, Special Paper No. 7, p. 253-272.
- Middleton, G.V. and Hampton, M.A.
1973: Sediment gravity flows: mechanics of flow and deposition; in *Turbidites and Deep Water Sedimentation*; Society of Economic Paleontologists and Mineralogists, Pacific Section, Short Course, Anaheim, p. 1-38.
1976: Subaqueous sediment transport and deposition by sediment gravity flows; in *Marine Sediment Transport and Environmental Management*, D.J. Stanley and P.S. Swift (eds.); John Wiley and Sons, New York, p. 197-218.
- Monger, J.W.H. and Price, R.A.
1979: Geodynamic evolution of the Canadian Cordillera - progress and problems; *Canadian Journal of Earth Sciences*, v. 16, p. 770-791.
- Morin, G.
1981: Mississippian porosity trends; confidential report, Applied Geoscience and Technology Consultants Ltd., phase III, v. 1, 63 p.
- Morrow, D.W.
1978: The Dunedin Formation: a transgressive shelf carbonate sequence; *Geological Survey of Canada, Paper* 76-12.
1982a: Diagenesis 1. Dolomite - part 1: the chemistry of dolomitization and dolomite precipitation; *Geoscience Canada*, v. 9, p. 5-13.
1982b: Diagenesis 2. Dolomite - part 2: dolomitization models and ancient dolostones; *Geoscience Canada*, v. 9, p. 95-107.
- Mount, J.F.
1982: Storm-surge-ebb origin of hummocky cross-stratified units of the Andrews Mountain Member, Campito Formation (Lower Cambrian), White-Inyo Mountains, eastern California; *Journal of Sedimentary Petrology*, v. 52, p. 941-958.
- Mullins, H.T. and Neumann, A.C.
1979: Deep carbonate bank margin structure and sedimentation in the northern Bahamas; in *Geology of Continental Slopes*, L.J. Doyle and O.H. Pilkey (eds.); Society of Economic Paleontologists and Mineralogists, Special Publication no. 27, p. 165-192.

- Mullins, H.T., Neumann, A.C., Wilber, R.J., and Boardman, M.R.
1980: Nodular carbonate sediment on Bahamian slopes: possible precursors to nodular limestones; *Journal of Sedimentary Petrology*, v. 50, p. 117-131.
- Murray, R.C.
1969: Hydrology of south Bonaire, N.A. - a rock selective dolomitization model; *Journal of Sedimentary Petrology*, v. 39, p. 1007-1013.
- Mutti, E.
1974: Examples of ancient deep-sea fan deposits from circum-Mediterranean geosynclines; in *Modern and Ancient Geosynclinal Sedimentation*, R.H. Dott, Jr. and R.H. Shaver (eds.); Society of Economic Paleontologists and Mineralogists, Special Publication no. 19, p. 92-105.
1977: Distinctive thin-bedded turbidite facies and related depositional environments in the Eocene Hecho Group (south-central Pyrenees, Spain); *Sedimentology*, v. 24, p. 107-131.
- Mutti, E. and Ghibaudo, G.
1972: Un esempio di torbiditi di conoide sottomarina esteri: le Arenarie di S. Salvatore (Formazione di Bibbio, Miocene) nell' Apennino di Piacenza; *Memoire Accademia Scienze Torino, Classe di Scienze Fisiche, Matematiche e Naturali, Serie 4*, no. 16, 40 p.
- Mutti, E. and Ricci-Lucchi, F.
1972: Le torbiditi dell' Apennino settentrionale: introduzione all' analisi di facies; *Società Geologica Italiana, Memorie*, v. 11, p. 161-199.
- Nassichuk, W.W.
1975: Carboniferous ammonoids and stratigraphy in the Canadian Arctic Archipelago; *Geological Survey of Canada, Bulletin* 237.
- Nelson, C.H.
1982: Modern shallow-water graded sand layers from storm surges, Bering Shelf: a mimic of Bouma sequences and turbidite systems; *Journal of Sedimentary Petrology*, v. 52, p. 537-545.
- Nelson, C.H. and Kulm, L.D.
1973: Submarine fans and deep-sea channels; in *Turbidites and Deep Water Sedimentation*; Society of Economic Paleontologists and Mineralogists, Pacific Section, Short Course, Anaheim, p. 39-78.
- Newell, N.D., Rigby J.K., Fisher, A.G., Whiteman, A.J., Hickon, J.E., and Bradley, J.S.
1953: The Permian reef complex of the Guadalupe Mountains region, Texas and New Mexico - a study in paleoecology; W.H. Freeman and Co., San Francisco, 236 p.
- Normark, W.R.
1970: Growth patterns of deep-sea fans; *American Association of Petroleum Geologists Bulletin*, v. 54, p. 2170-2195.
1974: Submarine canyons and fan valleys: factors affecting growth patterns of deep-sea fans; in *Modern and Ancient Geosynclinal Sedimentation*, R.H. Dott, Jr. and R.H. Shaver (eds.); Society of Economic Paleontologists and Mineralogists, Special Publication no. 19, p. 56-68.
- Patton, W.J.H.
1958: Mississippian succession in South Nahanni River area, Northwest Territories; in *Jurassic and Carboniferous of Western Canada*, A.J. Goodman (ed.); *American Association of Petroleum Geologists, Allan Memorial Volume*, p. 309-326.
- Pelzer, E.E.
1966: Mineralogy, geochemistry and stratigraphy of the Besa River shale, British Columbia; *Bulletin of Canadian Petroleum Geology*, v. 14, p. 273-321.
- Pettijohn, F.J., Potter, P.E., and Siever, R.
1972: *Sand and Sandstone*; Springer-Verlag, New York, 618 p.
- Pfeil, R.W. and Read, J.F.
1980: Cambrian carbonate platform margin facies, Shady Dolomite, southwestern Virginia, U.S.A.; *Journal of Sedimentary Petrology*, v. 50, p. 91-116.
- Porter, J.W., Price, A.A., and McCrossan, R.G.
1982: The western Canada sedimentary basin; *Philosophical Transactions of the Royal Society of London, Series A*, v. 305, p. 169-192.
- Prior, D.B. and Coleman, J.M.
1980: Sonograph mosaics of submarine slope instabilities, Mississippi River delta; *Marine Geology*, v. 36, p. 227-239.
- Prior, D.B., Coleman, J.M., and Garrison, L.E.
1979: Digitally acquired undistorted side-scan sonar images of submarine landslides, Mississippi River delta; *Geology*, v. 7, p. 423-425.
- Raaf, J.F.M. de, Boersma, J.R., and Gelder, A. van
1977: Wave-generated structures and sequences from a shallow marine succession, Lower Carboniferous, County Cork, Ireland; *Sedimentology*, v. 24, p. 451-483.
- Radke, B.M. and Mathis, R.L.
1980: On the formation and occurrence of saddle dolomite; *Journal of Sedimentary Petrology*, v. 50, p. 1150-1168.
- Ramsbottom, W.H.C.
1973: Transgressions and regressions in the Dinantian: a new synthesis of British Dinantian stratigraphy; *Proceedings of the Yorkshire Geological Society*, v. 39, p. 567-607.
- Reineck, H.E. and Singh, I.B.
1975: *Depositional Sedimentary Environments*; Springer-Verlag, New York, 439 p.
- Reinhardt, J.
1977: Cambrian off-shelf sedimentation, central Appalachians; in *Deep-water Carbonate Environments*, H.E. Cook and P. Enos (eds.); Society of Economic Paleontologists and Mineralogists, Special Publication no. 25, p. 83-112.
- Ricci-Lucchi, F.
1975: Depositional cycles in two turbidite formations of northern Apennines (Italy); *Journal of Sedimentary Petrology*, v. 45, p. 3-43.

- Richards, B.C.
1978: Submarine channels in the Flett Formation: a deeper water carbonate succession, District of Mackenzie, Canada; Abstracts with programs, Annual Meeting, Geological Society of America, v. 10, p. 478.
- 1983a: Uppermost Devonian and Lower Carboniferous stratigraphy, sedimentation and diagenesis, southwestern District of Mackenzie and southeastern Yukon Territory; unpublished Ph.D. thesis, University of Kansas, 373 p.
- 1983b: Uppermost Devonian and Lower Carboniferous stratigraphy, sedimentation and diagenesis, southwestern District of Mackenzie and southeastern Yukon Territory; Abstracts with programs, Joint Annual Meeting, Geological Association of Canada, Mineralogical Association of Canada, Canadian Geophysical Union, v. 8, p. A57.
- Richards, B.C., Bamber, E.W., Higgins, A.C., and Utting, J.
in press: Carboniferous; in *Sedimentary Cover of the North American Craton: Canada*, D.F. Stott and J.D. Aitken (eds.); Geological Survey of Canada, Special Publication (Volume D-1 of the series "Decade of North American Geology").
- Richter, D.K. and Füchtbauer, H.
1978: Ferroan calcite replacement indicates former magnesian calcite skeletons; *Sedimentology*, v. 25, p. 843-860.
- Rose, P.R.
1976: Mississippian carbonate shelf margins, western United States; *United States Geological Journal of Research*, v. 4, p. 449-466.
- Rupke, N.A.
1975: Deposition of fine-grained sediments in the abyssal environment of the Algéro-Balearic basin, western Mediterranean Sea; *Sedimentology*, v. 22, p. 95-109.
- Rupke, N.A. and Stanley, D.J.
1974: Distinctive properties of turbidites and hemipelagic mud layers in the Algéro-Balearic basin, western Mediterranean Sea; *Smithsonian Contributions to Earth Sciences*, v. 13, 40 p.
- Sandberg, C.A. and Gutschick, R.C.
1979: Guide to conodont biostratigraphy of Upper Devonian and Mississippian rocks along the Wasatch front and cordilleran hingeline, Utah; in *Conodont Biostratigraphy of the Great Basin and Rocky Mountains*, C.A. Sandberg and P.L. Clark (eds.); Brigham Young University Geology Studies, v. 26, Part 3, p. 107-134.
- 1980: Sedimentation and biostratigraphy of Osagean and Meramecian starved basin and foreslope, western United States; in *Paleozoic Paleogeography of the West-Central United States Rocky Mountain Paleogeography Symposium I*, T.D. Fouch and E.R. Magathan (eds.); Rocky Mountain Section, Society of Economic Paleontologists and Mineralogists, p. 129-147.
- Sandberg, C.A. and Mapel, W.J.
1967: Devonian of the northern Rocky Mountains and plains; in *International Symposium on the Devonian System*, Calgary, 1967, D.H. Oswald (ed.); Alberta Society of Petroleum Geologists, v. 1, p. 843-877.
- Sandberg, C.A. and Poole, F.G.
1977: Conodont biostratigraphy and depositional complexes of Upper Devonian cratonic-platform and continental-shelf rocks in the western United States; in *Western North America: Devonian*, M.A. Murphy, W.B.N. Berry, and C.A. Sandberg (eds.), California University, Riverside, Campus Museum Contributions, no. 4, p. 144-182.
- Sandberg, C.A., Streel, M., and Scott, R.A.
1972: Comparison between conodont zonation and spore assemblages at the Devonian-Carboniferous boundary in the western and central United States and Europe; in *Septième Congrès International de Stratigraphie et de Géologie du Carbonifère*, Krefeld 1971, *Compte-Rendu*, v. 1, p. 179-203.
- Sandberg, C.A., Ziegler, W., Leuteritz, K., and Brill, S.M.
1978: Phylogeny, speciation, and zonation of *Siphonodella* (Conodonta, Upper Devonian and Lower Carboniferous); *Newsletters on Stratigraphy*, v. 7, p. 102-120.
- Sanders, J.E.
1965: Primary sedimentary structures formed by turbidity currents and related resedimentation mechanisms; in *Primary sedimentary structures and their hydrodynamic interpretation*, G.V. Middleton (ed.); Society of Economic Paleontologists and Mineralogists, Special Publication no. 12, p. 192-219.
- Sando, W.J. and Bamber, E.W.
1979: Coral zonation of the Mississippian System of western North America; Abstracts of papers, Ninth International Congress of Carboniferous Stratigraphy and Geology, Urbana, p. 191.
- 1985: Coral zonation of the Mississippian System in the western interior province of North America; *United States Geological Survey, Professional Paper 1334*, 61 p.
- Schlager, W. and Chermak, A.
1979: Sediment facies of platform-basin transition, Tongue of The Ocean, Bahamas; in *Geology of continental slopes*, L.J. Doyle and O.H. Pilkey (eds.); Society of Economic Paleontologists and Mineralogists, Special Publication no. 27, p. 193-208.
- Scholle, P.A.
1971: Diagenesis of deep-water carbonate turbidites, Upper Cretaceous Monte Antola flysch, northern Apennines, Italy; *Journal of Sedimentary Petrology*, v. 41, p. 233-250.
- Seilacher, A.
1967: Bathymetry of trace fossils; *Marine Geology*, v. 5, p. 413-428.
- 1978: Use of trace fossil assemblages for recognizing depositional environments; in *Trace Fossil Concepts*, P.B. Basan (ed.); Society of Economic Paleontologists and Mineralogists, short course No. 5, Oklahoma City, p. 185-201.

- Shanmugam, G. and Walker, K.R.
1978: Tectonic significance of distal turbidites in the Middle Ordovician Blackhouse and lower Sevier formations in east Tennessee; *American Journal of Science*, v. 278, p. 551-578.
- Shepard, F.P. and Marshall, N.F.
1978: Currents in submarine canyons and other sea valleys; in *Sedimentation in Submarine Canyons, Fans, and Trenches*, D.J. Stanley and G. Kelling (eds.); Dowden, Hutchinson, and Ross Inc., Stroudsburg, Pennsylvania, p. 3-14.
- Shinn, E.A., Ginsburg, R.N., and Lloyd, R.M.
1965: Recent supratidal dolomite from Andros Island, Bahamas; in *Dolomitization and Limestone Diagenesis: a Symposium*, L.C. Pray and R.C. Murray (eds.); Society of Economic Paleontologists and Mineralogists, Special Publication no. 13, p. 112-123.
- Skipper, K. and Middleton, G.V.
1975: The sedimentary structures and depositional mechanics of certain Ordovician turbidites, Cloridorme Formation, Gaspé Peninsula, Quebec; *Canadian Journal of Earth Sciences*, v. 12, p. 1934-1952.
- Smith, D.L.
1977: Transition from deep- to shallow-water carbonates, Paine Member, Lodgepole Formation, central Montana; in *Deep-Water Carbonate Environments*, H.E. Cook and P. Enos (eds.); Society of Economic Paleontologists and Mineralogists, Special Publication no. 25, p. 187-201.
- Southard, J.B.
1975: Bed configurations; in *Depositional Environments as Interpreted from Primary Sedimentary Structures and Stratification Sequences*; Society of Economic Paleontologists and Mineralogists, Short Course no. 2, Dallas, p. 5-43.
- Spearing, D.R.
1975: Shallow marine sands; in *Depositional Environments as Interpreted from Primary Sedimentary Structures and Stratification Sequences*; Society of Economic Paleontologists and Mineralogists, Short Course no. 2, Dallas, p. 103-132.
- Speranza, A.
1984: Sedimentation and diagenesis of the Pekisko Formation (Mississippian), Canyon Creek, Alberta; unpublished Masters thesis, University of Waterloo, 178 p.
- Stanley, D.J. and Unrug, R.
1972: Submarine channel deposits, fluxoturbidites and other indicators of slope and base-of-slope environments in modern and ancient marine basins; in *Recognition of Ancient Sedimentary Environments*, J.K. Rigby and Wm. K. Hamblin (eds.); Society of Economic Paleontologists and Mineralogists, Special Publication no. 16, p. 287-340.
- Stow, D.A.V.
1979: Distinguishing between fine-grained turbidites and contourites on the Nova Scotian deep water margin; *Sedimentology*, v. 26, p. 371-387.
- Stow, D.A.V. and Bowen, A.J.
1980: A physical model for the transport and sorting of fine-grained sediment by turbidity currents; *Sedimentology*, v. 27, p. 31-46.
- Stow, D.A.V. and Lovell, J.P.B.
1979: Contourites: their recognition in modern and ancient sediments; *Earth-Science Reviews*, v. 14, p. 251-291.
- Stow, D.A.V. and Shanmugam, G.
1980: Sequence of structures in fine-grained turbidites: comparison of Recent deep-sea and ancient flysch sediments; *Sedimentary Geology*, v. 25, p. 23-42.
- Sullivan, H.J.
1965: Palynological evidence concerning the regional differentiation of Upper Mississippian floras; *Pollen et spores*, v. 7, p. 539-563.
- Sutherland, P.K.
1958: Carboniferous stratigraphy and rugose coral faunas of northeastern British Columbia; Geological Survey of Canada, Memoir 295.
- Thorsteinsson, R.
1974: Carboniferous and Permian stratigraphy of Axel Heiberg Island and western Ellesmere Island, Canadian Arctic Archipelago; Geological Survey of Canada, Bulletin 224.
- Thorsteinsson, R. and Tozer, E.T.
1970: Geology of the Arctic Archipelago; in *Geology and Economic Minerals of Canada*, R.J.W. Douglas (ed.); Economic Geology Report no. 1, Geological Survey of Canada, p. 548-590.
- Tiffin, D.L., Murray, J.W., Mayers, I.R., and Garrison, R.E.
1971: Structure and origin of foreslope hills, Fraser delta, British Columbia; *Bulletin of Canadian Petroleum Geology*, v. 19, p. 589-600.
- Trettin, H.P.
1973: Early Paleozoic evolution of northern parts of Canadian Arctic Archipelago; in *Arctic Geology*, M.G. Pitcher (ed.); American Association of Petroleum Geologists, Memoir 19, p. 57-75.
- Turnau, E.
1979: Correlations of Upper Devonian and Carboniferous deposits of western Pomerania, based on miospore study; *Rocznik Polskiego Towarzystwa Geologicznego*, v. 49, p. 231-269.
- Vail, P.R., Mitchum, R.M. Jr., and Thompson, S. III
1977a: Seismic stratigraphy and global changes of sea level, Part 3: Relative changes of sea level from coastal onlap; in *Seismic Stratigraphy - Applications to Hydrocarbon Exploration*, C.E. Payton (ed.); American Association of Petroleum Geologists, Memoir 26, p. 63-81.
1977b: Seismic stratigraphy and global changes of sea level, Part 4: Global cycles of relative change of sea level; in *Seismic Stratigraphy - Applications to Hydrocarbon Exploration*, C.E. Payton (ed.); American Association of Petroleum Geologists, Memoir 26, p. 83-97.

- Voges, A.
 1959: Conodonten aus dem Unterkarbon I und II (*Gattendorfia* - und *Pericyclus* - Stufe) des Sauerlandes; *Palaeontologische Zeitschrift*, v. 33, p. 266-314.
 1960: Die Bedeutung der Conodonten für die Stratigraphie des Unterkarbons I und II (*Gattendorfia* - und *Pericyclus* - Stufe) im Sauerland; *Fortschritte in der geologie von Rheinlan und Westfalen* 3, 1: p. 197-228.
- Walker, R.G.
 1975: Nested submarine-fan channels in the Capistrano Formation, San Clemente, California; *Geological Society of America, Bulletin*, v. 86, p. 915-924.
 1976: Facies models 2. Turbidites and associated coarse clastic deposits; *Geoscience Canada*, v. 3, p. 25-36.
 1979: Facies models 7. Shallow marine sands; in *Facies Models*, R.G. Walker (ed.); *Geoscience Canada Reprint Series* 1, p. 75-89.
- Walker, R.G. and Mutti, E.
 1973: Turbidite facies and facies associations; in *Turbidites and Deep Water Sedimentation*; Society of Economic Paleontologists and Mineralogists, Pacific Section, Short Course, Anaheim, p. 119-157.
- Walton, H.S. and Mason, D.
 1967: New data on the Devonian-Carboniferous boundary in Western Canada; in *International Symposium on the Devonian System (abs.)*; Alberta Society of Petroleum Geologists, p. 155.
- Warren, P.S.
 1927: Banff area, Alberta; *Geological Survey of Canada, Memoir* 153, 94 p.
- Wetzel, A.
 1982: Cyclic and dyscyclic black shale formation; in *Cyclic and Event Stratification*, G. Einsele and A. Seilacher (eds.); Springer-Verlag, New York, p. 431-455.
- Wilson, J.L.
 1975: Carbonate Facies in Geologic History; Springer-Verlag, New York, 471 p.
- Wit, R. de Gronberg, E.C., Richards, W.B. and Richmond, W.O.
 1973: Tathlina area, District of Mackenzie; in *The Future Petroleum Provinces of Canada - Their Geology and Potential*, R.G. McCrossan (ed.); Canadian Society of Petroleum Geologists, p. 187-212.
- Wood, G.V. and Armstrong, A.K.
 1975: Diagenesis and stratigraphy of the Lisburne Group limestones of the Sadlerochit Mountains and adjacent areas, northeastern Alaska; *United States Geological Survey, Professional Paper* 857, 47 p.
- Yurewicz, D.A.
 1977: Sedimentology of Mississippian basin-facies carbonates, New Mexico and west Texas - the Rancheria Formation; in *Deep-water Carbonate Environments*, H.E. Cook and P. Enos (eds.); Society of Economic Paleontologists and Mineralogists, Special Publication no. 25, p. 203-219.
- Zar, J.E.
 1974: Biostatistical Analysis; Prentice-Hall, New Jersey, 620 p.

APPENDIX A

FORAMINIFERS AND CALCAREOUS ALGAE (B.L. MAMET)

Data in this appendix are paraphrased from reports prepared in 1977 and 1981 by B.L. Mamet (University of Montréal). See Figure 1 for locations.

Locality 1. Bluefish Mountain; latitude 61°07'23"N, longitude 123°29'13"W, NTS 95 G/3; southwestern District of Mackenzie; Section 75MTA-BCR7 (GSC localities in metres above base of section).

(GSC loc. C-52280, 153.4 m) Banff(?) Formation, 260.3 m below top.

Archaeosphaera sp.
Earlandia elegans (Rauzer-Chernousova)
Biumbella sp.
Quasiumbella sp.

Age: inadequate assemblage; youngest possible age is Tournaisian.

(GSC loc. C-52288, 323.7 m) Banff(?) Formation, 90 m below top.

Earlandia elegans (Rauzer-Chernousova)
Girvanella problematica Nicholson and Etheridge

Age: inadequate assemblage; probably Tournaisian.

(GSC loc. C-52287, 323.9 m) Banff(?) Formation, 89.8 m below top.

Earlandia elegans (Rauzer-Chernousova)
Radiosphaera sp.

Age: inadequate assemblage; probably Tournaisian.

(GSC loc. C-52290, 400.9 m) Banff(?) Formation, 12.8 m below top.

Earlandia elegans (Rauzer-Chernousova)
Girvanella problematica Nicholson and Etheridge

Age: inadequate assemblage; probably Tournaisian.

(GSC loc. C-52284, 413.9 m) Yohin Formation, 0.2 m above base.

Archaeosphaera sp.
Calcisphaera laevis Williamson
Earlandia elegans (Rauzer-Chernousova)
Earlandia minima (Birina)
Girvanella problematica Nicholson and Etheridge

Age: inadequate assemblage; probably Tournaisian.

(GSC loc. C-52291, 415.9 m) Yohin Formation, 2.2 m above base.

Calcisphaera sp.
Earlandia elegans (Rauzer-Chernousova)
Girvanella problematica Nicholson and Etheridge

Age: inadequate assemblage; probably Tournaisian.

(GSC loc. C-52292, 420.9 m) Yohin Formation, 7.2 m above base.

Archaeosphaera sp.
Calcisphaera sp.
Earlandia elegans (Rauzer-Chernousova)

Age: inadequate assemblage; probably Tournaisian.

(GSC loc. C-52293, 423.9 m) Yohin Formation, 10.2 m above base.

Calcisphaera sp.
Earlandia elegans (Rauzer-Chernousova)
Girvanella problematica Nicholson and Etheridge

Age: inadequate assemblage; probably Tournaisian.

(GSC loc. C-52297, 431.4 m) Yohin Formation, 17.7 m above base.

Calcisphaera laevis Williamson
Earlandia elegans (Rauzer-Chernousova)
Girvanella problematica Nicholson and Etheridge

Age: inadequate assemblage; probably Tournaisian.

Locality 2. Twisted Mountain; latitude 61°11'00"N, longitude 123°37'38"W, NTS 95 G/4; southwestern District of Mackenzie; Section 76MTA-BCR9 (GSC localities in metres above base of section).

(GSC loc. C-58993, 0.5 m) Yohin Formation, 128.9 m below top.

Calcisphaera laevis Williamson
Earlandia elegans (Rauzer-Chernousova)
Issinella sp.

Age: inadequate assemblage; probably Tournaisian.

(GSC loc. C-58995, 6.0 m) Yohin Formation, 123.4 m below top.

Archaeosphaera sp.
Calcisphaera laevis Williamson
Earlandia elegans (Rauzer-Chernousova)
Girvanella problematica Nicholson and Etheridge

Age: inadequate assemblage; probably Tournaisian.

(GSC loc. C-58996, 12.0 m) Yohin Formation, 117.4 m below top.

Archaeosphaera sp.
Girvanella problematica

Age: inadequate assemblage; probably Tournaisian.

(GSC loc. C-58998, 13.0 m) Yohin Formation, 116.4 m below top.

Calcisphaera sp.
Earlandia elegans (Rauzer-Chernousova)
Girvanella sp.

Age: inadequate assemblage; probably Tournaisian.

(GSC loc. C-58999, 14.0 m) Yohin Formation, 115.4 m below top.

Calcisphaera sp.
Issinella devonica Reitlinger
Girvanella problematica Nicholson and Etheridge

Age: inadequate assemblage; probably Tournaisian.

(GSC loc. C-59003, 28.0 m) Yohin Formation, 101.4 m below top.

Calcisphaera sp.
Calcisphaera laevis Williamson
Earlandia elegans (Rauzer-Chernousova)
Earlandia minima (Birina)
Quasiumbella sp.

Age: inadequate assemblage; probably Tournaisian.

(GSC loc. C-59024, 273.0 m) Prophet Formation, 9.2 m above base.

Calcisphaera laevis Williamson
Earlandia clavatula (Howchin)
Earlandia elegans (Rauzer-Chernousova)
Earlandia moderata (Malakhova)
Palaeoberesella lahuseni (von Möller)

Age: latest Tournaisian, zone 9.

(GSC loc. C-59030, 327 m) Flett Formation, 18.8 m above base.

Calcisphaera laevis Williamson
Calcisphaera pachysphaerica (Pronina)
Earlandia clavatula (Howchin)
Earlandia vulgaris (Rauzer-Chernousova and Reitlinger)
Endothyra sp.
Issinella sp.
Issinella devonica Reitlinger
Priscella sp.
Pseudotaxis sp.

Age: earliest Viséan, zone 10.

(GSC loc. C-59033, 338 m) Flett Formation, 29.8 m above base.

Calcisphaera pachysphaerica (Pronina)
Earlandia sp.
Endothyra sp.
Issinella sp.
Priscella sp.
Pseudotaxis sp.

Age: late early Viséan, zone 11.

(GSC loc. C-59038, 361 m) Flett Formation, 52.8 m above base.

Calcisphaera pachysphaerica (Pronina)
Dainella sp.
Earlandia clavatula (Howchin)
Earlandia vulgaris (Rauzer-Chernousova and Reitlinger)
Endothyra sp.
Eoendothyranopsis of the group *E. spiroides* (Zeller)
Eoforschia sp.
Globoendothyra sp.
Latiendothyra sp. ("Laxoendothyra" sp.)
Palaeoberesella sp.
Stacheoides sp.
Tetrataxis sp.

Age: late early Viséan, zone 11.

(GSC loc. C-59041, 365 m) Flett Formation, 56.8 m above base.

Brunsia sp.
Calcisphaera laevis Williamson
Calcisphaera pachysphaerica (Pronina)
Dainella sp.
Earlandia clavatula (Howchin)
Earlandia vulgaris (Rauzer-Chernousova and Reitlinger)
Earlandinella sp.
Endothyra sp.
Eoendothyranopsis of the group *E. spiroides* (Zeller)
Eoendothyranopsis spiroides (Zeller)
Eogloboendothyra sp.
Eoforschia sp.
Globoendothyra of the group *G. baileyi* (Hall)
Latiendothyra sp. ("Laxoendothyra" sp.)
Palaeoberesella sp.
Priscella of the group *P. prisca* (Rauzer-Chernousova and Reitlinger)
Pseudoammodiscus sp.
Pseudokamaena sp.
Septabrunsiia? sp.
"Septatourmayella" henbesti (Skipp, Holcomb and Gutschick)
Spinoendothyra? or *Planoendothyra*? sp.
Tetrataxis sp.

Age: late early Viséan, zone 11.

(GSC loc. C-59044, 368 m) Flett Formation, 59.8 m above base.

Calcisphaera laevis Williamson
Calcisphaera pachysphaerica (Pronina)
Earlandia vulgaris (Rauzer-Chernousova and Reitlinger)
Endothyra sp.
Eoendothyranopsis sp.
Eogloboendothyra sp.
Globoendothyra sp.
Latiendothyra sp.
Pseudoammodiscus sp.
Tetrataxis sp.

Age: late early Viséan, zone 11.

(GSC loc. C-59045, 392 m) Flett Formation, 83.8 m above base.

Earlandia clavatula (Howchin)
Earlandia vulgaris (Rauzer-Chernousova and Reitlinger)

Age: inadequate assemblage; late early to early middle Viséan.

(GSC loc. C-59047, 423.5 m) Flett Formation, 115.3 m above base.

Calcisphaera laevis Williamson
Calcisphaera pachysphaerica (Pronina)
Earlandia sp.
Endothyra sp.
Eoendothyranopsis spiroides (Zeller)
Kamaena sp.
Palaeoberesella sp.
Parathuramina sp.

Age: inadequate assemblage; late early to early middle Viséan.

(GSC loc. C-59048, 458 m) Flett Formation, 149.8 m above base.

Calcisphaera laevis Williamson
Calcisphaera pachysphaerica (Pronina)
Dainella anivikensis Mamet
Earlandia sp.
Endothyra sp.
Eoendothyranopsis hinduensis (Skipp in McKee and Gutschick)
Eoendothyranopsis spiroides (Zeller)
Eoforschia moelleri (Malakhova in Dain)
Girvanella problematica Nicholson and Etheridge
Globoendothyra paula (Vissarionova)
Planoendothyra rotayi (Lebedeva)
Priscella prisca (Rauzer-Chernousova and Reitlinger)
Pseudoammodiscus sp.

Age: early middle Viséan, zone 12.

(GSC loc. C-59052, 502 m) Flett Formation, 193.8 m above base.

Calcisphaera laevis Williamson
Calcisphaera pachysphaerica (Pronina)
Dainella anivikensis Mamet
Earlandia clavatula (Howchin)
Earlandia vulgaris (Rauzer-Chernousova and Reitlinger)
Endothyra sp.
Eoendothyranopsis scitula (Toomey)
Eoendothyranopsis of the group *E. spiroides* (Zeller)
Eoforschia sp.
Girvanella problematica Nicholson and Etheridge
Globoendothyra paula (Vissarionova)
Issinella sp.
Mametella skimoensis (Mamet and Rudloff)
Planoendothyra rotayi (Lebedeva)
Pseudoammodiscus sp.
Priscella devera
Priscella prisca (Rauzer-Chernousova and Reitlinger)
Tetrataxis sp.

Age: early to late middle Viséan; zones 12/13, passage of 12 to 13.

(GSC loc. C-59053, 515 m) Flett Formation, 206.8 m above base.

Calcisphaera sp.
Eoendothyranopsis sp.
Globoendothyra sp.

Age: inadequate assemblage; middle Viséan.

(GSC loc. C-59056, 541 m) Flett Formation, 232.8 m above base.

Calcisphaera pachysphaerica (Pronina)
Earlandia clavatula (Howchin)
Earlandia vulgaris (Rauzer-Chernousova and Reitlinger)
Endothyra sp.
Endothyranella sp.
Eoendothyranopsis of the group *E. pressa* and *E. rara* (Grozdilova in Lebedeva)
Eoendothyranopsis cf. *E. prodigiosa* (Armstrong)
Eoendothyranopsis scitula (Toomey)
Eoforschia moelleri (Malakhova in Dain)
Globoendothyra paula (Vissarionova)
Septabrunciina? sp.
Skippella sp.
Priscella sp.
Tetrataxis sp.

Age: late middle Viséan, zone 13.

(GSC loc. C-59059, 552 m) Flett Formation, 243.8 m above base.

Calcisphaera sp.
Earlandia sp.
Endothyra of the group *E. bowmani* Phillips in Brown emend. Brady
Eoendothyranopsis sp.
Eoforschia sp.
Globoendothyra sp.
Parathuramina sp.
Pseudoammodiscus priscus (Rauzer-Chernousova)

Age: late middle Viséan, zone 13.

(GSC loc. C-59061, 570 m) Flett Formation, 261.8 m above base.

Asphaltina sp.
Brunsia sp.
Calcisphaera pachysphaerica (Pronina)
Earlandia vulgaris (Rauzer-Chernousova and Reitlinger)
Endothyra sp.
Eoendothyranopsis sp.
Eoendothyranopsis of the group *E. ermakiensis* (Grozdilova in Lebedeva)
Globoendothyra paula (Vissarionova)
Skippella sp.

Age: latest middle Viséan or possibly slightly younger, zone 13 or slightly younger.

(GSC loc. C-59060, 571 m) Flett Formation, 262.8 m above base.

Brunsia sp.
Calcisphaera pachysphaerica (Pronina)
Earlandia vulgaris (Rauzer-Chernousova and Reitlinger)
Endothyra of the group *E. bowmani* Phillips in Brown emend. Brady
Eoendothyranopsis sp.
Eoendothyranopsis of the group *E. ermakiensis* (Grozilova in Lebedeva)
Fasciella? sp.
Globoendothyra paula (Vissarionova)
Priscella sp.
Skippella sp.
Stacheoides tenuis Petryk and Mamet

Age: latest middle Viséan or possibly slightly younger, zone 13 or slightly younger.

(GSC loc. C-59063, 580 m) Flett Formation, 271.8 m above base.

Aoujgalia sp.
Calcisphaera sp.
Earlandia sp.
Eoendothyranopsis sp.
Eoforschia sp.
Globoendothyra sp.
Tetrataxis sp.

Age: latest middle Viséan or possibly slightly younger, zone 13 or slightly younger.

Locality 3. North end of Mattson anticline; latitude 61°06'38"N, longitude 123°45'54"W, NTS 95 G/4; southwestern District of Mackenzie; composite section 75MTA-BCR 4, 5, and 6 (GSC localities in metres above base of section).

(GSC loc. C-52200, 347.8 m) Prophet Formation, 106.5 m above base.

Archaeosphaera sp.
Calcisphaera laevis Williamson
Earlandia elegans (Rauzer-Chernousova)
Earlandia moderata (Malakhova)
Parathurammina sp.
Trochiliscus surmilovae Toyarkov

Age: latest Tournaisian, probably zone 9.

(GSC loc. C-52202, 365.1 m) Prophet Formation, 123.8 m above base.

Archaeosphaera sp.
Calcisphaera laevis Williamson
Earlandia clavatula (Howchin)
Earlandia elegans (Rauzer-Chernousova)
Earlandia moderata (Malakhova)
Girvanella problematica Nicholson and Etheridge
Latiendothyra sp. ("*Laxoendothyra*" sp.)
Priscella sp.
Septabruntiina sp.
Septaglomospiranella sp.

Age: latest Tournaisian, zone 9.

(GSC loc. C-52214, 439.4 m) Flett Formation, 46.6 m above base.

Calcisphaera laevis Williamson
Earlandia vulgaris (Rauzer-Chernousova and Reitlinger)
Earlandia clavatula (Howchin)
Endothyra sp.
Eoforschia sp.
Latiendothyra sp.
Parathurammina sp.
Priscella sp.
Pseudotaxis sp.

Age: earliest Viséan, zone 10.

(GSC loc. C-52226, 513.8 m) Flett Formation, 121 m above base.

Calcisphaera laevis Williamson
Calcisphaera pachysphaerica (Pronina)
Earlandia sp.
Endothyra sp.
Eogloboendothyra sp.
Globoendothyra of the group *G. baileyi* (Hall)
Latiendothyra sp.
Septaglomospiranella? sp.
Stacheoides sp.

Age: early Viséan, zone 11(?).

(GSC loc. C-52235, 561 m) Flett Formation, 168.2 m above base.

Calcisphaera sp.
Earlandia sp.
Earlandia vulgaris (Rauzer-Chernousova and Reitlinger)
Endothyra sp.
Eoendothyranopsis of the group *E. spiroides* (Zeller)
Eoforschia sp.
Globoendothyra paula (Vissarionova)
Kamaena sp.
Latiendothyra? sp.
Palaeoberesella sp.
Uviella sp.

Age: early middle Viséan, zone 12.

(GSC loc. C-52237, 572.9 m) Flett Formation, 180.1 m above base.

Calcisphaera sp.
Earlandia vulgaris (Rauzer-Chernousova and Reitlinger)
Endothyra sp.
Endothyranella sp.
Globoendothyra paula (Vissarionova)
Mametella? sp.
Priscella sp.
Tetrataxis sp.

Age: early middle Viséan, zone 12.

(GSC loc. C-52255, 627.8 m) Flett Formation, 235 m above base.

Calcisphaera pachysphaerica (Pronina)
Earlandia vulgaris (Rauzer-Chernousova and Reitlinger)
Endothyra sp.
Eoendothyranopsis scitula (Toomey)
Eoendothyranopsis of the group *E. spiroides* (Zeller)
Globoendothyra paula (Vissarionova)
Mametella sp.
Tetrataxis sp.

Age: early to late middle Viséan; zones 12/13, passage of 12 to 13.

(GSC loc. C-52263, 649.7 m) Flett Formation, 256.9 m above base.

Calcisphaera laevis Williamson
Calcisphaera pachysphaerica (Pronina)
Earlandia vulgaris (Rauzer-Chernousova and Reitlinger)
Endothyra of the group *E. bowmani* Phillips in Brown emend. Brady
Endothyranella sp.
Endothyranopsis sp.
Eoendothyranopsis prodigiosa (Armstrong)
Eoendothyranopsis scitula (Toomey)
Eoendothyranopsis thompsoni (Anisgard and Campau)
Eoforschia sp.
Globoendothyra paula (Vissarionova)
Septabrunsiina mackeei Skipp in Skipp, Holcomb and Gutschick
Skippella sp.
Stacheoides tenuis Petryk and Mamet
Tetrataxis sp.

Age: late middle Viséan, zone 13.

(GSC loc. C-52259, 653.3 m) Flett Formation, 260.5 m above base.

Calcisphaera sp.
Endothyra sp.
Endothyranella sp.
Eoendothyranopsis scitula (Toomey)
Eoforschia sp.
Priscella sp.
Tetrataxis sp.

Age: late middle Viséan, zone 13.

(GSC loc. C-52264, 688.3 m) Flett Formation, 295.5 m above base.

Calcisphaera pachysphaerica (Pronina)
Earlandia vulgaris (Rauzer-Chernousova and Reitlinger)
Endothyra of the group *E. bowmani* Phillips in Brown emend. Brady
Endothyranella sp.
Eoendothyranopsis sp.
Eoendothyranopsis prodigiosa (Armstrong)
Eoendothyranopsis scitula (Toomey)
Eoendothyranopsis of the group *E. ermakiensis* (Lebedeva)
Epistacheoides sp.
Globoendothyra sp.

Skippella sp.
Stacheoides sp.

Age: late middle Viséan, zone 13.

(GSC loc. C-52267, 700.8 m) Flett Formation, 308 m above base.

Calcisphaera laevis Williamson
Calcisphaera pachysphaerica (Pronina)
Earlandia clavatula (Howchin)
Earlandia vulgaris (Rauzer-Chernousova and Reitlinger)
Endothyra of the group *E. bowmani* Phillips in Brown emend. Brady
Endothyranella sp.
Eoendothyranopsis scitula (Toomey)
Eoendothyranopsis thompsoni (Anisgard and Campau)
Eoforschia sp.
Globoendothyra sp.
Septabrunsiina sp.
Stacheoides sp.
Tetrataxis sp.

Age: late middle Viséan, zone 13.

(GSC loc. C-52273, 730 m) Flett Formation, 337.2 m above base.

Calcisphaera sp.
Earlandia sp.
Endothyra similis Rauzer-Chernousova and Reitlinger
Endothyra of the group *E. bowmani* Phillips in Brown emend. Brady
Endothyra sp.
Endothyranopsis sp.
Eoendothyranopsis ermakiensis (Lebedeva)
Tetrataxis sp.

Age: latest middle Viséan or possibly slightly younger, zone 13 or possibly slightly younger.

(GSC loc. C-52275, 737.6 m) Flett Formation, 344.8 m above base.

Calcisphaera sp.
Earlandia sp.
Endothyra sp.
Endothyra of the group *E. bowmani* Phillips in Brown emend. Brady
Globoendothyra sp.
Priscella sp.
Tetrataxis sp.

Age: latest middle Viséan or possibly slightly younger, zone 13 or possibly slightly younger.

Locality 4. Jackfish Gap, latitude 61°05'54"N, longitude 123°59'26"W, NTS 95 G/4; southwestern District of Mackenzie; composite section 75MTA-BCR1, 2, and 3 (GSC localities in metres above base of section).

(GSC loc. C-52072, 492 m) Flett Formation, 14.6 m above base.

Archaeosphaera sp.
Calcisphaera laevis Williamson

Calcisphaera cf. *C. pachysphaerica* (Pronina)
Earlandia clavatula (Howchin)
Earlandia elegans (Rauzer-Chernousova)
Earlandia cf. *E. minima* (Bisina)
Endothyra sp.
Latiendothyra sp. ("*Laxoendothyra*" sp.)
Palaeoberesella sp.
Priscella sp.
Septabrinsiina parakrainica Skipp in Skipp, Holcomb
and Gutschick
Septabrinsiina sp.
Septaglomospiranella dainae Lipina
Septatourmayella sp.
Spinoendothyra sp.

Age: latest Tournaisian, zone 9.

(GSC loc. C-52091, 550.5 m) Flett Formation, 73.1 m
above base.

Archaeosphaera sp.
Calcisphaera pachysphaerica (Pronina)
Calcisphaera sp.
Earlandia clavatula (Howchin)
Earlandia vulgaris (Rauzer-Chernousova and
Reitlinger)
Endothyra sp.
Eoforschia sp.
Eoglobendothyra sp.
Girvanella problematica Nicholson and Etheridge
Girvanella staminea Garwood
Latiendothyra sp.
Priscella of the group *P. prisca* (Rauzer-Chernousova
and Reitlinger)
Pseudotaxis sp.
Septabrinsiina sp.
Septatourmayella pseudocamerata (Lipina in Lebedeva)
Spinoendothyra sp.
Tetrataxis sp.

Age: earliest Viséan, zone 10.

(GSC loc. C-52103, 598.3 m) Flett Formation, 120.9 m
above base.

Calcisphaera laevis Williamson
Calcisphaera pachysphaerica (Pronina)
Earlandia clavatula (Howchin)
Earlandia moderata (Malakhova)
Earlandia vulgaris (Rauzer-Chernousova and
Reitlinger)
Eoglobendothyra sp.
Mametella sp.

Age: inadequate assemblage; early Viséan.

(GSC loc. C-52110, 636.9 m) Flett Formation, 159.5 m
above base.

Calcisphaera pachysphaerica (Pronina)
Earlandia clavatula (Howchin)
Endothyra sp.
Mametella sp.
Septaglomospiranella sp.
Septatourmayella sp.

Age: late early Viséan, zone 11.

(GSC loc. C-52112, 649.4 m) Flett Formation, 172 m
above base.

Calcisphaera laevis Williamson
Calcisphaera pachysphaerica (Pronina)
Earlandia clavatula (Howchin)
Earlandia vulgaris (Rauzer-Chernousova and
Reitlinger)
Mametella sp.
Priscella sp.

Age: inadequate assemblage; early to middle
Viséan.

(GSC loc. C-52114, 659.4 m) Flett Formation, 182 m
above base.

Calcisphaera laevis Williamson
Calcisphaera pachysphaerica (Pronina)
Earlandia clavatula (Howchin)
Earlandia elegans (Rauzer-Chernousova)
Earlandia vulgaris (Rauzer-Chernousova and
Reitlinger)
Endothyra sp.
Eoendothyranopsis of the group *E. spiroides* (Zeller)
Globoendothyra of the group *G. baileyi* (Hall)
Latiendothyra sp. ("*Laxoendothyra*")
Mametella sp.
Priscella sp.
Septaglomospiranella sp.
Stacheoides sp.

Age: inadequate assemblage; late early to early
middle Viséan.

(GSC loc. C-52117, 688.8 m) Flett Formation, 211.4 m
above base.

Calcisphaera sp.
Earlandia sp.
Endothyra sp.
Mametella sp.
Priscella sp.
Stacheoides sp.

Age: inadequate assemblage; probably early middle
Viséan.

(GSC loc. C-52121, 697.8 m) Flett Formation, 220.4 m
above base.

Calcisphaera sp.
Earlandia sp.
Endothyra sp.
Mametella sp.
Priscella sp.
Stacheoides sp.

Age: inadequate assemblage; probably early middle
Viséan.

(GSC loc. C-52122, 698.8 m) Flett Formation, 221.4 m
above base.

Calcisphaera laevis Williamson
Calcisphaera pachysphaerica (Pronina)
Earlandia clavatula (Howchin)

Earlandia vulgaris (Rauzer-Chernousova and Reitlinger) (very abundant)
Endothyra sp.
Latiendothyra? sp.
Mametella sp.
Stacheoides sp.
Tetrataxis sp.

Age: inadequate assemblage; probably early middle Viséan.

(GSC loc. C-52123, 700 m) Flett Formation, 222.6 m above base.

Calcisphaera laevis Williamson
Calcisphaera pachysphaerica (Pronina)
Diplosphaerina sp.
Earlandia vulgaris (Rauzer-Chernousova and Reitlinger)
Endothyra sp.
Mametella sp.
Latiendothyra? sp.
Pseudotaxis sp.
Stacheoides sp.
Tetrataxis sp.

Age: inadequate assemblage; probably early middle Viséan.

(GSC loc. C-52132, 702.6 m) Flett Formation, 225.2 m above base.

Calcisphaera sp.
Earlandia vulgaris (Rauzer-Chernousova and Reitlinger)
Endothyra sp.
Eoendothyranopsis sp.
Eogloboendothyra sp.
Globoendothyra sp.
Mametella sp.
Priscella sp.

Age: inadequate assemblage; probably early middle Viséan.

(GSC loc. C-52129, 732.8 m) Flett Formation, 255.4 m above base.

Brunsiina sp.
Calcisphaera laevis Williamson
Calcisphaera pachysphaerica (Pronina)
Diplosphaerina sp.
Earlandia clavatula (Howchin)
Earlandia moderata (Malakhova)
Earlandia vulgaris (Rauzer-Chernousova and Reitlinger)
Endothyra sp.
Eoendothyranopsis of the group *E. spiroides*? (Zeller)
Eoendothyranopsis scitula (Toomey)
Eoendothyranopsis thompsoni (Anisgard and Campau)
Eoforschia sp.
Eogloboendothyra sp.
Globoendothyra paula (Vissarionova)
Globoendothyra of the group *G. tomiliensis* (Lebedeva)
Globoendothyra sp.
Issinella sp.
Mametella sp.
Planoendothyra sp.
Planoendothyra rotayi (Lebedeva)

Priscella sp.
Pseudoammodiscus sp.
Pseudotaxis sp.
Skippella sp.
Stacheoides tenuis Petryk and Mamet
"Septatournayella" sp.
Tetrataxis sp.

Age: early to late middle Viséan; zones 12/13, passage of 12 to 13.

(GSC loc. C-52131, 739 m) Flett Formation, 261.6 m above base.

Calcisphaera laevis Williamson
Calcisphaera pachysphaerica (Pronina)
Earlandia vulgaris (Rauzer-Chernousova and Reitlinger)
Eoendothyranopsis scitula (Toomey)
Eoendothyranopsis of the group *E. spiroides*? (Zeller)
Eoendothyranopsis thompsoni (Anisgard and Campau)
Eoforschia sp.
Globoendothyra of the group *G. tomiliensis* (Lebedeva)
Priscella sp.

Age: early to late middle Viséan; zones 12/13, passage of 12 to 13.

(GSC loc. C-52138, 767.8 m) Flett Formation, 290.4 m above base.

Calcisphaera sp.
Earlandia vulgaris (Rauzer-Chernousova and Reitlinger)
Endothyra sp.
Endothyra of the group *E. bowmani* Phillips in Brown emend. Brady
Eoendothyranopsis scitula (Toomey)
Eoforschia sp.
Globoendothyra paula (Vissarionova)
Globoendothyra sp.
Pseudotaxis sp.
Stacheoides sp.
Tetrataxis sp.

Age: late middle Viséan, zone 13.

(GSC loc. C-52139, 775.8 m) Flett Formation, 298.4 m above base.

Calcisphaera pachysphaerica (Pronina)
Earlandia vulgaris (Rauzer-Chernousova and Reitlinger)
Endothyra the group *E. bowmani* Phillips in Brown emend. Brady
Endothyra similis Rauzer-Chernousova and Reitlinger
Eoendothyranopsis scitula (Toomey)
Eoendothyranopsis of the group *E. ermakiensis* (Lebedeva)
Eoforschia moelleri (Malakhova in Dain)
Globoendothyra paula (Vissarionova)
Mametella sp.
Priscella sp.
Stacheoides sp.
Tetrataxis sp.

Age: late middle Viséan, zone 13.

(GSC loc. C-52145, 781 m) Flett Formation, 303.6 m above base.

Endothyra of the group *E. bowmani* Phillips in Brown emend. Brady
Eoendothyranopsis scitula (Toomey)
Globoendothyra paula (Vissarionova)
Priscella sp.

Age: late middle Viséan, zone 13.

(GSC loc. C-52147, 789 m) Flett Formation, 311.6 m above base.

Calcisphaera pachysphaerica (Pronina)
Earlandia vulgaris (Rauzer-Chernousova and Reitlinger)
Eoendothyranopsis scitula (Toomey)
Eoendothyranopsis of the group *E. ermakiensis* (Lebedeva)
Globoendothyra paula (Vissarionova)
Mametella sp.
Priscella sp.
Tetrataxis sp.

Age: late middle Viséan, zone 13.

(GSC loc. C-52148, 794.8 m) Flett Formation, 317.4 m above base.

Calcisphaera sp.
Earlandia vulgaris (Rauzer-Chernousova and Reitlinger)
Endothyra sp.
Endothyra of the group *E. bowmani* Phillips in Brown emend. Brady
Eoendothyranopsis scitula (Toomey)
Epistacheoides sp.
Globoendothyra paula (Vissarionova)
Mametella? sp.
Palaeoberesella sp.
Priscella sp.
Stacheoides sp.

Age: late middle Viséan, zone 13.

(GSC loc. C-52149, 796 m) Flett Formation, 318.6 m above base.

Calcisphaera pachysphaerica (Pronina)
Earlandia vulgaris (Rauzer-Chernousova and Reitlinger)
Endothyra sp.
Eoendothyranopsis sp.
Palaeoberesella sp.
Pseudotaxis sp.
Tetrataxis sp.

Age: late middle Viséan, zone 13.

(GSC loc. C-52151, 806.6 m) Flett Formation, 329.2 m above base.

Calcisphaera pachysphaerica (Pronina)
Earlandia vulgaris (Rauzer-Chernousova and Reitlinger)
Endothyra similis Rauzer-Chernousova and Reitlinger
Eoendothyranopsis sp.

Epistacheoides sp.
Globoendothyra sp.
Skippella sp.

Age: latest middle Viséan or possibly slightly younger, zone 13 or possibly slightly younger.

(GSC loc. C-52154, 814 m) Flett Formation, 336.6 m above base.

Calcisphaera pachysphaerica (Pronina)
Earlandia sp.
Endothyra sp.
Globoendothyra sp.
Planoendothyra sp.
Priscella sp.

Age: latest middle Viséan or possibly slightly younger, zone 13 or possibly slightly younger.

(GSC loc. C-52155, 819.4 m) Flett Formation, 342 m above base.

Earlandia sp.
Globoendothyra sp.
Pseudostacheoides sp.
Pseudotaxis sp.

Age: latest middle Viséan or possibly slightly younger, zone 13 or possibly slightly younger.

(GSC loc. C-52156, 821.3 m) Flett Formation, 343.9 m above base.

Earlandia sp.
Endothyra sp.
Eoendothyranopsis scitula (Toomey)
Globoendothyra paula (Vissarionova)
Issinella sp.
Planoendothyra sp.
Priscella sp.
Skippella sp.
Tetrataxis sp.

Age: latest middle Viséan or possibly slightly younger, zone 13 or possibly slightly younger.

Locality 5. Northeastern corner Tlogotsho Plateau; latitude 61°03'55"N, longitude 124°07'08"W, NTS 95 F/1; southwestern District of Mackenzie; Section 78BCR1 (GSC localities in metres above base of section).

(GSC loc. C-74243, 731 m) Flett Formation, 40 m above base.

Endothyra sp.
Latiendothyra sp.
Mametella skimoensis (Mamet and Rudloff)
Priscella sp.
Rectopriscella sp.

Age: inadequate assemblage; early to early middle Viséan.

(GSC loc. C-74248, 755.5 m) Flett Formation, 64.5 m above base.

Calcisphaera sp.
Earlandia clavatula (Howchin)
Mametella skimoensis (Mamet and Rudloff)

Age: inadequate assemblage; early to early middle Viséan.

(GSC loc. C-74249, 766.5 m) Flett Formation, 75.5 m above base.

Calcisphaera pachysphaerica (Pronina)
Calcisphaera sp.
Earlandia vulgaris (Rauzer-Chernousova and Reitlinger)
Earlandia sp.
Endothyra sp.
Eoendothyranopsis sp.
Eoforschia sp.
Globoendothyra paula (Vissarionova)
Globoendothyra sp.
Mametella sp.
Priscella sp.
Pseudotaxis sp.
Rectopriscella sp.
Tetrataxis angusta (Vissarionova)
Trochiliscus sp.

Age: early middle Viséan, zone 12.

(GSC loc. C-74251, 789.5 m) Flett Formation, 98.5 m above base.

Calcisphaera pachysphaerica (Pronina)
Earlandia vulgaris (Rauzer-Chernousova and Reitlinger)
Endothyra sp.
Pseudotaxis sp.
Tetrataxis angusta (Vissarionova)

Age: inadequate assemblage; middle Viséan.

(GSC loc. C-74252, 796.5 m) Flett Formation, 105.5 m above base.

Calcisphaera sp.
Earlandia sp.
Endothyra sp.
Globoendothyra sp.

Age: inadequate assemblage; middle Viséan.

(GSC loc. C-74260, 860 m) Flett Formation, 169.1 m above base.

Earlandia vulgaris (Rauzer-Chernousova and Reitlinger)
Endothyra sp.
Eoendothyranopsis sp.
Globoendothyra sp.

Age: inadequate assemblage; middle Viséan.

(GSC loc. C-74261, 868 m) Flett Formation, 177 m above base.

Earlandia vulgaris (Rauzer-Chernousova and Reitlinger)
Endothyra sp.
Globoendothyra sp.
Priscella sp.
Pseudotaxis sp.
Tetrataxis sp.

Age: inadequate assemblage; middle Viséan.

(GSC loc. C-74262, 882.5 m) Flett Formation, 191.5 m above base.

Mametella skimoensis (Mamet and Rudloff)
Priscella sp.

Age: inadequate assemblage; middle Viséan.

(GSC loc. C-74265, 903 m) Flett Formation, 212 m above base.

Asphaltina sp.
Endothyra sp.
Eoendothyranopsis of the group *E. rara* (Grozdilova in Lebedeva)
Eoendothyranopsis scitula (Toomey)
Globoendothyra sp.
Globoendothyra paula (Vissarionova)
Priscella sp.
Skippella sp.
Stacheoides meandriiformis Petryk and Mamet

Age: late middle Viséan, zone 13.

(GSC loc. C-74267, 915 m) Flett Formation, 224 m above base.

Earlandia sp.
Priscella sp.
Tetrataxis sp.

Age: insufficient assemblage; probably late middle Viséan.

Locality 6. Ram Creek; latitude 61°09'50"N, longitude 124°24'47"W, NTS 95 F/1; southwestern District of Mackenzie; Section 75MTA-BCR8 (GSC localities in metres above base of section).

(GSC loc. C-52308, 47 m) Prophet Formation, 156.6 m below top.

Calcisphaera laevis Williamson
Calcisphaera pachysphaerica (Pronina)
Earlandia clavatula (Howchin)
Earlandia vulgaris (Rauzer-Chernousova and Reitlinger)
Mametella sp.
Priscella sp.

Age: earliest Viséan, zone 10.

(GSC loc. C-52316, 126.5 m) Prophet Formation, 77.1 m below top.

Calcisphaera sp.
Earlandia vulgaris (Rauzer-Chernousova and Reitlinger)
Endothyra sp.
Eogloboendothyra sp.
Priscella sp.
Tetrataxis sp.
Trochiliscus surmilovae Toyarkov

Age: inadequate assemblage; early to middle Viséan.

(GSC loc. C-52320, 162.5 m) Prophet Formation, 41.1 m below top.

Earlandia vulgaris (Rauzer-Chernousova and Reitlinger)
Earlandia sp.
Endothyra sp.
Eoendothyranopsis scitula (Toomey)
Globoendothyra sp.
Priscella sp.

Age: late middle Viséan, zone 13.

(GSC loc. C-52323, 190.1 m) Prophet Formation, 13.5 m below top.

Calcisphaera pachysphaerica (Pronina)
Earlandia vulgaris (Rauzer-Chernousova and Reitlinger)
Endothyra bowmani Phillips emend. Brady
Eoendothyranopsis of the group *E. pressa* and *E. rara* (Grozilova in Lebedeva)
Mametella skimoensis (Mamet and Rudloff)
Priscella sp.
Pseudotaxis sp.
Tetrataxis sp.

Age: late middle Viséan, zone 13.

(GSC loc. C-52324, 203 m) Prophet Formation, 0.6 m below top.

Earlandia sp.
Priscella sp.
Radiospheres
Tetrataxis sp.

Age: inadequate assemblage; probably late middle Viséan.

Locality 7. Sheaf Creek, latitude 61°12'23"N, longitude 124°33'32"W, NTS 95 F/2; southwestern District of Mackenzie; Section 75MTA-BCR11 (GSC localities in metres above base of section).

(GSC loc. C-52458, 204.5 m) Prophet Formation, 35 m below top.

Earlandia vulgaris (Rauzer-Chernousova and Reitlinger)
Endothyra sp.
Eogloboendothyra sp.

Mametella sp.
Tetrataxis sp.

Age: inadequate assemblage; zone 10 or younger, earliest Viséan or younger.

(GSC loc. C-52461, 241 m) Flett Formation, 1.5 m above base.

Calcisphaera pachysphaerica (Pronina)
Earlandia clavatula (Howchin)
Earlandia vulgaris (Rauzer-Chernousova and Reitlinger)
Endothyra sp.
"Endothyranella" sp.
Eoendothyranopsis of the group *E. spiroides* (Zeller)
Eoparastaffella sp.
Globoendothyra sp.
Mametella sp.
Pseudotaxis sp.
Stacheoides sp.

Age: early to middle Viséan, zones 11 or 12, most probably 11.

(GSC loc. C-52469, 275 m) Flett Formation, 35.5 m above base.

Calcisphaera laevis Williamson
Calcisphaera pachysphaerica (Pronina)
Earlandia vulgaris (Rauzer-Chernousova and Reitlinger)
Endothyra sp.
Eoendothyranopsis sp.
Globoendothyra paula (Vissarionova)
Mametella sp.
Priscella sp.
Pseudotaxis sp.
Tetrataxis sp.

Age: early middle Viséan, zone 12.

(GSC loc. C-52470, 286.2 m) Flett Formation, 46.7 m above base.

Calcisphaera laevis Williamson
Calcisphaera pachysphaerica (Pronina)
Earlandia clavatula (Howchin)
Earlandia vulgaris (Rauzer-Chernousova and Reitlinger)
Endothyra sp.
Endothyranella sp.
Eogloboendothyra sp.
Eoendothyranopsis sp.
Globoendothyra paula (Vissarionova)
Mametella sp.
Priscella sp.
Pseudotaxis sp.

Age: early middle Viséan, zone 12.

(GSC loc. C-52484, 324 m) Flett Formation, 84.5 m above base.

Calcisphaera pachysphaerica (Pronina)
Earlandia vulgaris (Rauzer-Chernousova and Reitlinger)
Endothyra sp.

Globoendothyra paula (Vissarionova)
Latiendothyra? sp.
Priscella sp.
Parathurammina sp.

Age: inadequate assemblage; middle Viséan.

(GSC loc. C-57129, 349 m) Flett Formation, 109.5 m above base.

Endothyra sp.
Globoendothyra sp.
Mametella sp.
Paracalligelloides sp.
Priscella sp.
Tetrataxis sp.

Age: inadequate assemblage; middle Viséan.

(GSC loc. C-52493, 353.3 m) Flett Formation, 113.8 m above base.

Calcisphaera pachysphaerica (Pronina)
Earlandia sp.
Endothyra of the group *E. similis* Rauzer-Chernousova and Reitlinger
Eoendothyranopsis of the group *E. pressa* and *E. rara* (Grozdilova in Lebedeva)
Globoendothyra paula (Vissarionova)
Priscella sp.
Pseudotaxis sp.
Planoendothyra sp.
Skippella sp.
Stacheoides sp.
Tetrataxis sp.

Age: late middle Viséan, zone 13.

(GSC loc. C-52496, 365 m) Golata Formation, 7 m above base.

Calcisphaera sp.
Endothyra sp.
Priscella sp.
Pseudotaxis sp.
Tetrataxis sp.

Age: inadequate assemblage; probably late middle Viséan.

Locality 10. Central Liard Range; latitude 60°45'15"N, longitude 123°55'27"W, NTS 95 B/12; southwestern District of Mackenzie; Section 76MTA-BCR8 (GSC localities in metres above base of section).

(GSC loc. C-58955, 8.2 m) Prophet Formation, 195.5 m below top.

Earlandia clavatula (Howchin)
Earlandia elegans (Rauzer-Chernousova)
Endothyra sp.
Latiendothyra sp.
Mametella sp.
Priscella sp.

Age: latest Tournaisian, zone 9.

(GSC loc. C-58965, 90.2 m) Prophet Formation, 113.5 m below top.

Calcisphaera laevis Williamson
Earlandia clavatula (Howchin)
Earlandia vulgaris (Rauzer-Chernousova and Reitlinger)
Eogloboendothyra sp.
Priscella sp.
Pseudotaxis sp.

Age: earliest Viséan, zone 10.

(GSC loc. C-58978, 207.2 m) Flett Formation, 3.5 m above base.

Calcisphaera sp.
Earlandia sp.
Kamaena sp.
Globoendothyra sp.
Latiendothyra sp.

Age: inadequate assemblage; early to middle Viséan.

(GSC loc. C-58979, 211.2 m) Flett Formation, 7.5 m above base.

Calcisphaera sp.
Earlandia clavatula (Rauzer-Chernousova and Reitlinger)
Mametella sp.
Stacheoides tenuis Petryk and Mamet
Tetrataxis sp.

Age: inadequate assemblage; early to middle Viséan.

(GSC loc. C-58981, 225.2 m) Flett Formation, 21.5 m above base.

Calcisphaera laevis Williamson
Calcisphaera pachysphaerica (Pronina)
Earlandia vulgaris (Rauzer-Chernousova and Reitlinger)
Endothyra sp.
Eoendothyranopsis scitula (Toomey)
Eogloboendothyra sp.
Globoendothyra sp.
Globoendothyra paula (Vissarionova)
Priscella sp.
Pseudoammodiscus sp.
Pseudotaxis sp.
Stacheoides sp.
Tetrataxis sp.

Age: late middle Viséan, zone 13.

(GSC loc. C-58987, 266.2 m) Flett Formation, 62.5 m above base.

Calcisphaera sp.
Earlandia vulgaris (Rauzer-Chernousova and Reitlinger)
Endothyra sp.
Eoendothyranopsis prodigiosa (Armstrong)
Eoendothyranopsis scitula (Toomey)
Eoforschia sp.

Mametella sp.
Stacheoides? sp.
Tetrataxis sp.

Age: late middle Viséan, zone 13.

(GSC loc. C-58988, 271.2 m) Flett Formation, 67.5 m above base.

Calcisphaera sp.
Earlandia sp.
Endothyra sp.
Endothyra of the group *E. bowmani* Phillips in Brown
emend. Brady
Eoendothyranopsis scitula (Toomey)
Eoforschia sp.
Globoendothyra sp.
Priscella sp.
Pseudotaxis sp.

Age: late middle Viséan, zone 13.

Locality 11. North end Flett anticline; latitude 60°41'20"N, longitude 123°48'20"W, NTS 95 B/12; southwestern District of Mackenzie; Section 75MTA-BCR12 (GSC localities in metres above base of section).

(GSC loc. C-52507, 81.5 m) Besa River Formation, 149 m below top.

Archaeosphaera sp.
Calcisphaera laevis Williamson
Earlandia elegans (Rauzer-Chernousova)
Girvanella? sp.

Age: inadequate assemblage; probably Tournaisian.

(GSC loc. C-58554, 428 m) Prophet Formation, 197.5 m above base.

Earlandia elegans (Rauzer-Chernousova)
Earlandia vulgaris (Rauzer-Chernousova and
Reitlinger)
Mametella sp.

Age: inadequate assemblage; probably Tournaisian.

Locality 12. West flank Flett anticline; latitude 60°33'50"N, longitude 123°48'20"W, NTS 95 B/12; southwestern District of Mackenzie; Section 75MTA-BCR10 (GSC localities in metres above base of section).

(GSC loc. C-52372, 90.7 m) Clausen Formation, 41.7 m above base.

Archaeosphaera sp.
Calcisphaera laevis Williamson
Septaglomospiranella of the group *S. primaeva*
(Chernysheva) (non Rauzer-Chernousova)

Age: inadequate assemblage; Tournaisian.

(GSC loc. C-52385, 407.5 m) Prophet Formation, 138.5 m above base.

Asphaltinella sp.
Latiendothyra sp.
Mametella? sp.
Stacheins

Age: inadequate assemblage; probably middle to late Tournaisian.

Mametella is unknown before the Osagean, and
Asphaltinella is usually common in middle
Osagean.

(GSC loc. C-52482, 428.8 m) Prophet Formation, 159.8 m above base.

Calcisphaera sp.
Earlandia sp.
Mametella sp.
Stacheins

Age: inadequate assemblage; probably middle to late Tournaisian.

(GSC loc. C-52399, 572.5 m) Flett Formation, 23.5 m above base.

Calcisphaera laevis Williamson
Earlandia clavatula (Howchin)
"Endothyranella" sp.
Mametella sp.
Latiendothyra sp.
Priscella sp.
Spinoendothyra sp.

Age: latest Tournaisian, zone 9.

(GSC loc. C-52404, 594.7 m) Flett Formation, 45.7 m above base.

Calcisphaera laevis Williamson
Calcisphaera pachysphaerica (Pronina)
Earlandia clavatula (Howchin)
Earlandia vulgaris (Rauzer-Chernousova and
Reitlinger) (abundant)
Endothyra sp.
Latiendothyra sp. ("*Laxoendothyra*" sp.)
Mametella sp.
Priscella sp.
Spinoendothyra sp. (relict)

Age: earliest Viséan, zone 10.

(GSC loc. C-52409, 617.5 m) Flett Formation, 68.5 m above base.

Calcisphaera sp.
Endothyra sp.
Eogloboendothyra sp.
Mametella sp.
Priscella sp.

Age: inadequate assemblage; early to middle Viséan.

(GSC loc. C-52412, 660 m) Flett Formation, 111 m above base.

Earlandia vulgaris (Rauzer-Chernousova and Reitlinger)
Endothyra sp.
Globoendothyra sp.
Latiendothyra sp.
Priscella sp.
Pseudotaxis sp.

Age: inadequate assemblage; early to middle Viséan.

(GSC loc. C-52417, 690 m) Flett Formation, 141 m above base.

Calcisphaera laevis Williamson
Calcisphaera pachysphaerica (Pronina)
Earlandia vulgaris (Rauzer-Chernousova and Reitlinger)
Endothyra sp.
Globoendothyra sp.
Priscella sp.

Age: inadequate assemblage; early to middle Viséan.

(GSC loc. C-52422, 719 m) Flett Formation, 170 m above base.

Calcisphaera laevis Williamson
Calcisphaera pachysphaerica (Pronina)
Earlandia vulgaris (Rauzer-Chernousova and Reitlinger)
Endothyra sp.
Eoendothyranopsis sp.
Globoendothyra sp.
Priscella sp.
Pseudotaxis sp.

Age: inadequate assemblage; early to middle Viséan.

(GSC loc. C-52423, 721 m) Flett Formation, 172 m above base.

Calcisphaera sp.
Earlandia sp.
Endothyra sp.
Dainella sp.
Mametella sp.
Priscella sp.
Stacheoides sp.

Age: inadequate assemblage; early to middle Viséan.

(GSC loc. C-52520, 724 m) Flett Formation, 175 m above base.

Calcisphaera laevis Williamson
Calcisphaera pachysphaerica (Pronina)
Earlandia vulgaris (Rauzer-Chernousova and Reitlinger)
Endothyra sp.
Priscella sp.
Pseudotaxis sp.

Age: inadequate assemblage; early to middle Viséan.

(GSC loc. C-52427, 729 m) Flett Formation, 180 m above base.

Earlandia sp.
Endothyra sp.
Globoendothyra sp.
Priscella sp.
Tetrataxis sp.

Age: inadequate assemblage; early to middle Viséan.

(GSC loc. C-52428, 732.5 m) Flett Formation, 183.5 m above base.

Calcisphaera sp.
Earlandia sp.
Endothyra sp.
Globoendothyra sp.
Mametella sp.
Priscella sp.
Pseudotaxis sp.
Tetrataxis sp.

Age: inadequate assemblage; early to middle Viséan.

(GSC loc. C-52430, 743.5 m) Flett Formation, 194.5 m above base.

Calcisphaera sp.
Earlandia clavatula (Howchin)
Earlandia vulgaris (Rauzer-Chernousova and Reitlinger)
Endothyra sp.
Globoendothyra sp.
Priscella sp.

Age: inadequate assemblage; early to middle Viséan.

(GSC loc. C-52431, 750 m) Flett Formation, 201 m above base.

Calcisphaera laevis Williamson
Calcisphaera pachysphaerica (Pronina)
Earlandia clavatula (Howchin)
Earlandia moderata (Malakhova)
Earlandia vulgaris (Rauzer-Chernousova and Reitlinger)
Endothyra sp.
Eoendothyranopsis of the group *E. pressa* and *E. rara* (Grozdilova in Lebedeva)
Globoendothyra sp.
Priscella sp.
Pseudotaxis sp.
Tetrataxis sp.

Age: late middle Viséan, zone 13.

(GSC loc. C-52432, 755 m) Flett Formation, 206 m above base.

Calcisphaera sp.
Earlandia sp.
Endothyra sp.

Eoforschia sp.
Globoendothyra sp.
Priscella sp.
Tetrataxis sp.

Age: inadequate assemblage; probably late middle Viséan.

(GSC loc. C-52436, 766 m) Flett Formation, 217 m above base.

Calcisphaera pachysphaerica (Pronina)
Earlandia vulgaris (Rauzer-Chernousova and Reitlinger)
Eoendothyranopsis of the group *E. pressa* and *E. rara* (Grozilova in Lebedeva)
Globoendothyra paula (Vissarionova)
Priscella sp.
Pseudotaxis sp.

Age: late middle Viséan, zone 13.

(GSC loc. C-52437, 775 m) Flett Formation, 226 m above base.

Earlandia vulgaris (Rauzer-Chernousova and Reitlinger)
Endothyra sp.
Pseudotaxis sp.

Age: inadequate assemblage; probably late middle Viséan.

Locality 13. Southern Liard Range; latitude 60°29'46"N, longitude 123°38'53"W, NTS 95 B/5; southwestern District of Mackenzie; Section 75MTA-BCR9 (GSC localities in metres above base of section).

(GSC loc. C-52335, 154 m) Flett Formation, 6.8 m above base.

Calcisphaera sp.
Earlandia clavatula (Howchin)
Earlandia vulgaris (Rauzer-Chernousova and Reitlinger)
Mametella sp.
Priscella sp.

Age: earliest Viséan, basal zone 10.

(GSC loc. C-52336, 158 m) Flett Formation, 10.8 m above base.

Calcisphaera sp.
Earlandia clavatula (Howchin)
Earlandia vulgaris (Rauzer-Chernousova and Reitlinger)
Mametella sp.
Priscella sp.

Age: earliest Viséan, zone 10.

(GSC loc. C-52339, 194.7 m) Flett Formation, 47.5 m above base.

Calcisphaera sp.
Earlandia sp.
Eoendothyranopsis sp.
Mametella sp.
Priscella sp.

Age: inadequate assemblage; early to middle Viséan.

(GSC loc. C-52344, 235 m) Flett Formation, 87.8 m above base.

Calcisphaera sp.
Earlandia vulgaris (Rauzer-Chernousova and Reitlinger)
Endothyra sp.
Eoendothyranopsis cf. *E. hinduensis* (Skipp in McKee and Gutschick)
Eoforschia sp.
Globoendothyra sp.
Mametella sp.
Skippella sp.
Tetrataxis sp.

Age: late early to early middle Viséan, zone 11 or 12.

(GSC loc. C-52348, 253.3 m) Flett Formation, 106.1 m above base.

Brunsia sp.
Calcisphaera sp.
Earlandia vulgaris (Rauzer-Chernousova and Reitlinger)
Eoendothyranopsis of the group *E. spiroides* (Zeller)
Eoendothyranopsis scitula (Toomey)
Eoforschia sp.
Globoendothyra paula (Vissarionova)
Priscella prisca (Rauzer-Chernousova and Reitlinger)
Tetrataxis sp.

Age: early to late middle Viséan; zones 12/13, passage of 12 to 13.

(GSC loc. C-52349, 256.3 m) Flett Formation, 109.1 m above base.

Brunsia sp.
Calcisphaera sp.
Earlandia vulgaris (Rauzer-Chernousova and Reitlinger)
Endothyra sp.
Eoendothyranopsis scitula (Toomey)
Eoendothyranopsis thompsoni (Anisgard and Campau)
Evendothyranopsis of the group *E. pressa* and *E. rara* (Grozilova in Lebedeva)
Eoendothyranopsis of the group *E. spiroides* (Zeller)
Globoendothyra sp.
Priscella sp.
Tetrataxis sp.

Age: early to late middle Viséan; zones 12/13, passage of 12 to 13.

(GSC loc. C-52350, 263 m) Flett Formation, 115.8 m above base.

Calcisphaera sp.
Earlandia sp.
Endothyra sp.
Eoendothyranopsis sp.
Globoendothyra sp.
Tetrataxis sp.

Age: inadequate assemblage; probably middle Viséan.

(GSC loc. C-52416, 264 m) Flett Formation, 116.8 m above base.

Calcisphaera laevis Williamson
Calcisphaera pachysphaerica (Pronina)
Earlandia clavatula (Howchin)
Earlandia vulgaris (Rauzer-Chernousova and Reitlinger)
Endothyra sp.
Eoendothyranopsis of the group *E. spiroides* (Zeller)
Eoendothyranopsis hinduensis (Skipp in McKee and Gutschick)
Eogloboendothyra sp.
Eoforschia sp.
Globoendothyra sp.
Priscella sp.
Tetrataxis sp.

Age: early to late middle Viséan; zones 12/13, passage of 12 to 13.

(GSC loc. C-52359, 327 m) Flett Formation, 179.8 m above base.

Calcisphaera laevis Williamson
Calcisphaera pachysphaerica (Pronina)
Earlandia sp.
Endothyra sp.
Eoendothyranopsis of the group *E. pressa* and *E. rara* (Grozilova in Lebedeva)
Eoendothyranopsis cf. *E. prodigiosa* (Armstrong)
Eoforschia sp.
Mametella sp.
Pseudotaxis sp.
Stacheoides tenuis Petryk and Mamet
Tetrataxis sp.

Age: late middle Viséan, zone 13.

(GSC loc. C-52475, 341 m) Flett Formation, 193.8 m above base.

Earlandia vulgaris (Rauzer-Chernousova and Reitlinger)

Endothyra sp.
Globoendothyra sp.
Tetrataxis angusta Vissarionova

Age: inadequate assemblage; late middle Viséan.

(GSC loc. C-52362, 353.5 m) Flett Formation, 206.3 m above base.

Calcisphaera laevis Williamson
Calcisphaera pachysphaerica (Pronina)
Calcisphaera sp.
Earlandia clavatula (Howchin)
Earlandia vulgaris (Rauzer-Chernousova and Reitlinger)
Eoendothyranopsis scitula (Toomey)
Globoendothyra paula (Vissarionova)
Mametella sp.
Pseudotaxis sp.
Stacheoides sp.
Tetrataxis sp.

Age: late middle Viséan, zone 13.

(GSC loc. C-52478, 394.5 m) Flett Formation, 247.3 m above base.

Earlandia sp.
Endothyra sp.
Mametella sp.
Priscella sp.

Age: inadequate assemblage; probably late middle Viséan.

(GSC loc. C-52363, 425 m) Flett Formation, 277.8 m above base.

Calcisphaera sp.
Earlandia vulgaris (Rauzer-Chernousova and Reitlinger)
Eoendothyranopsis sp.
Eoforschia sp.
Globoendothyra sp.
Mametella sp.
Paracalligelloides sp.
Priscella sp.
Stacheoides sp.
Tetrataxis sp.

Age: inadequate assemblage; probably late middle Viséan.

APPENDIX B

CORALS (E.W. BAMBER)

Data in this appendix are paraphrased from a report prepared in 1977 by E.W. Bamber (Geological Survey of Canada, Calgary, Alberta). See Figure 1 for localities. The coral zones are those of Sando and Bamber (1979, p. 191; 1985).

Locality 2. Twisted Mountain; latitude 61°11'00"N, longitude 123°37'38"W, NTS 95 G/4; southwestern District of Mackenzie; Section 76 MTA-BCR9 (GSC localities in metres above base of section).

(GSC loc. C-59015, 121 m) Yohin Formation, 8.4 m below top.

polycoeliid coral, possibly *Calophyllum* sp.

Age: Early Carboniferous; zone not determined.

(GSC loc. C-59028, 311 m) Flett Formation, 2.8 m above base.

Siphonodendron sp. cf. *S. oculinum* Sando

Age: early to early middle Viséan (V1 to V2); zone IIIA or IIIB.

(GSC loc. C-59039, 349 m) Flett Formation, 40.8 m above base.

?*Zaphriphyllum* sp.
Lophophyllum? sp. cf. *L. proteus* (Sutherland)

Age: late early to early middle Viséan (V1 to V2); zone IIIA or IIIB.

(GSC loc. C-59036, 350.5 m) Flett Formation, 42.3 m above base.

Siphonodendron oculinum Sando
Amplexizaphrentis sp.

Age: early to early middle Viséan (V1 to V2); zone IIIA or IIIB.

(GSC loc. C-59040, 362 m) Flett Formation, 53.8 m above base.

Amplexizaphrentis sp.
?*Zaphriphyllum* sp.

Age: probably early to middle Viséan (V1 to V2); zone III (undifferentiated).

(GSC loc. C-59043, 362.4 - 366.4 m) Flett Formation, 54.2 - 58.2 m above base.

Zaphriphyllum sp.
Lophophyllum? sp. cf. *L. proteus* (Sutherland)
Vesiculophyllum sp.

Age: probably late early to early middle Viséan (V1 to V2); zone IIIA (upper) or IIIB.

(GSC loc. C-59049, 455 m) Flett Formation, 146.8 m above base.

Caninia sp.
?*Lophophyllum* spp.
Siphonodendron? sp.

Age: middle Viséan (V2); zone IIIB to lower IIID.

Locality 3. North end Mattson anticline; latitude 61°06'38"N, longitude 123°45'54"W, NTS 95 G/4; southwestern District of Mackenzie; composite section 75MTA-BCR4, 5, and 6 (GSC localities in metres above base of section).

(GSC loc. C-47925, 323.3 m) Prophet Formation, 82 m above base.

Amplexizaphrentis sp.

Age: Early Carboniferous; zone not determined.

(GSC loc. C-52205, 376.3 m) Prophet Formation, 135 m above base.

Siphonodendron oculinum Sando

Age: early to early middle Viséan (V1 to V2); zone IIIA or IIIB.

(GSC loc. C-47926, 398.8-400.3 m) Flett Formation, 6-7.5 m above base.

Vesiculophyllum sp.
cf. *Pleurosiphonella* sp.

Age: middle Tournaisian to early middle Viséan (Tn2 to V2); probably Viséan, zone not determined.

(GSC loc. C-47929, 459.8-461.1 m) Flett Formation, 67-68.3 m above base.

Siphonodendron oculinum Sando
Vesiculophyllum sp.
Zaphriphyllum sp.

Age: early to early middle Viséan (V1 to V2); zone IIIA or IIIB.

(GSC loc. C-47928, 461.1 m) Flett Formation, 68.3 m above base.

Zaphriphyllum cf. *disseptum* of Sando

Age: early to early middle Viséan (V1 to V2); zone IIIA or IIIB.

(GSC loc. C-52234, 558.5 m) Flett Formation, 165.7 m above base.

Lophophyllum? proteus (Sutherland)
Amplexizaphrentis sp.

Age: late Tournaisian to early late Viséan (Tn3 to V3); zone not determined.

(GSC loc. C-47930, 569.5 m) Flett Formation, 176.7 m above base.

Siphonodendron oculinum? Sando
?Zaphriphyllum sp.

Age: early to middle Viséan (V1 to V2); zone IIIA or IIIB.

(GSC loc. C-52238, 572.7-574.9 m) Flett Formation, 179.9-182.1 m above base.

?Vesiculophyllum sp.
Siphonodendron sp. cf. *S. oculinum* Sando

Age: early Viséan to early middle Viséan (V1 to V2), probably the latter; zone IIIA or IIIB.

(GSC loc. C-47933, 573.6 m) Flett Formation, 180.8 m above base.

Siphonodendron sp. cf. *S. oculinum* Sando

Age: early to early middle Viséan (V1 to V2); zone IIIA or IIIB.

(GSC loc. C-52239, 583.5 m) Flett Formation, 190.7 m above base.

Amplexizaphrentis sp.
?Lophophyllum sp.

Age: (?)late middle to early late Viséan (V2 to V3); zone IIIC or IIID.

(GSC loc. C-52240, 584.9 m) Flett Formation, 192.1 m above base.

?Lophophyllum sp.

Age: middle Tournaisian to (?)middle Viséan (Tn2 to V2); zone not determined.

(GSC loc. C-47948, 666.3 m) Flett Formation, 273.5 m above base.

?Lophophyllum sp.

Age: early to early late Viséan (V1 to V3); zone not determined.

(GSC loc. C-52268, 699.8-702.3 m) Flett Formation, 307-309.5 m above base.

cf. *Dorlodotia* sp.

Syringopora sp.
"Diphyphyllum" sp.

Age: probably late middle to early late Viséan (V2 to V3); probably zone IIIC or IIID.

(GSC loc. C-52269, 700.8 m) Flett Formation, 308 m above base.

clisiophyllid coral
hypsiphyllid coral
cf. *Dorlodotia* sp.

Age: probably late middle to early late Viséan (V2 to V3); probably zone IIIC or IIID.

Locality 4. Jackfish Gap; latitude 61°05'54"N, longitude 123°59'26"W, NTS 95 G/4; southwestern District of Mackenzie; composite section 75MTA-BCR1, 2, and 3 (GSC localities in metres above base of section).

(GSC loc. C-52534, 431.8-436.1 m) Prophet Formation, 81.4-85.7 m above base.

Amplexizaphrentis sp.

Age: Early Carboniferous; zone not determined.

(GSC loc. C-52087, 536 m) Flett Formation, 58.6 m above base.

Vesiculophyllum sp.

Age: middle Tournaisian to early middle Viséan (Tn2 to V2); zone not determined.

(GSC loc. C-52089, 541 m) Flett Formation, 63.6 m above base.

Vesiculophyllum sp.
Zaphriphyllum disseptum? Sutherland

Age: latest Tournaisian to early Viséan; (Tn3 to V1); zone IIB (upper) to IIA.

(GSC loc. C-52541, 551 m) Flett Formation, 73.6 m above base.

?Zaphriphyllum sp.
Amplexizaphrentis sp.

Age: latest Tournaisian to middle Viséan (Tn3 to V2); zone IIB (upper) to IIIC.

(GSC loc. C-52108, 619.3 m) Flett Formation, 141.9 m above base.

?Amplexizaphrentis sp.

Age: Early Carboniferous; zone not determined.

(GSC loc. C-52111, 635.4 m) Flett Formation, 158 m above base.

Amplexizaphrentis sp.

Age: Early Carboniferous; zone not determined.

(GSC loc. C-52544, 644.4 m) Flett Formation, 167 m above base.

Amplexizaphrentis sp.

Ekvasophyllum? *harkeri* Sutherland

Age: early to early late Viséan (V1 to V3); zone III (undifferentiated).

(GSC loc. C-52113, 648.8 m) Flett Formation, 171.4 m above base.

Ekvasophyllum sp. cf. *E. inclinatum* Parks

Age: early to early late Viséan (V1 to V3); zone III (undifferentiated).

(GSC loc. C-52119, 692.3 m) Flett Formation, 214.9 m above base.

Ekvasophyllum enclinotabulatum Sutherland

Age: early to early late Viséan (V1 to V3); zone III (undifferentiated).

(GSC loc. C-52120, 693.8 m) Flett Formation, 216.4 m above base.

Syringopora sp.

Age: inadequate for age determination.

(GSC loc. C-52124, 697.8 m) Flett Formation, 220.4 m above base.

"*Diphyphyllum*" sp.

Age: probably early to middle Viséan (V1 to V2); zone not determined.

(GSC loc. C-52126, 705 m) Flett Formation, 227.6 m above base.

?*Lophophyllum* sp.

Age: middle Tournaisian to early middle Viséan (Tn2 to V2); zone not determined.

(GSC loc. C-52538, 730.3 m) Flett Formation, 252.9 m above base.

Amplexizaphrentis sp.

Lophophyllum? *proteus* (Sutherland)

Age: late Tournaisian to early late Viséan (Tn3 to V3); zone IIB or III (undifferentiated).

(GSC loc. C-52546, 730.3-730.8 m) Flett Formation, 252.9-253.4 m above base.

Syringopora sp.

Ekvasophyllum enclinotabulatum Sutherland
"*Diphyphyllum*" sp.

Age: early to early late Viséan (V1 to V3); zone III (undifferentiated).

(GSC loc. C-52543, 732.3 m) Flett Formation, 254.9 m above base.

Ekvasophyllum enclinotabulatum Sutherland

Age: early to early late Viséan (V1 to V3); zone III (undifferentiated).

(GSC loc. C-52545, 735.9 m) Flett Formation, 258.5 m above base.

Amplexizaphrentis sp.

Age: Early Carboniferous; zone not determined.

(GSC loc. C-52549, 777.2 m) Flett Formation, 299.8 m above base.

Amplexizaphrentis sp.

?*Canadiphyllum* sp.

Age: probably middle Viséan (V2); probably zone IIIB to IIID.

(GSC loc. C-47950, 822.2 m) Flett Formation, 344.8 m above base.

Ekvasophyllum? sp. cf. *E.?* *harkeri* Sutherland

Age: early to early late Viséan (V1 to V3); zone III (undifferentiated).

(GSC loc. C-52157, 823.5 m) Flett Formation, 346.1 m above base.

?*Zaphriphyllum* sp.

Lophophyllum? *proteus* (Sutherland)

Age: probably middle Viséan (V2); probably zone IIIB or IIIC.

Locality 7. Sheaf Creek; latitude 61°12'23"N, longitude 124°33'32"W, NTS 95 F/2; southwestern District of Mackenzie; Section 75MTA-BCR11 (GSC localities in metres above base of section).

(GSC loc. C-52462, 239.5-242.5 m) Flett Formation, 0-3 m above base.

?*Amplexizaphrentis* sp.

Age: Early Carboniferous; zone not determined.

(GSC loc. C-52463, 253.5-255 m) Flett Formation, 14-15.5 m above base.

Amplexizaphrentis sp.

Age: Early Carboniferous; zone not determined.

(GSC loc. C-52472, 279.5-286.5 m) Flett Formation, 40-47 m above base.

Ekvasophyllum? sp. cf. *E. harkeri* Sutherland

Age: early to early late Viséan (V1 to V3); zone III (undifferentiated).

(GSC loc. C-52479, 293.5 m) Flett Formation, 54 m above base.

Siphonodendron sp. cf. *S. whitneyi* of Meek
Siphonodendron n. sp.

Age: probably middle to early late Viséan (V2 to V3); probably zone IIIB or IIID.

(GSC loc. C-47942, 308-309 m) Flett Formation, 68.5-69.5 m above base.

Siphonodendron whitneyi of Meek
"*Diphyphyllum*" sp.
Syringopora sp.

Age: late middle to early late Viséan (V2 to V3); zone IIID.

(GSC loc. C-52485, 328 m) Flett Formation, 88.5 m above base.

Ekvasophyllum? *harkeri* Sutherland

Age: early to middle Viséan (V1 to V2); zone III (undifferentiated).

(GSC loc. C-52489, 341.5 m) Flett Formation, 102 m above base.

Siphonodendron n. sp.
Siphonodendron sp. cf. *S. mutabile* (Kelly)

Age: early to middle Viséan (V1 to V2), probably early middle Viséan; probably zone IIIB.

(GSC loc. C-52490, 342 m) Flett Formation, 102.5 m above base.

Siphonodendron n. sp.

Age: This coral also occurs in the Debolt Formation of northeastern British Columbia, where it has been dated as early middle Viséan (V2); probably zone IIIB.

Locality 11. North end of Flett anticline; latitude 60°41'20"N, longitude 123°48'20"W, NTS 95 B/12; southwestern District of Mackenzie; Section 75MTA-BCR12 (GSC localities in metres above base of section).

(GSC loc. C-52523, 405.5-412 m) Prophet Formation, 175-181.5m above base.

Amplexizaphrentis sp.

Age: Early Carboniferous; zone not determined.

Locality 12. West flank of Flett anticline; latitude 60°33'50"N, longitude 123°48'20"W, NTS 95 B/12; southwestern District of Mackenzie; Section 75MTA-BCR10 (GSC localities in metres above base of section).

(GSC loc. C-52368, 39 m) Pekisko Formation, 8 m above base.

?*Vesiculophyllum* sp.

Age: probably middle to late Tournaisian (Tn2 to Tn3); zone not determined.

(GSC loc. C-47938, 489-490.6 m) Prophet Formation, 220-221.6 m above base.

Amplexizaphrentis sp.

Age: Early Carboniferous; zone not determined.

(GSC loc. C-52396, 553.2 m) Flett Formation, 4.2 m above base.

Amplexizaphrentis sp.

Age: Early Carboniferous; zone not determined.

(GSC loc. C-47941, ~ 693-694 m) Flett Formation, 144-145 m above base.

Siphonodendron whitneyi of Meek
Siphonodendron sp. cf. *S. warreni* Nelson

Age: late middle to early late Viséan (V2 to V3); zone IIID.

(GSC loc. C-52434, 762 m) Flett Formation, 213 m above base.

Stelechophyllum? *mclareni* (Sutherland)

Age: late middle to early late Viséan (V2 to V3); zone IIID.

Locality 13. Southern Liard Range; latitude 60°29'46"N; longitude 123°38'53"W, NTS 95 B/5; southwestern District of Mackenzie; Section 75MTA-BCR9 (GSC localities in metres above base of section).

(GSC loc. C-52361, 340.5 m) Flett Formation, 193.3 m above base.

Siphonodendron sp. cf. *S. mutabile* (Kelly)

Age: Range uncertain, middle Tournaisian to middle Viséan (Tn2 to V2); zone not determined.

(GSC loc. C-68829, 423-425 m) Flett Formation, 275.8-277.8 m above base.

Siphonodendron sinuosum (Kelly)
Siphonodendron whitneyi of Meek
Stelechophyllum? mclareni (Sutherland)
Stelechophyllum sp.

Age: late middle to early late Viséan (V2 to V3); zone IIID.

APPENDIX C

CONODONTS (A.C. HIGGINS)

Data in this appendix are paraphrased from a report prepared in 1981 by A.C. Higgins (The British Petroleum Company, B.P. Research Centre, Sunbury-on-Thames, Middlesex, England); formerly Geological Survey of Canada. See Figure 1 for locations.

Locality 1. Bluefish Mountain; latitude 61°07'23"N, longitude 123°29'13"W, NTS 95 G/3; southwestern District of Mackenzie; Section 75MTA-BCR7 (GSC localities in metres above base of section).

(GSC loc. C-47936, 283.9-284.2 m) Banff(?) Formation, 129.8-129.5 m below top.

Bispathodus aculeatus aculeatus (Branson and Mehl)
Bispathodus aculeatus anteposicornis Rexroad and Scott
Polygnathus communis Branson and Mehl
Polygnathus inornatus inornatus E.R. Branson
Polygnathus longiposticus Branson and Mehl
Polygnathus n. sp.
Siphonodella sulcata (Huddle)

Age: early Tournaisian (Tn1b), earliest Carboniferous; (?) *Siphonodella sulcata* zone.

Maturity: 1-1.5 (see Epstein, Epstein and Harris, 1977).

(GSC loc. C-58529, 293.9 m) Banff(?) Formation, 119.8 m below top.

Bispathodus aculeatus aculeatus (Branson and Mehl)
Bispathodus stabilis Branson and Mehl
Polygnathus communis Branson and Mehl
Polygnathus inornatus E.R. Branson
Siphonodella duplicata morphotype 1 Branson and Mehl

Age: early Tournaisian (Tn1b), earliest Carboniferous; Lower *Siphonodella duplicata* zone.

Maturity: 1-1.5.

(GSC loc. C-52289, 326.9 m) Banff(?) Formation, 86.8 m below top.

Bispathodus aculeatus aculeatus (Branson and Mehl)
Bispathodus stabilis Branson and Mehl
Polygnathus inornatus E.R. Branson

Age: early Tournaisian (Tn1b); *Siphonodella sulcata*-*Siphonodella duplicata* zones, most likely *S. duplicata* zone.

Maturity: 1-1.5.

(GSC loc. C-58530, 425.9 m) Yohin Formation, 12.2 m above base.

Bispathodus aculeatus aculeatus (Branson and Mehl)
Neoprioniodus barbatus (Branson and Mehl)
Polygnathus inornatus E.R. Branson
Polygnathus spicatus E.R. Branson

Age: early Tournaisian (Tn1b), earliest Carboniferous; *Siphonodella sulcata*-*Siphonodella duplicata* zones, most likely *S. duplicata* zone.

Locality 2. Twisted Mountain; latitude 61°11'00"N, longitude 123°37'38"W, NTS 95 G/4; southwestern District of Mackenzie; Section 76MTA-BCR9 (GSC localities in metres above base of section).

(GSC loc. C-58994, 0.6 m) Yohin Formation, 128.8 m below top.

Archignathodus penescitulus (Rexroad and Scott)

Bispathodus stabilis (Branson and Mehl)
Polygnathus communis Branson and Mehl
Polygnathus inornatus E.R. Branson

Age: middle Tournaisian (Tn2); Lower *Siphonodella crenulata* zone.

Maturity: 1-1.5.

(GSC loc. C-58997, 11.5 m) Yohin Formation, 117.9 m below top.

Archignathodus penescitulus (Rexroad and Scott)
Bispathodus stabilis (Branson and Mehl)
Polygnathus communis communis Branson and Mehl
Polygnathus inornatus E.R. Branson

Age: middle Tournaisian (Tn2); Lower *Siphonodella crenulata* zone.

APPENDIX D

PALYNOMORPHS (D.C. MCGREGOR)

Data in this appendix are paraphrased from a report prepared in 1980 by D.C. McGregor (Geological Survey of Canada, Ottawa, Ontario).

Locality 33, Table 1. Imperial Island River No.1 well; latitude 60°09'29"N, longitude 121°08'16"W, NTS 95 A/3; southwestern District of Mackenzie (GSC localities in metres below Kelly Bushing).

[GSC loc. C-82856K, core from 1062 m (3484 ft)] Kotcho Formation, 5.2 m (17 ft) below top.

Archaeozonotriletes dedaleus Naumova
Archaeozonotriletes famenensis Naumova
Auroraspora macra Sullivan
Cornispora bicornata Nazarenko
Cyrtospora cristifer (Luber) van der Zwan
Grandispora cf. *G. gracilis* (Kedo) Streel
Perotriletes perinatus Hughes and Playford
Retusotriletes incohatus Sullivan
Rugospora versabilis (Kedo) Streel

Age: This assemblage is mid-Famennian, about equivalent to a part of the interval Fa2a to Fa2b in terms of the Famennian type area in Belgium, and to the Dankov-Lebedyan beds of the Russian Platform. Reworked Frasnian spores are also present and include *Archaeoperisaccus*? *timanicus* Pashkevich, *Cymbosporites cyathus* Allen, and *Hymenozonotriletes* cf. *H. bistchoensis* Staplin and Jansonius.

[GSC loc. C-82856I, core from 997.6 m (3273 ft)] Banff Formation, 52.4 m (172 ft) above base, 348.3 m (1143 ft) below top.

Retispora lepidophyta (Kedo) Playford
Rugospora versabilis (Kedo) Streel
Tumulispora (*Lophozonotriletes*) *malevkensis* (Kedo) Turnau

Age: Spores are rare but sufficient to indicate the *Vallatisporites pusillites*-*Spelaeotriletes lepidophytus* (PL) zone or the *Spelaeotriletes lepidophytus*-*Verrucosporites nitidus* (LN) Subzone of post-Famennian Devonian age, which is equivalent to the early Tournaisian Tn1a or early Tn1b.

[GSC loc. C-82856H, core from 915.3 m (3003 ft)] Banff Formation, 134.7 m (442 ft) above base, 266.1 m (873 ft) below top.

Auroraspora micromanifesta (Hacquebard) Richardson
Convolutispora spp.
? *Corbulispora cancellata* (Waltz) Bharadwaj and Venkatachala
Cyrtospora cristifer (Luber) van der Zwan
Dictyotriletes? *trivialis* Kedo
Grandispora echinata Hacquebard
Retispora lepidophyta (Kedo) Playford
Retusotriletes incohatus Sullivan
Rugospora versabilis (Kedo) Streel
Vallatisporites sp.

Age: This assemblage, like the previous one, is assignable to the PL zone or the LN Subzone, of Late Devonian (early Tournaisian) age.

[GSC loc. C-82856F, core from 837.5 m (2747.9 ft)] Banff Formation, 212.5 m (697.1 ft) above base, 188.3 m (617.9 ft) below top.

Convolutispora harlandii Playford
Dibolisporites (*Umbonatisporites*) *distinctus* (Clayton) Playford
Dictyotriletes? *similis* Kedo
Dictyotriletes? *trivialis* Naumova ex Kedo
Grandispora cf. *G. echinata* Hacquebard
Grandispora uncata (Hacquebard) Playford
Hystricosporites sp.
Knoxisporites hederatus Playford
Lophozonotriletes curvatus Naumova
Lophozonotriletes triangulatus (Ishchenko) Hughes and Playford
Lophozonotriletes variverrucatus Playford
Retispora lepidophyta (Kedo) Playford
Vallatisporites pusillites (Kedo) Dolby and Neves

Age: This assemblage is close to the Devonian-Carboniferous boundary in age. *Retispora lepidophyta* is abundant, which indicates that the strata at 837.5 m are of Devonian age. The assemblage is exceptionally diverse and well preserved.

[GSC loc. C-82856C, core from 707.7 m (2322 ft)]
Banff Formation, 342.3 m (1123 ft) above base, 58.5 m
(192 ft) below top.

Auroraspora macra Sullivan
Crassispora drucei Playford
Crassispora kosankei (Potonié and Kremp) Bharadwaj
Grandispora uncata Hacquebard

Lophozonotriletes triangulatus (Ishchenko) Hughes
and Playford
Lophozonotriletes variverrucatus Playford
Murospora? friendii Playford
Murospora sp.
Raistrickia corynogenes Sullivan
Tumulispota ordinaria Staplin and Jansonius

Age: This assemblage is definitely of Early
Carboniferous (Tournaisian) age.

APPENDIX E

PALYNOMORPHS (J. UTTING)

Data in this appendix are paraphrased from reports prepared in 1981 by
J. Utting (Geological Survey of Canada, Calgary, Alberta). See Figure 1
for locations.

Locality 1. Bluefish Mountain; latitude 61°07'23"N, longitude
123°29'13"W, NTS 95 G/3; southwestern District of
Mackenzie; Section 75MTA-BCR7 (GSC localities in metres
above base of section).

(GSC loc. C-58524, 154.9 m) middle Banff(?) Formation,
258.8 m below top.

Acanthotriletes sp.
Auroraspora macra Sullivan
Cyrtospora cristifer (Luber) Van der Zwan
Grandispora sp.
Hystricosporites sp.
Knoxisporites? sp.
Punctatisporites planus Hacquebard
Punctatisporites sp.
Retusotriletes incohatus Sullivan
Spelaetriletes sp.

Age: The presence of *Cyrtospora cristifer* along with
the lack of *Retispora lepidophyta* (Kedo)
Playford suggest an age no older than the
uppermost part of Tn1b. In contrast to other
assemblages from the Banff and Yohin
formations studied for this report, this
assemblage lacks the species *Dibolisporites*
distinctus, which appears in Europe at the base
of Tn2. Therefore, the assemblage may be of
latest Tn1b (late early Tournaisian) age.

Thermal Alteration Index: 2-2+.

(GSC loc. C-58527, 205.9 m) middle Banff(?) Formation,
207.8 m below top.

Acanthotriletes multisetus Playford
Auroraspora macra Sullivan
Cyrtospora cristifer (Luber) Van der Zwan
Densosporites anulatus (Loose) Smith and Butterworth
Dibolisporites sp.
Grandispora echinata Hacquebard
Hystricosporites sp.
Leiotriletes sp.
Lophozonotriletes rarituberculatus (Luber) Kedo

Spelaetriletes sp.
Tumulispota variverrucata Staplin and Jansonius

Age: probably latest Tn1b (latest early Tournaisian).

Thermal Alteration Index: 3-.

Locality 2. Twisted Mountain; latitude 61°11'00"N, longitude
123°37'38"W, NTS 95 G/4; southwestern District of
Mackenzie; Section 76MTA-BCR9 (GSC localities in metres
above base of section).

(GSC loc. C-59008, 79 m) Yohin Formation, 50.4 m below
top.

Apiculatisporis sp.
Corbulispora cancellata (Waltz) Bharadwaj and
Venkatachala
Cyrtospora cristifer (Luber) Van der Zwan
Densosporites anulatus (Loose) Smith and
Butterworth
Densosporites spitsbergensis Playford
Dibolisporites distinctus (Clayton) Playford
Grandispora echinata Hacquebard
Knoxisporites literatus (Waltz) Playford
Latosporites sp.
Leiotriletes sp.
Punctatisporites glaber (Naumova) Playford
Pustulatisporites gibberosus (Hacquebard) Playford
Reticulatisporites cancellatus (Waltz) Playford
Tumulispota variverrucata Staplin and Jansonius
Spelaetriletes sp.
Vallatisporites banffensis Staplin and Jansonius

Age: Comparison with the miospore zones of
western Europe proposed by Clayton et al.
(1977) suggests an age younger than Tn1b. For
example, in Europe, *Dibolisporites distinctus*
appears near the base of Tn2. Also, an age
younger than Tn1b would explain the lack of
forms such as *Retispora lepidophyta* (Kedo)
Playford. There is insufficient evidence to
determine whether the sample is of Tn2 or Tn3
age (middle or late Tournaisian), although, in
Europe, *Cyrtospora cristifer* does not extend

above the lower part of Tn3. Should the upper part of the range of this species prove similar in western Canada, an age of Tn2 to early Tn3 would seem reasonable.

Thermal Alteration Index: 2+ to 3-.

(GSC loc. C-59009, 83 m) Yohin Formation, 46.4 m below top.

Acanthotriletes sp.
Apiculatisporis sp.
Corbulispora cancellata (Waltz) Bharadwaj and Venkatachala
Densosporites anulatus (Loose) Smith and Butterworth
Densosporites spitsbergensis Playford
Dibolisporites distinctus (Clayton) Playford
Grandispora echinata Hacquebard
Knoxisporites literatus (Waltz) Playford
Pustulatisporites gibberosus (Hacquebard) Playford
Reticulatisporites peltatus Playford
Retusotriletes sp.
Spelaeotriletes sp.
Vallatisporites banffensis Staplin and Jansonius

Age: This assemblage is similar to the one above (C-59008), and the same age is suggested.

Thermal Alteration Index: 2+ to 3-

(GSC loc. C-59014, 123 m) Yohin Formation, 6.4 m below top.

Apiculatisporis sp.
Densosporites anulatus (Loose) Smith and Butterworth
Grandispora echinata Hacquebard
Lophozotriletes rarituberculatus (Luber) Kedo
Punctatisporites sp.
Pustulatisporites gibberosus (Hacquebard) Playford
Spelaeotriletes sp.
Vallatisporites banffensis Staplin and Jansonius

Age: This assemblage is similar to the one from locality C-59008; it is, therefore, probably of Tn2 to early Tn3 age (middle to early late Tournaisian)

Thermal Alteration Index: 2+-3-.

(GSC loc. C-59021, 192 m) Clausen Formation, 62.6 m above base.

Densosporites spitsbergensis Playford
Knoxisporites literatus (Waltz) Playford
Lophozotriletes rarituberculatus (Luber) Kedo
Monilospira sp.
Pustulatisporites sp.
Raistrickia golatensis Staplin
Raistrickia sp.
Reticulatisporites cancellatus (Waltz) Playford
Tripartites incisotrilobus (Naumova) Karczewska and Turnau
Vallatisporites banffensis Staplin and Jansonius

Age: *Tripartites incisotrilobus* is common, and this differentiates the assemblage from those found

in the underlying upper Yohin Formation between 79.0 and 123 m. The general similarity of this assemblage to those from the upper Yohin suggests it is approximately the same age or slightly younger than that interval. The possible age range suggested for the upper Yohin assemblages was Tn2 to lower Tn3. In Poland, *T. incisotrilobus* appears in the Tn3 and also is present in the Viséan (Turnau, 1979); this may imply an age no older than Tn3 for the assemblage from C-59021. In addition, the base of the overlying Prophet Formation at Twisted Mountain contains foraminifers that are of latest Tournaisian age and assignable to Mamet and Skipp's (1970, 1971) zone 9 (Mamet, Appendix A). The assemblage from C-59021 is, therefore, probably of Tn3 age (latest Tournaisian).

Thermal Alteration Index: 3-.

Locality 4. Jackfish Gap; latitude 61°05'54"N, longitude 123°59'26"W, NTS 95 G/4; southwestern District of Mackenzie; composite section 75MTA-BCR1, 2, 3 and 76MTA-BCR4 (GSC localities in metres above base of section).

(GSC loc. C-58503, 93 m) Yohin Formation, 64.2 m below top.

Densosporites anulatus (Loose) Smith and Butterworth
Densosporites spitsbergensis Playford
Punctatisporites glaber (Naumova) Playford

Age: Not determined.

Thermal Alteration Index: 3- to 3.

(GSC loc. C-58502, 144 m) Yohin Formation, 13.2 m below top.

Apiculatisporis sp.
Densosporites spitsbergensis Playford
Lophozotriletes rarituberculatus (Luber) Kedo
Punctatisporites glaber (Naumova) Playford
Spelaeotriletes sp.
Vallatisporites banffensis Staplin and Jansonius

Age: No precise age can be determined; however, all of the species listed here were also found in the Yohin Formation at Location 2, Twisted Mountain.

Thermal Alteration Index: 3- to 3.

(GSC loc. C-58501, 156-157 m) Yohin Formation, 1.2-0.2 m below top.

Cyclogranisporites sp.
Densosporites anulatus (Loose) Smith and Butterworth
Densosporites spitsbergensis Playford
Lophozotriletes rarituberculatus (Luber) Kedo
Punctatisporites glaber (Naumova) Playford
Vallatisporites banffensis Staplin and Jansonius

Age: This assemblage is similar to that described from GSC loc. C-58502.

Thermal Alteration Index: 3⁻ to 3.

(GSC loc. C-52180, 267.9 m) Clausen Formation, 104.7 m above base.

Leiotriletes sp.
Lophozonotriletes rarituberculatus (Luber) Kedo
Punctatisporites sp.
Spelaeotriletes sp.
Tripartites incisotrilobus (Naumova) Karczewska and Turnau
Vallatisporites banffensis Staplin and Jansonius

Age: This assemblage is similar to that of C-59021 from the Clausen Formation at Twisted Mountain, and it was collected at a similar stratigraphic level. A probable Tn3 age (late Tournaisian) was suggested for the C-59021 assemblage.

Thermal Alteration Index: 3⁻.

Locality 11. North end of Flett anticline; latitude 60°41'20"N, longitude 123°48'20"W, NTS 95 B/12; southwestern District of Mackenzie; Section 75MTA-BCR12 (GSC localities in metres above base of section).

(GSC loc. C-52508, 97.5 m) Besa River Formation, 133 m below top.

Densosporites sp.
Leiotriletes sp.
Retusotriletes sp.
Tripartites incisotrilobus (Naumova) Karczewska and Turnau
Vallatisporites banffensis Staplin and Jansonius

Age: Although this assemblage is relatively limited, it was collected from a stratigraphic position similar to that of the Clausen Formation, and it contains *Tripartites incisotrilobus*. This suggests that the assemblage is similar in age to miospores from the Clausen; miospore assemblages from the latter (C-59021 and C-52180) are of probable Tn3 age (late Tournaisian).

Thermal Alteration Index: about 3.

Locality 33 (Table 1). Imperial Island River No. 1 well; latitude 60°09'29"N, longitude 121°08'16"W, NTS 95 A/3; southwestern District of Mackenzie (GSC localities in metres below Kelly Bushing).

[GSC loc. C-82856B, core from 655.9 m (2152 ft)] Banff Formation, 394.1 m (1293 ft) above base, 6.7 m (22 ft) below top.

Acanthotriletes multisetus (Luber) Potonié and Kremp
Anaplanisporites sp.
Apiculatisporis sp.
Auroraspora macra Sullivan
Auroraspora solisorta Hoffmeister, Staplin, and Malloy
Convolutispora flexuosa forma *minor* Hacquebard
Corbulispora cancellata (Waltz) Bharadwaj and Venkatachala
Cyclogranisporites sp.
Cyrtospora cristifer (Luber) Van der Zwan
Densosporites anulatus (Loose) Smith and Butterworth
Densosporites? *banffensis* Staplin and Jansonius
Densosporites simplex Staplin
Dibolisporites distinctus (Clayton) Playford
Dictyotriletes trivialis Naumova
Grandispora echinata Hacquebard
Knoxisporites literatus (Waltz) Playford
Microreticulatisporites hortonensis Playford
Punctatisporites planus Hacquebard
Spelaeotriletes pretiosus (Playford) Neves and Belt
Spelaeotriletes sp.
Vallatisporites banffensis Staplin and Jansonius

Age: Comparison of this assemblage with those of western Europe described by Clayton et al. (1977) suggests an age younger than Tn1b. For example, in Europe, *Dibolisporites distinctus* appears near the base of the Tn2, and *Spelaeotriletes pretiosus* appears near the middle of Tn2. The lack of species of *Lycospora* suggests an age older than Viséan, and in Europe the presence of *Cyrtospora cristifer* may imply an age older than late Tn3. Therefore, a tentative age range for this sample is Tn2 to early Tn3 (middle to early late Tournaisian).

Thermal Alteration Index: 3⁻.

APPENDIX F

Point count analyses

Analyses for clast composition and types of quartz clasts are based on 500 and 400 counts per thin section, respectively.

Yohin Formation													
GSC loc. no.	Locality Figure 1	Metres above base of section	Clast composition (per cent)							Quartz clasts (per cent)			
			quartz	chert rock fragments	other rock fragments	feldspar	heavy minerals	opaque	mica	straight extinction	undulous extinction	polycrystalline 2-3 units	polycrystalline > 3 units
C-52165	4	32.0	76.20	15.80	5.80	1.00	0.40	0.20	0.60	35.50	53.75	4.75	6.00
C-52177	4	155.8	81.80	13.20	2.20	1.00	0.80	0.40	0.60	35.25	53.50	3.50	7.50
C-52184	3	13.5	90.00	7.60	0.40	1.20	0.20	0.20	0.40	40.00	50.00	3.50	6.75
C-52188	3	35.6	83.20	11.40	2.20	1.40	1.20	0.20	0.40	--	--	--	--
C-52298	1	434.9	--	--	--	--	--	--	--	44.75	48.5	2.75	4.0
C-52300	1	448.9	79.00	15.40	2.80	1.00	1.00	1.20	1.20	--	--	--	--
C-52302	1	445.9	87.40	11.00	0.20	1.00	0.00	0.20	0.40	36.25	51.50	4.75	7.50
C-59012	2	107.0	85.20	10.80	2.20	0.80	0.60	0.00	0.40	37.25	51.50	4.50	6.75
mean per cent			83.26	12.17	2.26	1.06	0.60	0.34	0.57	38.17	51.46	3.96	6.42
standard deviation			4.77	2.87	1.85	0.19	0.43	0.40	0.29	3.66	2.02	0.83	1.31
Flett Formation													
C-52248	3	604.3	84.00	11.60	3.40	0.20	0.00	0.40	0.40	--	--	--	--
C-52249	3	607.3	90.80	4.20	3.80	0.00	0.40	0.20	0.60	70.00	27.00	0.50	2.50
C-52250	3	611.6	83.20	8.00	6.80	0.40	0.60	0.00	1.00	--	--	--	--
C-52252	3	617.1	84.40	13.00	2.00	0.00	0.00	0.60	0.00	61.50	33.50	1.25	3.75
C-52528	4	671.9	82.80	10.60	4.00	0.00	0.40	1.00	1.20	--	--	--	--
C-52529	4	673.5	85.20	8.00	5.60	0.40	0.00	0.00	0.80	61.75	31.00	2.00	5.25
C-52531	4	679.3	85.80	8.80	3.40	0.20	0.40	0.40	1.00	--	--	--	--
C-52532	4	685.7	92.20	7.20	0.20	0.40	0.00	0.00	0.00	55.75	38.00	2.25	4.00
C-59050	2	469.0	89.80	6.60	1.80	0.20	1.00	0.40	0.20	--	--	--	--
C-59051	2	490.0	88.60	10.40	0.80	0.00	0.20	0.00	0.00	66.75	29.50	1.00	2.75
mean per cent			86.68	8.84	3.18	0.18	0.30	0.30	0.52	63.15	31.80	1.4	3.65
standard deviation			3.22	2.47	1.94	0.17	0.31	0.30	0.44	4.89	3.75	0.64	0.98
Golata Formation													
C-58870	8	481.0	98.20	0.20	0.20	0.40	0.40	0.20	0.40	54.25	44.75	0.25	0.75
C-58871	8	476.0	95.20	0.60	3.20	0.20	0.20	0.40	0.20	56.25	41.75	0.50	1.50
mean per cent			96.70	0.40	1.70	0.30	0.30	0.30	0.30	55.25	43.25	0.38	1.13
standard deviation			2.12	0.28	2.12	0.14	0.14	0.14	0.14	1.40	2.12	0.18	0.53

APPENDIX G

Semiquantitative, whole-rock, X-ray diffraction analyses

This appendix is based on data prepared by A.G. Heinrich and colleagues at the Institute of Sedimentary and Petroleum Geology, Calgary, Alberta, between 1977 and 1981. Semiquantitative results were obtained from diffractograms, which may vary with degree of crystallinity, crystal size, and amount of amorphous material present.

GSC loc. number	Locality (Figure 1)	Metres above base of section	Lithology	Minerals present (per cent)													
				mixed-layer clays	illite	kaolinite	chlorite	quartz or chalcedony	feldspar	calcite	dolomite and ankerite	siderite	gypsum	pyrite	hematite	Total	
Clausen Formation																	
C-52180	4	261.9	shale	14	10	17	11	48	--	--	--	--	--	--	--	--	100
C-59021	2	192.0	mudstone	7	7	8	4	72	2	--	--	--	--	--	--	--	100
Prophet Formation																	
C-52311	6	80.0	limestone*	--	--	--	--	24	6	65	5	--	--	--	--	--	100
C-52316	6	126.5	limestone*	--	--	--	--	20	5	75	--	--	--	--	--	--	100
C-52326	13	1.5	limestone*	--	--	--	--	35	--	58	7	--	--	--	--	--	100
C-52327	13	52.5	limestone*	--	--	--	--	23	--	77	--	--	--	--	--	--	100
C-52514	11	254.2	limestone*	--	--	--	--	33	--	58	9	--	--	--	--	--	100
C-74223	5	541.0	limestone*	1	tr	tr	3	28	--	65	3	--	--	--	--	--	100
C-52056	4	365.4	spiculite	7	--	3	2	71	--	17	tr	--	--	--	tr	--	100
C-52058	4	390.4	spiculite	3	tr	--	--	47	1	42	7	--	--	--	--	--	100
C-52352	6	1.0	spiculite	--	--	--	--	93	--	7	--	--	--	--	--	--	100
C-58536	6	23.0	spiculite	6	--	tr	--	54	--	38	2	--	--	--	--	--	100
C-58842	8	1.0	spiculite	--	tr	--	tr	51	--	3	44	--	--	--	1	--	100
C-74217	5	421.0	spiculite	2	1	1.6	1.4	49	--	44	1	--	--	--	--	--	100
C-74228	5	593.6	spiculite	2	--	tr	4	65	--	22	6	--	--	--	1	--	99
C-52443	7	1.0	spiculite	7	tr	2	--	90	1	tr	--	--	--	--	--	--	100
C-52449	7	122.0	spiculite	11	--	4	--	71	--	14	tr	--	--	--	--	--	100
C-52067	4	467.3	shale	14	7	5	10	62	tr	2	tr	--	--	--	--	--	100
C-52460	7	213.2	shale	20	7	5	10	46	tr	9	3	--	--	--	--	--	100
C-58848	8	67.0	shale	25	9	--	16	42	tr	8	--	--	--	--	--	--	100
C-74220	5	470.0	shale	5	7	11	9	64	1	3	--	--	--	--	--	--	100
C-74234	5	654.0	mudstone	13	10	8	5	64	--	--	--	--	--	--	--	--	100
Flett Formation																	
C-58523	4	723.0	mudstone	4	5	4 ⁺		40	4	41	--	--	2	--	--	--	100
C-74330	4	528.8	mudstone	2	3	2 ⁺		69	3	20	--	--	--	1	--	--	100
C-74331	4	570.3	mudstone	2	4	2 ⁺		53	5	24	8	--	--	2	--	--	100
C-74336	4	764.9	mudstone	5	5	--	3	48	2	34	--	--	--	3	--	--	100
C-74338	4	767.8	shale	6	4	3 ⁺		52	2	28	2	--	--	3	--	--	100
C-52265	3	693.3	limestone*	1	tr	tr ⁺		26	3	70	--	--	--	--	--	--	100
C-74242	5	722.0	limestone*	1	3	--	--	17	tr	75	4	--	--	--	--	--	100
C-74249	5	766.5	limestone*	tr	--	--	--	6	2	92	--	--	--	--	--	--	100
C-74253	5	804.8	limestone*	tr	--	--	--	9	2	89	--	--	--	--	--	--	100
C-74255	5	819.0	limestone*	2	tr	--	--	22	--	71	2	--	--	3	--	--	100
C-74258	5	838.5	limestone*	3	--	tr ⁺		38	--	56	3	--	--	--	--	--	100
C-74264	5	894.5	limestone*	2	--	--	--	10	--	86	2	--	--	--	--	--	100
Golata Formation																	
C-58853	8	132.0	shale	3	4	4	7	70	1	2	8	--	--	1	--	--	100
C-58857	8	214.0	shale	3	6	--	12	76	--	--	3	--	--	--	--	--	100
C-58858	8	229.0	shale	3	8	3	8	73	--	1	4	--	--	--	--	--	100
C-58859	8	244.0	shale	5	8	6	9	65	2	--	5	--	--	--	--	--	100
C-58869	8	437.0	shale	6	9	12	8	65	--	--	--	--	--	--	--	--	100

+ chlorite and kaolinite

* Limestone is either skeletal lime packstone or lime wackestone.

tr = trace

